Reduced replication origin licensing selectively kills KRAS-mutant colorectal cancer cells via mitotic catastrophe

---

D I S S E R T A T I O N

zur Erlangung des akademischen Grades

Doctor rerum naturalium

(Dr. rer. nat.)

eingereicht an der Lebenswissenschaftlichen Fakultät

der Humboldt-Universität zu Berlin

von

M.Sc. Bastian Gastl

Die Präsidentin der Humboldt-Universität zu Berlin
Prof. Dr.-Ing. Dr. Sabine Kunst

Dekan der Lebenswissenschaftlichen Fakultät der Humboldt-Universität zu Berlin
Prof. Dr. Bernhard Grimm

Gutachter/innen:

Erstgutachterin:	Prof. Dr. Christine Sers
Zweitgutachter:	Prof. Dr. Nils Blüthgen
Drittgutachterin:	Prof. Dr. Lisa Wiesmüller

Eingereicht am:	21. Juni 2018
Tag der mündlichen Prüfung:	15. Oktober 2018

Acknowledgments

First of all, I want to thank my supervisor Prof. Dr. Christine Sers for giving me the chance to work in her lab in great independence and freedom. She has been an enormous inspiration to me - not only scientifically, but also personally.

I also want to thank Dr. Kathleen Klotz-Noack, Dr. Pamela Riemer, Soulafa Mamlouk, Ph.D., and PD Dr. Markus Morkel for lots of scientific advice and fun during my whole time in the lab. I want to thank Dr. Kathleen Klotz-Noack in particular for setting the foundation for this work. Furthermore, I want to thank Krenoula Hani Fouad Salib and Ángel Gil Nolskog for their help during their internships in the framework of the Master's program Molecular Medicine at the Charité. Lots of thanks also to Dr. Bertram Klinger for his help with handling the raw sequencing data of the RNAi screen.

Special thanks go to Cornelia Gieseler for handling basically every single problem in the lab. CO_2 supply is malfunctioning? No space left in the freezer? Do we have sodium deoxycholate? Conny always knew how to help. I also want to thank Birgit Schaefer for her unchallenged western blot skills.

Many thanks also to Julia Hoffmann, Tincy Simon, Sylvia Ispasanie, Prof. Dr. Reinhold Schäfer, Natalia Kuhn, Natalie Bublitz, Kerstin Wanke-Möhr, Maryam Sheykholeslami, Raphael Brandt, Manuela Pacyna, Slim Khouja, Andrea Menne, Dr. Katharina Kasack, and Silvia Schulze for great 3.5 years in the lab.

Finally, I want to express my sincere gratitude to my parents for supporting me throughout. Without your support, I would probably have to work in a bank of some kind and do boring stuff.

Thank you.

Memorandum

Partial results of the presented work have been submitted for publication at:

Journal: Cell Reports

Title: Reduced replication origin licensing selectively kills KRAS mutant colorectal cancer cells via mitotic catastrophe

Authors: Bastian Gastl, Kathleen Klotz-Noack, Bertram Klinger, Sylvia Ispasanie, Krenoula Hani Fouad Salib, Johannes Zuber, Nils Blüthgen, Reinhold Schäfer, Christine Sers

Date: June 19th, 2018

Author contributions: Conceptualization, B.G., C.S., R.S.; Methodology, B.G., K.K-N., J.Z., and C.S.; Validation, K.K-N. and K.H.F.S.; Formal Analyses, B.K.; Investigation, B.G.; Resources, K.K-N., J.Z., and S.I.; Writing – Original Draft, B.G.; Writing – Review & Editing, B.G., C.S., and R.S.; Visualization, B.G.; Supervision; C.S. and N.B.; Project Administration, C.S.; Funding Acquisition, B.G., C.S., N.B., and R.S.

Table of Contents

Abstract

With KRAS being one of the most frequently altered oncogenes in colorectal cancer (CRC), it is an obvious target for cancer therapy. However, despite enormous efforts over the past three decades to target mutated KRAS, not a single drug has made it to the clinic.

To unravel vulnerabilities of KRAS-mutant CRC cells, a shRNA-based screen was performed in CaCo2 cells harboring conditional oncogenic $KRAS^{G12V}$. The custom-designed shRNA library comprised 121 selected genes, which were previously identified to be strongly up- or downregulated in response to MEK inhibition.

The screen as well as the subsequent validations showed that CaCo2 cells expressing $KRAS^{G12V}$ were sensitive to the suppression of the DNA replication licensing factor Minichromosome Maintenance Complex Component 7 (MCM7), whereas $KRAS^{wt}$ CaCo2 cells were largely resistant to MCM7 suppression. Similar results were obtained in an isogenic DLD-1 cell culture model. Knockdown of MCM7 in a KRAS-mutant background led to replication stress as indicated by increased nuclear RPA focalization. Further investigation showed a significant increase in mitotic cells after simultaneous MCM7 knockdown and $KRAS^{G12V}$ expression. The increased percentage of mitotic cells coincided with strongly increased DNA damage in mitosis. Taken together, the accumulation of DNA damage in mitotic cells is due to replication stress that remained unresolved, which results in mitotic catastrophe and cell death.

In summary, the data show a vulnerability of KRAS-mutant cells towards suppression of MCM7 and suggest that inhibiting DNA replication licensing might be a viable strategy to target KRAS-mutant cancers.

Zusammenfassung

KRAS ist eines der am häufigsten mutierten Onkogene in Darmkrebspatienten. Dies macht es zu einem guten Ansatzpunkt für gezielte Krebstherapien. Trotz jahrzehntelanger Forschungsbemühungen hat sich jedoch keines der zur Inhibition des mutierten KRAS entwickelten Medikamente klinisch etablieren können.

Um eventuelle Schwachstellen von KRAS mutierten Darmkrebszellen aufzudecken, wurde in der vorliegenden Studie ein shRNA basierter Screen in CaCo2 Zellen mit konditioneller $KRAS^{G12V}$ Expression ausgeführt. Die maßangefertigte shRNA-Bibliothek umfasste 121 ausgewählte Gene, die zuvor nach MEK Inhibition als stark hoch- oder herunterreguliert identifiziert wurden.

Der Screen sowie die Screen-Validierung zeigten, dass $KRAS^{G12V}$ exprimierende CaCo2 Zellen besonders sensitiv für den Knockdown des DNA Replikationslizensierungsfaktors Minichromosome Maintenance Complex Component 7 (MCM7) waren, wohingegen sich $KRAS^{wt}$ CaCo2 Zellen als weitestgehend resistent gegenüber des MCM7 Knockdowns erwiesen. Ähnliche Ergebnisse wurden im isogenen DLD-1 Zellmodell erzielt. Des Weiteren hat der Knockdown von MCM7 spezifisch in KRAS mutierten Zellen zu erhöhtem Replikationsstress geführt, der durch gesteigerte nukleare RPA Fokalisierung nachgewiesen wurde. Weitere Untersuchungen haben außerdem eine signifikant erhöhte Anzahl an mitotischen Zellen nach gleichzeitigem MCM7 Knockdown und $KRAS^{G12V}$ Expression ergeben. Diese Zunahme an mitotischen Zellen wurde zusätzlich von einer stark angestiegenen Anzahl an DNS Schäden in der Mitose begleitet. Das hohe Maß an DNS Schäden in der Mitose kann auf den gesteigerten Replikationsstress zurückgeführt werden, der ungelöst zu einer gestörten Segregation der Chromosomen in der Mitose führt.

Zusammenfassend zeigen die Ergebnisse, dass KRAS mutierte Darmkrebszellen sensitiv auf den Knockdown von MCM7 sind. Demzufolge könnte die Inhibition von DNS Replikationslizensierung ein geeigneter Ansatz für die gezielte Therapie von KRAS mutierten Darmkrebs sein.

List of Figures

List of Tables

1. Introduction

Life is only possible because cells can store and pass on information through encoded deoxyribonucleic acid (DNA). Its code is composed of four distinct letters, which are read and translated into the building blocks that make up all living organisms. To pass on this information, the code has to be faithfully copied in a process called DNA replication. This process is highly efficient and accurate, nevertheless, rare copying mistakes do occur. These errors are necessary in the long run since they are the basis for genetic diversity and therefore evolution. However, mistakes at the wrong position of the genetic code can alter the building blocks of a cell in a way that is detrimental for regulated growth. By losing the ability to regulate and control their growth, healthy cells can be transformed into malignant cancer cells.

Since the basis of life and cancer are so closely linked, it is not surprising that cancer is considered to be an “ancient disease” (Faltas, 2011). The term “cancer” originates from the Greek physician Hippocrates (460-375 BC) as it reminded him of a crab or καρκίνος (karkinos) in Greek (Hajdu, 2011). The first descriptions of cancer, however, dates back even further to about 3,000 BC. The Edwin Smith Surgical Papyrus is the oldest document found to this date to mention cancer as a disease. It describes “bulging tumors” in the breast for which “there is no treatment” (Breasted, 1930; Donegang, 2006) (Figure 1).

In the following 5,000 years, treatment of cancerous growths was largely limited to surgical removal. This was until the late 20th century when chemotherapy and radiation combined with surgery started to become the standard for cancer treatment (Sudhakar, 2009). Despite the fact that cancer treatments have improved, it is still one of the biggest burdens on health up to this day. According to estimations of the World Health Organization, cancer contributed to 27% of all deaths in Germany in 2015 and was next to cardiovascular diseases the second most common cause of death (World Health Organization, 2015).

A

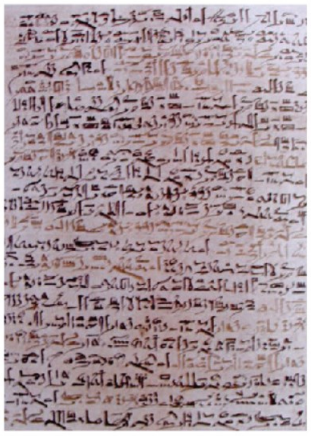

B

Translation

If thou examinest a man having bulging tumors on his breast, (and) thou findest that [swellings] have spread over his breast ; if thou puttest thy hand upon his breast upon these tumors, (and) thou findest them very cool, there being no fever at all therein when thy hand touches him ; they have no granulation, they form no fluid, they do not generate secretions of fluid, and they are bulging to thy hand

Figure 1: Excerpt from the Edwin Smith Surgical Papyrus from ca 3,000 B.C. (A) Image of case 45 the original Edwin Smith Surgical Papyrus (Donegang, 2006). (B) Transcription and translation of the earliest description of tumors (Breasted, 1930).

Cancer, with very few exceptions, is – as mentioned before - almost always caused by several separately occurring alterations to the DNA code, which either activate tumor-driving oncogenes or disable tumor suppressors. These alterations are what differentiate malignant cells from healthy cells. Douglas Hanahan and Robert Weinberg summarized the properties of cancer cells in their famous paper “The hallmarks of cancer” in 2000. They concluded that most cancers acquire the following properties: self-sufficiency in growth signals, insensitivity to anti-growth signals, tissue invasion and metastasis, limitless replicative capacity, sustained angiogenesis, and the evasion from apoptosis. 11 years later, they further expanded upon these six hallmarks by adding four additional hallmarks: deregulating cellular energetics, avoiding immune destruction, genome instability and mutation, and tumor-promoting inflammation (Hanahan and Weinberg, 2000, 2011). Interestingly, KRAS is one single oncogene that can feed into several different hallmarks of cancer simultaneously, such as self-sufficiency in growth signals, insensitivity to anti-growth signals, sustained angiogenesis, and deregulating cellular energetics (Bryant et al., 2014; Matsuo et al., 2009; Pylayeva-Gupta et al., 2011; Yang et al., 2013).

Nonetheless, these differences of cancerous cells compared to healthy cells also open up opportunities for treatments. In this thesis, I will focus on how mutations in the KRAS gene can be exploited for cancer therapy.

1.1. Colorectal Cancer

It is important to understand that cancer is not one single disease. One of the most common types of cancer is colorectal cancer (CRC). CRC is the second most frequent type of cancer in women after breast cancer and the third most common type in men after lung and prostate cancer. In total, there are about 1.4 million new cases and 694,000 deaths reported worldwide each year (Ferlay et al., 2015).

Colorectal cancers are in the clinical routine most commonly sub-classified in the following genetic and epigenetic groups: microsatellite instable (MSI), chromosome instable (CIN), and CpG island methylator phenotype (CIMP), as well as BRAF and KRAS mutant or wild-type (Jass, 2007). All of these classifications have been shown to have a prognostic value on patient survival (Phipps et al., 2015). A more recent and comprehensive attempt of subclassification proposed four sub-types of colorectal cancer that are defined by their distinct transcription profiles. The authors of the study concluded that colorectal cancer can be grouped into four types: MSI immune, canonical, metabolic, and mesenchymal. These groups also demonstrated prognostic value (Guinney et al., 2015). Those groups, however, do not overlap with the above mentioned genetic and epigenetic subtypes. Therefore, they can serve as a separate classifier rather than an extension of the former system.

Treatment in CRC still relies heavily on conventional chemotherapy. The most common therapy regimens for metastatic CRC combine 5-fluorouracil (5-FU) and folinic acid with oxaliplatin or irinotecan (FOLFOX/FOLFIRI). Another common strategy is the combination of capecitabine (a 5-FU precursor) with oxaliplatin or irinotecan (CAPOX/CAPIRI). Both strategies result in an average overall survival of about 18 months. In addition to conventional chemotherapy, more targeted therapies such as epidermal growth factor receptor (EGFR) and vascular endothelial growth factor (VEGF) inhibition have emerged in the recent years. Since then, the addition of targeted therapy has significantly improved overall survival of metastatic CRC patients to 22-29 months (Ciombor and Berlin, 2014; Van Cutsem et al., 2014; Martini et al., 2017). A prerequisite for effective targeted EGFR inhibition in CRC is the lack of activating mutations in the RAS genes downstream of EGFR (Amado et al., 2008; Douillard et al.,

2013). The RAS genes are, however, are mutated in about 50% of all CRC patients and are one of the most commonly mutated oncogenes in CRC next to the tumor suppressor genes APC (75%) and TP53 (53%) (The Cancer Genome Atlas, 2012).

1.2. The Ras Pathway in Cancer

RAS was one of the first oncogenes to be identified in the late 1970s (Malumbres and Barbacid, 2003). It was later discovered that there are three very homologous but distinct human RAS genes: Kirsten rat sarcoma viral oncogene homolog (KRAS), neuroblastoma RAS viral oncogene homolog (NRAS), and Harvey rat sarcoma viral oncogene homolog (HRAS). Additionally, KRAS has two splicing isoforms, namely KRAS4A and KRAS4B, of which the latter is the most prevalent variant (Hobbs et al., 2016). The RAS proteins are small GTPases that cycle between its inactive and active state, which depends on the binding of GDP or GTP, respectively. Almost all RAS mutations are found in one of three hotspot locations on the gene (G12, G13, and Q61). Mutations at these sites prevent the hydrolysis of GTP to GDP and thereby leave RAS permanently in its active GTP bound state, which leads to a constitutive activation of a variety of downstream pathways (COSMIC v83; Forbes et al., 2017; Pylayeva-Gupta et al., 2011). Overall, the RAS genes are mutated in about 27% of all human cancers (Hobbs et al., 2016). Despite the fact that all RAS homologs are highly similar and feed into the same pathways, they seem to have distinct functions. For example, a complete Kras knockout in mice leads to the death of the mouse embryos during gestation (Johnson et al., 1997). Nras and Hras knockouts in mice, on the other hand, do not lead to changes in viability of the offspring (Esteban et al., 2001). Additionally, KRAS is by far the most commonly mutated homolog (85%) followed by NRAS (11%) and HRAS (4%) (Hobbs et al., 2016). Nevertheless, the exact differences of the RAS homologs on their downstream pathways and the following cellular effects are still a matter of investigation.

The distinct importance of the three RAS homologs in different tissues is also well illustrated by the occurrence of mutations in different cancer entities. In pancreatic

ductal adenocarcinomas (PDAC) and colorectal cancer (CRC) KRAS is by far the most commonly mutated RAS homolog (PDAC: KRAS 90%, NRAS 0.3%, HRAS 0% - CRC: KRAS 42%, NRAS 9%, HRAS 0%) (Bailey et al., 2016; Cerami et al., 2012; The Cancer Genome Atlas, 2012). In melanoma, however, NRAS mutations (26%) play a far bigger role than KRAS (0%) or HRAS (0.8%) (Cancer Genome Atlas Network et al., 2015; Cerami et al., 2012). Figure 2 summarizes the occurrence of mutations for each RAS homolog across different cancer types.

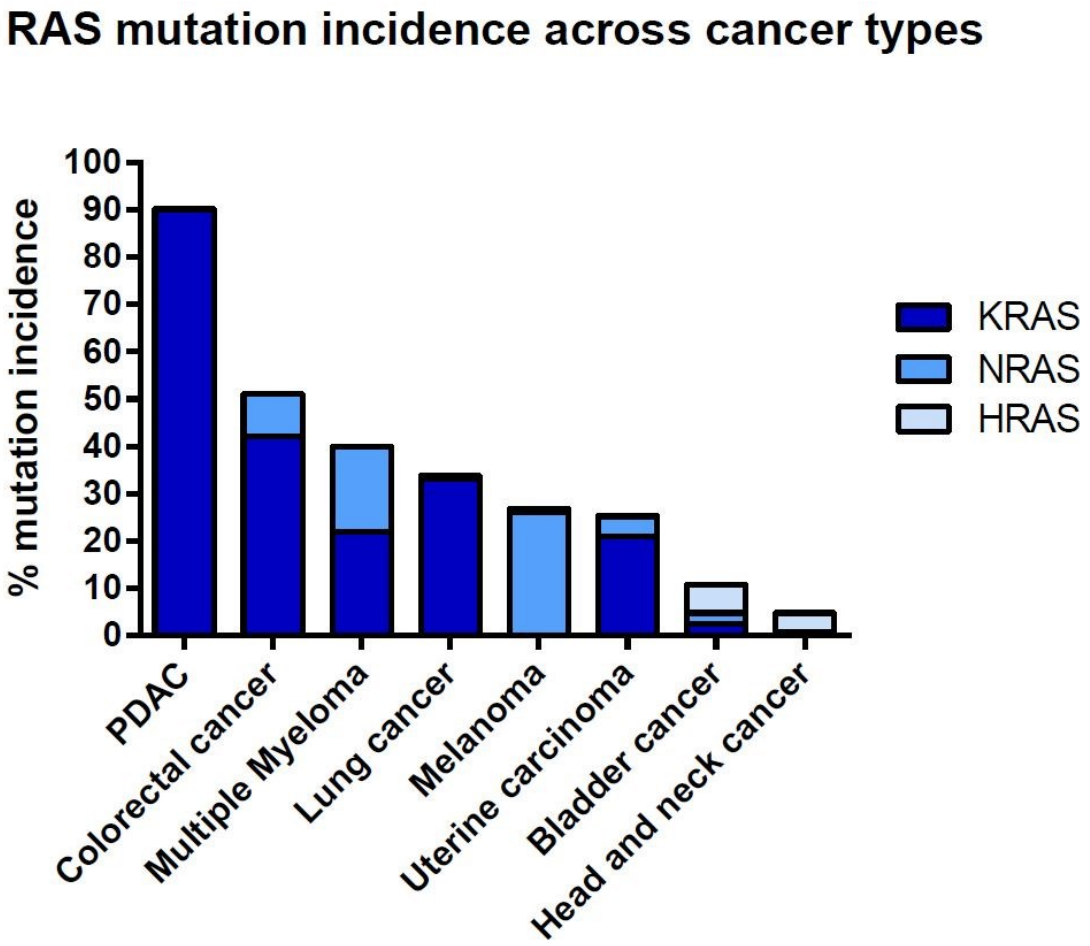

Figure 2: Mutation incidence of KRAS, NRAS, and HRAS across different cancer entities. Different cancer types show diverse mutation frequencies of the three RAS homologs. KRAS is the most frequently altered homolog. NRAS exhibits a high mutation rate specifically in multiple myeloma and melanoma. HRAS shows the highest mutation rate across the RAS homologs in bladder cancer and head and neck cancer (Bailey et al., 2016; Cancer Genome Atlas Network et al., 2015; Cerami et al., 2012; Collisson et al., 2014; Getz et al., 2013; Lawrence et al., 2015; Lohr et al., 2014; The Cancer Genome Atlas, 2012; Weinstein et al., 2014).

1.2.1. RAS signaling

In normal physiological conditions, RAS serves as a signal transducer of extracellular stimuli. It is activated through a wide variety of cell surface receptors such as receptor tyrosine kinases (RTKs) as well as G-protein-coupled-receptors (GPCRs). One of the most intensively studied pathways of RAS activation starts at the RTK epidermal growth factor receptor (EGFR). Upon ligand binding, EGFR dimerizes and auto-phosphorylates itself. The phosphorylation creates a binding site for the SH2-domain of growth-factor-receptor-bound protein 2 (GRB2), which is bound to the guanine nucleotide exchange factor (GEF) son of sevenless (SOS). GEFs activate plasma membrane-associated RAS by facilitating the exchange of GDP to GTP (Downward, 2003). RAS has a weak intrinsic GTPase activity, which means it can inactivate itself to a small degree. However, inactivation of RAS is mainly achieved through a number of GTPase activating proteins (GAPs), which promote the hydrolysis of RAS bound GTP to GDP. There are 14 known GAPs, e.g. neurofibromin or DAB2IP, which play a role in limiting the signal transduction through RAS (Maertens and Cichowski, 2014) (Figure 3).

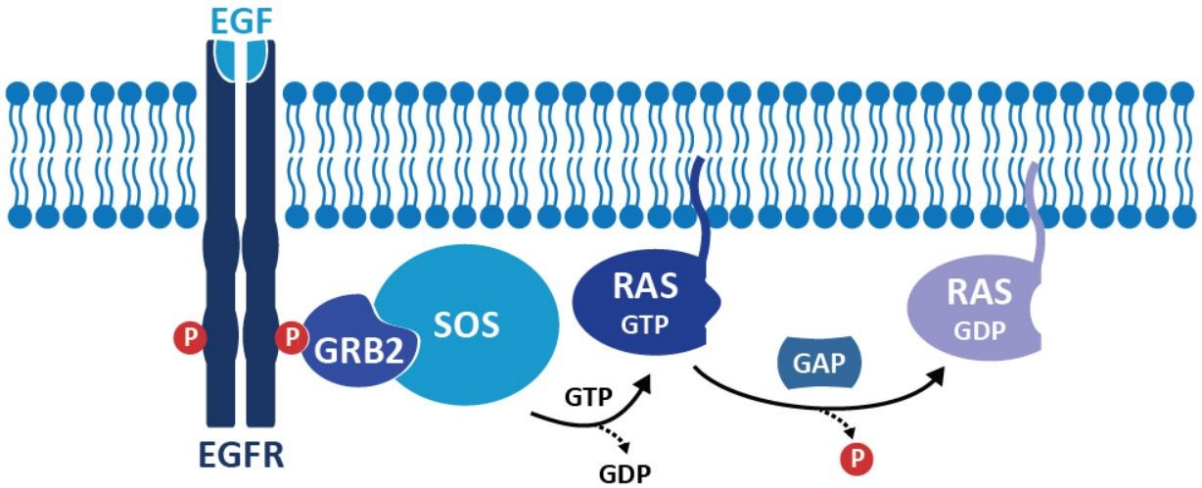

Figure 3: EGFR driven activation of RAS. Upon EGF binding, EGFR can autophosphorylate itself, which facilitates GRB2 binding. GRB2 then recruits the GEF SOS, which activates RAS by facilitating the exchange of GDP to GTP of RAS (adapted from Downward, 2003).

The conformational change upon GTP binding of RAS allows binding and activation of its downstream targets in different effector pathways. One of the most well-known downstream pathways of RAS is the mitogen-activated protein kinase (MAPK) pathway. The immediate targets of RAS in the MAPK pathway are the RAF proteins (ARAF, BRAF, c-RAF1), which in turn phosphorylate mitogen-activated protein kinase kinases 1 and 2 (MEK1/2). Phosphorylated MEK1/2 can then activate extracellular signal-regulated kinases 1 and 2 (ERK1/2), which in turn targets a wide variety of kinases and transcription factors, e.g. ELK1, p90RSK, or c-JUN (Downward, 2003). The cellular responses of activated MAPK signaling are diverse. They include increased proliferation by stimulating cell cycle progression, interfering with DNA damage checkpoint signaling, preventing apoptosis, as well as several metabolic changes (Downward, 2003; Knauf et al., 2006; Pylayeva-Gupta et al., 2011). RAS also activates the phosphatidylinositol 3-kinase (PI3K) pathway that is known for its pro-survival signaling. GTP bound RAS can recruit PI3K to the membrane and activate it. PI3K indirectly activates AKT, which phosphorylates and inhibits several pro-apoptotic targets like BAD and FORKHEAD. Moreover, RAS influences vesicle transport and cell cycle progression through the ral guanine nucleotide dissociation stimulator (RALGDS) pathway and has been shown to contribute towards calcium signaling via the 1-phosphatidylinositol-4,5-bisphosphate phosphodiesterase ε (PLCε) pathway (Figure 4) (Downward, 2003; Pylayeva-Gupta et al., 2011).

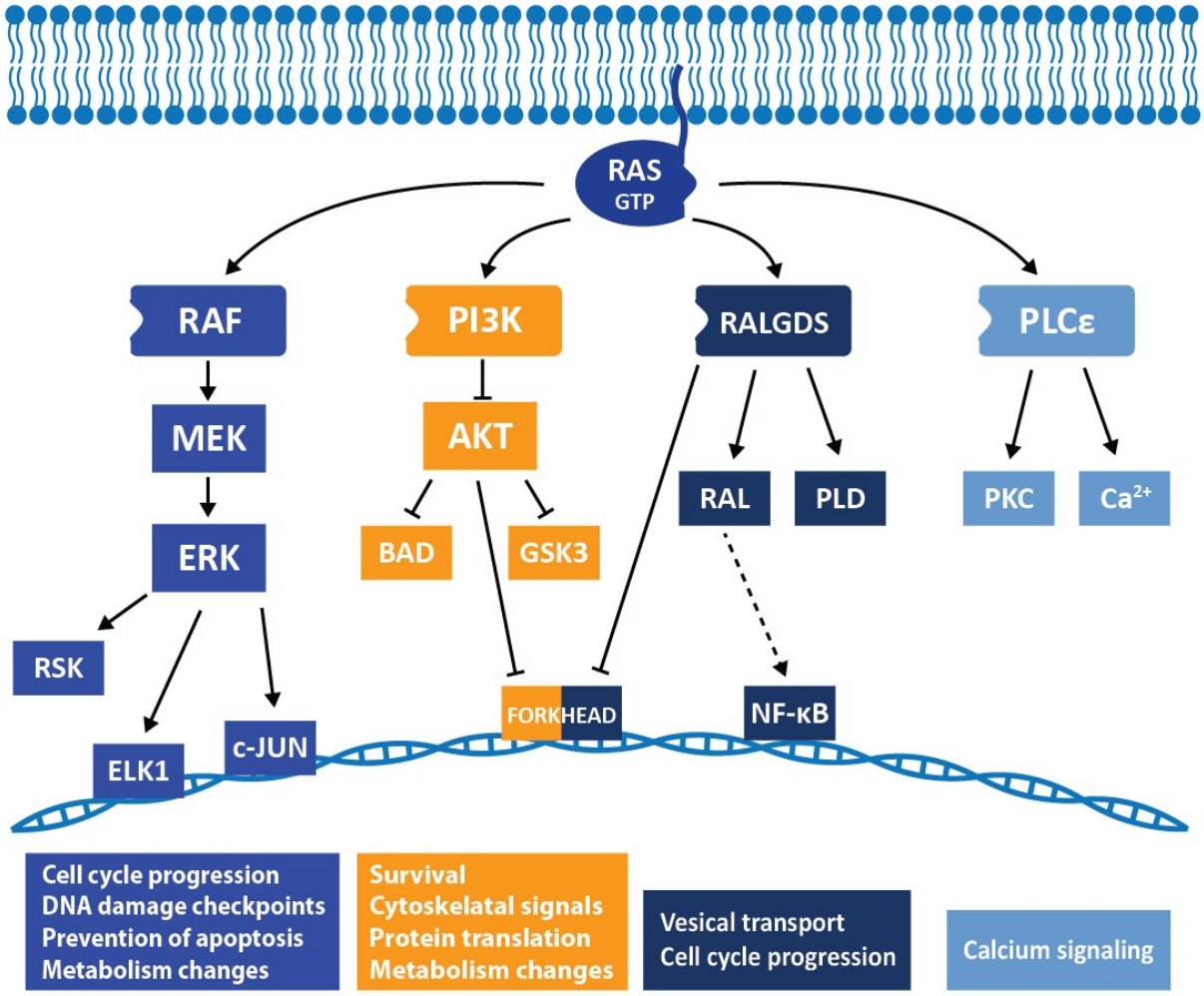

Figure 4: Downstream targets of RAS signaling. Active RAS can activate multiple different downstream pathways. Besides the most prominent MAPK and PI3K pathway, RAS also signals into the RALGDS and PLCε pathway (adapted from Downward, 2003; Neel et al., 2011).

1.2.2. Targeting oncogenic RAS

The significant role of mutant RAS in cancer renders it an obvious therapeutic target. This has, however, turned out to be remarkably challenging - so challenging that RAS has previously been coined to be “undruggable” (Cox et al., 2014). This chapter will summarize different strategies of targeting aberrant RAS signaling and explain why most of these approaches have not been successful so far (Figure 5).

The most straightforward approach is to target the RAS protein itself directly. To be active, RAS has to bind GTP. Therefore, targeting the GTP binding pocket with a small-

molecule antagonist, similar to kinase inhibitors, which target ATP binding pockets, seemed like an apparent strategy. The problem is that RAS has an affinity towards GTP in the picomolar range, which makes it virtually impossible to develop a GTP-competitive inhibitor for RAS (Cox et al., 2014). Nevertheless, some studies have shown that it is possible to specifically target and inhibit the mutant $KRAS^{G12C}$ variant. These inhibitors covalently bind the mutated cysteine in the GDP/GTP binding pocket of KRAS and thereby promote GDP instead of GTP binding, which inactivates mutant KRAS (Janes et al., 2018; Lim et al., 2014; Ostrem et al., 2013; Zeng et al., 2017). While these are promising results, they only address a rather rare mutation in KRAS. $KRAS^{G12C}$ mutations make up only 3% in PDACs and 11% in CRCs of all KRAS mutations (Cox et al., 2014). Furthermore, the efficacy has yet to be shown in clinical trials.

Other attempts focused on interfering with RAS localization. In addition to GTP binding, RAS has to be localized at the plasma membrane to be active. Initially, RAS is translated as an inactive, cytosolic protein. At its C-terminus, it has a CAAX site (C =cysteine, A = aliphatic amino acid, X = any amino acid), which directs a post-translational farnesyl moiety to the cysteine via the farnesyltransferase (FTase). The farnesylation allows then for the membrane localization of the otherwise hydrophobic RAS protein (Ahearn et al., 2011). Therefore, inhibition of FTase activity was thought to prevent proper RAS localization and thus inhibit KRAS activity. Initial studies on FTase inhibitors showed promising results in HRAS driven tumors but subsequent clinical trials failed to demonstrate the efficacy of FTase inhibitors in KRAS mutated cancers (Papke and Der, 2017). The reason for the low efficacy is that KRAS and NRAS can - in contrast to HRAS - be alternatively prenylated via geranylgeranylation by the geranylgeranyltransferase (GGTase) in the presence of FTase inhibitors (Whyte et al., 1997). More recently, two small-molecule inhibitors were described that prevent membrane association of KRAS through inhibition of phosphodiesterase δ (PDEδ). PDEδ shuttles prenylated KRAS to the Golgi or endosomes from where its transported to the plasma membrane. The PDEδ inhibitors have been shown to reduce RAS signaling and growth of RAS-mutated cancer cells. On the other hand, PDEδ inhibitors have a similarly high risk of off-target effects as FTase and GGTase inhibitors (Papke and Der, 2017; Papke et al., 2016; Zimmermann et al., 2013). It is estimated that over

100 proteins are prenylated by FTase and GGTase, many of which would also be affected by the inhibition of PDEδ (Lane and Beese, 2006).

Since targeting RAS activity directly has been proven to be problematic, another approach is to target downstream effectors of RAS signaling. While RAS activates several downstream effector pathways, there is evidence that at least in some cancers such as CRC and lung cancer the RAF-MEK-ERK pathway might be the one with the greatest impact (Collisson et al., 2012; Papke and Der, 2017; Ryan et al., 2015). However, the results of MEK inhibition with trametinib and cobimetinib in clinical trials have been underwhelming. MEK inhibition abolishes an inhibitory feedback-loop via activated ERK through RAF. This results in a reactivation of the pathway despite MEK inhibition and thus would require administration of high MEK inhibitor doses that are not applicable in a clinical setting (Duncan et al., 2012; Papke and Der, 2017). A similar problem of paradoxical MAPK activation upon BRAF inhibition has recently been overcome with the development of RAF inhibitors that show efficacy in RAS-driven cancers and do not lead to a MAPK activation (Holderfield et al., 2014; Peng et al., 2015; Zhang et al., 2015). However, another mechanism preventing MAPK signaling inhibition from efficiently preventing cancer cells growth is that cancer cells evade the treatment by activating PI3K signaling. Colorectal cancer cells have been shown to activate AKT upon MEK inhibition. This is mediated via a lack of a negative feedback from ERK to EGFR, which then, in turn, activates the PI3K pathway (Klinger et al., 2013; Prahallad et al., 2012). Unfortunately, blocking both pathways simultaneously has proven to be clinically not practicable mainly due to the high toxicity observed in clinical trials (Papke and Der, 2017). Recently, an inhibitor was published that was suggested to inhibit RAS signaling in several pathways simultaneously. Rigosertib acts as a RAS mimetic that binds and blocks the RAS-binding domain of several downstream effectors such as RAF, PI3K, and RALGDS (Athuluri-Divakar et al., 2016). Another study suggested, however, that the reduction in MAPK signaling by rigosertib was not due to inhibition of RAS-RAF interaction, but is rather an indirect effect of stress-induced JNK activity, followed by inhibition of RAF and SOS1 (Ritt et al., 2016). Rigosertib was also recently identified as a microtubule-destabilizing agent, which might hint towards rigosertib affecting a much broader spectrum of cellular processes, which raises the risk of unwanted side effects (Jost et al., 2017).

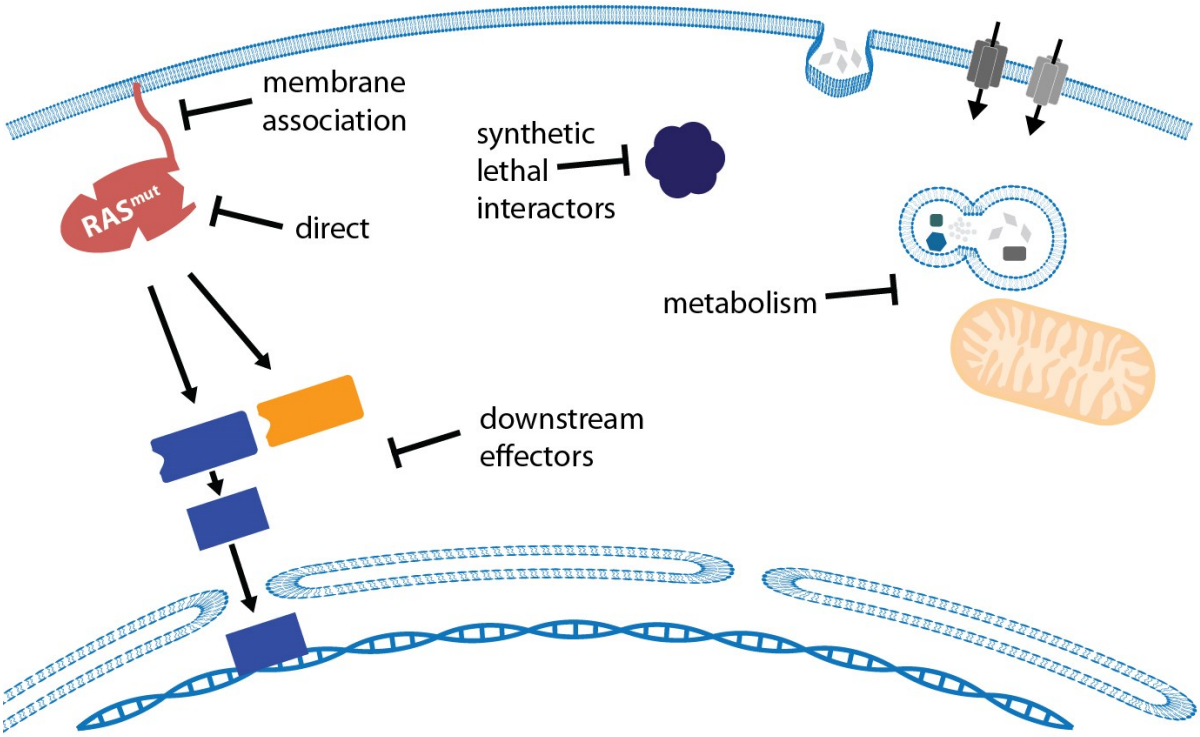

Figure 5: Strategies for drugging oncogenic RAS signaling. Several different strategies for targeting RAS signaling in cancer have been under investigation in the past decades. Next to the straightforward strategies of direct inhibition, inhibition of membrane association, and inhibition of downstream effectors, more indirect strategies are also under consideration. Namely, inhibition of the metabolism and inhibition of synthetic lethal interactors (adapted from Papke and Der, 2017).

Among the many additional cellular downstream effects of mutant KRAS signaling are also metabolic changes. RAS shifts the cellular energy production machinery from oxidative phosphorylation towards glycolysis by upregulating hypoxia-inducible factor 1α (HIF1α) via the MAPK and PI3K pathway. HIF1α leads to the elevated production of glucose transporter 1 (GLUT1) and thereby to increased glucose uptake (Blum et al., 2005; Chen et al., 2001; Flier et al., 1987; Pylayeva-Gupta et al., 2011). Glycolysis is further promoted by RAS through upregulation of several glycolytic enzymes such as 6-phosphofructo-1-kinase and lactate dehydrogenase (Chiaradonna et al., 2006; Kole et al., 1991; Pylayeva-Gupta et al., 2011). Moreover, mutant KRAS has also been shown to rewire the glutamine metabolism away from the TCA cycle towards the reduction of $NADP^+$ to NADPH and the production of pyruvate (Gaglio et al., 2011; Papke and Der, 2017; Son et al., 2013). To further fuel cancer cells, RAS also increases extracellular nutrient uptake by micropinocytosis and recycling of cell components through

autophagy. Several studies indicate that RAS driven cancer cells might rely on these two processes in order manage their metabolic needs (Commisso et al., 2013; Guo et al., 2011; Lock et al., 2011; White, 2013; Yang et al., 2011). Since the approach to target metabolic dependencies of KRAS-mutant cancers is relatively new, there have not been many clinical studies so far. However, some metabolic inhibitors are currently in clinical trials. The unspecific autophagy and micropinocytosis inhibitor chloroquine is currently in clinical trials for PDACs (clinicaltrials.gov, identifier: NCT01506973). Another inhibitor of the glutamine metabolism (CB-839) is also in several clinical trials (Cox et al., 2014; National Institutes of Health (NIH); Papke and Der, 2017).

In summary, targeting mutant RAS in cancer still constitutes a major hurdle up to this day. The broad variety of downstream effects that mutant RAS elicits in cells is only one reason why targeting RAS has proven to be so difficult. The next chapter focuses on another strategy that might allow specific targeting of RAS-mutant cancer cells in a more indirect manner.

1.2.3. Synthetic lethality

Since KRAS has proven to be notoriously hard to be inhibited directly, indirect targeting strategies could be a more promising strategy. An approach to indirectly but specifically target oncogenic KRAS signaling is the concept of synthetic lethality. The term “synthetic lethality” was coined by Theodore Dobzhansky. He observed that in *Drosophila melanogaster* flies that inherited two different deleterious genes were non-viable. In contrast, the parent generation harboring only one of these mutant genes was viable (Dobzhansky, 1946; Nijman, 2011).

The most prominent example for a successful synthetic lethal therapy is the inhibition of poly (ADP-ribose) polymerase (PARP) in Breast Cancer 1/2 (BRCA1/2) defective cancers (Bryant et al., 2005; Farmer et al., 2005). BRCA1 and BRCA2 are tumor suppressors involved in homologous recombination (HR), which is in addition to non-homologous end joining (NHEJ) one of the two major DNA double-strand break (DSB) repair mechanisms. PARP, on the other hand, facilitates DNA single-strand break (SSB) repair by binding SSBs and recruiting other DNA repair proteins to the site of DNA

damage. Inhibition of PARP by olaparib traps it on the DNA. The trapped PARP presents an obstacle for approaching DNA replication forks, which in turn cause replication fork stalling and eventually fork collapse. Collapsed forks can efficiently be repaired via HR, for which BRCA is required. Therefore, BRCA proficient cells survive the perturbation on PARP, whereas BRCA deficient cells accumulate non-repairable DNA damage and eventually die. In 2014, the PARP inhibitor olaparib was approved by the FDA for the treatment of BRCA mutated ovarian cancer (Dziadkowiec et al., 2016). Very recently, it was additionally approved for therapy of BCRA mutant breast cancers (U.S. Food & Drug Administration, 2018).

The idea of using the synthetic lethality approach in KRAS-mutant cancers is very similar: While inhibition or depletion of some proteins is tolerable for normal, non-transformed cells, KRAS mutated cells might heavily rely on the activity or presence of distinct proteins. Therefore, targeting a synthetic lethal interactor of mutant KRAS would specifically kill KRAS transformed cancer cells, while normal cells remain largely unaffected (Figure 6).

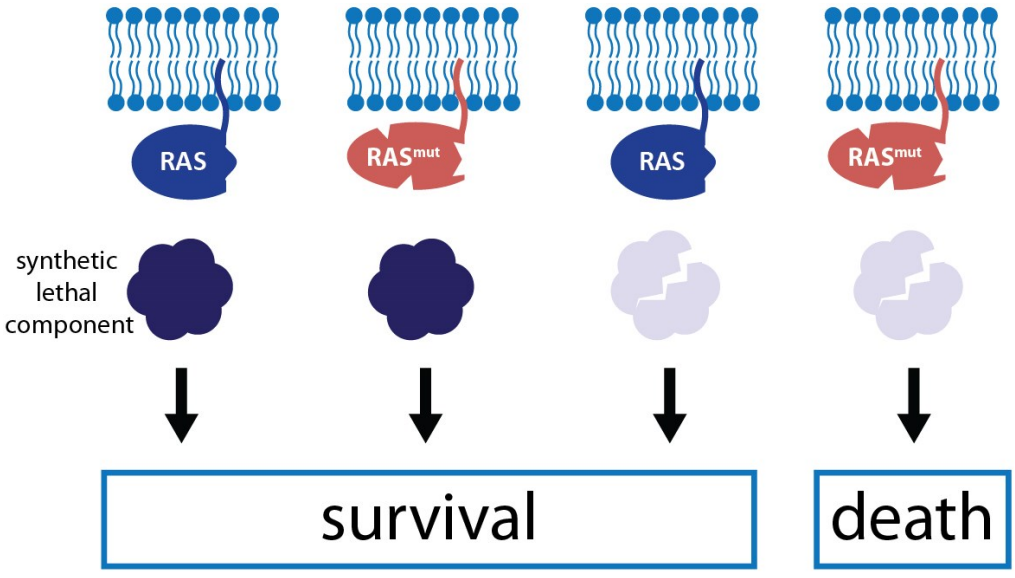

Figure 6: The concept of synthetic lethality. The concept of targeting mutant RAS via synthetic lethal interactors relies on the idea that oncogenic RAS signaling creates specific dependencies on other proteins or pathways for the cell. While these synthetic lethal components are dispensable for RAS wild-type cells, RAS-mutant cells heavily rely on them. Thus, inhibition or depletion of synthetic lethal components is compatible with RAS wild-type cell's survival but lethal for RAS-mutant cells.

RNAi or CRISPR/Cas9 based screens are the current state of the art methodology for identifying synthetic lethal interactors of RAS without prior knowledge or assumptions. Most screens knock down (RNAi screens) or knock out (CRISPR/Cas9 screens) a library of genes in a panel of RAS^{mut} and RAS^{wt} cells, in isogenic cell lines, or a combination of both. While there have been multiple attempts to identify synthetic lethal interactors of mutant RAS, there is only very little overlap in their identified synthetic lethal targets across most screens. Julian Downward reviewed and summarized the results from all RAS focused synthetic lethality screens in 2015. Table 1 shows the summary of Julian Downward's review and additionally other targets that have been identified since then (Downward, 2015). Although the individual genes identified do not show a big overlap between screens, two cellular processes dominate the collective results. For one, several components of the proteasome have been identified across different screens to be synthetic lethal with mutant RAS (Barbie et al., 2009; Luo et al., 2009; Steckel et al., 2012). Independent studies, however, showed poor selectivity of proteasome targeting drugs towards cancer cells with mutated RAS (Barretina et al., 2012; Downward, 2015; Garnett et al., 2012). The other process commonly identified in screens is the regulation of the cell cycle (Costa-Cabral et al., 2016; Luo et al., 2009; Sarthy et al., 2007; Steckel et al., 2012; Wang et al., 2016). The next chapter will thus focus on cell cycle regulation, DNA replication, and how RAS signaling influences those processes.

Table 1: Summary of synthetic lethal targets derived from synthetic lethality screens targeting RAS (adapted and expanded from Downward, 2015).

target(s)	Cell culture model	Screen setup	Reference
RAN, TPX1, SDC1	H1299 $NRAS^{Q61K}$ mutant human lung cancer cells	~3,700 druggable genes, siRNA, multi-well cell death	(Morgan-Lappe et al., 2007)
Survivin	DLD-1 $KRAS^{G13D}$ isogenic colon cancer cell lines	~4,000 druggable genes, siRNA, multi-well cell death	(Sarthy et al., 2007)
PLK1, APC/C, proteasome	DLD-1 and HCT116 $KRAS^{G13D}$ isogenic colon cancer cell lines	Whole-genome retroviral shRNA library, pooled proliferation screen microarray readout	(Luo et al., 2009)
STK33, AKT3, DGKZ	Panel of 4 KRAS-mutant and 4 wild-type pan-cancer cell lines, plus 2 normal cell lines	~1,000 druggable genes, lentiviral shRNA, multi-well proliferation	(Scholl et al., 2009)

TBK1, PSKH2, PSMD14, PTCH2	Human pan-cancer cell line panel	~1,000 druggable genes, lentiviral shRNA, multi-well proliferation	(Barbie et al., 2009)
WT1	Mouse lung cancer cells LKR10 and LKR13 $Kras^{G12D}$	162 KRAS relevant genes, shRNA pooled screen *in vivo*, bead array readout	(Vicent et al., 2010)
SNAI2	HCT116 isogenic colon cancer cell lines	~2,500 druggable genes, retroviral shRNA pooled proliferation screen, microarray readout	(Wang et al., 2010)
GATA2, CDC6, proteasome	HCT116 isogenic colon cancer cells and pan-cancer 26 cell line panel	~8,000 genes siRNA, multi-well cell proliferation and apoptosis	(Kumar et al., 2012; Steckel et al., 2012)
TAK1	$SW620^{G12V}$ KRAS and $SW837^{G12C}$ KRAS human colon cancer cell lines	Lentiviral shRNA screen with 17 selected kinases, multi-well proliferation	(Singh et al., 2012)
BCL-X_L	KRAS-mutant colon cancer cell lines HCT116 and SW620	~1,200 druggable genes, shRNA, pooled NGS readout, synergistic death with MEK inhibitor	(Corcoran et al., 2013)
Ctnnb1, Mllt6	$Hras^{G12V}$–mutant mouse keratinocytes in vivo	Whole-genome lentiviral shRNA library, pooled *in vivo* proliferation screen NGS readout	(Beronja et al., 2013)
COPI coatomer	KRAS plus LKB1-mutant lung cancer 17–cell line panel	Whole-genome siRNA, multi-well cell proliferation	(Kim et al., 2013)
ARHGEF2	Human pan-cancer 72–cell line panel	Whole-genome lentiviral shRNA library, pooled proliferation screen NGS readout	(Cullis et al., 2014)
CDK1	Isogenic LIM1215 colorectal cancer cell line and 26-cell line panel	784 genes, multi-well proliferation	(Costa-Cabral et al., 2016)
combined PLK1 and ROCK inhibition	Isogenic T29 ovarian surface epithelial cells +/- $KRAS^{G12V}$	20 drugs in pairs (190 combinations), multi-well proliferation	(Wang et al., 2016)
XPO1	12 non-small-cell lung cancer cell lines	genome-wide siRNA screen, multi-well proliferation	(Kim et al., 2016)
PREX1 (Rac pathway)	14 human acute myeloid leukemia cell lines	genome-wide viral CRISPR screen, pooled proliferation screen NGS readout	(Wang et al., 2017)
Mitochondrial translation	Isogenic HT116 and DLD-1 colorectal cancer cell lines	genome-wide lentiviral CRISPR screen, pooled proliferation screen NGS readout	(Martin et al., 2017)

1.3. Cell cycle, DNA replication, and stress

All proliferating cells go through a tightly regulated series of events in their goal of faithful DNA replication and cell division called the cell cycle. The cell cycle can be subdivided into four different phases: G1, S, G2, M. The “G” in G1 and G2 stands for “gap” since these are the cell states between DNA synthesis (S) and mitotic cell division (M). Cells that have ceased to proliferate remain in a similar state as cells in G1 referred to as G0 (Schafer, 1998). The transitions between the cell cycle phases are controlled by cyclins and cyclin-dependent kinases (CDKs). There are four different CDKs (CDK1, CDK2, CDK4, and CDK6) and four classes of cyclins (cyclin A, B, D, and E). As their names suggest, the activity of CDKs relies on binding of cyclins, whose expression cycle between specific cell cycle phases (Malumbres and Barbacid, 2009). Interestingly, only the mitotic CDK1 seems to be essential for the mammalian cell cycle, whereas the interphase CDKs (CDK2, CDK4, and CDK6) are largely dispensable and merely lead to defects in some specialized cell types (Barrière et al., 2007; Berthet et al., 2003; Diril et al., 2012; Malumbres and Barbacid, 2009; Malumbres et al., 2004; Ortega et al., 2003; Santamaría et al., 2007; Tsutsui et al., 1999). For example, simultaneous knockout of CDK2 and CDK4 results in a normal embryogenesis in mice. However, they die shortly after birth due to cardiological complication. In contrast, if CDK2 is conditionally knocked out after birth in a $CDK4^{-/-}$ background, mice show no observable phenotype (Barrière et al., 2007). An additional layer of cell cycle control in response to DNA damage are the cell cycle checkpoints. They are mainly executed through the two checkpoint kinases CHK1 and CHK2. Canonically, CHK1 is activated by ATR upon replication stress and is required for a robust G2/M arrest. CHK2, on the other hand, is activated by ATM upon DNA damage such as DSB and is primarily implicated in the G1/S arrest. However, these activation schemes have been challenged, since ATM has been shown to be able to activate CHK1. In addition, ATM-independent activations of CHK2 have been reported (Bartek and Lukas, 2003; Kastan and Bartek, 2004). Figure 7 shows a summary of the cell cycle regulation.

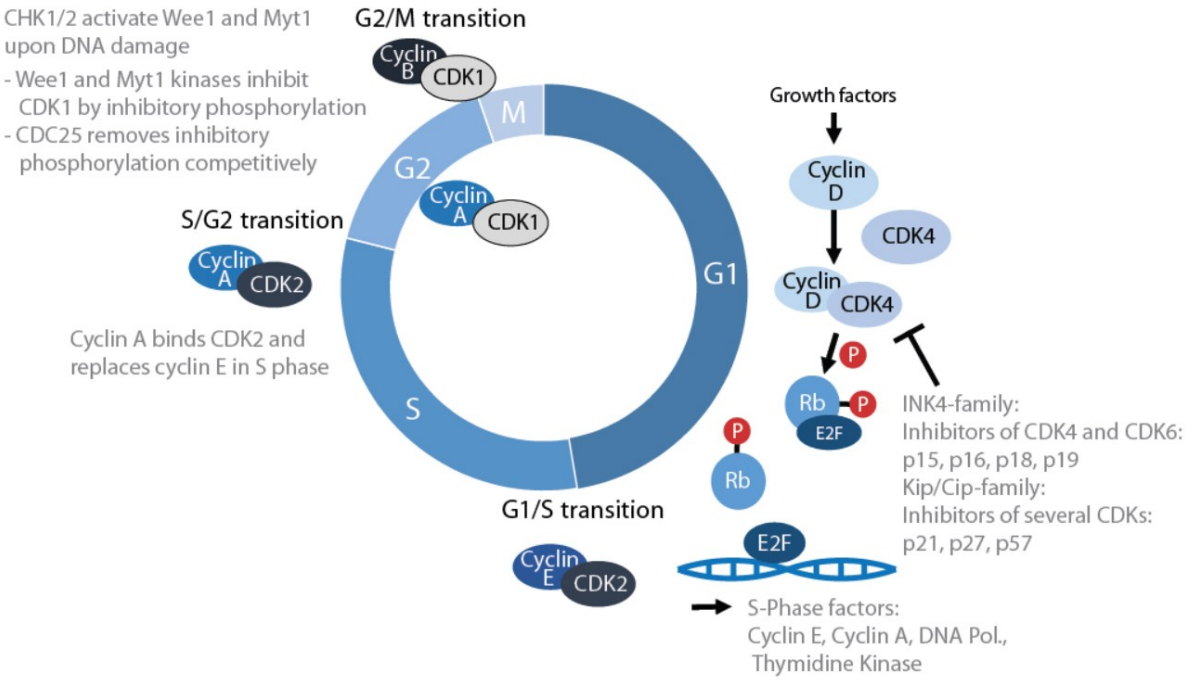

Figure 7: Regulation of the cell cycle. The different cell cycle phases are regulated by the expression of different cyclins and their binding to cyclin-dependent kinases (CDKs). Furthermore, several other regulators like the INK4-family and Kip/Cip-family proteins play a role in the G1/S transition, as well as WEE1, MYT1, and CDC25 in the G2/M transition (Malumbres and Barbacid, 2009).

1.3.1. DNA replication licensing and initiation by the MCM complex

The tight regulation of the cell cycle is a prerequisite for a complete and accurate duplication of the genome throughout the lifetime of each cell. One of the key players ensuring complete replication is the replicative helicase Minichromosome Maintenance protein complex (MCM). It is a hexameric complex, which consists of the six related proteins MCM2-7. To control DNA replication, the cell utilizes the MCM complex in a two-step process throughout the cell cycle (Deegan and Diffley, 2016).

First, MCM is recruited as a double hexamer to the origins of replication in a process called DNA replication licensing (Evrin et al., 2009; Gambus et al., 2011; Remus et al., 2009). To recruit MCM to the origins of replication, the origin recognition complex (ORC) first binds the origins of replication, which are spread throughout the genome. Then CDC6 can be recruited to the ORC. Recruitment of CDC6 creates a binding hub for CDT1, which is bound to the MCM complex and thereby recruits MCM to the origins

of replication. Upon binding of the first MCM complex, a second CDT1-MCM complex is recruited under involvement of a second CDC6 forming the pre-replication complex (pre-RC) (Figure 8) (Deegan and Diffley, 2016; Evrin et al., 2009; Gambus et al., 2011). To prevent re-replication of the same genomic areas, DNA licensing is strictly limited to late mitosis and G1. This is mainly accomplished by the expression of CDT1 inhibitor geminin from S-phase to mid of mitosis, thereby effectively preventing replication licensing during replicative states of the cell cycle (Klotz-Noack et al., 2012; Nishitani and Lygerou, 2002).

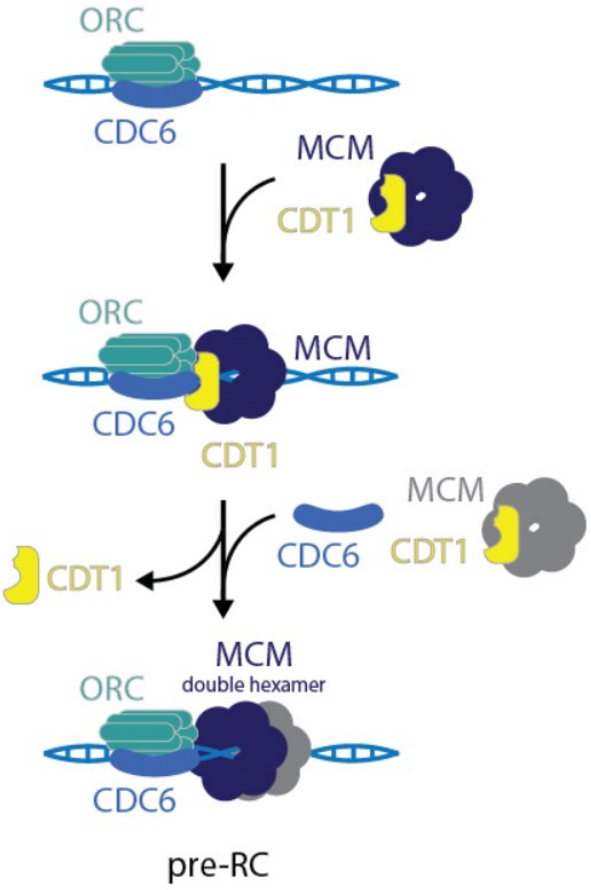

Figure 8: Mechanism of replication origin loading. Loading of the MCM complex is a stepwise process. First ORC binds DNA at origins of replication and recruits CDC6. Then CDT1 can recruit the MCM complex to the ORC and CDC6 bound sites. To obtain the necessary MCM double-hexamer, two different CDC6 and CDT1 proteins are required to load the second MCM complex onto the DNA and thereby form the final pre-replication complex (pre-RC) (adapted from Deegan and Diffley, 2016).

Upon S-phase entry, the pre-RC complex undergoes further modifications to initiate the second step: DNA replication. While the exact mechanism of DNA replication initiation

is not fully understood, it is clear that it is a multi-step process, of which the order of the steps is yet to be determined. Several replication factors have to bind and remodel the two MCM complexes. The two kinases cyclin-dependent kinase (CDK) and Dbf4-dependent kinase CDC7 (DDK) play a crucial role in the remodeling of the MCM double-hexamer. DDK phosphorylates MCM, which promotes the recruitment of SLD3/7 and CDC45. CDK also phosphorylates SLD2 and SLD3. This facilitates the binding of SLD2/3 to DPB11, which subsequently leads to the recruitment of GINS to MCM. The recruitment of CDC45 and GINS to both MCM complexes creates the active CMG (CDC45-MCM-GINS) helicases and is essential for the assembly of the complete replisome later on (Deegan and Diffley, 2016; Heller et al., 2011; Yeeles et al., 2015). The segregation of the two CMG helicases and assembly of the complete replisome leads then to the start of two replication forks per origin in a process called origin firing (Deegan and Diffley, 2016; Gambus et al., 2006; Ilves et al., 2010; Moyer et al., 2006). Thereby, the two MCM complexes unwind the DNA in both directions and provide a single-stranded DNA template for the DNA polymerase (Bochman and Schwacha, 2008, 2009) (Figure 9). As soon as two replication forks converge, MCM7 is polyubiquitinated by SCF^{Dia2} (in yeast) which causes the subsequent CMG removal by Cdc48/p97 (Deegan and Diffley, 2016; Dewar et al., 2015; Labib et al., 2000; Maculins et al., 2015).

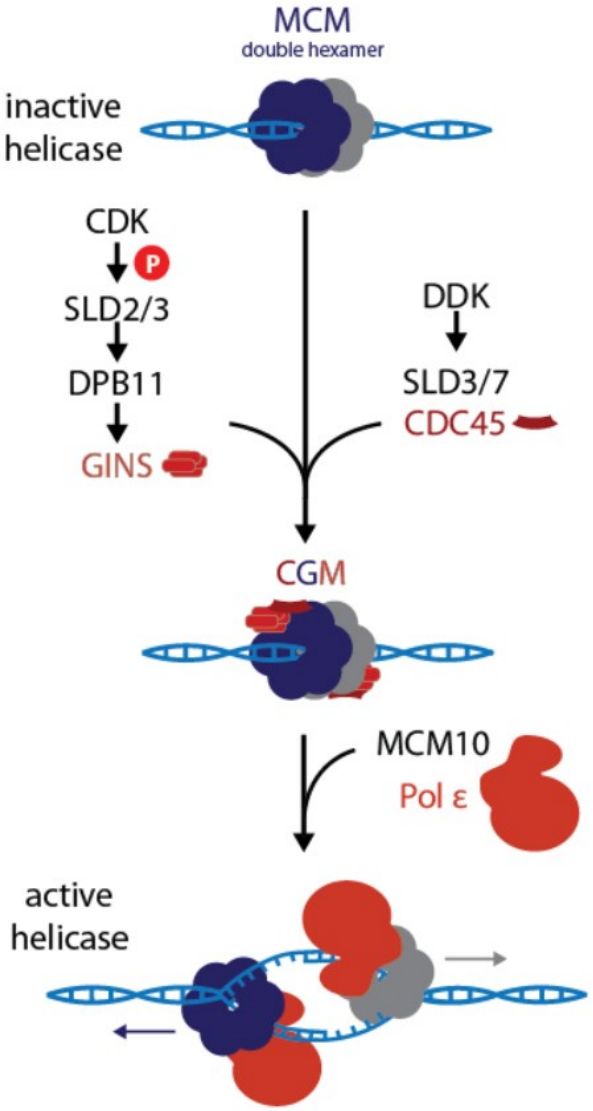

Figure 9: Assembly of the active helicase during replication origin firing. To initiate DNA replication cyclin-dependent kinase (CDK) and the Dbf4-dependent kinase CDC7 (DDK) remodel the pre-RC, which facilitates the recruitment of GINS and CDC45 to the MCM complex. Thereby, the active replicative CGM helicase is formed. Subsequently, MCM10 and DNA polymerase ε are recruited to facilitate DNA replication (adapted from Deegan and Diffley, 2016).

Interestingly, only a small fraction of the licensed origins (~10%) is used during unperturbed replication. The vast majority of licensed origins remain dormant during S phase and serve as a back-up to resolve perturbations such as stalled replication forks (Burkhart et al., 1995; Mahbubani et al., 1997; McIntosh and Blow, 2012; Wong et al., 2011).

Since the MCM complex plays a central role in DNA replication, it is also a crucial player in cancer cell proliferation. Several MCM subunits have been shown to be amplified in a variety of cancers including pancreatic cancer (MCM4 4-5%, MCM7 5-20%), breast cancer (MCM4 7%, MCM7 2.3%), and colorectal cancer (MCM4 4%, MCM7 2.3%) (Cerami et al., 2012; Ciriello et al., 2015; TCGA provisional; Witkiewicz et al., 2015). Additionally, MCM2 over-expression has been suggested to be a marker for the diagnosis of cervical cancer (Zheng, 2015). Additionally, MCM7 was proposed to be a prognostic marker for hepatocellular carcinoma (Qu et al., 2017) and prostate cancer (Padmanabhan et al., 2004; Ren et al., 2006).

1.3.2. RAS and replication stress

Oncogenes and their ability to drive abnormal proliferation are closely related to the regulation of DNA replication. The term replication stress is not well defined but can be understood as a collective term for perturbations of DNA replication that eventually lead to slowing or stalling of replication forks. A hallmark of replication stress are stretches of unreplicated, single-stranded DNA. The main source for this is double-stranded DNA that is unwound by the MCM complex but because following DNA replication machinery is stalled, two unwound single strands of DNA are left behind (Zou et al., 2000). The RPA complex binds this single-stranded DNA and thereby serves as a sensor for replication stress (Zeman and Cimprich, 2014; Zou and Elledge, 2003). Expression of oncogenic RAS proteins has previously been implicated in causing replication stress (Hills and Diffley, 2014). A term that is commonly used to describe replication stress caused by oncogenes, such as RAS, is oncogene-induced genotoxic stress (Dietlein et al., 2015; Grabocka et al., 2014, 2015). It is an elegantly simple term that masks the complexity of the many distinct mechanisms by which mutated RAS can disturb DNA replication and cause replicative stress.

For one, expression of mutant HRAS and NRAS have been reported to diminish the cellular nucleotide pool, whose depletion is a known cause of replication stress and genomic instability. The depletion is caused by RAS dependent downregulation of ribonucleotide reductase and thymidylate synthase - both crucial enzymes in the

nucleotide synthesis. Since a constant supply of nucleotides is essential for DNA synthesis, deoxyribose nucleoside triphosphate (dNTP) depletion can cause replication fork slowing or stalling (Aird et al., 2013; Bester et al., 2011; Mannava et al., 2013; Zeman and Cimprich, 2014).

RAS also targets the nucleotide pool via another mechanism: reactive oxygen species (ROS). It is well established that expression of oncogenic RAS increases cellular ROS levels (Irani et al., 1997; Lee et al., 1999; Ogrunc et al., 2014). While it seems to be clear that mutant RAS expression causes an increase in ROS, the source of ROS is still being discussed. Accumulation of ROS is assumed to be due to an upregulation of the mitochondrial NADPH oxidases NOX1 and NOX4 upon RAS expression (Mitsushita et al., 2004; Ogrunc et al., 2014; Weyemi et al., 2012). However, other results suggest that the ROS source is mitochondria independent (Maya-Mendoza et al., 2015). Increased cellular ROS levels indirectly impede replication fork progression by oxidating DNA and dNTPs, most prominently the oxidation of GTP to 8-oxo-dGTP, which perturbs replication fork progression (Rai et al., 2009).

An increase in transcription has also been discussed as a cause for RAS driven replication stress. Transcription can cause interference with DNA replication when transcription machineries collide with oncoming replication forks. As one study showed, overexpression of RAS causes a global increase of transcription and leads to replication fork slowing, which could be partially rescued by inhibition of RNA transcription (Kotsantis et al., 2016). Additionally, nascent RNA can become a hurdle for DNA replication by incorrectly forming a three-stranded RNA/DNA-hybrid – a so-called R-loop (Zeman and Cimprich, 2014).

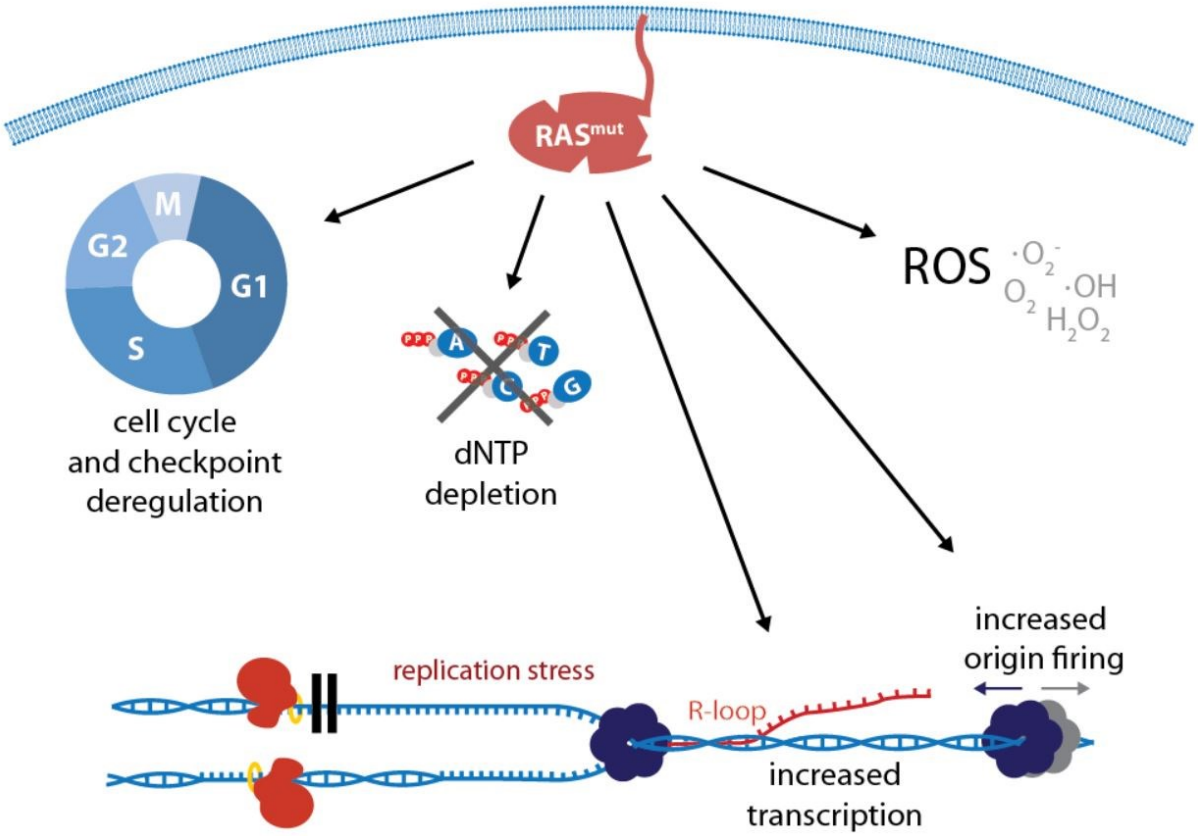

Figure 10: Sources of RAS-driven replication stress. Oncogenic RAS can cause replication stress via multiple mechanisms including deregulation of cell cycle checkpoints, dNTP depletion, generation of reactive oxygen species, R-loop formation via increased transcription, and increased replication origin firing.

Overexpression of HRAS has also been shown to cause increased replication origin firing (Di Micco et al., 2006). As mentioned in the last chapter, dormant origins are needed as a fail-safe mechanism in the case of perturbations during DNA synthesis. Increased origin firing could lead to stalled replication forks that cannot be resolved due to the lack of remaining adjacent dormant origins. However, the exact mechanism of how mutant RAS promotes origin firing is not fully understood.

Lastly, RAS has a well-established impact on the regulation of the cell cycle. RAS driven overexpression of cyclin D has been linked to triggering S-phase entry via retinoblastoma (Rb) phosphorylation (Figure 7) and thereby reduces the duration of the G1 phase (Filmus et al., 1994; Hitomi and Stacey, 1999; Liu et al., 1995). Since DNA replication licensing takes place primarily in G1, a shortened G1 phase can lead to an S-phase entry with an under-licensed genome and thereby cause replication stress.

Additionally, mutant RAS has been shown to interfere with the G2/M checkpoint and cause premature entry into mitosis (Grabocka et al., 2014; Knauf et al., 2006).

In summary, RAS causes oncogene-induced replication stress via diverse mechanisms (Figure 10). The so-called "genotoxic stress" inflicted by RAS is probably the result of a combination of several of the factors discussed above. However, which of these mechanisms is most decisive and if this is cell type-dependent has yet to be determined.

1.4. Aims and objectives

Despite enormous efforts that have been undertaken to disrupt the RAS pathway since its discovery, no targeted therapy for RAS-mutant cancers has successfully made its way to the clinic, yet (Cox et al., 2014; Malumbres and Barbacid, 2003; Papke and Der, 2017). Therefore, the purpose of this thesis is to identify novel synthetic lethal interactors with oncogenic KRAS in colorectal cancer cells. To find synthetic lethal interactions, a CaCo2 cell culture model with doxycycline (DOX) inducible expression of $KRAS^{G12V}$ will first be characterized to assess its suitability as an isogenic KRAS cell culture model for further investigations. Next, the transgenic cell line will be used as a model system in an RNAi-based screen to identify genes that are essential for proliferation and survival with oncogenic KRAS signaling (+DOX) yet are dispensable in the absence of mutant KRAS (-DOX). To this end, the cells will be transfected with a custom designed short hairpin RNA (shRNA) library consisting of 625 shRNAs targeting 121 genes (Table A 1), which were previously shown to be highly regulated upon MEK inhibition (Jürchott et al., 2010). The screening results will then be verified using functional growth assays. Subsequently, the mechanism behind the synthetic lethal interaction of the most promising target will be further investigated.

2. Results

2.1. Characterization of the KRAS^{G12V} inducible CaCo2 cell line

CaCo2 cells with DOX-inducible KRAS^{G12V} were chosen as a model for cancer cells harboring oncogenic KRAS mutations. CaCo2 are colorectal cancer cells that retained their epithelial-like growth. A genetic characterization of CaCo2 was performed by Ahmed and colleagues in 2013, in which they described CaCo2 as microsatellite stable (MSS) and CIN^{+} (chromosomal instability). They are furthermore wild-type for KRAS and important downstream effectors such as BRAF, PIK3CA, and PTEN. They do, however, harbor a TP53^{E204X} nonsense mutation (Ahmed et al., 2013). To test how efficiently KRAS^{G12V} expression could be induced in the CaCo2 model, doxycycline was added to the cells for 1-3 days and KRAS protein expression, as well as downstream activation of ERK1/2, was analyzed. In contrast to many conditional expression systems, induced KRAS^{G12V} expression in this CaCo2 model system remained at around two-fold compared to the endogenous KRAS expression instead of being highly overexpressed. Yet, expression of mutant KRAS^{G12V} at low levels led to a potent phosphorylation and activation of ERK1/2 (Figure 11).

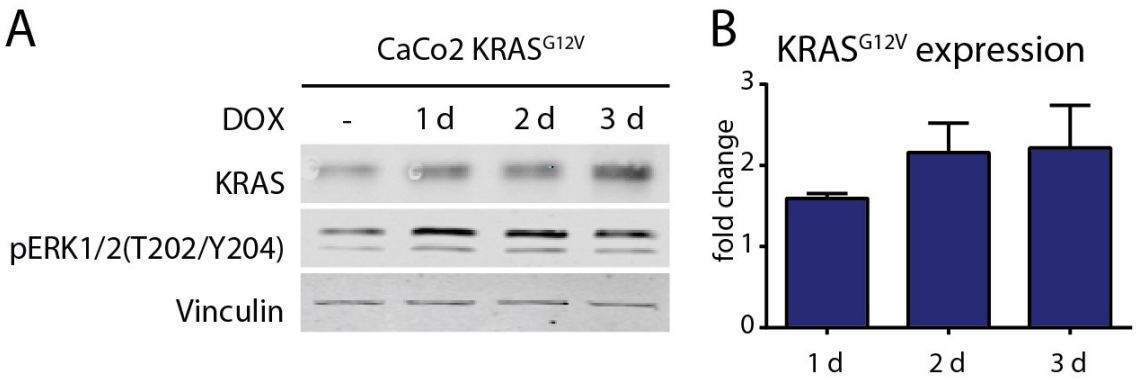

Figure 11: Doxycycline inducible KRAS^{G12V} expression level in CaCo2 cells over time. (A) Western blot of KRAS^{G12V} induced CaCo2 cells shows overexpression of KRAS and increased ERK1/2 phosphorylation after 1-3 days. Vinculin served as a loading control. (B) Quantification of total KRAS protein expression from 1-3 days. Mean fold change ± SEM is shown (n=2-3).

Since ectopic expression of RAS is often associated with reduced proliferation due to oncogene-induced senescence (Dimauro and David, 2010; Kilbey et al., 2008), the

growth of KRAS^{G12V} expressing CaCo2 cells was compared to cells with an empty vector control (vector) using live cell imaging. Interestingly, there was no difference in growth observed upon expression of oncogenic KRAS over the course of one week (Figure 12).

Taken together, the CaCo2 cell culture model provided a suitable platform to investigate characteristics of mutant KRAS in an otherwise isogenic background.

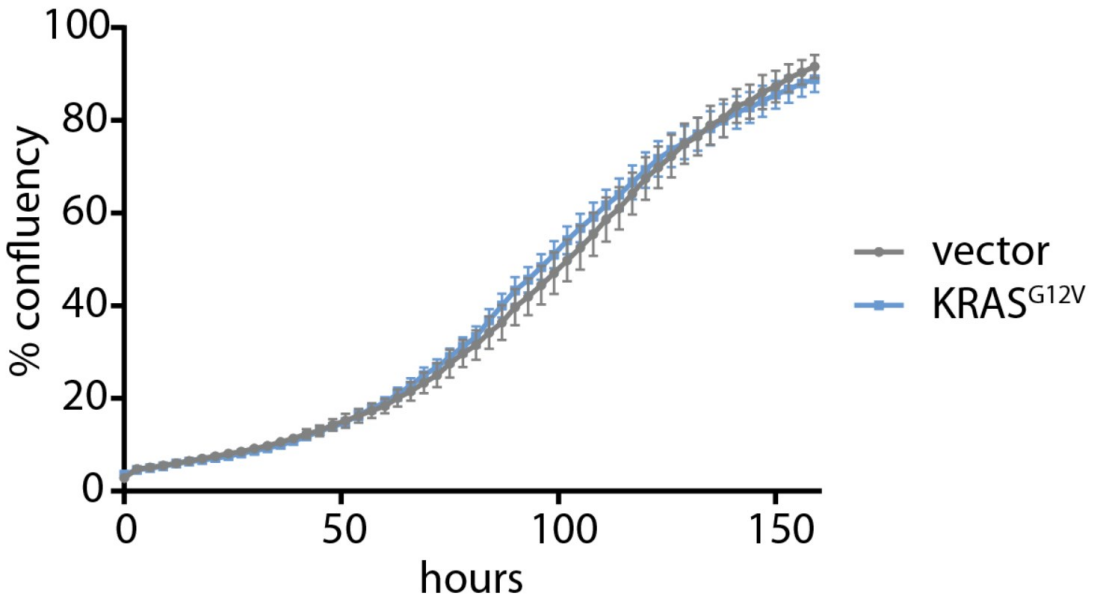

Figure 12: Representative growth curve of CaCo2 cells after KRAS^{G12V} induction. No difference in growth with or without KRAS^{G12V} expression was observed over a period of approx. one week. (n=6 technical replicates; error bars=SEM).

2.2. RNAi screen

To identify new synthetic lethal interactors of oncogenic KRAS, an RNAi-based proliferation screen was performed over a total of 21 days. Figure 13 shows a schematic outline of the screen.

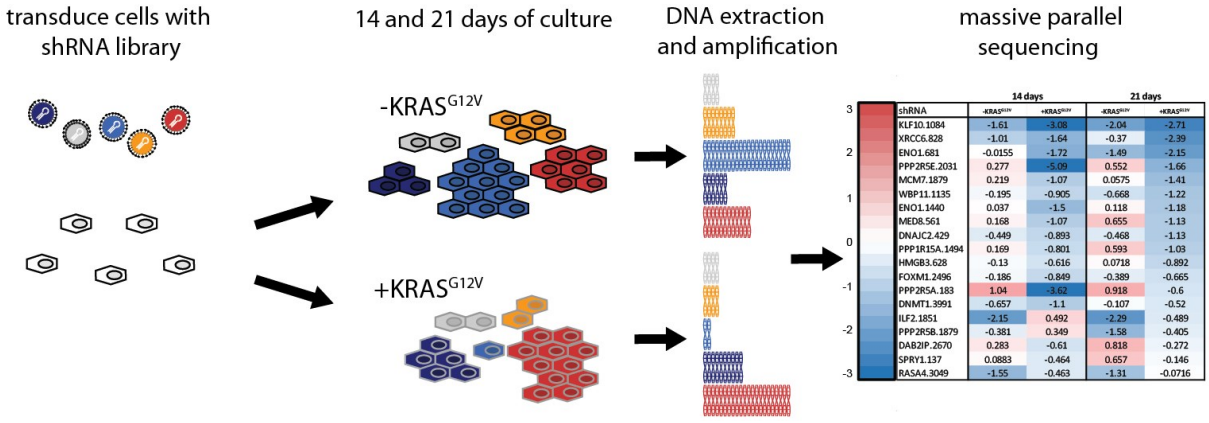

Figure 13: Outline of the RNAi screen. CaCo2 cells with doxycycline-inducible KRAS^{G12V} expression were transduced with an shRNA library by retroviral transduction. After 3 days of selection, a control sample was taken. The remaining cells were split into two populations and KRAS^{G12V} expression was induced in one of the two populations. After each 14 and 21 days of culture, a sample was taken. Subsequently, the genomic DNA, which contained the respective shRNA cassette, was isolated and the integrated shRNA cassettes were PCR amplified. The amplified cassettes were then sequenced via massive parallel sequencing.

First, CaCo2 cells harboring a doxycycline-inducible KRAS^{G12V} were transduced with a retroviral shRNA library targeting 121 genes, previously shown to be highly regulated upon MEK inhibition, using a retroviral transfection system. To avoid multiple transductions of a single cell, a transduction efficiency of less than 20% was aimed at. Three days after transduction the baseline control sample was taken and a transduction efficiency of 16.5% was observed (Figure 14). The cell population was then split into two populations and cultured with or without KRAS^{G12V} induction, respectively. After 14 and 21 more days of culture, the shRNA expressing cells (mCherry^{+}) were sorted and a sample was taken from the -KRAS^{G12V} and the +KRAS^{G12V} populations. At the end of the screening period of 21 days, the amount of shRNA

expressing cells in the two populations had increased from 16.5% to 70.0% (-KRAS^{G12V}) and 77.6% (+KRAS^{G12V}), respectively (Figure 14).

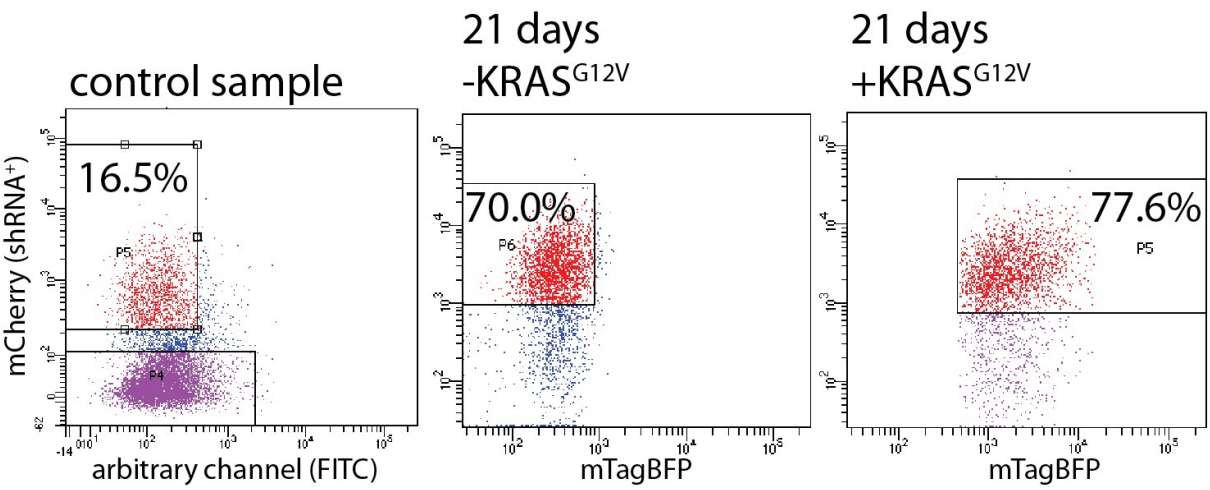

Figure 14: Fluorescence-activated cell sorting (FACS) of CaCo2 cells after transduction of the retroviral shRNA library. After 3 days of G418 selection, 16.5% of the cells constitutively expressed an shRNA (mCherry$^+$). An arbitrary channel (FITC), which presents no further information, was used for the x-axis. After 21 days, 77.6% of KRAS^{G12V} induced cells and 70.0% of uninduced cells expressed an shRNA construct (mCherry$^+$). To monitor the induction of KRAS^{G12V}, mTagBFP was used as a fluorescent reporter protein. Thus, cells exhibited an increased mTagBFP intensity upon KRAS^{G12V} induction.

After that, genomic DNA of all samples was isolated and the stably integrated shRNA cassettes were amplified via PCR. The relative abundance of each shRNA in both populations was determined by massive parallel sequencing. As a measurement of sequencing quality, the reads per shRNA were compared across all samples including the input library. All samples showed a median read count of over 15,000 reads/shRNA. In detail, the input library displayed 15,548 reads/shRNA and the control sample 17,084 reads/shRNA. The -KRAS^{G12V} samples exhibited medians of 16,333 reads/shRNA after 14 days and 16,029 reads/shRNA after 21 days. The KRAS^{G12V} induced samples displayed medians of 15,529 reads/shRNA after 14 days and 15,838 reads/shRNA after 21 days. Overall, the distribution of the reads/shRNA were highly similar across all samples (Figure 15).

Processing of the raw sequencing data as well as quality control was performed by Dr. Bertram Klinger, Institute of Pathology, Charité and IRI Life Sciences, Humboldt-University.

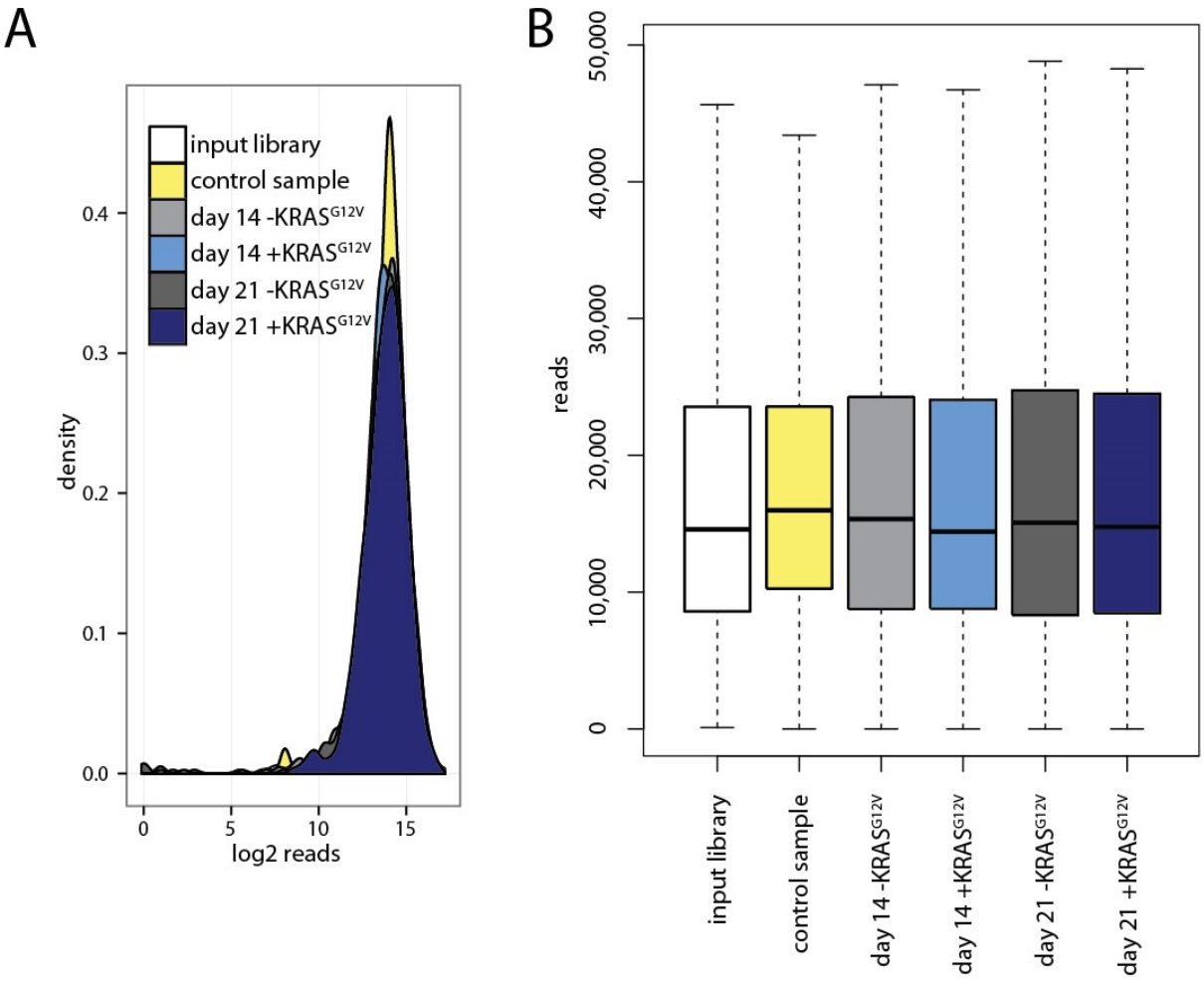

Figure 15: Distributions of number of reads after massive parallel sequencing as an indicator for sequencing quality. (A) Histogram of the sequencing reads (log_2) of all shRNA cassettes showed a highly similar distribution across all samples with a median of about 16,000 reads/shRNA. (B) The same data represented as boxplots showed comparable distributions of reads/shRNA across all samples (outliers excluded).

2.2.1. RNAi screen results

To identify potentially interesting targets from all screened shRNAs, the list of enriched and depleted shRNAs in both populations (+/- $KRAS^{G12V}$) compared to the control sample (Table A 2) was manually evaluated. shRNAs were picked for further

investigation if they showed a consistent difference in enrichment or depletion at both time points. Of all 625 shRNAs, 18 shRNAs showed a consistent change in abundance in a $KRAS^{G12V}$ dependent manner after 14 and 21 days, namely XRCC6.828, ENO1.681, PPP2R5E.2031, MCM7.1879, WBP11.1135, ENO1.1440, MED8.561, DNAJC2.429, PPP1R15A.1494, HMGB3.628, FOXM1.2496, PPP2R5A.183, DNMT1.3991, ILF2.1851, PPP2R5B.1879, DAB2IP.2670, SPRY1.137, RASA4.3049. Therein, only one gene was targeted by two independent shRNAs (ENO1) (Table 2, Figure 16). All of these 18 shRNAs that showed a consistent $KRAS^{G12V}$ dependent change in abundance were selected for further validation. Interestingly, only four shRNAs showed a consistent suppression of more than two-fold across all samples and time points, suggesting $KRAS^{G12V}$ independent lethality (ZNF207.1051, KLF10.1084, SRF.901, and ETV5.390) (Table A 2). One of these lethal targets (KLF10) was selected for further verification. In contrast, not a single shRNA in the screen showed an enrichment of more than two-fold across both samples and time points. Table 2 summarizes the shRNAs that were selected for further validation including their respective log_2 fold change +/- $KRAS^{G12V}$ compared to the control sample.

Table 2: List of selected shRNAs targeting 18 genes for further verification. Values indicate the log_2 fold change of shRNA abundance compared to the control sample after massive parallel sequencing. (blue = depletion; red = enrichment).

	14 days		21 days	
shRNA	**-$KRAS^{G12V}$**	**+ $KRAS^{G12V}$**	**- $KRAS^{G12V}$**	**+ $KRAS^{G12V}$**
KLF10.1084	-1.61	-3.08	-2.04	-2.71
XRCC6.828	-1.01	-1.64	-0.37	-2.39
ENO1.681	-0.02	-1.72	-1.49	-2.15
PPP2R5E.2031	0.28	-5.09	0.55	-1.66
MCM7.1879	0.22	-1.07	0.06	-1.41
WBP11.1135	-0.20	-0.91	-0.67	-1.22
ENO1.1440	0.04	-1.5	0.12	-1.18
MED8.561	0.17	-1.07	0.66	-1.13
DNAJC2.429	-0.45	-0.89	-0.47	-1.13
PPP1R15A.1494	0.17	-0.80	0.59	-1.03
HMGB3.628	-0.13	-0.62	0.07	-0.89
FOXM1.2496	-0.19	-0.85	-0.39	-0.67
PPP2R5A.183	1.04	-3.62	0.92	-0.60

DNMT1.3991	-0.66	-1.10	-0.11	-0.52
ILF2.1851	-2.15	0.49	-2.29	-0.49
PPP2R5B.1879	-0.38	0.35	-1.58	-0.41
DAB2IP.2670	0.28	-0.61	0.82	-0.27
SPRY1.137	0.09	-0.46	0.66	-0.15
RASA4.3049	-1.55	-0.46	-1.31	-0.07

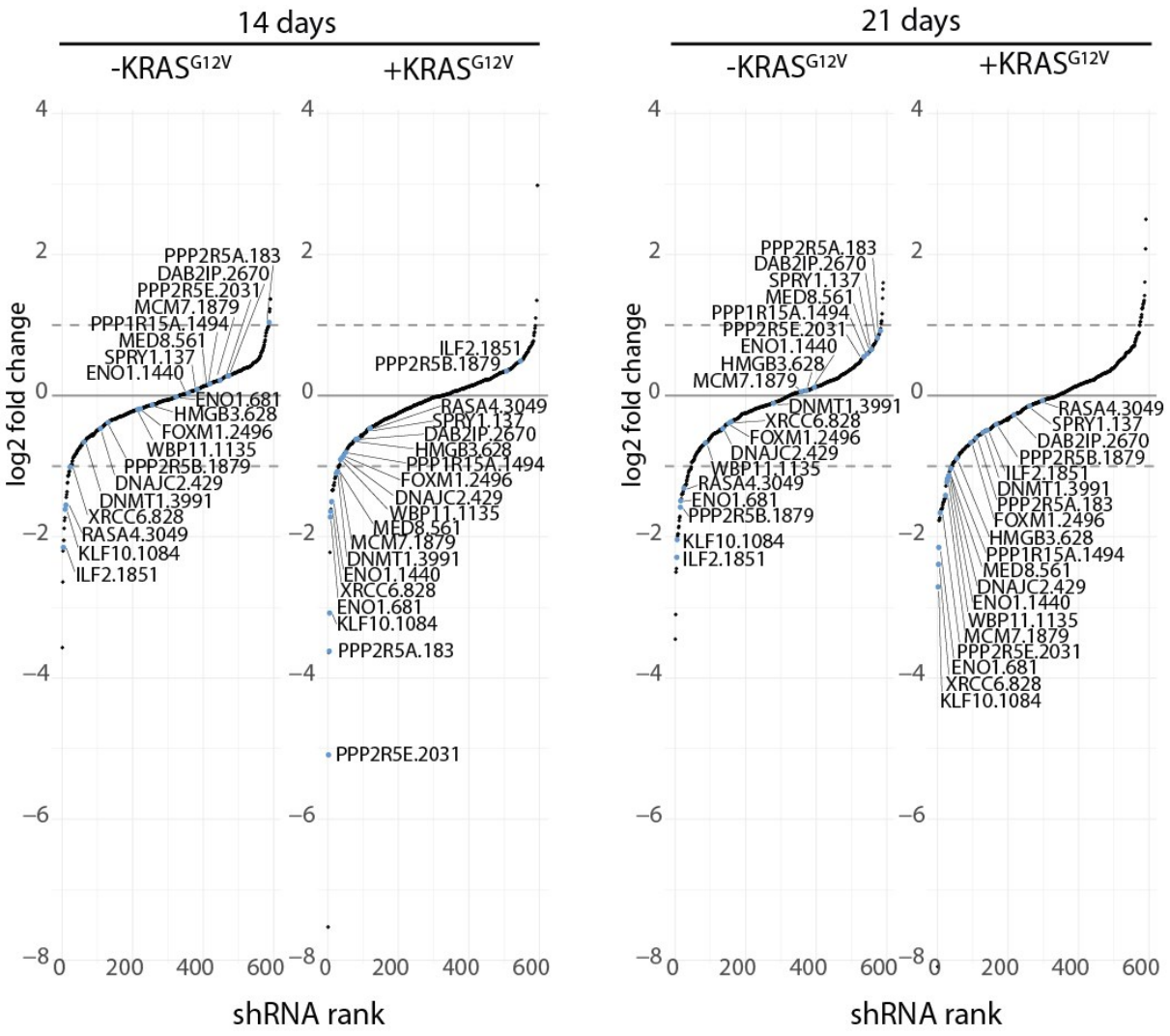

Figure 16: Ranked shRNAs or RNAi screen after 14 and 21 days. All shRNAs were ranked according to their change in abundance compared to the control sample and plotted according to their rank and $\log_2$ fold-change. Selected shRNAs for further verification are annotated and marked in blue.

2.2.2. Target validation

To validate the results obtained from the RNAi screen, all selected shRNAs (Table 2) were cloned into a doxycycline-inducible expression vector (p425, Table 15). For eight targets, one to two additional independent shRNAs were introduced. Furthermore, a scrambled shRNA (scrbl) was used as a control. The DOX-inducible knockdown constructs were then transduced into CaCo2 cells with either DOX-inducible $KRAS^{G12V}$ or an empty vector control via a retroviral delivery system. To investigate the effect of each shRNA on cell growth, the transduced cells were plated at low density and cultured for 10–13 days with or without doxycycline addition. Subsequently, the colonies were stained with methylene blue and their confluency was assessed using CellProfiler v2.2.0 (http://cellprofiler.org/) (Carpenter et al., 2006) (Figure 17 A). The outcome of the screen validation is depicted in Figure 17B. Half of the 18 investigated genes did not lead to any substantial alteration in growth upon knockdown (DAB2IP, DNMT1, FOXM1, XRCC6, HMBG3, PPP1R15A, PPP2R5B, PPP2R5E, and RASA4). KLF10.1084, which was identified in the screen to be essential independently of $KRAS^{G12V}$, did not show any lethality upon closer investigation. In contrast, the shRNA targeting MED8 caused strong lethality in the control cells as well as the $KRAS^{G12V}$ expressing cells. Knockdown of only four genes showed a similar pattern as predicted by the screen (MCM7, DNAJC2, PPP2R5A, and SPRY1). SPRY1.137 caused a $KRAS^{G12V}$ specific growth reduction of about 28%, however, it also led to a noticeable growth reduction in the control cells. DNAJC2.428 and PPP2R5A.1879 lead to a $KRAS^{G12V}$ specific decrease in growth of about 37% and 40%, respectively. The highest degree of synthetic lethality was observed with the knockdown of MCM7. MCM7.1879 and MCM7.sh3 led to a reduction in growth in $KRAS^{G12V}$ expressing cells of about 57% and 59%, respectively. MCM7.1534v had a lesser impact but still surpassed all other genes in validation with about 46% $KRAS^{G12V}$ specific growth reduction.

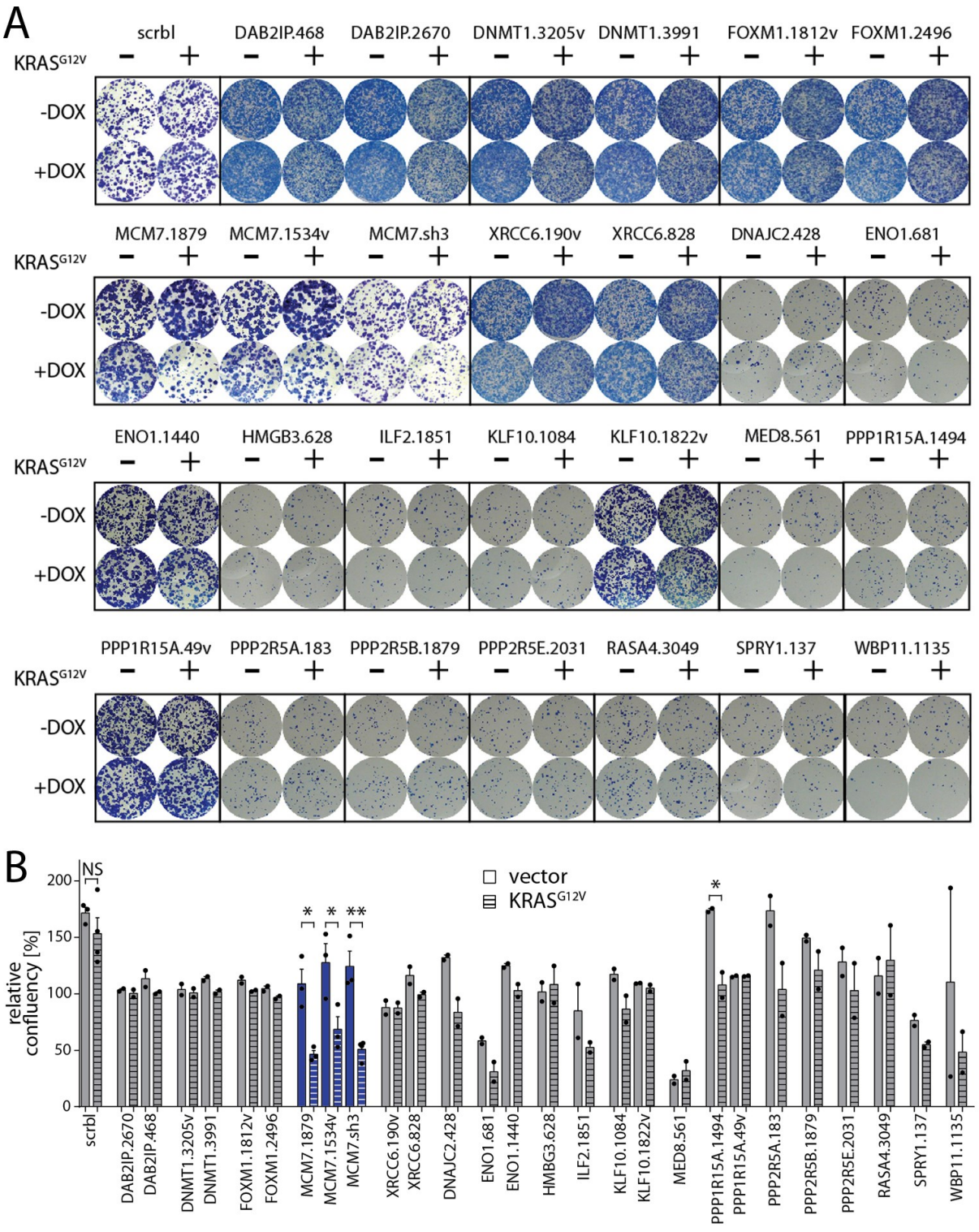

Figure 17: Validation of selected shRNAs by clonogenic assays. (A) Representative clonogenic assays of CaCo2 cells with knockdown of selected genes from the RNAi screen. (B) Quantification of the clonogenic assays cells after knockdown of respective targets. Only shRNAs against MCM7 showed a consistent growth reduction in a $KRAS^{G12V}$ dependent manner. Mean relative confluency in % ± SEM is shown (n= 2-4). Student's t-test (unpaired); * = $p < 0.05$; ** = $p < 0.01$.

2.3. MCM7 suppression is synthetic lethal with mutant KRAS

The screen validation results clearly identified MCM7 as the most promising candidate from the shRNA screen as a synthetic lethal interactor of mutant KRAS signaling. Therefore, MCM7 was chosen to be the focus of all further investigations.

2.3.1. Knockdown efficiencies of shRNAs targeting MCM7

First, the knockdown efficiency of the shRNAs targeting MCM7 was examined by western blot. MCM7.1879 and MCM7.sh3 led to an efficient knockdown of MCM7 in cells expressing $KRAS^{G12V}$ or an empty vector, whereas MCM7.1534v exhibited a less effective knockdown of MCM7 (Figure 18). This is in line with the previous result that showed a lower degree of synthetic lethality with MCM7.1534v than MCM7.1879 and MCM7.sh3 (Figure 17).

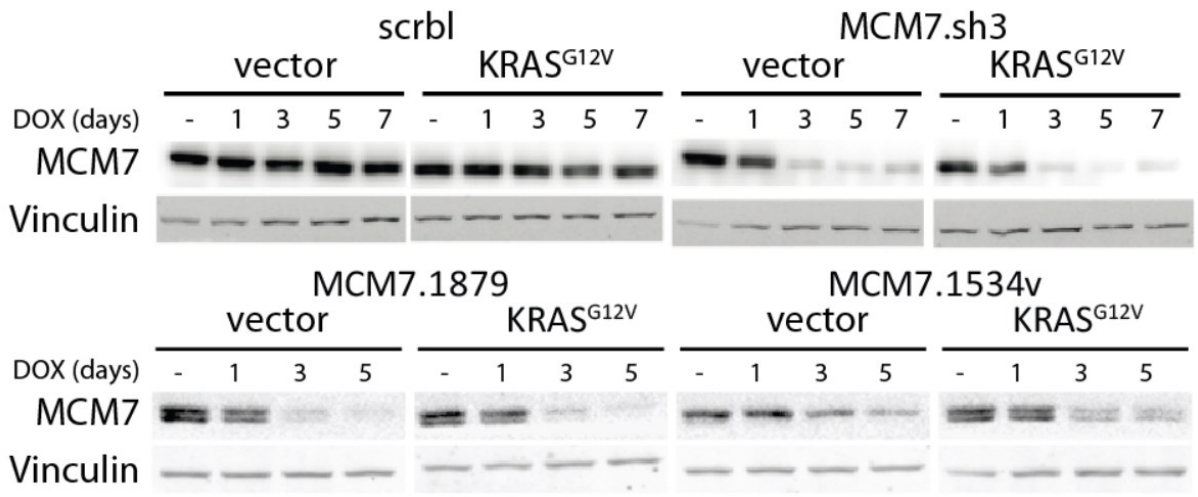

Figure 18: Knockdown efficiency of three different shRNAs against MCM7 in CaCo2 cells detected by western blot analysis after 1-5 or 1-7 days. MCM7.1879 and MCM7.sh3 led to a strong knockdown of MCM7, whereas MCM7.1534v showed a less efficient knockdown potential. Vinculin served as a loading control.

Since MCM7 is part of the MCM complex, which is in its functional state bound to DNA, the knockdown efficiency of MCM7.sh3 was additionally examined on chromatin level. MCM7 was efficiently suppressed in the soluble and chromatin-bound fraction after

the knockdown. Furthermore, MCM2, another MCM subunit, was only depleted in the chromatin fraction but not in the soluble fraction (Figure 19A). This was additionally visualized after an *in situ* chromatin fractionation of adherent cells and subsequent immunofluorescence straining that showed specific depletion of chromatin-bound MCM2 after seven days of MCM7 knockdown (Figure 19B).

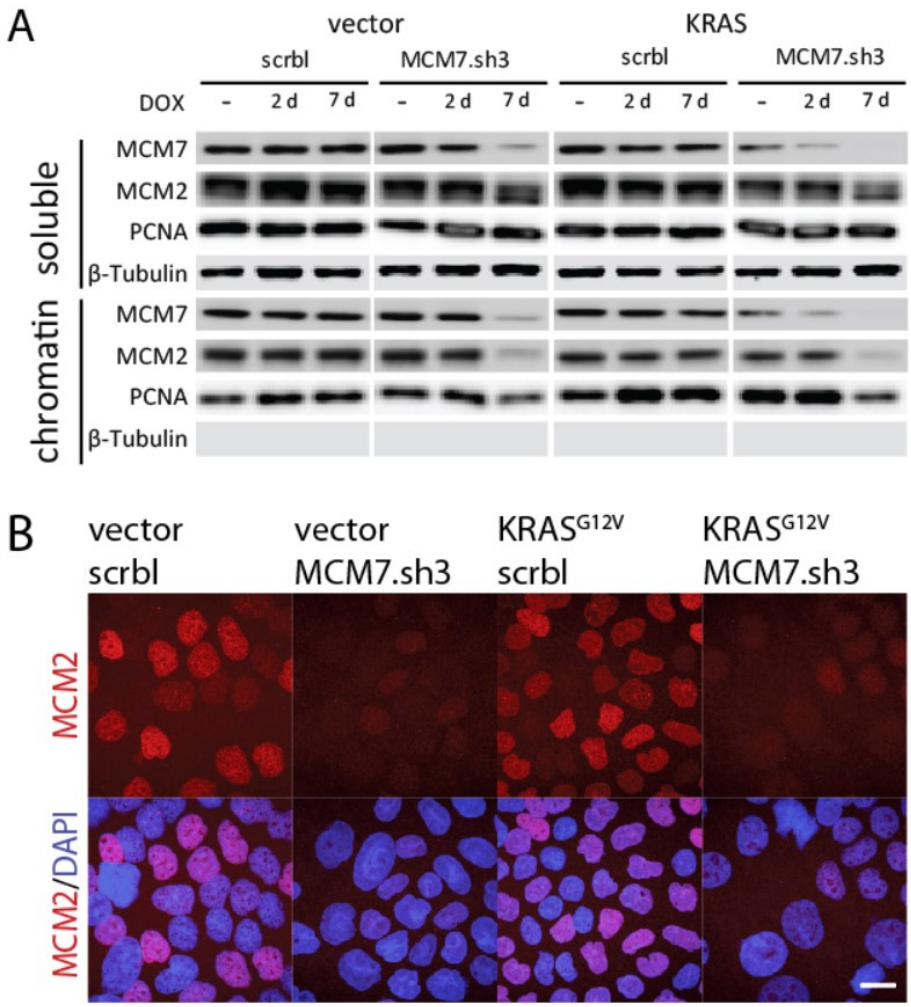

Figure 19: Knockdown efficiency of MCM7.sh3 in CaCo2 cells on chromatin level. (A) Western blot of the soluble (including soluble nuclear proteins) and chromatin-bound cell fraction after two and seven days of MCM7 knockdown. PCNA served as a loading control for soluble and chromatin-bound protein. β-tubulin served as a loading control which is only present in the soluble fraction. (B) Immunofluorescence of *in situ* chromatin fractionation of adherent cells shows efficient suppression of chromatin-bound MCM2 (red) after seven days of MCM7 knockdown in CaCo2 cells. DAPI (blue) was used as nuclear counter-staining. Scale bar = 20 µm.

2.3.2. Suppression of MCM7 reduces growth in KRAS^{G12V} expressing CaCo2 cells in 3D culture conditions

A hallmark of RAS-transformed cells is anchorage-independent growth (Kang and Krauss, 1996). To test the KRAS^{G12V} dependent growth inhibition of MCM7 suppression in 3D growth conditions, cells were seeded in soft agar and cultured for 5 weeks until visible colonies had formed. CaCo2 cells, which lack any MAPK activating mutations, showed an inherently low anchorage-independent growth capacity. Expression of oncogenic KRAS increased colony formation efficiency of CaCo2 cells about five-fold compared to the vector control. While the knockdown of MCM7 had no impact on colony formation in cells expressing the vector control, CaCo2 cells expressing KRAS^{G12V} showed a marked reduction of colonies (Figure 20).

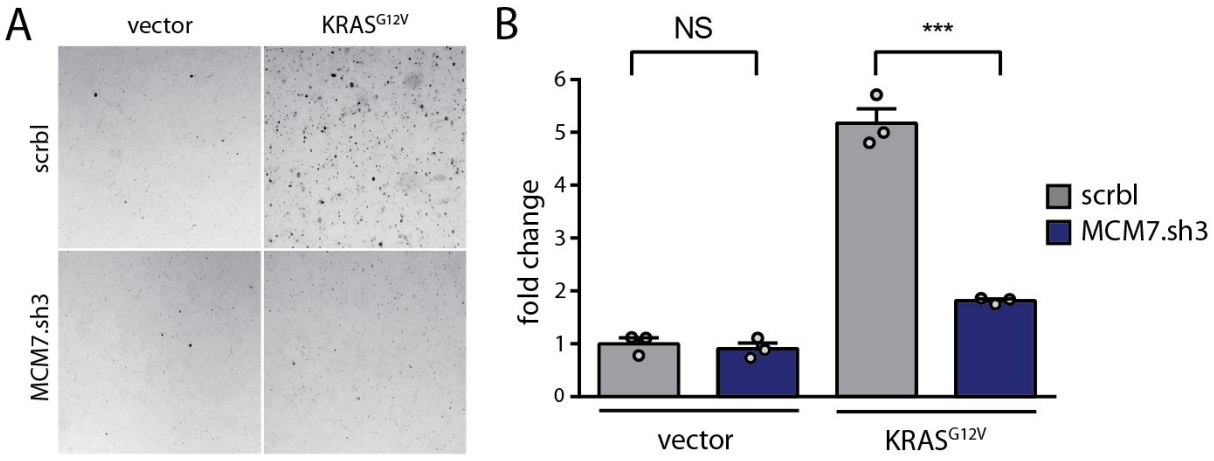

Figure 20: Soft agar assay of CaCo2 cells after MCM7 knockdown. (A) Representative soft agar assays after KRAS^{G12V} expression and MCM7 knockdown. (B) Quantification of soft agar assays. KRAS^{G12V} expression increased colony formation in CaCo2 cells about five-fold. MCM7 knockdown had no detectable effect on cells expressing a vector control, whereas cells expressing additionally KRAS^{G12V} showed significantly reduced colony formation. Mean fold change of colonies formed after five weeks of culture is shown ± SEM (n = 3 per group). Student's t-test (unpaired); NS = not significant; *** = $p < 0.001$.

2.3.3. MCM7 knockdown causes apoptosis in KRAS^{G12V} expressing CaCo2 cells

To assess whether the observed growth reduction is solely due to reduced cell growth or is accompanied with increased cell death, the presence of cleaved poly(ADP ribose) polymerase (clPARP) and cleaved Caspase 3 as indicators for apoptosis was investigated. Cells with reduced MCM7 levels alone showed only modest cleavage of PARP and caspase 3. In contrast, MCM7 suppression in KRAS^{G12V} expressing cells led to a pronounced increase in clPARP (Figure 21) and in cleaved caspase 3^{+} cells to around 10% (Figure 22).

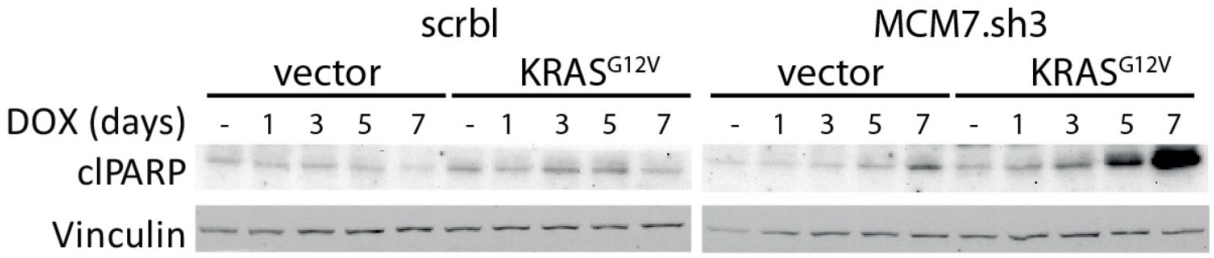

Figure 21: Western blot of CaCo2 cells assessing cleaved PARP expression after 1-7 days of MCM7 knockdown. Cleaved PARP was specifically enriched after 5 and 7 days after KRAS^{G12V} and MCM7.sh3 induction. Vinculin served as a loading control.

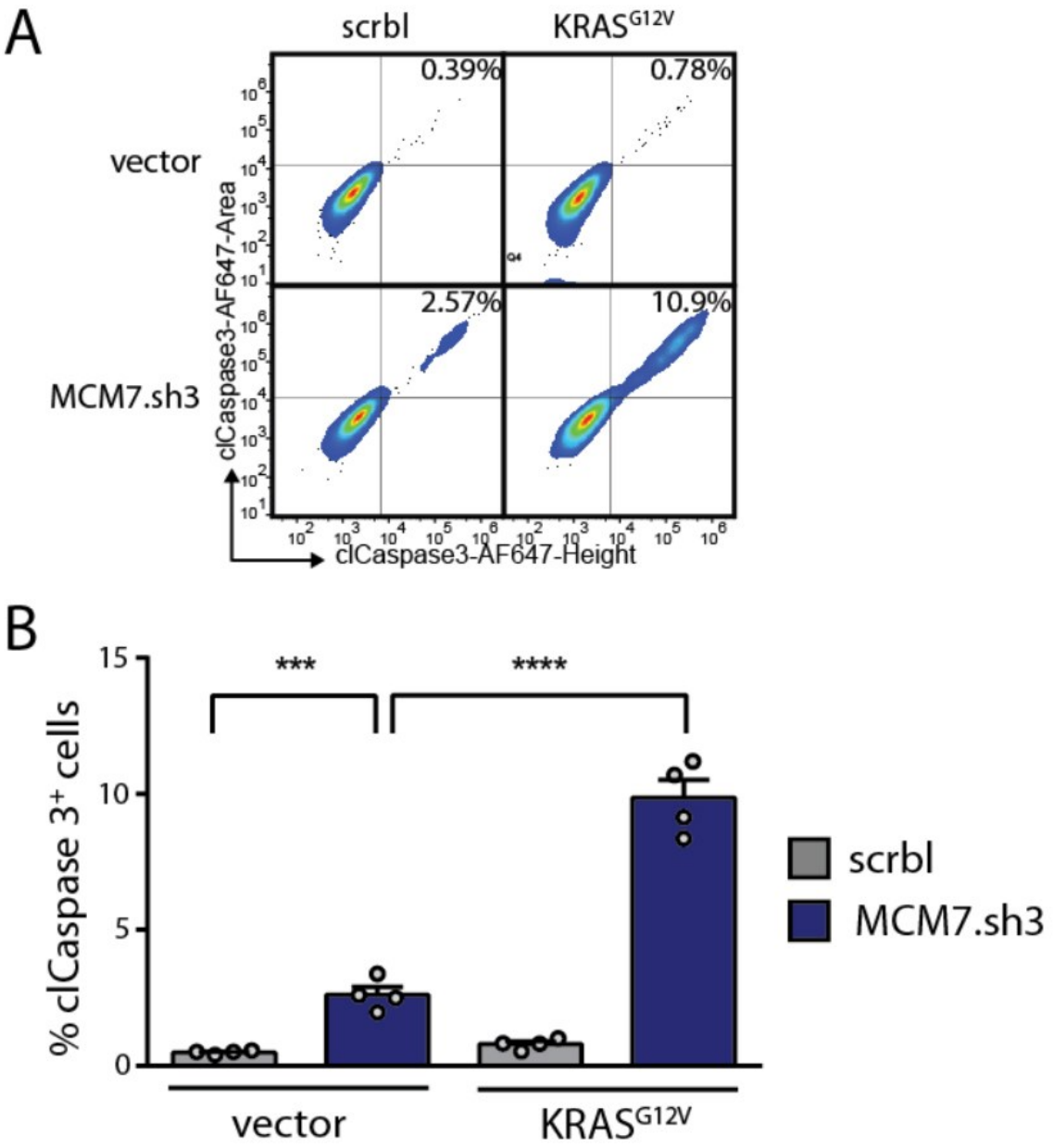

Figure 22: Flow cytometry analysis of cleaved Caspase 3 (clCaspase 3).
(A) Representative plot of cleaved caspase+ cells assessed via flow cytometry after induction of KRAS^{G12V} and knockdown of MCM7. (B) Cells co-expressing KRAS^{G12V} and MCM7.sh3 showed a significantly higher increase of apoptosis than cells expressing MCM7.sh3 alone. Mean percentage of clCaspase 3+ cells ± SEM is shown (n = 4 per group). Student's t-test (unpaired); *** = $p < 0.001$; **** = $p < 0.0001$.

2.3.4. MCM7 suppression is lethal in other colorectal cancer cell lines

So far, all experiments have focused on CaCo2 cells as a model for mutant KRAS expression, yet it was unclear whether KRAS sensitizes other colorectal cancer cell lines to MCM7 suppression, as well. Therefore, DLD-1 cells ($KRAS^{wt/G13D}$) were compared to an isogenic derivative cell line lacking the mutated KRAS allele ($KRAS^{wt/-}$) (Shirasawa et al., 1993). MCM7.sh3 induction in both cell lines resulted in a specific knockdown of MCM7 in the soluble as well as the chromatin fraction. Similar to CaCo2 cells, MCM2 followed the MCM7 depletion only in the chromatin fraction. After seven days of MCM7.sh3 induction, MCM7 levels increased again in DLD-1 ($KRAS^{wt/G13D}$) cells and to a lesser extent in DLD-1 ($KRAS^{wt/-}$) cells (Figure 23) probably due to the selective pressure exerted by MCM7.sh3 induction. In colony formation assays, both cell lines showed decreased growth upon MCM7 suppression. However, DLD-1 cells that harbor the mutant KRAS allele were, in fact, more sensitive to reduced MCM7 levels than the KRAS wild-type cell line. DLD-1 ($KRAS^{wt/-}$) cells displayed a confluence of about 39% after 10 days of MCM7 knockdown, whereas the parental KRAS-mutant cell line exhibited a final confluence of only approx. 20% (Figure 24).

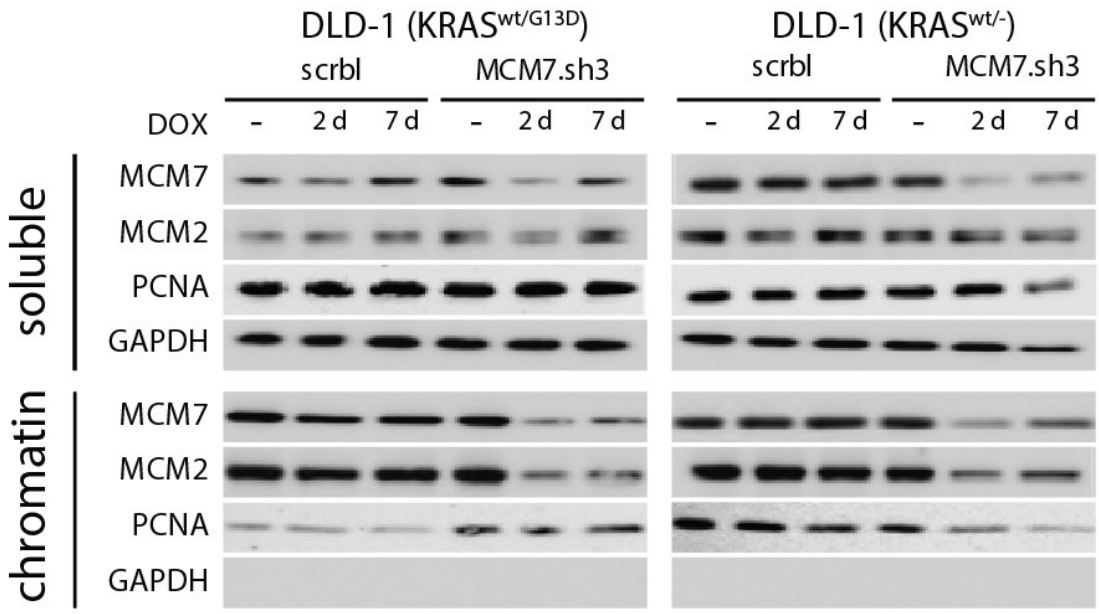

Figure 23: Knockdown efficiency of MCM7.sh3 in DLD-1 cells on chromatin level. Western blot of the soluble and chromatin-bound cell fraction after two and seven days of doxycycline induction showed efficient MCM7 knockdown in both DLD-1 cell lines.

PCNA served as a loading control for soluble and chromatin-bound protein. GAPDH served as a loading control that is only present in the soluble fraction.

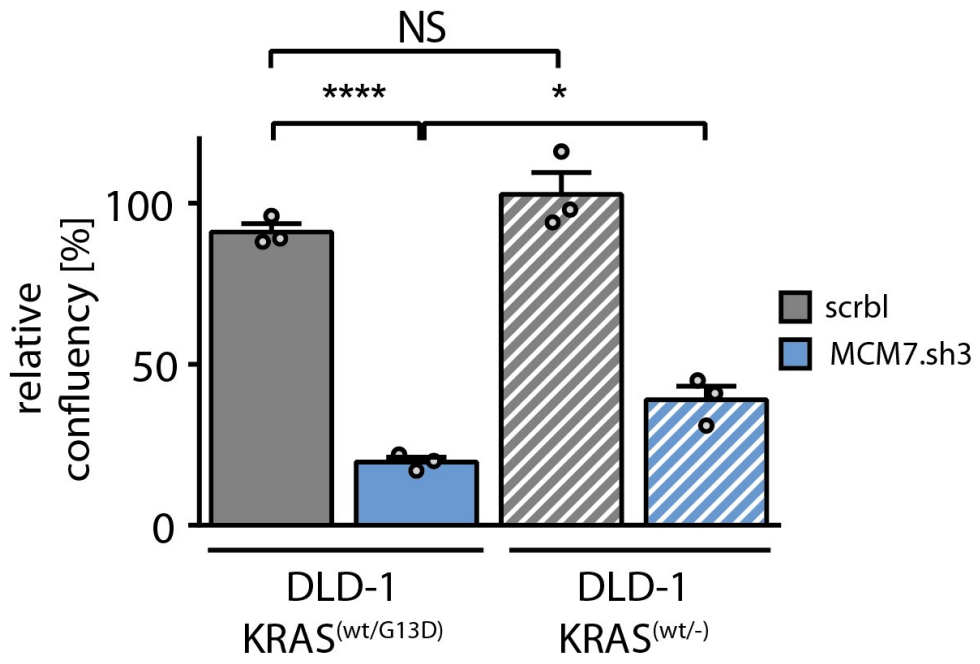

Figure 24: Quantification of clonogenic assays in DLD-1 ($KRAS^{(wt/-)}$) and DLD-1 ($KRAS^{wt/G13D}$) after MCM7 knockdown. Both cell lines are sensitive to MCM7 suppression, but DLD-1 cells lacking mutated KRAS showed decreased sensitivity to the MCM7 knockdown. Mean relative confluency ± SEM is shown (n = 3 per group). Student's t-test (unpaired); * = $p < 0.05$; **** = $p < 0.0001$.

Next, the impact of MCM7 knockdown in additional, non-isogenic colorectal cancer cell lines was investigated. All of these cell lines harbor either KRAS or BRAF mutations, leading to constitutive MAPK signaling. The cell lines were transduced with a control shRNA (scrbl) or an MCM7 targeting shRNA (MCM7.sh3) and evaluated in long-term growth assays after testing the knockdown efficiency via qPCR. Induction of MCM7.sh3 led to a similarly efficient knockdown in SW480 ($KRAS^{G12V}$), HT-29 ($BRAF^{V600E}$), and WiDr ($BRAF^{V600E}$) cells with about 20% remaining MCM7 mRNA expression. MCM7 expression in HCT-8 ($KRAS^{G13D}$) remained at about 39% (Figure 25).

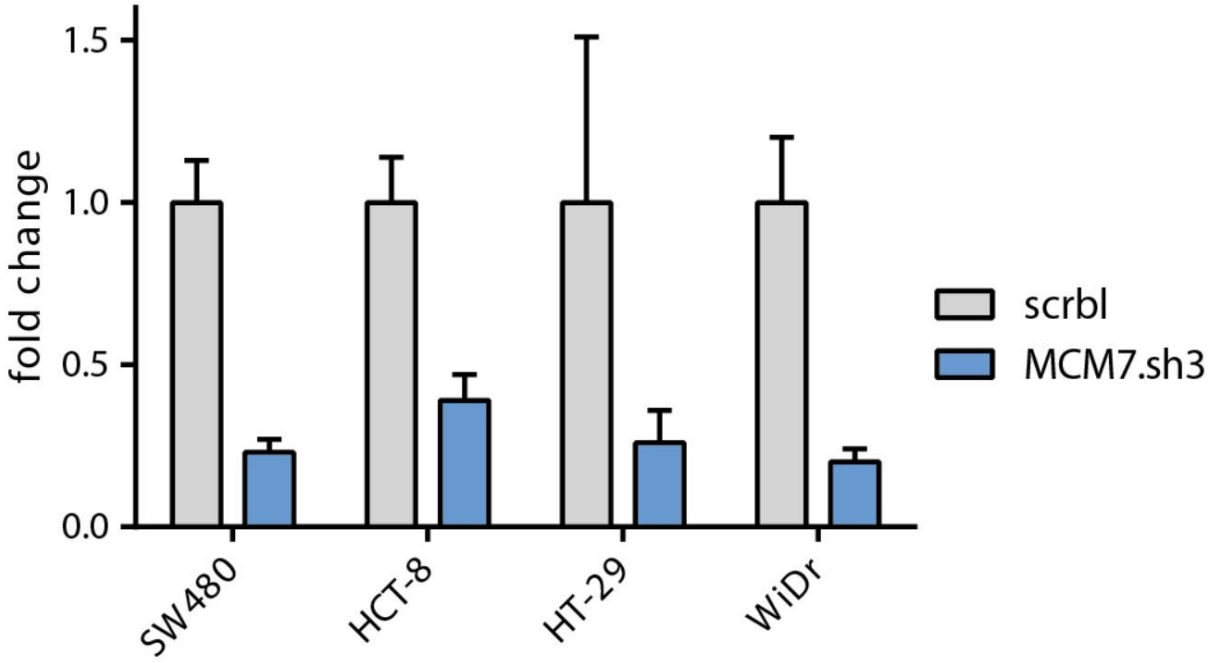

Figure 25: mRNA expression of SW480, HCT-8, HT-29, and WiDr cells three days after induction of MCM7.sh3. Knockdown of MCM7 caused an efficient suppression of MCM7 expression in all four cell lines after 3 days of doxycycline induction. Mean fold change normalized to scrbl control ± SD is shown (n = 2-3 technical replicates per group).

Next, the effect of MCM7 suppression on cell growth was assessed. In all cell lines, a significant growth reduction was observed upon MCM7 knockdown (Figure 26). Similarly, MCM7 suppression in anchorage-independent growth assays resulted in a reduction of colonies for both KRAS mutated cell lines, DLD-1 and SW480 (Figure 27).

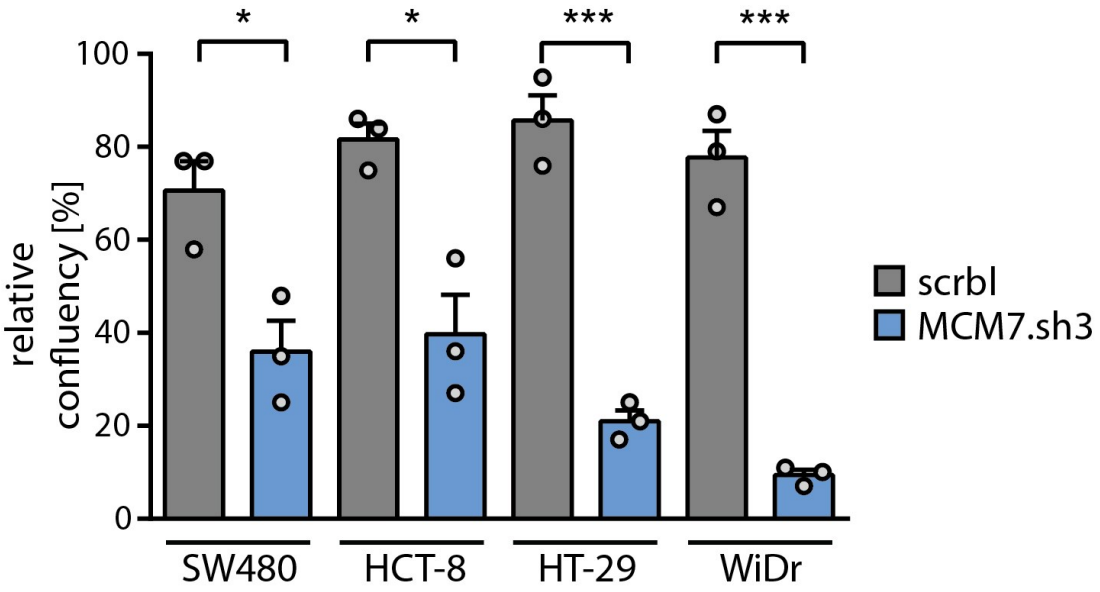

Figure 26: Quantification of clonogenic assays in SW480 ($KRAS^{G12V}$), HCT-8 ($KRAS^{G13D}$), HT-29 ($BRAF^{V600E}$), WiDr ($BRAF^{V600E}$). All cell lines showed decreased growth after doxycycline induction of MCM7.sh3 compared to the control shRNA (scrbl). Mean relative confluency ± SEM is shown (n = 3 per group). Student's t-test (unpaired); * = $p < 0.05$; *** = $p < 0.001$.

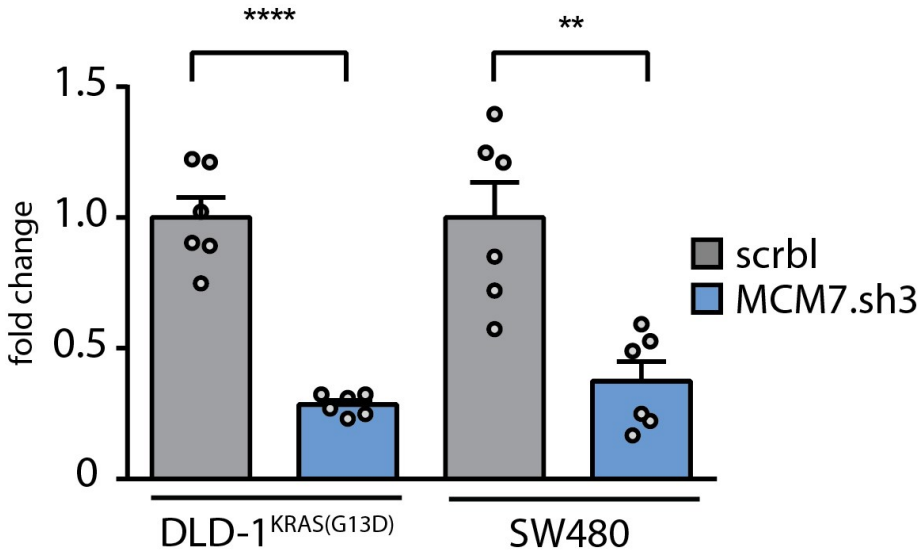

Figure 27: Quantification of colony formation in soft agar assays in KRAS mutated DLD-1 and SW480 cells. Both DLD-1 and SW480 cells showed a significant decrease in colony formation after three weeks of MCM7 knockdown in soft agar assays. Mean fold change of colonies ± SEM is shown (n = 6 per group). Student's t-test (unpaired); ** = $p < 0.01$; **** = $p < 0.0001$.

Krenoula Hani Fouad Salib contributed to obtaining the results shown in Figure 23, Figure 25, and Figure 26 in the framework of a laboratory rotation of the Master's program Molecular Medicine (https://molecular-medicine.charite.de/) at the Charité – Universitätsmedizin Berlin.

2.4. Mutant KRAS causes replicative stress in cells with low MCM7 levels

From the results obtained so far, it was clear that MCM7 suppression led to decreased cell growth in colorectal cancer cells and mutant KRAS additionally sensitized cells to the knockdown of MCM7. The following experiments focused on the underlying molecular mechanism responsible for the role of oncogenic KRAS in sensitizing colorectal cancer cells to MCM7 suppression.

2.4.1. KRAS-mutant cells show increased formation of RPA foci after MCM7 knockdown

The MCM complex is the key component of the replicative helicase and therefore a major player in DNA replication (Deegan and Diffley, 2016). Additionally, mutant RAS expression has been shown to influence DNA replication and to be a trigger for replication stress (reviewed in 1.3.2 RAS and replication stress). To investigate the impact of mutant KRAS expression in the context of MCM7 suppression on replication stress, replication protein A (RPA) focalization was assessed. RPA specifically binds single-stranded DNA (ssDNA), which is abundantly present in stalled replication forks. Therefore, the resulting nuclear RPA focalization can be used as a reliable cellular marker of replication stress (Zeman and Cimprich, 2014; Zou and Elledge, 2003).

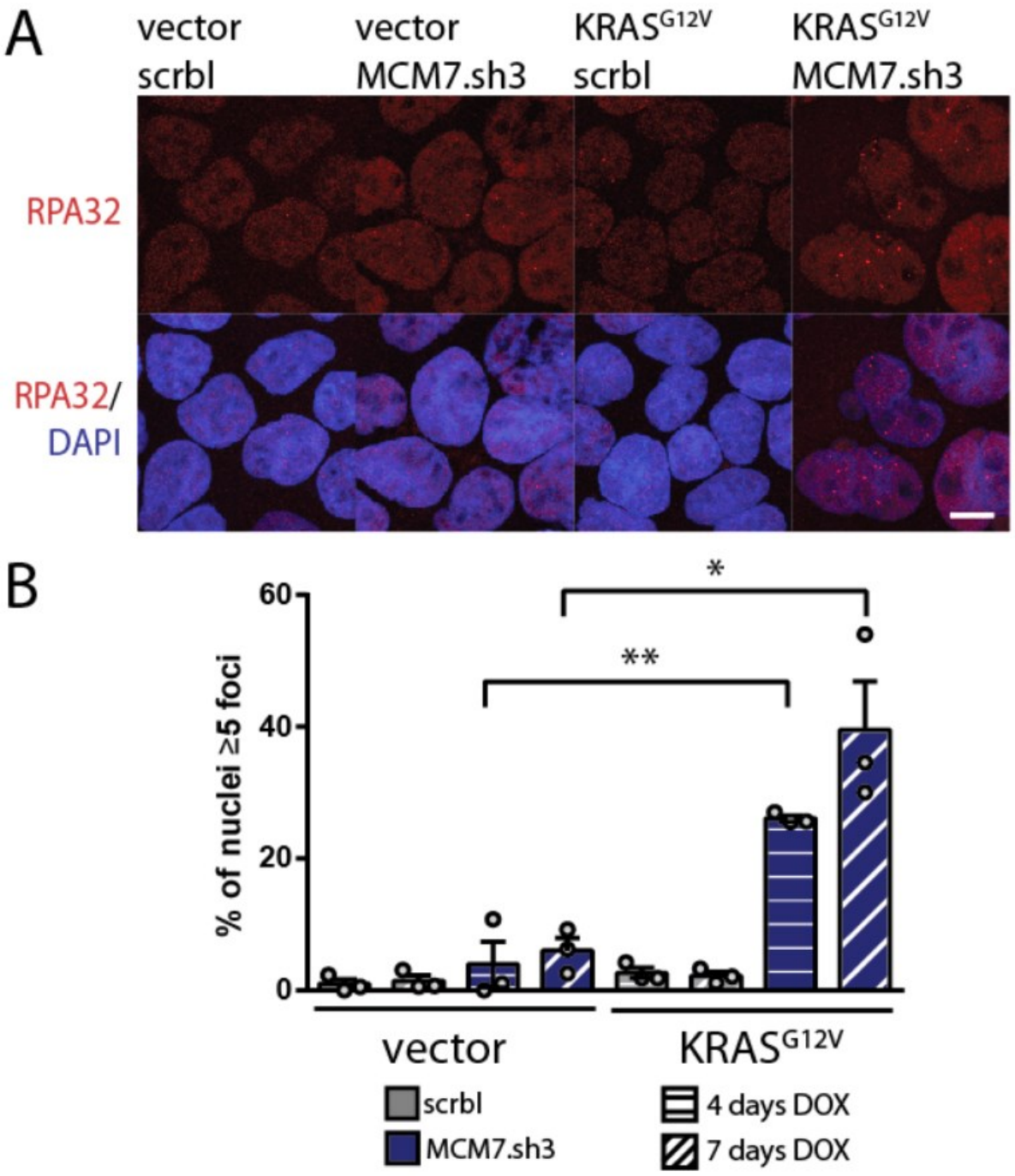

Figure 28: RPA focalization after KRAS^{G12V} expression and MCM7 knockdown in CaCo2 cells. (A) Representative immunofluorescence images after 7 days of doxycycline induction showed RPA2 foci formation in CaCo2 cells after simultaneous KRAS^{G12V} expression and MCM7 knockdown. Scale bar = 10µm. (B) Quantification of nuclei with 5 or more RPA2 foci showed a significant increase of RPA2 focalization only when KRAS^{G12V} and MCM7.sh3 were co-expressed in CaCo2 cells. After 4 and 7 days, ~26% and ~40% of cells exhibited 5 or more RPA2 foci, respectively. Mean percentage of cells with ≥5 RPA2 foci ± SEM is shown (n = 3 per group). At least 50 cells per experiment were counted. Student's t-test (unpaired); * = $p < 0.05$, ** = $p < 0.01$.

Expression of KRAS^{G12V} and knockdown of MCM7 was induced in CaCo2 cells for 4 and 7 days and the RPA subunit RPA2 was visualized using immunofluorescence. Neither KRAS^{G12V} expression nor MCM7 suppression alone led to a significant change in number of cells exhibiting RPA foci. However, knockdown of MCM7 in KRAS-mutant CaCo2 cells caused a substantial increase of cells exhibiting RPA foci to approx. 26% after 4 days of induction and approx. 40% after 7 days (Figure 28). Additionally, western blot analysis showed RPA2 phosphorylation at T21 exclusively upon MCM7 suppression in KRAS^{G12V} expressing cells, confirming the previous observation (Figure 29). Similarly, increased RPA foci formation was observed in KRAS-mutant DLD-1 and SW480 cells upon MCM7 suppression (Figure 30). Interestingly, RPA foci co-localized well with 53BP1 nuclear bodies (Figure 31).

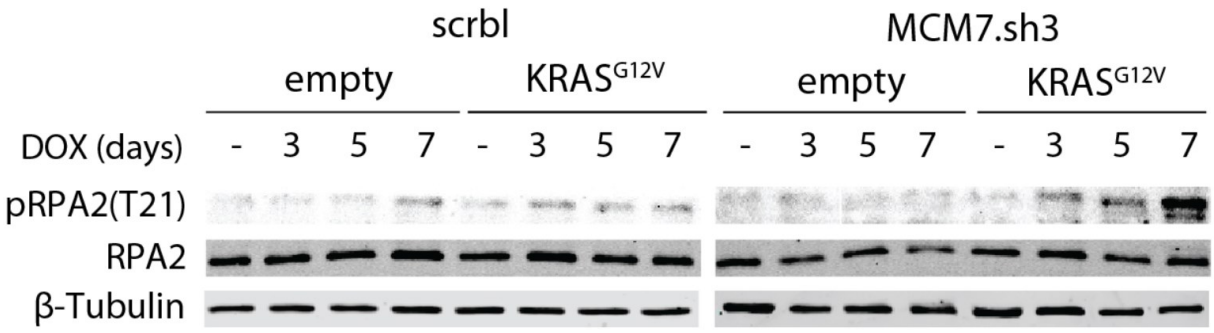

Figure 29: Western blot analysis of RPA2(T21) phosphorylation in CaCo2 cells after KRAS^{G12V} expression and MCM7 knockdown. RPA2 was specifically phosphorylated at the T21 site in KRAS^{G12V} expressing CaCo2 cells after MCM7 knockdown. Tubulin served as a loading control. Western blot was performed by Birgit Schaefer, medical technical assistant, Institute of Pathology, Charité.

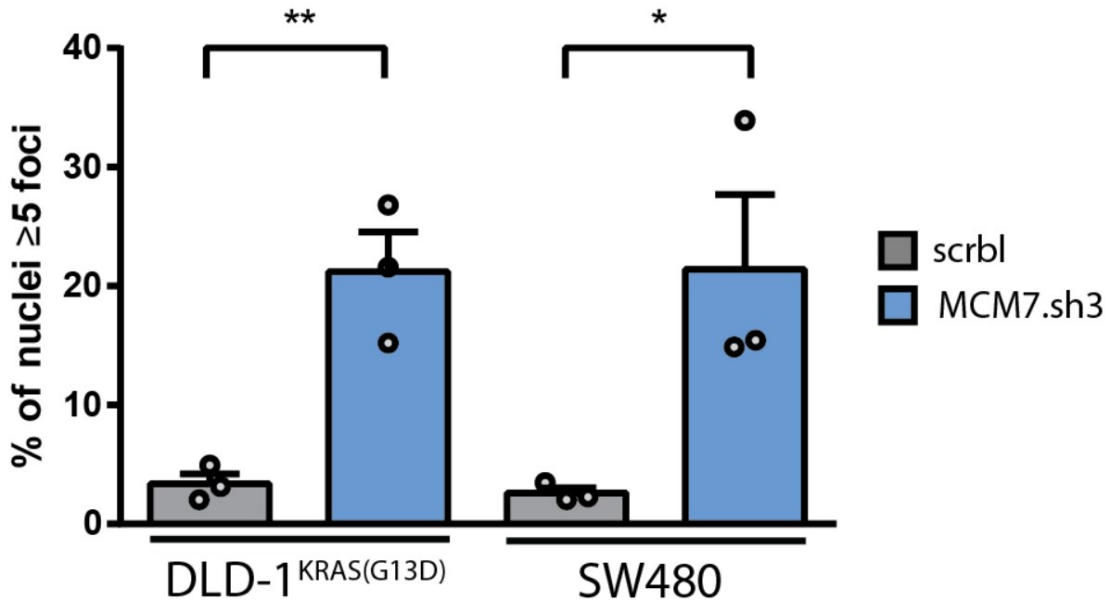

Figure 30: Quantification of RPA focalization in DLD-1 and SW480 cells. The quantification of immunofluorescence images revealed an increase of cells with RPA foci after 4 days of MCM7 knockdown. Mean percentage of cells with ≥5 RPA foci ± SEM is shown (n = 3 per group). At least 50 cells per experiment were counted. Student's t-test (unpaired); * = $p < 0.05$; ** = $p < 0.01$.

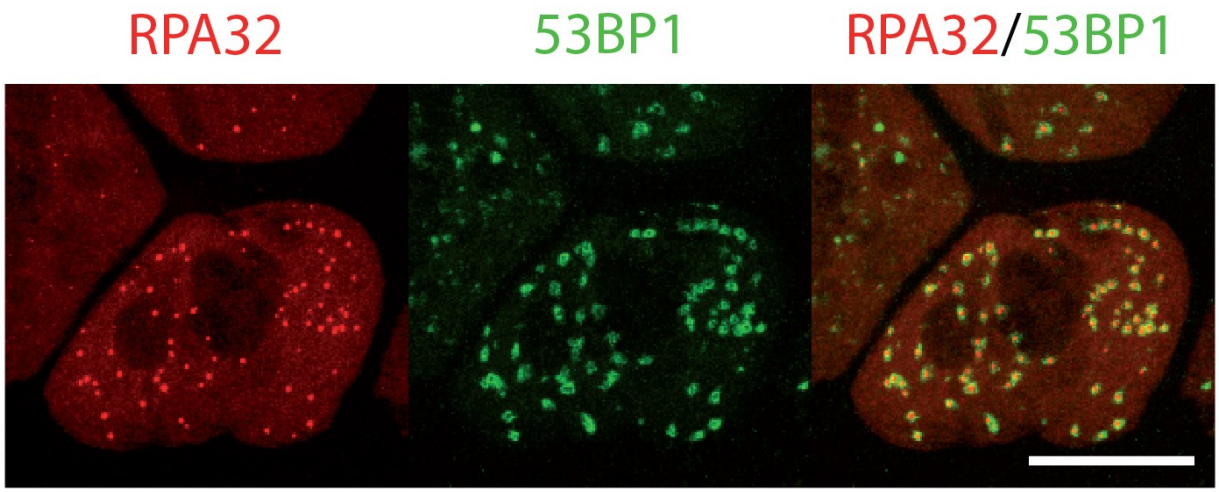

Figure 31: Immunofluorescence of RPA2 and 53BP1 in CaCo2 cells after simultaneous KRAS^{G12V} and MCM7.sh3 expression. RPA foci showed co-localization with 53BP1 nuclear bodies in CaCo2 cells after 7 days of KRAS^{G12V} induction and MCM7 knockdown. Scale bar = 10 µm.

2.4.2. Mutant KRAS confers resistance to CDC7 inhibition

The source of mutant KRAS inflicted replication stress in the background of low replication licensing is still elusive. Previously, expression of oncogenic RAS has been linked to replication stress due to an increase in replication origin firing (Hills and Diffley, 2014; Di Micco et al., 2006). Aberrant origin firing can deplete dormant origins that function as a fail-safe mechanism to recover stalled replication forks (Burkhart et al., 1995; Mahbubani et al., 1997; McIntosh and Blow, 2012; Wong et al., 2011). Therefore, the influence of mutant KRAS on the pharmacological inhibition of origin firing was investigated. CDC7 is one of the kinases that initiate origin firing via phosphorylation and subsequent remodeling of the MCM complex (Deegan and Diffley, 2016; Heller et al., 2011). Thus, the link between oncogenic KRAS and origin firing in colorectal cancer cells, the effect of the CDC7 inhibitor PHA 767491 on growth in KRAS-mutant and KRAS wild-type cells was assessed. Indeed, a decrease in phosphorylation of MCM2 at serine 40, an indicator for CDC7 activity and origin firing (Montagnoli et al., 2006, 2008), was observed upon 24 h of CDC7 inhibition with 10 µM PHA 767491 (Figure 32). CaCo2 cells expressing mutant $KRAS^{G12V}$ showed a slightly increased resistance to CDC7 inhibition, as indicated by a shift in IC_{50} of PHA 767491 from 0.576 µM (95% CI: 0.467 µM-0.710 µM) to 0.851 µM (95% CI: 0.662 µM-1.095 µM). An even more pronounced shift was observed in DLD-1 cells with $KRAS^{G13D}$ compared to the isogenic cells harboring only a KRAS wild-type allele from 1.406 µM (95% CI: 1.140 µM to 1.735 µM) to 3.086 µM (95% CI: 2.777 µM to 3.431 µM) (Figure 32, Figure 33).

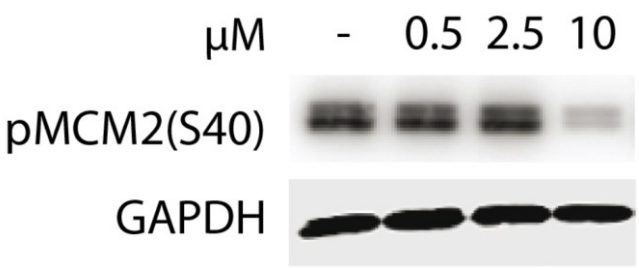

Figure 32: Western blot of pMCM2 (S40) as an indicator for origin firing after CDC7 inhibition CaCo2 cells showed decreased phosphorylation of MCM2 at serine 40 after 24 h of pharmacological CDC7 inhibition with 10 µM PHA 767491.

The 0.5 µM and 2.5 µM concentrations did not cause an observable change in MCM2 phosphorylation after 24 h. GAPDH served as a loading control.

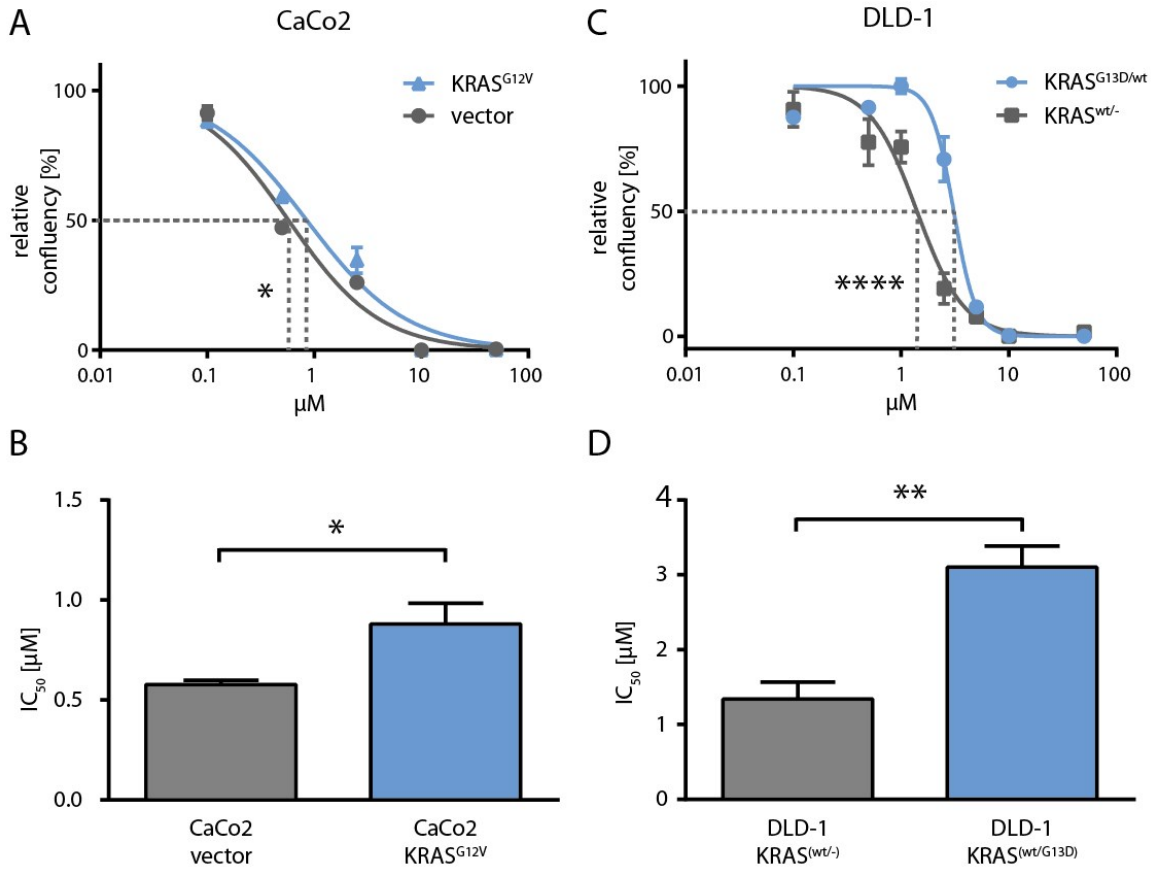

Figure 33: IC_{50} determination of $KRAS^{mut}$ and $KRAS^{wt}$ cells to the CDC7 inhibitor PHA 767491. (A,B) CaCo2 cells exhibited a slight shift in IC_{50} from 0.576 µM (95% CI: 0.467 µM - 0.710 µM) to 0.851 µM (95% CI: 0.662 µM - 1.095 µM) upon $KRAS^{G12V}$ expression. R^2_{vector}=0.9675; $R^2_{KRAS(G12V)}$= 0.9574 (C,D) DLD-1 cells harboring $KRAS^{G13D}$ were substantially more resistance to CDC7 inhibition exhibiting an IC_{50} of 1.406 µM (95% CI: 1.140 µM - 1.735 µM) compared to the $KRAS^{wt}$ DLD-1 cells with an IC_{50} of 3.086 µM (95% CI: 2.777 µM - 3.431 µM). $R^2_{KRAS(wt/-)}$=0,9267; $R^2_{KRAS(G13D/wt)}$=0.9662. Mean relative confluency ± SEM is shown (n = 3-4 per group). Nonlinear regression - extra sum-of-squares F test (A, C). Mean IC_{50} ± SEM is shown (n = 4). Student's t-test (unpaired) (B, D); * = $p < 0.05$; ** = $p < 0.01$; **** = $p < 0.0001$.

2.4.3. MCM7 knockdown causes checkpoint activation

Consistent with the observed replicative stress, increased CHK1 activation was detected specifically in CaCo2 cells with simultaneous $KRAS^{G12V}$ expression and

MCM7 knockdown. In contrast, CHK2 was activated after MCM7 suppression independently of KRAS^{G12V} expression (Figure 34).

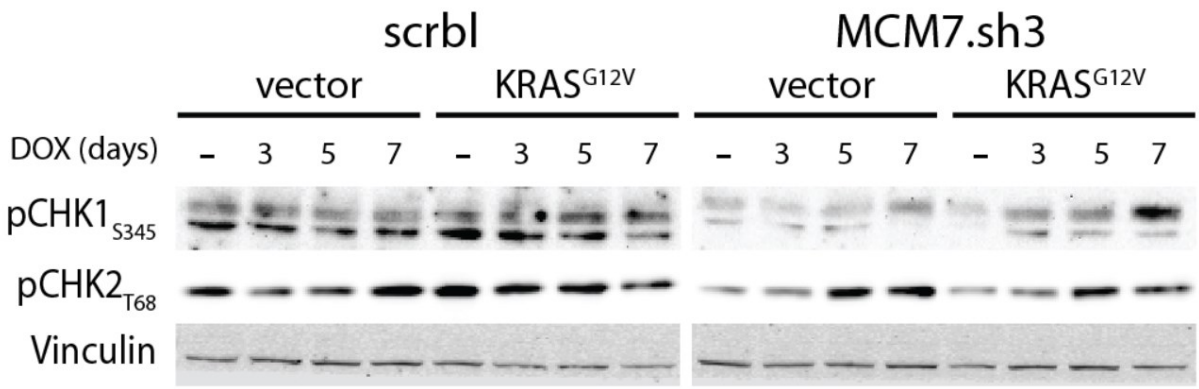

Figure 34: Western blot analysis of pCHK1(S345) and pCHK2(T68). CHK1 is specifically activated after 7 days of KRAS^{G12V} and MCM7.sh3 co-expression. CHK2 is activated after 5 days of MCM7 knockdown, independently of KRAS^{G12V} expression. Vinculin served as a loading control.

2.5. Knockdown of MCM7 leads to a shift in cell cycle distribution

Activation of the checkpoint kinases CHK1 and CHK2 can trigger a delay in cell cycle progression until the cause of their activation is resolved (Bartek and Lukas, 2003). Therefore, cell cycle distributions were analyzed in CaCo2 cells after MCM7 knockdown in a KRAS wild-type and mutant background.

2.5.1. Cells accumulate in G2/M phase after MCM7 suppression independently of mutant KRAS expression

To assess the impact of MCM7 and KRAS^{G12V} induced replication stress on the cell cycle distribution, CaCo2 cells were analyzed after 7 days of MCM7 knockdown with or without KRAS^{G12V} expression and 30 minutes of BrdU incorporation by flow cytometry. CaCo2 cells did not arrest in G1 after MCM7 knockdown, despite decreased DNA replication licensing, as indicated by the loss of chromatin-bound MCM7 and MCM2 (Figure 19). In contrast, the cells accumulated in G2/M after MCM7 knockdown.

This was seen independently of KRAS^{G12V} expression. KRAS^{G12V} expression itself had no major impact on the cell cycle distribution. A slight increase in G1 as observed after KRAS^{G12V} expression. However, this might be the consequence of slight differences in initial plating densities that resulted in a higher confluency in KRAS^{G12V} expressing cells and thus in a higher G1 population due to increased cell-cell contact inhibition. (Figure 35).

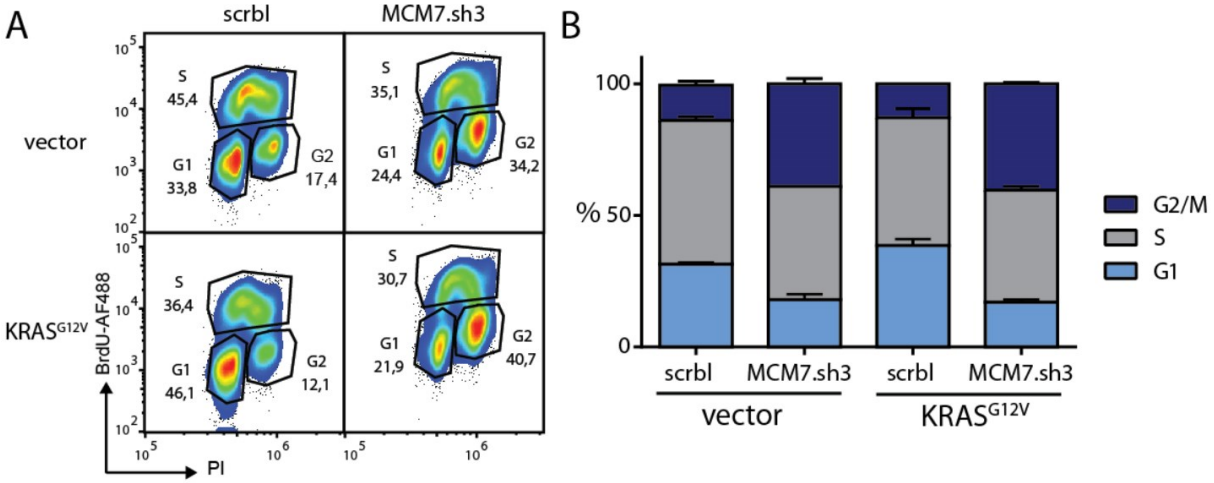

Figure 35: Analysis of cell cycle distributions in CaCo2 cells after 7 days of KRAS^{G12V} and MCM7.sh3 expression. BrdU was added to the cells 30 min before they were harvested and stained with propidium iodide (PI) and an anti BrdU-AF488 antibody. (A) Representative plot of cell cycle distributions in CaCo2 cells after KRAS^{G12V} expression and MCM7 knockdown. (B) Flow cytometry analysis revealed increased persistence of CaCo2 cells with low levels of MCM7 in G2/M phase independently of KRAS^{G12V} seven days after induction. (n=2 per group).

2.5.2. KRAS-mutant cells accumulate specifically in mitosis after MCM7 knockdown

To differentiate between G2 and M phase arrest, CaCo2 cells were stained for phospho-Histone H3 (pHH3), which is specifically phosphorylated at serine 10 in mitosis (Hans and Dimitrov, 2001). Analysis of immunofluorescence images showed that KRAS^{G12V} expression or knockdown of MCM7 alone did not change the number of cells in mitosis after 7 days of induction. This indicates that cells halt in G2 after MCM7 suppression but still enter mitosis eventually, albeit with some delay. Remarkably, cells

co-expressing KRAS^{G12V} and MCM7.sh3 show a robust increase of cells in mitosis from approximately 5% to 11% (Figure 36).

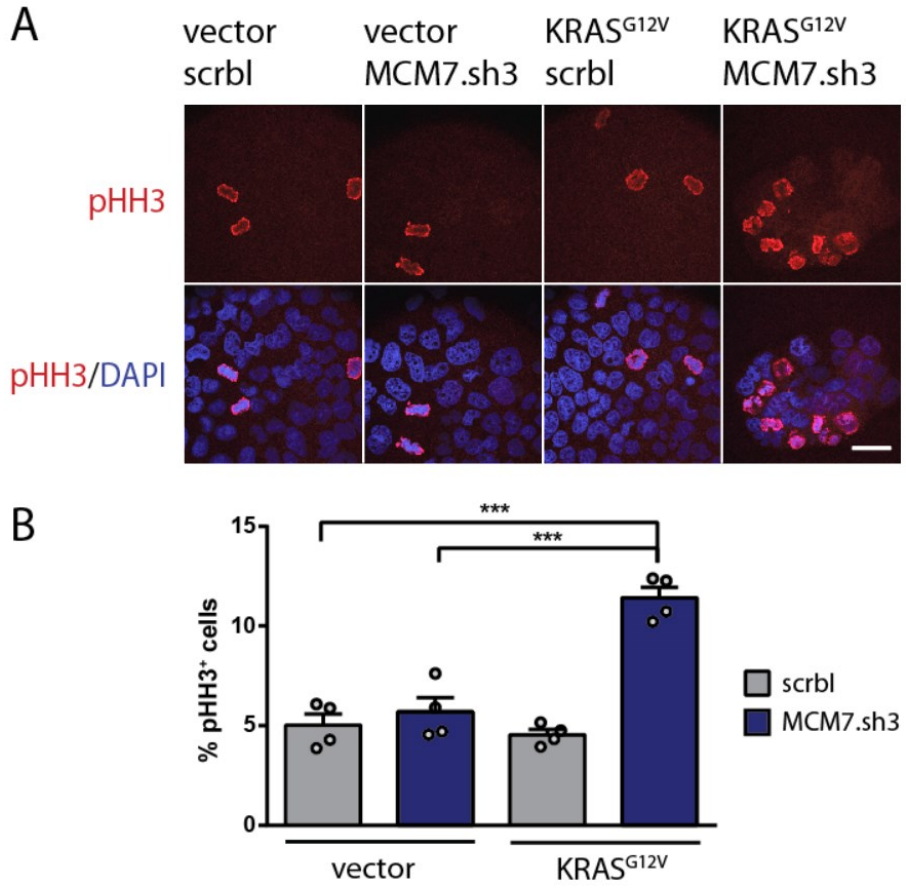

Figure 36: Fluorescence microscopy analysis of pHH3(S10) positive CaCo2 cells after 7 days of KRAS^{G12V} expression and MCM7 knockdown. (A) Representative immunofluorescence images of CaCo2 cells stained for phospho-Histone H3 (pHH3) after 7 days of induction. Scale bar = 40 µm. (B) Quantification of pHH3^{+} stained cells revealed that about 5% of all cells stained positive for pHH3 after 7 days of doxycycline addition except cells co-expressing KRAS^{G12V} and MCM7.sh3, which exhibited an increase of mitotic cells to over 11%. Mean percentage of pHH3^{+} cells ± SEM is shown (n = 4 per group). At least 200 cells were counted per experiment. Student's t-test (unpaired); *** = $p < 0.001$.

Comparable results were obtained in an independent experiment after measuring pHH3^{+} cells via flow cytometry. Again, CaCo2 cells showed the highest increase in pHH3^{+} cells after simultaneous KRAS^{G12V} expression and MCM7 knockdown (Figure 37). However, the flow cytometry analysis showed a more pronounced increase in pHH3 positive cells after MCM7 knockdown in the absence of KRAS^{G12V}. The reason for the slight differences between immunofluorescence and flow cytometry

experiments is not entirely clear, however, it might be due to not further known technical discrepancies between the two experimental procedures.

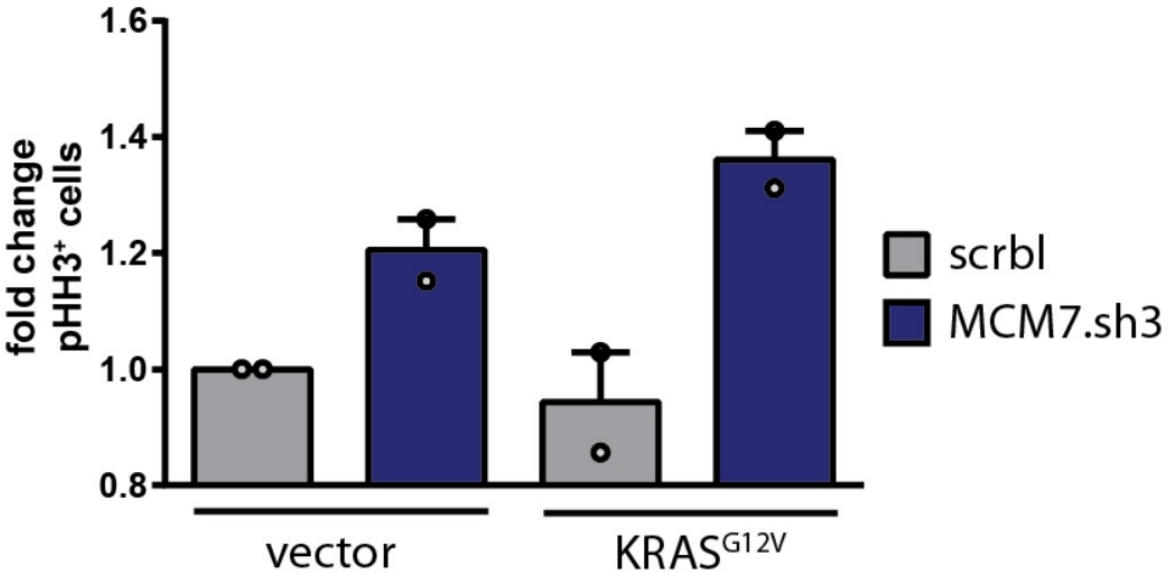

Figure 37: Flow cytometry analysis of pHH3(S10) positive CaCo2 cells after 7 days of KRAS^{G12V} and MCM7.sh3 expression. A higher fraction of mitotic cells was observed after MCM7 knockdown, which was further increased after additional KRAS^{G12V} expression. Mean percentage of pHH3^{+} cells ± SEM is shown (n = 2 per group). Flow cytometry was performed by Kathleen Klotz-Noack, Institute of Pathology, Charité.

2.6. KRAS-mutant cells are driven into mitotic catastrophe after MCM7 suppression

2.6.1. KRAS-mutant cells enter mitosis with damaged DNA

Premature entry into mitosis in the presence of DNA damage due to the lack of a functional G2/M checkpoint is a hallmark of mitotic catastrophe (Castedo et al., 2004; Vakifahmetoglu et al., 2008). Thus, the hypothesis that mitotic catastrophe is the underlying mechanism of oncogenic KRAS dependent cell death in MCM7 depleted cells was assessed. To test this, KRAS^{G12V} expression and MCM7 knockdown were induced in CaCo2 cells for 7 days before the cells were stained for pHH3 (S10) and phospho-H2AX at Ser139 (γH2AX). Cells with either KRAS^{G12V} expression or MCM7 suppression alone showed no significant increase of γH2AX foci in mitosis. However,

a striking 61% of cells with simultaneous KRAS^{G12V} expression and MCM7 knockdown exhibited DNA damage in mitosis (Figure 38).

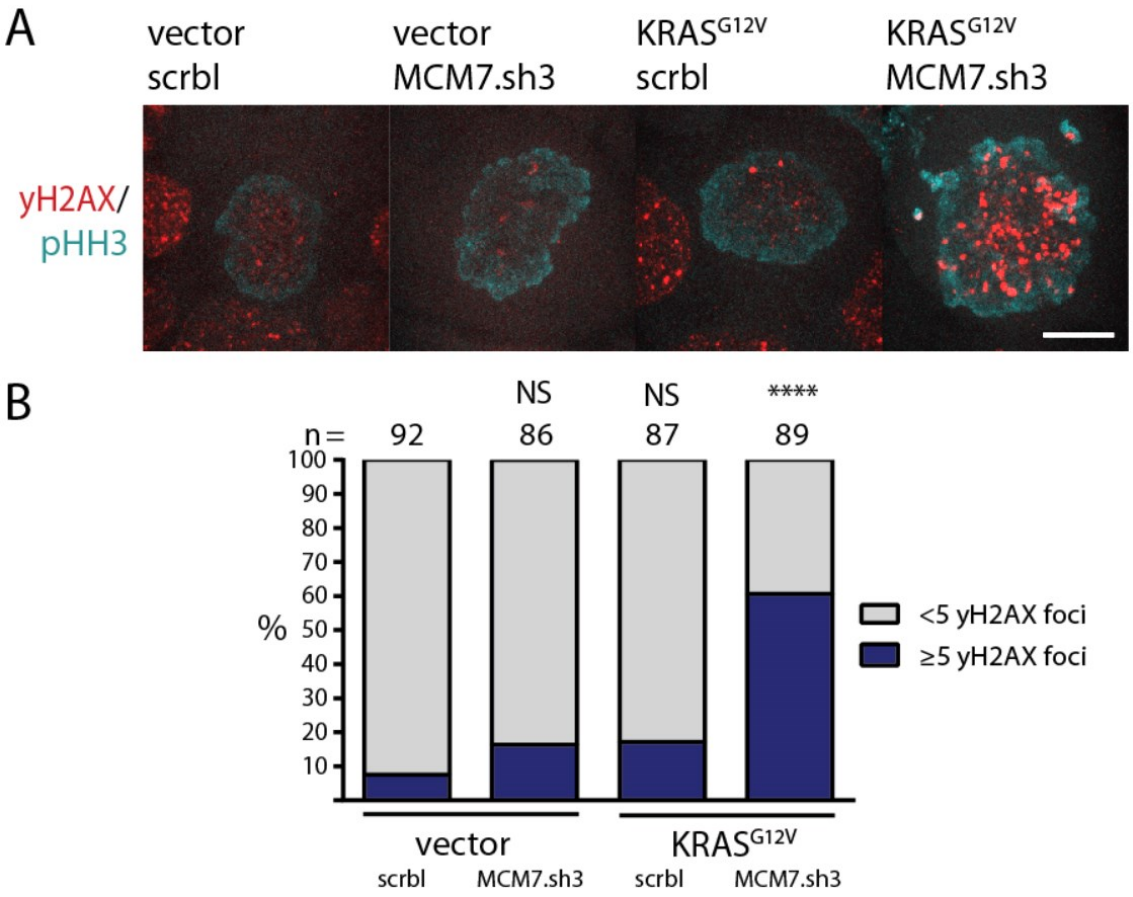

Figure 38: Fluorescence microscopy analysis of DNA damage (γH2AX$^+$) during mitosis (pHH3$^+$) in CaC2 cells after KRAS^{G12V} and MCM7.sh3 expression. (A) Representative immunofluorescence images of phospho-Histone H3 (pHH3) and γH2AX stained CaCo2 cells after 7 days of doxycycline induction. (B) Quantification of γH2AX foci in pHH3$^+$ CaCo2 cells. KRAS^{G12V} or MCM7.sh3 expression alone did not significantly change the number of mitotic cells with 5 or more γH2AX foci. Co-expression of KRAS^{G12V} and MCM7.sh3 caused an increase of mitotic γH2AX$^+$ cells to about 61%. At least 86 cells per group were counted through the course of 5 independent experiments. Fisher's exact test; **** = $p < 0.0001$.

The increased DNA damage during mitosis observed in cells simultaneously expressing KRAS^{G12V} and MCM7.sh3 was confirmed in an independent flow cytometry experiment. About 13.5% of KRAS-mutant cells showed high γH2AX levels during mitosis after MCM7 knockdown, whereas cells with MCM7 knockdown alone remained at low levels of γH2AX$^+$ cells during mitosis (Figure 39). Again, the

fluorescence microscopy experiment and the flow cytometry experiment showed slightly different outcomes. The fluorescence microscopy experiment showed DNA damage in about 61% of all mitotic cells, whereas only about 14% of cells were γH2AX positive in the flow cytometry experiment. This difference can be explained by the different sensitivities of the two assays. While single sites of DNA damage are visible in fluorescence microscopy (each γH2AX focus is a site of DNA damage), high levels of DNA damage are required to display a cell as γH2AX positive in flow cytometry. Therefore, the absolute numbers of γH2AX positive cells in mitosis were lower in the flow cytometry experiment, however, the relative proportions between samples were similar in both experiments.

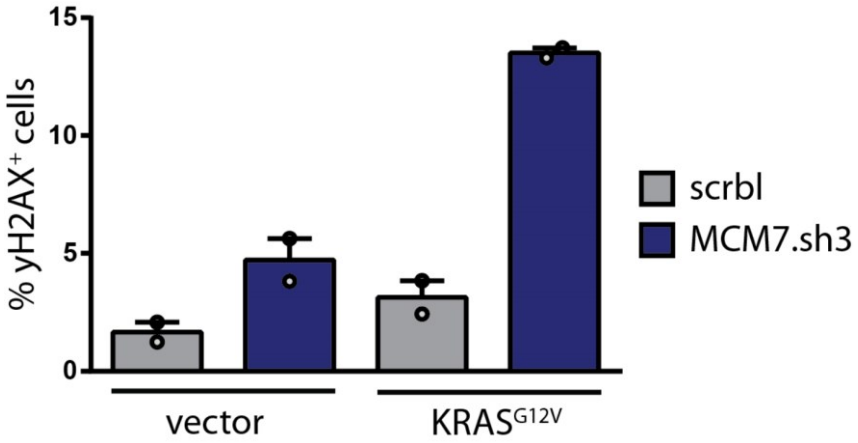

Figure 39: Flow cytometry analysis of γH2AX⁺/pHH3⁺ CaCo2 cells. CaCo2 cells showed a pronounced increase of γH2AX⁺ cells in mitosis specifically after simultaneous expression of $KRAS^{G12V}$ and knockdown of MCM7 for 7 days. Mean percentage of γH2AX⁺ cells (gated on pHH3⁺ cells) ± SEM is shown (n = 2 per group). Flow cytometry was performed by Kathleen Klotz Noack, Institute of Pathology, Charité.

As a consequence of DNA damage in mitosis and the resulting mitotic catastrophe, random distributions of condensed chromosomes throughout the cell (Figure 40) and massive chromosomal aberrations during mitosis (Figure 41) were frequently observed after simultaneous $KRAS^{G12V}$ expression and MCM7 knockdown.

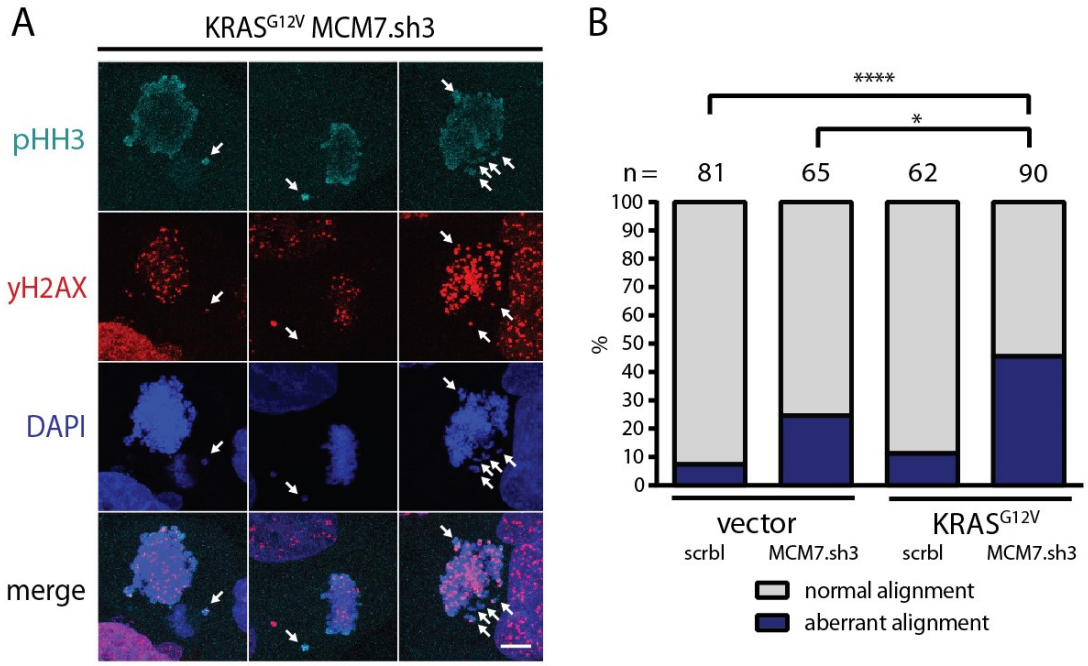

Figure 40: Analysis of aberrant chromosome alignments during mitosis. Immunofluorescence imaging (A) and subsequent quantification (B). CaCo2 cells showed an increased number of cells with DNA damage and randomly distributed chromosomes throughout the cell during mitosis after 7 days of KRAS^{G12V} expression and MCM7 knockdown. Arrows indicate misaligned chromosomes. Scale bar = 10 µm. Fisher's exact test; * = $p < 0.05$; **** = $p < 0.0001$.

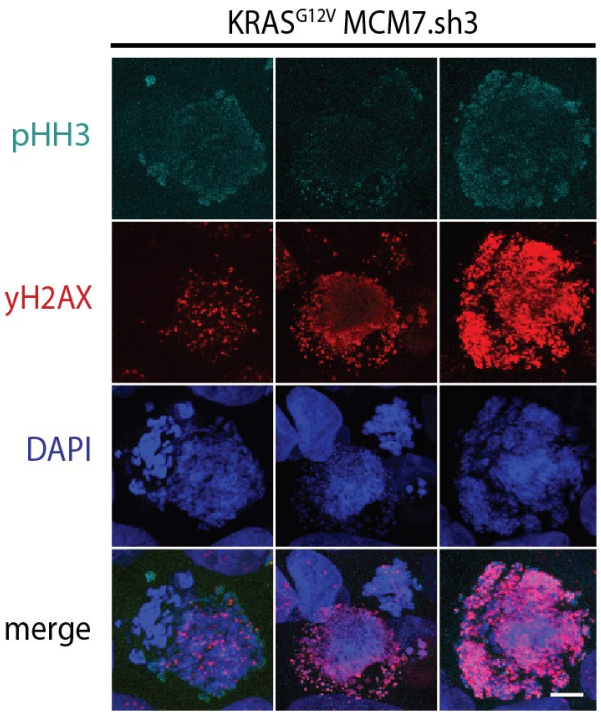

Figure 41: Immunofluorescence of massively aberrated chromosomes during mitosis after 7 days of KRAS^{G12V} expression and MCM7 knockdown. CaCo2 cells expression KRAS^{G12V} and MCM7.sh3 simultaneously for 7 days exhibit in part massive chromosomal aberrations and DNA damage during mitosis. Scale bar = 10 µm.

2.6.1. The influence of KRAS^{G12V} on the G2/M checkpoint

The results so far showed that KRAS-mutant cells display an increased mitotic cell population as well as DNA damage in mitosis after MCM7 suppression. It was previously suggested that oncogenic RAS might promote the G2/M transition via ERK1/2 and p90RSK and therefore might be able to push cells with unreplicated DNA in mitosis (Grabocka et al., 2014; Knauf et al., 2006). To assess the impact of oncogenic KRAS in the G2/M transition after MCM7 suppression, several downstream targets of p90RSK that are linked to the regulation of mitotic entry were analyzed, including CHK1, CDC25B/C, and MYT1, as indicators for functional G2 arrest. The output of all analyzed proteins converges in the mitotic kinase CDK1. The active CDK1-cyclin B complex phosphorylates numerous targets involved in chromosome condensation, spindle assembly, and nuclear membrane breakdown among other processes that lead to mitotic entry. Its activity can be inhibited by phosphorylation at Thr14 and Tyr15 via WEE1 and MYT1 (Booher et al., 1997; Mueller et al., 1995; Nigg, 2001). The hypothetical molecular connecting KRAS and the G2/M transition is summarized in Figure 42.

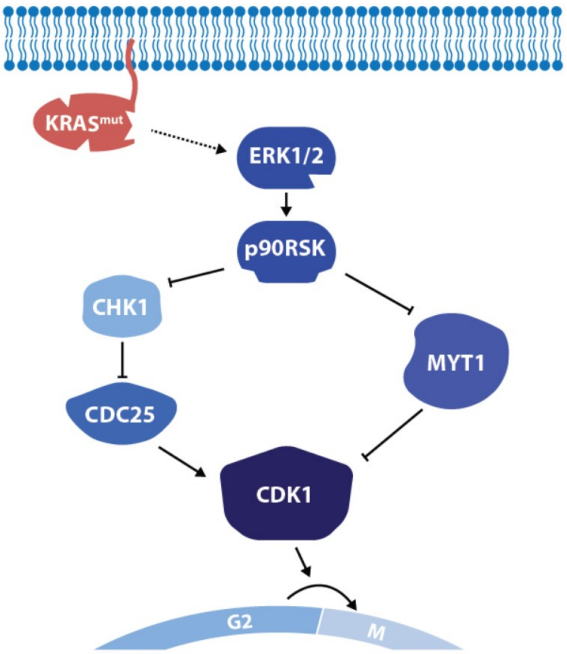

Figure 42: Hypothetical molecular impact of oncogenic KRAS on the G2/M transition. Mutant KRAS causes activation of p90RSK via its downstream targets ERK1/2 (Grabocka et al., 2014; Knauf et al., 2006). p90RSK inhibits MYT1 by phosphorylation and thus prevents MYT1 from inhibiting CDK1, thereby triggering entry into mitosis

(Palmer et al., 1998). Additionally, p90RSK can also phosphorylate CHK1 at the inhibitory site S280. Without CHK1 activity upon DNA damage, the phosphatase CDC25 remains active and removes inhibitory phosphorylations from CDK1, allowing cells to proceed into mitosis (Donzelli and Draetta, 2003; Ray-David et al., 2013).

No changes in the activity of the ERK1/2 downstream target p90RSK, as measured by the phosphorylation at T359/S363, were observed upon $KRAS^{G12V}$ expression or MCM7 knockdown. Similarly, the inhibitory phosphorylation site serine 280 in CHK1 showed no increase after $KRAS^{G12V}$ or MCM7.sh3 induction (Figure 43A). The CDK1 activating phosphatases CDC25B and CDC25C also showed no change in activation after neither after $KRAS^{G12V}$ expression nor after MCM7 knockdown (Figure 43B). In contrast, MYT1 was hyperphosphorylated after knockdown of MCM7. This hyperphosphorylation was highest after simultaneous MCM7 knockdown and $KRAS^{G12V}$ expression. $KRAS^{G12V}$ expression alone did not induce increased MYT1 phosphorylation. However, the inhibitory phosphorylation of MYT1 did not result in changes in CDK1 phosphorylation (Figure 43C).

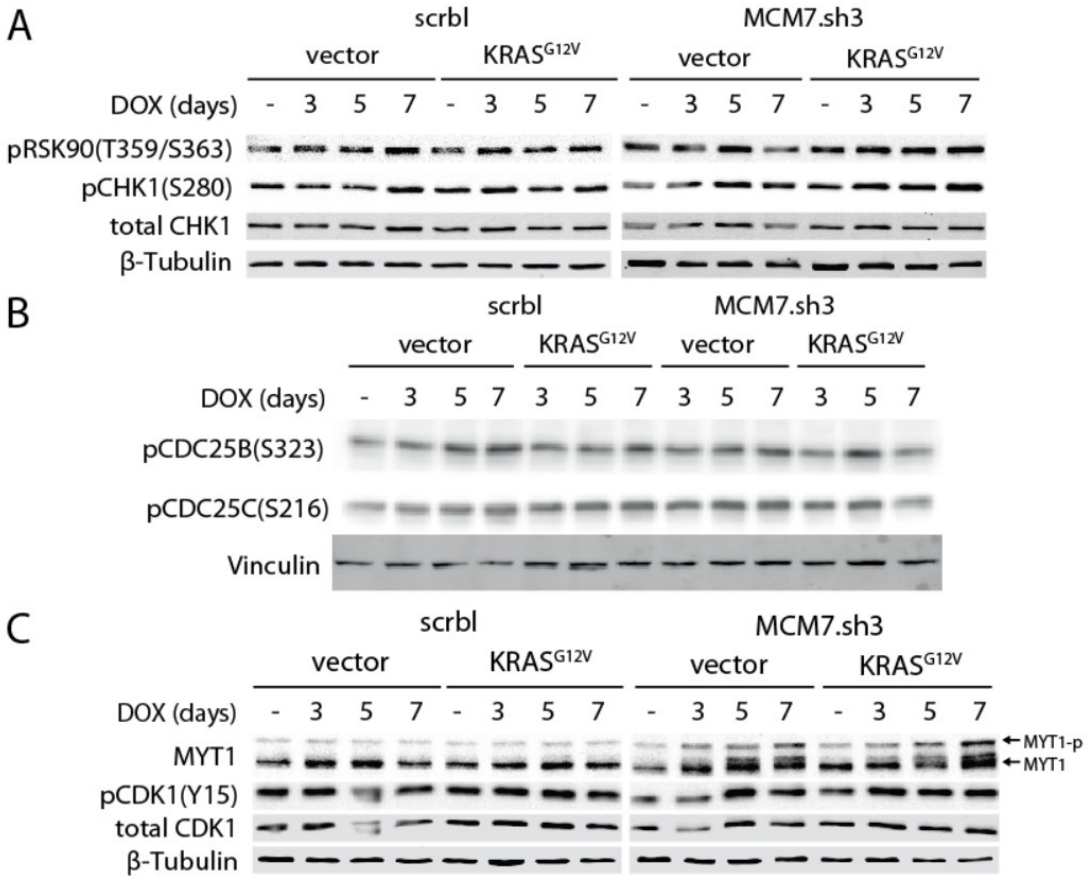

Figure 43: Analysis of G2/M checkpoint transition protein activation by western blot. CaCo2 cells were induced for 3, 5, and 7 days and then analyzed by western blot. (A) Phosphorylation of pRSK90 did not increase after 3, 5, or 7 days of doxycycline induction at the activating sites T359 and S363 in any of the samples. Similarly, CHK1 showed no increased inhibition by phosphorylation at S280. (B) The phosphatases CDC25B and CDC25C also exhibited no change in phosphorylation at S323 or S216, respectively. (C) MYT1 was hyperphosphorylated after MCM7 suppression. This was more prominent after simultaneous $KRAS^{G12V}$ expression. No change in the inhibitory phosphorylation at Y15 of CDK1 was observed. Vinculin and β-tubulin served as loading controls. Western blot was performed by Birgit Schaefer, medical technical assistant, Institute of Pathology, Charité.

To test the dynamics of CDK1 phosphorylation, the cells were treated with hydroxyurea to elicit inhibition of CDK1. However, despite the efficient reduction of MYT1 hyperphosphorylation upon hydroxyurea treatment, no increased CDK1 phosphorylation at Y15 was observed (Figure 44).

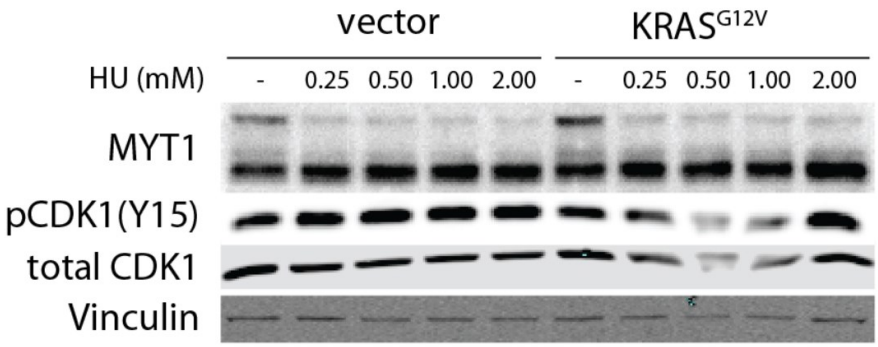

Figure 44: Western blot analysis of MYT1 and CDK1 phosphorylation after treatment with hydroxyurea. CaCo2 cells were induced with doxycycline for 3 days and treated with 0.25-2 mM hydroxyurea for 4 hours. Hyperphosphorylation of MYT1 was decreased after treatment with hydroxyurea. pCDK1(Y15) remained unchanged upon hydroxyurea treatment. Vinculin served as a loading control. Western blot was performed by Birgit Schaefer, medical technical assistant, Institute of Pathology, Charité.

2.7. Mutated KRAS confers increased sensitivity towards perturbation of replication fork progression

Currently, there are no pharmacological inhibitors of DNA replication licensing available. However, DNA replication as a process is a major target in cancer therapy. To assess whether KRAS-mutant cells are also sensitive to pharmacological perturbations of DNA replication progression, CaCo2 cells were exposed to hydroxyurea and oxaliplatin, which both lead to perturbations in DNA synthesis through different mechanisms. Hydroxyurea depletes the dNTP pool by inhibiting the ribonucleotide reductase and thereby prevents the incorporation of nucleotides during DNA replication, which leads to stalled replication forks (Singh and Xu, 2016; Yarbro, 1992). Oxaliplatin, on the other hand, inhibits replication by generating DNA inter- and intra-strand crosslinks (Alcindor and Beauger, 2011). Indeed, increased sensitivity of CaCo2 cells to hydroxyurea and oxaliplatin was observed when $KRAS^{G12V}$ was expressed. $KRAS^{G12V}$ expression in CaCo2 cells caused a shift in the IC_{50} of hydroxyurea from 207.3 µM (95% CI: 192.7 µM-223.0 µM) to 154.7 µM (95% CI: 142.1 µM-168.4 µM) upon $KRAS^{G12V}$ induction. Likewise, $KRAS^{G12V}$ expression resulted in a shift in oxaliplatin IC_{50} from 0.157 µM (95% CI: 0.1342 µM-0.1826 µM) to

0.076 µM (95% CI: 0.066 µM-0.088 µM) (Figure 45). These results suggest that mutant KRAS expression can indeed sensitize cells to perturbations of DNA replication.

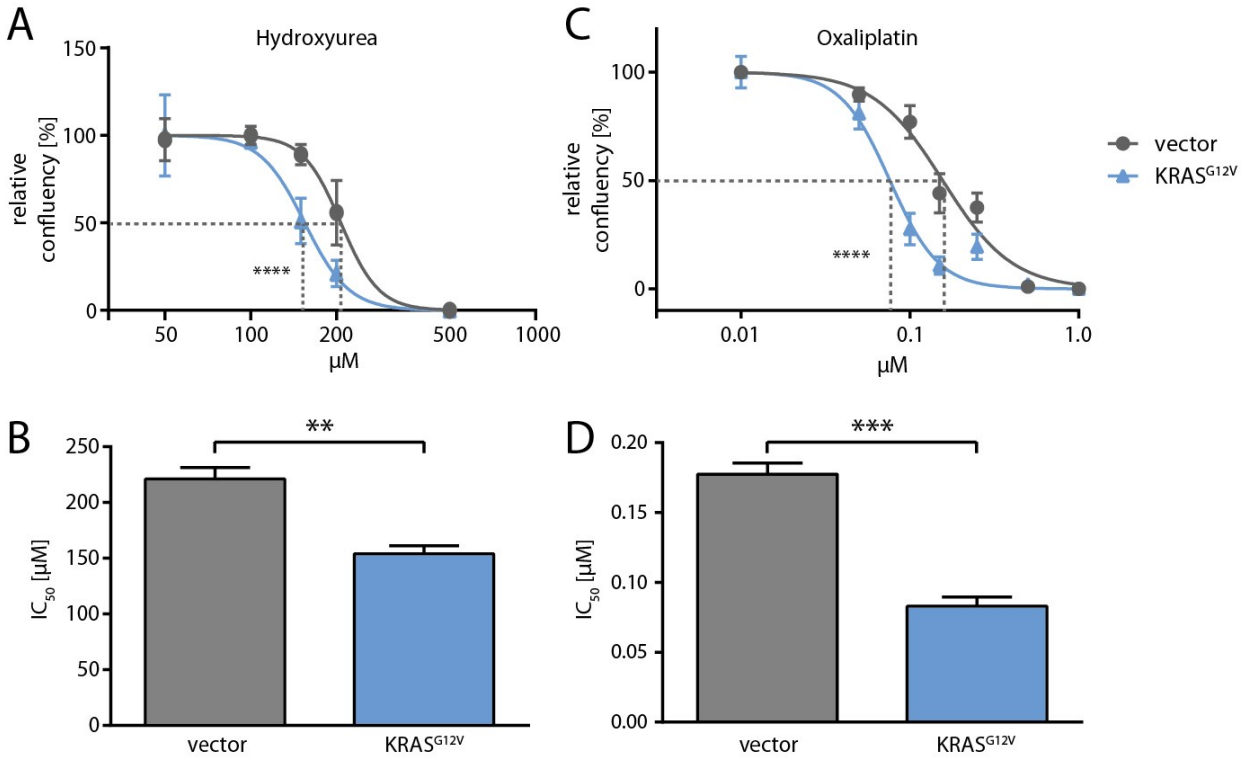

Figure 45: Perturbations of replication fork progression by hydroxyurea and oxaliplatin in CaCo2 cells. Hydroxyurea and oxaliplatin showed increased efficacy in KRAS-mutant CaCo2 cells. KRAS induction caused a shift in IC_{50} from 207.3 µM to 154.7 µM with hydroxyurea (R^2_{vector}=0.9379; $R^2_{KRAS(G12V)}$=0.9257) (A,B) and 0.157 µM to 0.076 µM with oxaliplatin (R^2_{vector}=0.9123; $R^2_{KRAS(G12V)}$=0.9155) (C,D). Mean relative confluency ± SEM is shown (n = 3-5 per group). Nonlinear regression - extra sum-of-squares F test; Mean IC_{50} ± SEM is shown (n = 3). Student's t-test (unpaired) (B,D); ** = $p < 0.01$; *** = $p < 0.001$; **** = $p < 0.0001$.

3. Discussion

KRAS is one of the most commonly mutated oncogenes in human cancers. Therefore, specific inhibition of oncogenic KRAS signaling would be an obvious choice for targeted cancer therapy. However, through the past decades, it has become clear that this is agonizingly difficult to achieve. Despite enormous efforts to specifically target KRAS mutant cells in cancer therapy, no sustainable treatment targeting KRAS directly has made its way to the clinic up to this date (Cox et al., 2014; Papke and Der, 2017). For a while, KRAS has even been coined "undruggable" (Cox et al., 2014). Figure 5 summarizes the different strategies of targeting oncogenic KRAS in cancer that have been explored so far. One of the approaches to target mutant KRAS is the concept of synthetic lethality (Figure 6). By inhibiting synthetic lethal interactors, cells with a specific alteration such as KRAS mutations can be targeted indirectly. This approach has been proven to be successful in BRCA-deficient ovarian cancers and breast cancers and thus the PARP inhibitor olaparib was approved by the FDA for the treatment of BRCA-deficient ovarian and breast cancer (Dziadkowiec et al., 2016; U.S. Food & Drug Administration, 2018).

To identify synthetic lethal interactors of oncogenic KRAS, I performed an RNAi screen in an isogenic CaCo2 cell culture model targeting genes, which have been previously found to be highly regulated upon MEK inhibition (Jürchott et al., 2010). I demonstrated that KRAS mutated colorectal cancer cells specifically rely on high MCM7 levels and its suppression is synthetically lethal with KRAS mutated cells.

3.1. Lethality of MCM7 knockdown in KRAS-mutant cancer cell lines

The synthetic lethality of MCM7 suppression in KRAS-mutant CaCo2 cells was predicted by one shRNA that was specifically depleted in the $KRAS^{G12V}$ induced samples after 14 and 21 days in the RNAi screen (Table 2, Figure 16). Subsequent validation with two additional and independent shRNAs confirmed the sensitivity of $KRAS^{G12V}$ expressing CaCo2 cells to the knockdown of MCM7 (Figure 17, Figure 20).

This indicates that the observed synthetic lethality is the result of a specific MCM7 suppression and not due to off-target effects. Additionally, it is worth noting that the strength of synthetic lethality correlated with the knockdown efficiency of the respective shRNAs. While the shRNAs MCM7.1879 and MCM7.sh3 showed a high knockdown efficiency and high synthetic lethality with $KRAS^{G12V}$, MCM7.1534v exhibited a lower potency of MCM7 suppression and $KRAS^{G12V}$ specific growth reduction. Thus, MCM7 was confirmed to act in a synthetic lethal manner with $KRAS^{G12V}$ in CaCo2 cells with three independent shRNAs (Figure 17, Figure 18). Importantly, overall MCM7 suppression led to a simultaneous depletion of chromatin-bound MCM2, but not of soluble MCM2 (Figure 19). This suggests that the knockdown was specific for MCM7 but the suppression of MCM7 expression led to a disruption of proper MCM complex formation or recruitment to the DNA as it was previously described (Ibarra et al., 2008). Therefore, by suppressing MCM7 expression, the entire origin licensing process could be targeted.

The specific growth reduction in $KRAS^{G12V}$ expressing CaCo2 cells after MCM7 suppression could at least partially be attributed to the induction of apoptosis as it was shown by the increased presence of cleaved PARP and cleaved caspase 3 (Figure 21, Figure 22). Nevertheless, a slight increase of apoptotic cells was also observed in CaCo2 cells that expressed MCM7.sh3 in the absence of $KRAS^{G12V}$, suggesting a mild toxicity of MCM7 suppression in the parental CaCo2 cells. However, decreased proliferation or non-apoptotic cell death mechanisms cannot be excluded to play an additional role in the observed overall growth reduction in $KRAS^{G12V}$ expressing cells after MCM7 suppression.

The synthetic lethality could additionally be verified in an isogenic DLD-1 cell culture model. In contrast to KRAS wild-type CaCo2 cells, DLD-1 cells harbor an endogenous $KRAS^{G13D}$ mutation (Ahmed et al., 2013). Indeed, the parental DLD-1 ($KRAS^{wt/G13D}$) cells were more sensitive to MCM7 suppression than their derivative KRAS wild-type DLD-1 ($KRAS^{wt/-}$), confirming the observations made in the CaCo2 cell culture model (Figure 17, Figure 24). However, in contrast to the CaCo2 model, DLD-1 cells without oncogenic KRAS showed a marked growth reduction after MCM7 knockdown. The reason for this sensitivity is not clear. It is possible that the DLD-1 $KRAS^{G13D}$ knockout clone has adapted in a way that phenocopies the lacking oncogenic KRAS signal. This is further

supported by increased endogenous activation of ERK1/2 in DLD-1 ($KRAS^{wt/-}$) compared to DLD-1 ($KRAS^{wt/G13D}$) cells (not shown, data courtesy of Sylvia Ispasanie, Institute of Pathology, Charité). In addition, DLD-1 cells might exhibit higher endogenous replication stress, which requires higher levels of DNA replication licensing.

Lastly, a panel of four non-isogenic colorectal cancer cell lines showed a sensitivity to MCM7 suppression (Figure 26). Interestingly, not only the KRAS-mutant cell lines SW480 and HCT-8, but also the KRAS wild-type HT-29 and WiDr cells were sensitive to the knockdown of MCM7. Both HT-29 and WiDr harbor a $BRAF^{V600E}$ mutation that leads to constitutive activation of the MAPK pathway (Ahmed et al., 2013; Davies et al., 2002) and might function as a substitute for the sensitizing KRAS mutation. This would indicate a central role of MAPK signaling, which was however not further investigated.

In summary, the presented data showed that KRAS mutations sensitize colorectal cancer cells to decreased replication licensing via the suppression of the replication factor MCM7. Additionally, colorectal cancer cells with constitutive MAPK activity via $BRAF^{V600E}$ mutations exhibited a strong sensitivity to the knockdown of MCM7.

3.2. KRAS and replication stress

The major distinctive phenotype induced in $KRAS^{mut}$ cells after MCM7 knockdown was the presence of RPA foci, which is considered to be a hallmark of replication stress (Zeman and Cimprich, 2014; Zou and Elledge, 2003; Zou et al., 2000). $KRAS^{G12V}$ expressing CaCo2 cells showed a drastic increase in replication stress as indicated by nuclear RPA2 focalization and phosphorylation (Figure 28, Figure 29). Consistent with the observed replicative stress, increased CHK1 activation was specifically detected in cells with simultaneous $KRAS^{G12V}$ expression and MCM7 knockdown (Figure 34). Additionally, an increase of RPA2 focalization upon MCM7 knockdown was observed in the KRAS-mutant cell lines DLD-1 and SW480 (Figure 30). As mentioned in 1.3.2 RAS and replication stress, RPA binds single-stranded DNA, which is abundantly present in stalled replication forks. Stalled replication forks and unreplicated DNA are a hallmark

of replication stress, which renders RPA focalization a robust marker for replication stress (Zeman and Cimprich, 2014; Zou and Elledge, 2003; Zou et al., 2000).

Interestingly, $KRAS^{G12V}$ expression alone did not cause any observable replication stress in CaCo2 cells (Figure 28, Figure 29). This finding is in strong contrast to previous publications, which show that oncogenic RAS expression alone causes replication stress (reviewed in 1.3.2 RAS and replication stress). Di Micco and colleagues, for example, showed that expression of oncogenic $HRAS^{G12V}$ expression in normal human fibroblasts leads to a marked increase of RPA foci formation (Di Micco et al., 2006). However, the authors worked with a strong overexpression of mutant HRAS, which is not considered to reflect physiological conditions. While amplifications (~0.5-1.6% of patients) and upregulation of gene expression (~5-7% of patients) of the RAS homologs do occur in colorectal cancer patients, most patients show unaltered expression levels of RAS compared to a reference population (Cerami et al., 2012; Muzny et al., 2012). Therefore, high RAS overexpression could result in observations that do not reflect normal cancer biology. Nevertheless, nine publications cited in 1.3.2 RAS and replication stress that showed replication stress upon oncogenic RAS expression used cell culture models with high RAS overexpression (Aird et al., 2013; Kotsantis et al., 2016; Lee et al., 1999; Mannava et al., 2013; Maya-Mendoza et al., 2015; Di Micco et al., 2006; Mitsushita et al., 2004; Ogrunc et al., 2014; Weyemi et al., 2012). Only Irani and colleagues used a cell culture model with ectopic HRAS expression close to endogenous levels (Irani et al., 1997). Four publications did not indicate the respective RAS expression levels (Filmus et al., 1994; Hitomi and Stacey, 1999; Knauf et al., 2006; Liu et al., 1995). This begs the question: Does oncogenic KRAS expression at physiological levels actually result in enough replication stress to disturb cell proliferation and survival? Ectopic oncogenic RAS expression is commonly attributed to cause oncogene-induced senescence due to increased replication stress (Dimauro and David, 2010). Expression of $KRAS^{G12V}$ at low levels in CaCo2 cells, however, had no observable effect on cell growth as well as on replication stress. Only in combination with knockdown of MCM7, a pronounced increase in replication stress was detected (Figure 11, Figure 12, Figure 28, Figure 29). This suggests that oncogenic KRAS expression at low levels alone is not sufficient to cause detectable replication stress. However, oncogenic KRAS expression can

sensitize cells towards additional perturbations of replication in the form of decreased origin licensing. Furthermore, knockdown of MCM7 alone did not lead to an increase of RPA focalization in CaCo2 cells. This result is consistent with previous findings, which showed that MCM2-7 levels can be decreased several-fold in human cancer cells (U2OS and HeLa) without major effects on replication (Ge et al., 2007; Ibarra et al., 2008). The strong reduction of MCM2-7 levels is probably possible because about 90% of licensed origins remain dormant during unperturbed replication and are only activated upon nearby fork stalling to resume DNA replication (Burkhart et al., 1995; Mahbubani et al., 1997; McIntosh and Blow, 2012; Wong et al., 2011). Therefore, decreased origin licensing can be compatible with cell proliferation in the absence of additional replication stress such as oncogene-induced origin firing.

How $KRAS^{G12V}$ expression causes this additional replication stress that sensitizes cells to MCM7 suppression is not entirely clear. Oncogenic $HRAS^{G12V}$ expression has previously been shown to cause decreased distance between active replicons – a sign for increased origin firing (Hills and Diffley, 2014; Di Micco et al., 2006). This finding is substantiated by the increased resistance of KRAS-mutant cells to inhibition of origin firing with the CDC7 inhibitor PHA 767491 (Figure 33). Moreover, pharmacological inhibition of origin firing with PHA 767491 could partially counteract the $KRAS^{G12V}$ dependent lethality of CaCo2 cells after MCM7 knockdown (Figure A 1). Therefore, it is plausible that $KRAS^{G12V}$ expression triggers origin firing, which additionally to the MCM7 knockdown further reduces the presence of dormant origins. As a consequence, KRAS-mutant cells would have an increased dependency on high levels of DNA replication licensing components. Still, the exact mechanism by which RAS increases origin firing is not yet clear. One possibility is that RAS directly regulates origin firing by modulating CHK1 activity via p90RSK. Since CHK1 controls dormant origin firing, RAS driven inhibition of CHK1 could lead to increased origin firing (Blow et al., 2011; Ge and Blow, 2010; Ray-David et al., 2013). However, no indications for this could be detected in CaCo2 cells by western blot analysis (Figure 43). Another possibility is the RAS-dependent upregulation of cyclins and CDKs that promote origin firing (Hills and Diffley, 2014). Finally, increased origin firing by RAS could merely be an indirect effect. It is possible that excessive dormant origin firing is due to increased replicative stress caused by RAS-dependent dNTP depletion (Aird et al., 2013; Bester

et al., 2011; Mannava et al., 2013), ROS accumulation (Irani et al., 1997; Lee et al., 1999; Ogrunc et al., 2014), and increased transcription (Kotsantis et al., 2016). These processes could trigger additional firing of dormant origins.

In summary, mutant KRAS expression is likely to cause replication stress. However, the extent of this stress is probably low when oncogenic KRAS is expressed at physiological levels. Nevertheless, the mild replication stress caused by mutant KRAS can sensitize cells towards decreased replication origin licensing as seen with the suppression of MCM7 expression.

3.3. KRAS, MCM7 knockdown, and their influence on the cell cycle

Depletion of DNA replication licensing factors such as ORC, CDC6, or CDT1, or MCM2-7 itself prevents full licensing of DNA replication origins. It was previously reported that inhibition of DNA replication origin licensing leads to the activation of the licensing checkpoint in G1. Activation of this checkpoint prevents cells from entering S-phase with an under-licensed genome, which would render cells susceptible to replication stress due to the reduction of dormant origins (Feng et al., 2003; Machida et al., 2005; McIntosh and Blow, 2012; Shreeram et al., 2002). Conversely, decreasing origin licensing in CaCo2 cells by knockdown of MCM7 did not lead to an accumulation in G1, indicating that the licensing checkpoint is not being activated in CaCo2 cells. Instead of a G1 arrest, CaCo2 cells accumulated in G2/M following MCM7 knockdown independently of $KRAS^{G12V}$ expression (Figure 35). It was previously suggested that the tumor suppressor p53 is required for a sufficient G1 arrest as a response to the licensing checkpoint (Nevis et al., 2009). CaCo2 cells, as well as the majority of colorectal cancers, harbor TP53 alterations that render it p53-deficient (Ahmed et al., 2013; The Cancer Genome Atlas, 2012). This can explain why CaCo2 cells lack a functional licensing checkpoint. The observed cell cycle delay in G2/M is also in line with previous findings by Ibarra and colleagues, who showed an accumulation in G2/M in cancer cell lines after MCM2 and MCM3 knockdown (Ibarra et al., 2008). The G2/M

checkpoint activation is likely the result of DNA damage caused by stalled and unresolved replication forks in the absence of p53.

While there was no difference in the G2/M accumulation after MCM7 suppression in KRAS wild-type or KRAS-mutant CaCo2 cells, $KRAS^{G12V}$ expressing cells showed a marked increase in the number of mitotic cells (Figure 36, Figure 37). This might suggest that oncogenic KRAS can deregulate the G2/M checkpoint and drive cells into mitosis. Mutant KRAS and HRAS signaling have previously been shown to overwrite the G2/M checkpoint by activating p90RSK via ERK (Grabocka et al., 2014; Knauf et al., 2006). p90RSK can phosphorylate CHK1 at its inhibitory site S280 and thereby prevents DNA damage-induced inhibition of CDC25. Active CDC25, in turn, activates the mitotic kinase CDK1 by dephosphorylation and initiates mitosis (Donzelli and Draetta, 2003; Ray-David et al., 2013). Additionally, p90RSK has been shown to regulate mitotic entry through MYT1 inhibition, which is an inhibitory kinase of CDK1 (Palmer et al., 1998). Thus, oncogenic KRAS might shift the CDC25/MYT1 balance towards mitosis promoting CDC25 and away from MYT1, thereby overwriting the G2/M checkpoint (Figure 42).

However, western blot analysis of p90RSK(T359/S363), CHK1(S280), CDC25B(S323), CDC25C(S216), as well as CDK1(Y15) showed no marked difference in their respective activation status in a $KRAS^{G12V}$ dependent manner. Only MYT1 exhibited strong hyperphosphorylation upon simultaneous $KRAS^{G12V}$ expression and MCM7 knockdown. Yet, this signal was not noticeably transduced to CDK1 (Figure 43). The increased hyperphosphorylation of MYT1 is also not necessarily proof of increased G2/M transition signaling since MYT1 is inhibited by hyperphosphorylation throughout mitosis (Booher et al., 1997; Chow and Poon, 2013) and CaCo2 cells showed an increased mitotic population after $KRAS^{G12V}$ expression and MCM7 knockdown (Figure 36, Figure 37). Thus, increased MYT1 hyperphosphorylation could be solely due to an increased number of mitotic cells.

To test whether the inhibitory phosphorylation of CDK1 can be detected by western blot at all in CaCo2 cells, the cells were exposed to different concentrations of hydroxyurea, which has been shown to elicit CDK1 phosphorylation at Y15 (Chow and Poon, 2013). While MYT1 efficiently lost its hyperphosphorylation at all tested hydroxyurea concentrations, inhibition of CDK1 could not be detected (Figure 44). This

indicates that changes in CDK1 activity might be below the detection limit of western blot assays in asynchronous CaCo2 cells. On the other hand, it cannot be ruled out entirely that the reason no change in CDK1 inhibition was observed is that CaCo2 cells are possibly deficient in the G2/M checkpoint control regulation in general. This, however, is unlikely to fully explain why no CDK1 inhibition could be detected since a consistent accumulation of cells in G2/M was observed after MCM7 knockdown that could not completely be attributed to cells in mitosis (Figure 35, Figure 36). Also, results from RNA sequencing data derived from CaCo2 $KRAS^{G12V}$ cells showed a two-fold upregulation of the CDK1 interaction partner cyclin B3. The binding of cyclin B3 to CDK1 is required for CDK1 activity. Therefore, increased cyclin B3 levels could promote the transition from G2 to M in a KRAS dependent manner (not shown, data courtesy of Sylvia Ispasanie, Institute of Pathology, Charité). Similar observations have been made by Knauf and colleagues, who showed that oncogenic HRAS causes an upregulation of cyclin B1 that lead to an accelerated G2/M transition (Knauf et al., 2006).

While the role of oncogenic KRAS in the G2/M transition is not fully understood, it is clear that $KRAS^{G12V}$ expressing cells could enter mitosis despite the presence of DNA perturbations. Cells that were depleted for MCM7 and expressed $KRAS^{G12V}$ simultaneously displayed an increased number of mitotic cells and exhibited DNA damage in mitosis as marked by γH2AX foci accumulation (Figure 36, Figure 37, Figure 38, Figure 39). The high ratio of mitotic cells with DNA damage was not observed in cells with only MCM7 suppression or only $KRAS^{G12V}$ expression (Figure 38, Figure 39). The DNA perturbations in mitotic KRAS-mutant cells after MCM7 knockdown were likely derived from increased levels of unresolved replication stress (Figure 28, Figure 29).

In summary, knockdown of MCM7 caused a shift in the cell cycle from G1 to G2/M independent of oncogenic KRAS expression. Published data suggest that oncogenic RAS signaling can accelerate the G2/M transition. From the data presented here, however, it is not entirely clear to which extend oncogenic KRAS signaling contributes to the G2/M transition in the presence of replication stress. Therefore, further experiments are required to fully elucidate the connections between mutant KRAS and

the G2/M checkpoint. Still, it is clear that $KRAS^{G12V}$ expressing cells specifically exhibited a mitotic delay and DNA damage during mitosis.

3.4. Mechanism of KRAS-mutant cell's sensitivity to MCM7 suppression

During my work, I showed that KRAS-mutant cells are specifically susceptible to MCM7 suppression. The mechanism behind this sensitivity is that KRAS-mutant cells showed higher levels of replication stress after MCM7 suppression, which resulted in unreplicated DNA (Figure 28, Figure 30). Unreplicated DNA cannot be resolved through conventional replication once there are no dormant origins remaining to resolve sites of stalled replication forks as origins cannot be re-licensed in G2 (Klotz-Noack et al., 2012; Nishitani and Lygerou, 2002). Homologous recombination has been suggested as a possible mechanism to rescue stalled replication forks and complete DNA replication in G2 (Michel et al., 2001). However, when cells fail to resolve stretches of unreplicated DNA before entering mitosis, they become prone to mitotic catastrophe (Aarts et al., 2012; O'Connor, 2015). This was specifically observed in cells expressing $KRAS^{G12V}$ after MCM7 knockdown as marked by the presence of γH2AX foci in mitotic cells (Figure 38, Figure 39). Additionally, $KRAS^{G12V}$ expressing cells showed the highest proportion of cells with randomly distributed chromosomes throughout the cell and massive chromosomal aberrations during mitosis (Figure 40, Figure 41), which is characteristic for mitotic catastrophe (Vakifahmetoglu et al., 2008). In conclusion, my work provides evidence that even low levels of oncogenic KRAS expression sensitize colorectal cancer cells to inhibition of DNA replication origin licensing via the suppression of the replication factor MCM7. Mechanistically, KRAS-mutant cells – in comparison to KRAS wild-type cells - displayed higher levels of unreplicated DNA after MCM7 knockdown that could not be resolved before entering mitosis. The presence of unreplicated DNA in mitosis led to a strongly perturbed mitosis, resulting in mitotic catastrophe followed by cell death. The mechanism behind the synthetic lethality of MCM7 suppression with mutant KRAS cancer cells is summarized in Figure 46.

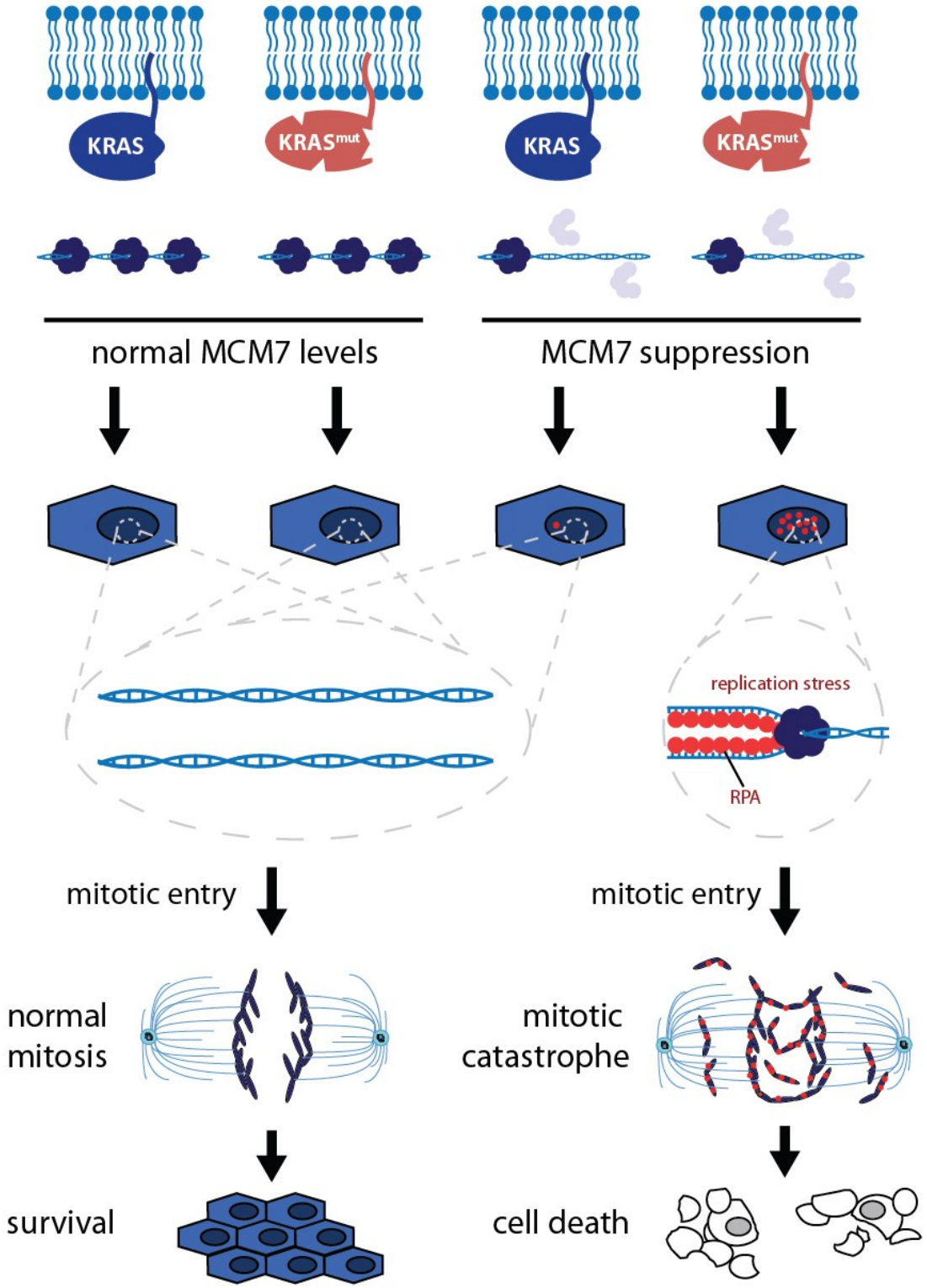

Figure 46: Mechanism of synthetic lethality of mutant KRAS and MCM7 suppression. Knockdown of MCM7 in KRAS-mutant cells causes excessive replication stress, which results in unreplicated DNA. The presence of unreplicated DNA in mitosis leads then to mitotic catastrophe and cell death.

There are three potential outcomes of mitotic catastrophe: cell death by either apoptosis or necrosis, senescence, and survival with aneuploidy or polyploidy. Cells can either succumb without completing mitosis or die a mitotic death. This can happen in a directed apoptotic death or in undirected necrosis. In contrast, cells can complete mitosis after mitotic catastrophe and become senescent or die in the following G1 phase. However, cells can potentially also continue to proliferate with aneuploid or polyploid nuclei (Figure 47) (Vitale et al., 2011).

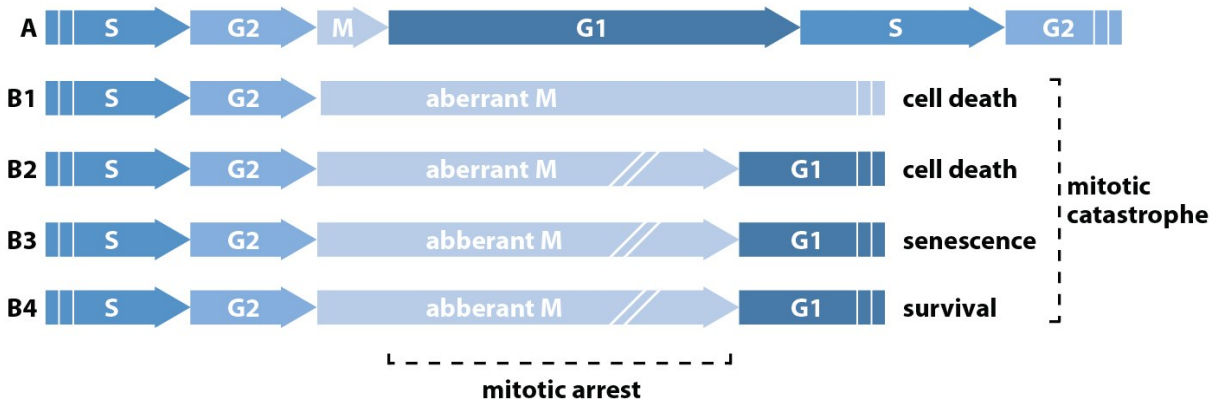

Figure 47: Potential cell fates after mitotic catastrophe. (A) Unperturbed cells progress normally through all cell cycle phases. Cells with perturbations during mitosis exhibit a mitotic arrest followed by mitotic catastrophe. There are three main outcomes of mitotic catastrophe: Cells can (B1) fail to exit mitosis and therefore die directly in mitosis, (B2) exit mitosis and die in the following G1 phase, (B3) become senescent in G1 after mitotic exit, (B4) or continue proliferating as aneuploid or polyploid cells (adapted from Vitale et al., 2011).

There is evidence that some cells completed mitosis despite the presence of unreplicated DNA since co-localization of RPA foci and 53BP1 nuclear bodies were observed (Figure 31). 53BP1 has been implicated in the repair of under-replicated DNA after mitosis, suggesting increased transmission of unreplicated DNA through cell division (Lukas et al., 2011; Moreno et al., 2016). This can then result in apoptosis or senescence as mentioned above (Figure 47). Even though senescence following mitotic catastrophe cannot be excluded entirely, it is probably not the main mechanism of growth reduction. Senescent cells would be expected to accumulate in G1 after mitotic catastrophe (Vakifahmetoglu et al., 2008), however, there was no significant increase in the G1 cell cycle population observed (Figure 35). Additionally, cells could

be equally well synchronized in mitosis with nocodazole independent of $KRAS^{G12V}$ expression or MCM7 knockdown, which indicates that most cells still show an active cell cycle (Figure A 2). On the other hand, only about 10% of $KRAS^{G12V}$ and MCM7.sh3 co-expressing cells exhibited an induction of the apoptosis marker cleaved caspase 3 (Figure 22). Additional necrotic cell death could explain the strong $KRAS^{G12V}$ dependent growth reduction after MCM7 knockdown. Therefore, it is likely that $KRAS^{G12V}$ and MCM7.sh3 co-expressing cells died from a combination of necrosis and apoptosis due to mitotic catastrophe.

3.5. Limitations

3.5.1. RNAi screen

The RNAi screen performed far below expectations and the raw results obtained from it should be regarded with caution. From 121 genes, only one gene (ENO1) showed a $KRAS^{G12V}$ specific effect on cell proliferation with two independent shRNAs at both day 14 and day 21 in the screen (Table A 2). Despite this, a $KRAS^{G12V}$ specific lethality could not be validated for ENO1 in long-term growth assays. In fact, out of the 19 genes that were selected for further validation, only MCM7 could be verified with more than one shRNA to cause a $KRAS^{G12V}$ specific effect on cell growth (due to the low level of synthetic lethality with $KRAS^{G12V}$ found in DNAJC2, PPP2R5A, and SPRY1 with one shRNA, no further shRNAs were tested) (Figure 17). Interestingly, although suppression of MCM7 was successfully identified to be synthetic lethal with mutant KRAS, only one out of the five shRNAs in the RNAi screen showed $KRAS^{G12V}$ specific lethality (Table A 2).

There are multiple reasons for the poor performance of the shRNA screen: First, CaCo2 cells that were used is the screen are not an ideal cell line for proliferation screens. CaCo2 cells are rather slowly proliferating cells with a doubling time of over 30 h (inferred from live cell imaging growth curves). Therefore, specific and detectable depletion of shRNAs during the selection period might remain below thresholds even after 21 days. Additionally, CaCo2 cells have retained a solid epithelial phenotype with

strong cell-cell adhesion. This makes it difficult to obtain single cell suspensions when passaging the cells during the screen. Both of these attributes hamper efficient selection in a proliferation screen. In retrospect, the faster proliferating DLD-1 cells might have been a more promising choice as an isogenic KRAS-mutant cell culture model and should be considered for future screening attempts.

Another culprit is the shRNA technology. Testing of several shRNAs targeting a single gene by Kathleen Klotz-Noack (Institute of Pathology, Charité) revealed that on average only three out of five shRNAs produced a knockdown of more than 50% of the target gene expression levels (data not shown). Additionally, the knockdown efficiency can vary vastly between different shRNAs. Therefore, shRNAs with merely a mild knockdown might not elicit a functionally relevant effect in the cell. An alternative to shRNA screens are CRISPR/Cas screens. CRISPR is a technology that allows a fast and specific knockout of genes of interest, which ideally results in a complete loss of function of the gene. Knockdown of genes with shRNAs, on the other hand, causes merely a decrease in the abundance of a gene product. Therefore, even an efficient knockdown of a gene product that functions at low abundances might not be sufficient to effectively block its function. A systematic comparison of shRNA and CRISPR screens by Evers and colleagues showed that CRISPR knockout screens outperform shRNA screens in several aspects. The CRISPR knockout screens showed a lower variability between separate screens and less off-target effects than shRNA screens. This resulted in overall decreased noise in CRISPR screens (Evers et al., 2016). Therefore, CRISPR screens might produce more reliable results in screens in the future.

Nevertheless, shRNA screens clearly have some merit. MCM7 would not have been identified if a CRISPR screen had been employed instead of an RNAi screen. The MCM complex is essential for proliferation. In a CRISPR screen that strived to identify essential genes in the human genome, constructs against all MCM2-7 components were found to be strongly depleted (Wang et al., 2015). Since shRNAs merely reduce the abundance of a gene product, some residual activity remains. In the case of MCM2-7, this residual protein amount is enough for proliferation in otherwise unperturbed cells (Ge et al., 2007; Ibarra et al., 2008).

In conclusion, for future screening endeavors, it is recommended to change the cell culture model to a more suitable cell line that exhibits a higher proliferation rate and has a lower cell-cell adhesion. Additionally, CRISPR knockout screens should be preferred over RNAi screens for more reliable results, even with the disadvantages of missing subtle quantitative effects.

3.5.2. Targeting DNA replication licensing in cancer therapy

This work demonstrated that KRAS-mutant cancer cells are susceptible to decreased DNA replication licensing in cell culture models. Therefore, the next step is to theoretically assess if targeting DNA replication licensing could be a viable strategy in cancer therapy.

A major drawback of inhibiting DNA replication licensing in therapy is that only proliferating cells are targeted, similar to other conventional chemotherapies like oxaliplatin or irinotecan. Only proliferating cells require DNA replication licensing. In fact, cells in a quiescent G0 phase downregulate replication licensing factors such as CDC6 and MCM2-7 (Song et al., 2013). Quiescent cancer stem cells can reside in tumors in a senescence-like G0 cell cycle phase and possess the ability to re-enter the cell cycle (Chen et al., 2016). Therefore, quiescent cells would be entirely unaffected by the treatment and could allow the tumor to re-emerge after treatment as it is observed in many other therapeutic approaches (Housman et al., 2014).

Another concern is cells that slip through perturbed mitosis and manage to stay viable as aneuploid cells after decreased replication licensing induced chromosomal instability (CIN). CIN is associated with aneuploidy in cancer and is linked to drug resistance and an overall poor patient outcome (McGranahan et al., 2012). This is probably due to the fact that chromosomally aberrated tumors exhibit increased intra-tumor heterogeneity and therefore an evolutionary advantage of having more chromosomes and thereby a higher chance of functionally beneficial mutations (McGranahan et al., 2012). Therefore, any treatment that drives cancer cells into mitotic catastrophe might show promising results in short-term, however, could potentially have detrimental effects in the long run.

Additionally, it is difficult to estimate the potential toxicity of decreased replication licensing compared to standard chemotherapy since the sensitivity of MCM7 suppression was only tested in cancer cell lines and no healthy cell lines in this study. Considering that DNA replication licensing is an essential process in all proliferating cells, targeting replication licensing might not come entirely without adverse effects. Nonetheless, previous data suggests it might be a viable approach with low toxicity. For example, while mice with decreased replication origin licensing due to MCM2 level reduction are cancer-prone (Pruitt et al., 2007), patients with Meier-Gorline Syndrome, which is caused by mutations in proteins required for replication licensing, show a primordial dwarfism phenotype but no higher cancer incidence rate. They also do not show severely health compromising symptoms (Bicknell et al., 2011; Bongers et al., 2001; Klingseisen and Jackson, 2011). Furthermore, MCM2-7 levels can be decreased several-fold in human cells without major effects on replication (Ge et al., 2007; Ibarra et al., 2008). This is most likely due to the fact that most origins stay dormant, only a small fraction of the licensed origins (~10%) is used during unperturbed replication. This might suggest a low toxicity of a potential therapy targeting replication licensing for normal cells. Additionally, the presence of the licensing checkpoint might prevent healthy cells from entering S-phase before the genome is fully licensed (Feng et al., 2003). This could avert healthy cells from experiencing replication stress caused by inhibition of origin licensing. However, further investigations are necessary to draw a definitive conclusion about potential toxicities.

3.6. Outlook

While there are no direct replication licensing inhibitors available at the time of writing, there are efforts being made to develop inhibitors of DNA replication licensing. Currently, there are nanobodies in development in the Stephen Bell lab (Massachusetts Institute of Technology, USA) that inhibit loading of the replicative helicase onto the origins of replication (according to a personal conversation with Lorraine De Jesús Kim, Massachusetts Institute of Technology, USA). It will be interesting to further

investigate our findings in clinically relevant models with a small molecule inhibitor of replication licensing.

Additionally, this work indicates that oncogenic KRAS can sensitize cells to agents that interfere with DNA replication such as hydroxyurea and oxaliplatin (Figure 45). Therefore, eliciting replication stress by additional means than decreased origin licensing might also be a viable approach to specifically target KRAS-mutant cancer cells. That notion is further strengthened by previous studies that came to similar results (Lin et al., 2014; Steckel et al., 2012).

On the contrary, inhibiting origin firing might result in a low efficacy in KRAS-mutant cancers as increased resistance to CDC7 inhibition was shown in KRAS-mutant cells (Figure 33). This is probably because mutant KRAS results in aberrant origin firing as it has been reported for $HRAS^{G12V}$ expressing cells (Di Micco et al., 2006). This could explain why mutant KRAS can rescue cells from CDC7 inhibition. At the time of writing, Cancer Research UK and Millennium Pharmaceuticals, Inc. are recruiting patients for phase I clinical trials to test the CDC7 inhibitor LY3143921 and TAK-931, respectively, in a variety of solid tumors including highly KRAS mutated cancers such as colorectal cancer, pancreatic cancer and lung cancer (clinicaltrials.gov, identifiers: NCT03096054, NCT02699749). According to the results presented here, patients with KRAS mutated tumors might show lower treatment efficacy. To better interpret the results of the study, it could be helpful to stratify patient groups in KRAS wild-type and mutant patients.

In conclusion, the data collected during this work is unlikely to be directly translated into a cure for KRAS-mutant colorectal cancer patients. However, it sheds more light on the mechanism how mutant KRAS sensitizes cancer cells to additional replication stress. Hopefully, these insights will provide a valuable foundation for future studies to further elucidate how KRAS influences DNA replication and how these properties can be exploited in cancer therapy.

4. Materials and Methods

4.1. Materials

4.1.1. Consumables

Table 3: Consumables

Product	Manufacturer	#
0.45 µm syringe filters	Sarstedt	83.1826
96 Well PCR plate, colorless, "Fast" Type	Biozym	710888
Adhesive Clear qPCR Seals, Sheets	Biozym	600238
Amersham Protran 0.2 NC	GE Healthcare	10600001
Cell Scraper 2-Posit. Blade 25	Sarstedt	83.1830
CellTrics 30 µm, sterile	Sysmex Partec GmbH	04-004-2325
CryoPure Tube 1.8 ml	Sarstedt	72.379
Falcon® 100 mm Cell Culture Dish	Corning	353003
Falcon® 12 Well Clear Flat Bottom plates	Corning	353043
Falcon® 15 ml Conical Centrifuge Tubes	Corning	352097
Falcon® 150 mm Cell Culture Dish	Corning	353025
Falcon® 175cm² Rectangular Straight Neck Cell Culture Flask with Vented Cap	Corning	353118
Falcon® 25cm² Rectangular Canted Neck Cell Culture Flask with Vented Cap	Corning	353108
Falcon® 50 ml Conical Centrifuge Tubes	Corning	352098
Falcon® 5mL Round Bottom Polystyrene Test Tube	Corning	352054
Falcon® 6 Well Clear Flat Bottom plates	Corning	353046
Falcon® 75cm² Rectangular Canted Neck Cell Culture Flask with Vented Cap	Corning	353136
Falcon® 96 Well Clear Flat Bottom plates	Corning	353072
Falcon® Polystyrene Serological Pipets (5 ml, 10 ml, 25 ml)	Corning	357543, 357551, 357525
Microscope cover glasses	VWR	631-1578
Microscopy slides	R. Langenbrinck	03-0004
Pasteur pipettes	Brand GmbH	7477 20
Phase Lock Gel light tubes	5 Prime	2302800
Pipette Filter Tips Biosphere (10 µl, 100 µl, 300 µl, 1000 µl, 1250 µl)	Sarstedt	70.1116.210, 70.760.212, 70.765.210, 70.762.211
SafeSeal 0.5 ml PCR tubes	Sarstedt	72.704
SafeSeal 1.5 ml reaction tubes	Sarstedt	72.706
SafeSeal 2.0 ml reaction tubes	Sarstedt	72.695.500
Whatman® cellulose papers	GE Healthcare	3030-931

Table 4: Commercial kits

Product	Manufacturer	#
Amplitaq Gold	Applied Biosystems	N8080241
GoTaq qPCR Master Mix	Promega	A6002
High-Capacity cDNA ReverseTranscription Kit	Roche	4368814
Phusion High-Fidelity DNA Polymerase	Thermo Fisher	F-553L
Pierce BCA protein assay kit	Thermo Fisher	23225
QIAGEN Plasmid Maxi Kit	QIAGEN	12163
QIAGEN Plasmid Midi kit	QIAGEN	12145
QIAGEN Plasmid Mini kit	QIAGEN	12125
QIAquick gel extraction kit	QIAGEN	28704
QIAquick PCR Purification kit	QIAGEN	28104
RNase-free DNase Set	QIAGEN	79254
RNeasy Mini kit	QIAGEN	74104

4.1.2. Devices

Table 5: Devices

Product	Manufacturer
8-Channel Multipipet 300 µl Xplorer	Eppendorf
Agarose gel chamber	Bio-Rad
ASPIRE Laboratory Aspirator	Accuris
Balance BP toploader 2100S	Sartorius
Balance RC210P	Sartorius
BD Accuri C6 flow cytometer	BD Biosciences
Bioruptor	Diagenode
Camera Lumix DMC-TZ3	Panasonic
Camera Nexus 5X	LG
Centrifuge 5415C	Eppendorf
Centrifuge 5417R	Eppendorf
Centrifuge 5810	Eppendorf
Centrifuge 8510R	Eppendorf
Centrifuge Avanti J-25	Beckman
Clean Bench LaminAir HBB2448	Heraeus
Clean Bench Maxisafe 2020	Thermo Fisher
Clean Bench NU-437-600E	NuAire
Electrophoresis power supply EPS 200	Amersham parmacia biotech
Electrophoresis power supply EPS 301	Amersham parmacia biotech
Electrophoresis power supply PowerPac 300	Bio-Rad
FACSAria II	BD Biosciences
FluorChem M System	Protein Simple
Incubator B6120 microbiological	Heraeus
Incubator Heracell 240i	Heraeus
IncuCyte Zoom	Essen BioScience

Magnetic Stirrers RCT basic	IKA
Microscope TCS SPE confocal system	Leica
Microskope Axiovert 40 CFL	Zeiss
Microwave M1913	Samsung
Mini-PROTEAN Tetra Cell	Bio-Rad
Miscellaneous glasware	Duran
Neubauer Improved cell counting chamber	Carl Roth
Odyssey Infrared System 9120	LI-COR
PCR cycler T Gradient	Biometra
PCR cycler T1 Thermocycler	Biometra
PerfectBlue Semi-Dry Electroblotter	Peqlab
pH-meter CG 840	Schott
PIPETBOY	INTEGRA Biosciences
Plate reader Synergy 2	BioTek
Research pipette 0.1-2.5 µl	Eppendorf
Research pipette 0.5-10 µl	Eppendorf
Research pipette 2-20 µl	Eppendorf
Research pipette 10-100 µl	Eppendorf
Research pipette 100-1000 µl	Eppendorf
Rocking Platform Duomax 1030	Heidolph
Rocking Platform STR9	Stuart scientific
Roller 6	IKA
Roller SRT6D	Stuart scientific
Shaking Incubator Type 3031	GFL
StepOnePlus Real-Time PCR System	Applied Biosystems
Thermocell Cooling & Heating Block	Biozym Scientific
Thermomixer 5436	Eppendorf
Transiluminator Bioview UST-20M-8R	Biostep
Vortex mixer MSI Minishaker	IKA
Vortex mixer REAX 2000	Heidolph
Water Bath 1004	GFL
Water Bath 61569	Köttermann
Water purification system Classic	ELGA

4.1.3. Chemicals, drugs, and enzymes

Table 6: Chemicals

Product	Manufacturer	#
2-Mercaptoethanol (C2H6OS)	Applichem	A1108,0250
Agarose	Serva	11404.07
Albumin bovine (BSA)	Serva	11926.03
Ammonium persulfate (APS)	Merck	1.01200.1000
Bacto Agar	BD Bioscience	214010
Bacto Tryptone	BD Bioscience	211705
Bacto Yeast Extract	BD Bioscience	212750
Bromodeoxyuridine (BrdU)	Sigma-Aldrich	B5002
Bromphenol Blue	Sigma-Aldrich	B-6896
Calcium chloride (CaCl2)	Merck	1.02382.0500
cOmplete Protease Inhibitor Cocktail Tablets	Roche	11697498001
DAPI (4',6-diamidino-2-phenylindole)	Sigma-Aldrich	D9542
Dimethyl sulfoxide (DMSO)	Applichem	A3672,0050
Disodium hydrogen phosphate (Na2HPO2)	Merck	1.06559.0500
Dithiothreitol (DTT)	Biomol	04010.25
Ethanol (CH3CH2OH)	J.T. Baker	2606
Ethidium bromide	Sigma-Aldrich	E1510
Ethylenediaminetetraacetic acid (EDTA)	Invitrogen	15576-028
Formalin solution, neutral buffered, 10%	Sigma-Aldrich	HT501128
GelRed	Biotium	41001
Glycerol	Merck	1.04093.1000
Glycin	Merck	1.04169.1000
HEPES	Sigma-Aldrich	H3375-100G
Hydrogen chloride (HCl)	Merck	HC825345
Isopropanol	Merck	8.18766.1000
Magnesium chloride	Merck	1.05833.8250
Methanol (CH3OH)	J.T. Baker	8045
Methylene blue	Applichem	A4261
Noble Agar	BD Bioscience	214220
Nonfat dried milk powder	Applichem	A0830
NP-40, 10 % solution	Merck	492018
Paraformaldehyde (PFA)	Merck	1.04005.1000
Pellet Paint Co-Precipitant	Novagen	69049
Phenol	Sigma-Aldrich	P4557
PhosSTOP Phosphatase Inhibitor Cocktail Tablets	Roche	4906845001
Poly-L-lysine	Sigma-Aldrich	P9155
Polyoxyethylene sorbitan monolaurate (Tween-20)	DAKO	S1966
Potassium chloride (KCl)	Merck	1.04936
Potassium dihydrogen phosphate (H2KO4P)	Merck	1.04873.1000
Propidium iodide	Sigma-Aldrich	P4170
Sodium acetate (CH3COONa)	Merck	1.06267.0500

Sodium chloride (NaCl)	Merck	567440-1KG
Sodium deoxycholate	Sigma-Aldrich	D5670-5G
Sodium dodecyl sulfate (SDS)	Serva	20765.03
Sodium hydroxide (NaOH)	Applichem	141687.1211
Sodium phosphate (NaH2PO4)	Merck	6345.1000
TEMED (N,N,N',N'-tetramethylethane-1,2-diamine)	Sigma-Aldrich	T-9281
Tris-Base	Merck	1.08382.0500
Triton X-100	Sigma-Aldrich	T8532-500ml
UltraPure™ Agarose	Invitrogen	16500500

Table 7: Enzymes

Product	Manufacturer	#
Alkaline Phosphatase, Calf Intestinal (CIP)	New England Biolabs	M0290S
EcoRI	New England Biolabs	R0101S
Proteinase K	Ambion	AM2546
RNase, DNase-free	Roche	11119915001
T4 DNA Ligase	New England Biolabs	M0202S
XhoI	New England Biolabs	R0146S

Table 8: Drugs

Product	Manufacturer	#
5-Fluorouracil	Sigma-Aldrich	F6627
Ampicilin	Sigma-Aldrich	A9518-5G
Blasticidin	Applichem	A3784,0025
Doxycycline	Applichem	A2951,0025
Etoposide	Sigma-Aldrich	E1383
Geneticindisulfat (G418)	Roth	CP11.3
Hydroxyurea	Sigma-Aldrich	H8627
Hygromycin B	Roche	10843555001
Nocodazole	Sigma-Aldrich	M1404
Oxaliplatin	Sigma-Aldrich	O9512
PHA 767491	Sigma-Aldrich	PZ0178
Puromycin dihydrochloride	Sigma-Aldrich	P8833

4.1.4. Buffers, solutions, and media

Table 9: Commercial buffers, solutions, and media

Product	Manufacturer	#
1 kb DNA ladder	New England Biolabs	N3232L
100 bp DNA ladder	New England Biolabs	N3231L
10x DMEM	Sigma-Aldrich	D2429
10x DPBS	Gibco	14200-067
10x RPMI-1640	Sigma-Aldrich	R1145
6 x DNA loading dye	Thermo Fisher	R0611
Amersham ECL Western Blotting Detection Reagent	GE Healthcare	RPN2235
D-(+)-Glucose solution	Sigma	G8769
DMEM	Lonza	BE12-707F
Fetal calve serum (FCS)	PAN Biotech	P30-1506 Lot No. P130902
M-PER Mammalian Protein Extraction Reagent	Thermo Scientific	78501
NEBuffer 3.1	New England Biolabs	B7203S
Odyssey Blocking Buffer	LI-COR Bioscience	P/N 927
PageRuler™ Prestained Protein Ladder	Thermo Fisher	26616
Penicillin/Streptomycin	Biochrom	A 2212
Polybrene	Merck Millipore	TR-1003
Rotiphorese Gel 30	Roth	3029
RPMI 1640	Biochrom	FG1385
Sodium Bicarbonate 7.5%	Biochrom	L 1713
Sodium Pyruvate	Gibco	11360070
SuperSignal™ West Femto Maximum Sensitivity Substrate	Thermo Fisher	34095
TrypLE Express	Gibco	12604-013
Ultraglutamine 1	Lonza	BE17-605E/U1
VECTASHIELD HardSet Antifade Mounting Medium	Vector Laboratories	H-1400

Table 10: Self-made solutions

Solution	Recipe
Running buffer (1x)	5.02 g Tris-base, 15 g Glycine, 1 g SDS, add H_2O to 1,000 ml
Blotting buffer (1x)	5.812 g Tris-base, 2.932 g Glycine, 1.876 ml 20% SDS, 200 ml Methanol, add H_2O to 1,000 ml
Separation gel (8%)	4.6 ml H_2O, 2.5 ml 1.5 M Tris-HCl pH=8.6, 100 µl 10% SDS, 2.7 ml 30% Acrylamide, 100 µl 10% APS, 6 µl TEMED
Separation gel (10%)	4 ml H_2O, 2.5 ml 1.5 M Tris-HCl pH=8.6, 100 µl 10% SDS, 3.33 ml 30% Acrylamide, 100 µl 10% APS, 4 µl TEMED
Separation gel (12%)	3.33 ml H_2O, 2.5 ml 1.5 M Tris-HCl pH=8.6, 100 µl 10% SDS, 4 ml 30% Acrylamide, 100 µl 10% APS, 4 µl TEMED
Stacking gel (2%)	3.05 ml H_2O, 1.25 ml 0.5 M Tris-HCl pH=6.8, 50 µl 10% SDS, 0.665 ml 30% Acrylamide, 25 µl 10% APS, 5 µl TEMED
1x LB medium	10 g Bacto™ Tryptone, 5 g Bacto Yeast Extract, 10 g NaCl, pH 7.5, add H_2O to 1,000 ml
1x LB agar	15 g Bacto Agar per 1 l H_2O
50x Tris-acetate EDTA buffer (TAE)	242 g Tris-Base, 57.1 ml Glacial acetic acid, 18.6 g EDTA, pH=7.5 - 7.8, add 1 l H_2O

Phosphate buffered saline (PBS)	137 mM NaCl, 2.7 mM KCl, 10 mM Na_2HPO_4, 1.8 mM KH_2PO_4, pH=7.4
Tris-buffered saline (TBS)	50 mM Tris-base, 150 mM NaCl, pH=7.6
RIPA	50 mM Tris-HCl pH=7.4, 150 mM NaCl, 1% NP-40, 1 mM EDTA, 0.5% Na-deoxycholate
CSK buffer	10 mM Hepes pH=7.4, 300 mM Sucrose, 100 mM NaCl, 3 mM $MgCl_2$, 0.5% Triton X-100
PO_4 solution	70 mM Na_2HPO_4, 70 mM NaH_2PO_4
2x HBS	41.96 mM Hepes, 273.78 mM NaCl, pH=7.15
6x SDS-sample-buffer	300 mM Tris-HCl pH=6.8, 600 mM DTT, 12% SDS, 60% Glycerol, 0.6% w/v Bromophenol blue
DNA extraction buffer	10 mM Tris-HCl pH=8.0, 150 mM NaCl, 10 mM EDTA

4.1.5. Antibodies

Table 11: Primary antibodies

Antibody target	Manufacturer	#	dilution WB	dilution IF	dilution FACS
53BP1	Biomol Bethyl	A300-272A-M		1:100	
BrdU	BD Bioscience	#347580			1:50
pCDC25B (S323)	Sigma	SAB4503810	1:200		
pCDC25C (S216)	CST	4901	1:1,000		
CDK1	CST	3652	1:1,000		
pCDK1 (Y15)	CST	9111	1:1,000		
CHK1	Santa Cruz	sc-8408	1:200		
pCHK1 (S280)	Abcam	ab92630	1:2,500		
pCHK1 (S345)	CST	2341	1:1,000		
pCHK2 (T68)	CST	2661	1:2,000		
Cleaved Caspase 3 (Asp175) Alexa Fluor® 647 Conjugate	CST	9602			1:50
cleaved PARP	CST	9541	1:1,000		
pERK1/2	CST	4370	1:2,000		
γH2AX	Millipore	05-636		1:100	1:250
γH2AX	CST	9718		1:200	
GAPDH	Invitrogen	AM4300	1:10,000		
pHH3 (Ser10)	CST	9701		1:200	
pHH3 (Ser10) (PE Conjugate)	CST	5764			1:50
KRAS	OriGene	TA801672	1:2,000		
MCM2	BD	610701	1:2,000	1:50	
pMCM2	Abcam	ab133243	1:1,000		
MCM7	Santa Cruz	sc-9966	1:200		
PCNA	Santa Cruz	sc-56	1:200		
p-p90RSK (T359/S363)	CST	9344	1:1,000		
RPA2	Abcam	ab2175	1:500	1:300	
pRPA2 (Thr21)	Abcam	ab61065	1:500		
β-Tubulin	CST	2146	1:1,000		
Vinculin	CST	4650	1:1,000		

Table 12: Secondary antibodies

Antibody target	Manufacturer	#	dilution WB	dilution IF	dilution FACS
α-mouse Alexa Fluor 488	Invitrogen	A-21204		1:400	1:1,000
α-mouse Alexa Fluor 568	Invitrogen	A-11031		1:400	
α-mouse Alexa Fluor 647	Invitrogen	A-21237		1:400	
α-mouse HRP-linked	CST	7076	1:2,000		
α-mouse IRDye 680RD	LI-COR	925-68070	1:10,000		
α-mouse IRDye 800CW	LI-COR	925-32210	1:10,000		
α-rabbit Alexa Fluor 488	Invitrogen	A-11008		1:400	
α-rabbit Alexa Fluor 568	Invitrogen	A-11036		1:400	
α-rabbit HRP-linked	CST	7074	1:2,000		
α-rabbit IRDye 680RD	LI-COR	925-68071	1:10,000		
α-rabbit IRDye 800CW	LI-COR	925-32211	1:10,000		

4.1.6. Cell lines

Table 13: Human cell lines and culture conditions

cell line	authentic-cation	medium	additions	Hygro-mycin	Puro-mycin	G418	Blasti-cidin
CaCo2 (ATCC)	13 Feb 2018, CLS GmbH	DMEM	10% FCS, 1% Pen/Strep, 1% Ultraglutamine solution	250 µg/ml	5.0 µg/ml	1250 µg/ml	---
HT29 (ATCC)	11 Nov 2018, CLS GmbH	DMEM	10% FCS, 1% Pen/Strep, 1% Ultraglutamine solution	---	1.0 µg/ml	1000 µg/ml	---
WiDr (provided by Prof. Reinhold Schäfer)	29 May 2015, CLS GmbH	DMEM	10% FCS, 1% Pen/Strep, 1% Ultraglutamine solution	---	1.0 µg/ml	1000 µg/ml	---
SW480 (ATCC)	13 Feb 2018, CLS GmbH	DMEM	10% FCS, 1% Pen/Strep, 1% Ultraglutamine solution	---	5.0 µg/ml	1250 µg/ml	---
HCT8 (ATCC)	12 Apr 2016, CLS GmbH	DMEM	10% FCS, 1% Pen/Strep, 1% Ultraglutamine solution, 4g/L glucose	---	5.0 µg/ml	1250 µg/ml	---
DLD-1 ($KRAS^{wt/G13D}$) (Horizon Discovery)	May 2016, freshly purchased	RPMI	10% FCS, 1% Pen/Strep	---	2.5 µg/ml	1250 µg/ml	---
DLD-1 ($KRAS^{wt/-}$) (Horizon Discovery)	May 2016, freshly purchased	RPMI	10% FCS, 1% Pen/Strep	---	2.5 µg/ml	1250 µg/ml	---
PlatE (HEK293T) (provided by Prof. Johannes Zuber, IMP)	---	DMEM	10% FCS, 1% Pen/Strep, 1% Ultraglutamine solution, 4g/L glucose	---	1.0 µg/ml	---	10 µg/ml

Table 14: Bacteria

cell line:	medium	manufacturer	#
E. coli (OneShot) Stabl3	LB	Invitrogen	C737303

4.1.7. Plasmids

Table 15: Plasmids used to generate transgenic cell lines

Plasmid	provided by	Gene/shRNA	Resistance	Fluorescent marker
TRE3G_KRAS_IRES_TagBFP_SV40polyA	Dr. Kathleen Klotz-Noack	$KRAS^{G12V}$	Hygromycin	BFP
TRE3G_IRES_TagBFP_SV40polyA	Dr. Kathleen Klotz-Noack	---	Hygromycin	BFP
gagpol	Prof. Johannes Zuber, IMP	viral group antigens and reverse transcriptase	---	---
00419_pRRL-SFFV-rtTA3-IRES-EcoRec-PGK-Puro (pRRL-RIEP)	Prof. Johannes Zuber, IMP	SLC7A1 (M. musculus)/ reverse tetracycline-controlled transactivator 3	Puromycin	---
00409_LMN.miRE.mCherry.shX	Dr. Kathleen Klotz-Noack	shRNA library	G418	mCherry
(p425) 00425_pSIN-TRE3G-turboGFP-miRE-Ren.713-PGK-Neo	Prof. Johannes Zuber, IMP	Renilla.713	G418	TurboGFP
00425_pSIN-TRE3G-turboGFP-miRE-scrbl-PGK-Neo	derived from p425	scrbl control shRNA	G418	TurboGFP
00425_pSIN-TRE3G-turboGFP-miRE-MCM7.1879-PGK-Neo	derived from p425	MCM7.1879	G418	TurboGFP
00425_pSIN-TRE3G-turboGFP-miRE-MCM7.1534v-PGK-Neo	derived from p425	MCM7.1534v	G418	TurboGFP
00425_pSIN-TRE3G-turboGFP-miRE-MCM7.sh3-PGK-Neo	derived from p425	MCM7.sh3	G418	TurboGFP
00425_pSIN-TRE3G-turboGFP-miRE-DAB2IP.2670-PGK-Neo	derived from p425	DAB2IP.2670	G418	TurboGFP
00425_pSIN-TRE3G-turboGFP-miRE-DAB2IP.468-PGK-Neo	derived from p425	DAB2IP.468	G418	TurboGFP
00425_pSIN-TRE3G-turboGFP-miRE-DNMT1.3205v-PGK-Neo	derived from p425	DNMT1.3205v	G418	TurboGFP
00425_pSIN-TRE3G-turboGFP-miRE-DNMT1.3991-PGK-Neo	derived from p425	DNMT1.3991	G418	TurboGFP
00425_pSIN-TRE3G-turboGFP-miRE-FOXM1.1812v-PGK-Neo	derived from p425	FOXM1.1812v	G418	TurboGFP

00425_pSIN-TRE3G-turboGFP-miRE-FOXM1.2496-PGK-Neo	derived from p425	FOXM1.2496	G418	TurboGFP
00425_pSIN-TRE3G-turboGFP-miRE-XRCC6.190v-PGK-Neo	derived from p425	XRCC6.190v	G418	TurboGFP
00425_pSIN-TRE3G-turboGFP-miRE-XRCC6.828-PGK-Neo	derived from p425	XRCC6.828	G418	TurboGFP
00425_pSIN-TRE3G-turboGFP-miRE-DNAJC2.428-PGK-Neo	derived from p425	DNAJC2.428	G418	TurboGFP
00425_pSIN-TRE3G-turboGFP-miRE-ENO1.681-PGK-Neo	derived from p425	ENO1.681	G418	TurboGFP
00425_pSIN-TRE3G-turboGFP-miRE-ENO1.1440-PGK-Neo	derived from p425	ENO1.1440	G418	TurboGFP
00425_pSIN-TRE3G-turboGFP-miRE-HMBG3.628-PGK-Neo	derived from p425	HMBG3.628	G418	TurboGFP
00425_pSIN-TRE3G-turboGFP-miRE-ILF2.1851-PGK-Neo	derived from p425	ILF2.1851	G418	TurboGFP
00425_pSIN-TRE3G-turboGFP-miRE-KLF10.1084-PGK-Neo	derived from p425	KLF10.1084	G418	TurboGFP
00425_pSIN-TRE3G-turboGFP-miRE-KLF1.1822v-PGK-Neo	derived from p425	KLF1.1822v	G418	TurboGFP
00425_pSIN-TRE3G-turboGFP-miRE-MED8.561-PGK-Neo	derived from p425	MED8.561	G418	TurboGFP
00425_pSIN-TRE3G-turboGFP-miRE-PPP1R15A.1494-PGK-Neo	derived from p425	PPP1R15A.1494	G418	TurboGFP
00425_pSIN-TRE3G-turboGFP-miRE-PPP1R15A.49v-PGK-Neo	derived from p425	PPP1R15A.49v	G418	TurboGFP
00425_pSIN-TRE3G-turboGFP-miRE-PPP2R5A.183-PGK-Neo	derived from p425	PPP2R5A.183	G418	TurboGFP
00425_pSIN-TRE3G-turboGFP-miRE-PPP2R5B.1879-PGK-Neo	derived from p425	PPP2R5B.1879	G418	TurboGFP
00425_pSIN-TRE3G-turboGFP-miRE-PPP2R5E.2031-PGK-Neo	derived from p425	PPP2R5E.2031	G418	TurboGFP
00425_pSIN-TRE3G-turboGFP-miRE-RASA4.3049-PGK-Neo	derived from p425	RASA4.3049	G418	TurboGFP
00425_pSIN-TRE3G-turboGFP-miRE-SPRY1.137-PGK-Neo	derived from p425	SPRY1.137	G418	TurboGFP
00425_pSIN-TRE3G-turboGFP-miRE-WBP11.1135-PGK-Neo	derived from p425	WBP11.1135	G418	TurboGFP

4.1.8. shRNAs

Table 16: shRNAs used for target validation of the RNAi screen

Name	Guide	97mere sequence
scrbl	TATTCATCTGAGCATCTTCG CA	TGCTGTTGACAGTGAGCGAGCGAAGATGC TCAGATGAATATAGTGAAGCCACAGATGTA TATTCATCTGAGCATCTTCGCATGCCTACT GCCTCGGA
MCM7.1879	TTTGACATCTCCATTAGCCT GA	TGCTGTTGACAGTGAGCGCCAGGCTAATG GAGATGTCAAATAGTGAAGCCACAGATGTA TTTGACATCTCCATTAGCCTGATGCCTACT GCCTCGGA
MCM7.1534v	TAGGTCATTGTCTCGGTCGG GC	TGCTGTTGACAGTGAGCGACCCGACCGAG ACAATGACCTATAGTGAAGCCACAGATGTA TAGGTCATTGTCTCGGTCGGGCTGCCTACT GCCTCGGA
MCM7.sh3	TTTTCGTAGAAATCCTCCTC TG	TGCTGTTGACAGTGAGCGAAGAGGAGGAT TTCTACGAAAATAGTGAAGCCACAGATGTA TTTTCGTAGAAATCCTCCTCTGTGCCTACT GCCTCGGA
DAB2IP.468	TTCTTCTTGTCGGTCTCCCG GT	TGCTGTTGACAGTGAGCGCCCGGGAGACC GACAAGAAGAATAGTGAAGCCACAGATGT ATTCTTCTTGTCGGTCTCCCGGTTGCCTAC TGCCTCGGA
DAB2IP.2670	TCGTCTTCTAACAACTGCGC GT	TGCTGTTGACAGTGAGCGCCGCGCAGTTGT TAGAAGACGATAGTGAAGCCACAGATGTAT CGTCTTCTAACAACTGCGCGTTGCCTACTG CCTCGGA
DNMT1.3991	TTGAAGGAGACAAAGTTCCT GA	TGCTGTTGACAGTGAGCGCCAGGAACTTTG TCTCCTTCAATAGTGAAGCCACAGATGTAT TGAAGGAGACAAAGTTCCTGATGCCTACTG CCTCGGA
DNMT1.3205v	TTTGATGTCAGTCTCATTGG GC	TGCTGTTGACAGTGAGCGACCCAATGAGA CTGACATCAAATAGTGAAGCCACAGATGTA TTTGATGTCAGTCTCATTGGGCTGCCTACT GCCTCGGA
FOXM1.2496	TAGCTCAGGAATAAACTGGG AC	TGCTGTTGACAGTGAGCGATCCCAGTTTAT TCCTGAGCTATAGTGAAGCCACAGATGTAT AGCTCAGGAATAAACTGGGACTGCCTACTG CCTCGGA
FOXM1.1812v	TTGAATCACAAGCATTTCCG AG	TGCTGTTGACAGTGAGCGATCGGAAATGCT TGTGATTCAATAGTGAAGCCACAGATGTAT TGAATCACAAGCATTTCCGAGTGCCTACTG CCTCGGA
XRCC6.828	TTAACCTGCTGAGTGCTCGC TT	TGCTGTTGACAGTGAGCGCAGCGAGCACT CAGCAGGTTAATAGTGAAGCCACAGATGTA TTAACCTGCTGAGTGCTCGCTTTGCCTACT GCCTCGGA
XRCC6.190v	TGAGTGAGTAGTCAGATCCG TG	TGCTGTTGACAGTGAGCGAACGGATCTGAC TACTCACTCATAGTGAAGCCACAGATGTAT GAGTGAGTAGTCAGATCCGTGTGCCTACTG CCTCGGA
DNAJC2.428	TTCATCTTCTGATTCCTCGG AT	TGCTGTTGACAGTGAGCGCTCCGAGGAATC AGAAGATGAATAGTGAAGCCACAGATGTAT TCATCTTCTGATTCCTCGGATTGCCTACTG CCTCGGA
ENO1.681	TCTTCGATAGACACCACTGG GT	TGCTGTTGACAGTGAGCGCCCCAGTGGTGT CTATCGAAGATAGTGAAGCCACAGATGTAT

		CTTCGATAGACACCACTGGGTTGCCTACTG CCTCGGA
ENO1.1440	TTTGAGCACAAAACCACCGG GG	TGCTGTTGACAGTGAGCGACCCGGTGGTTT TGTGCTCAAATAGTGAAGCCACAGATGTAT TTGAGCACAAAACCACCGGGGTGCCTACT GCCTCGGA
HMGB3.628	TTCATCTTCCTCTTCCACCT TT	TGCTGTTGACAGTGAGCGCAAGGTGGAAG AGGAAGATGAATAGTGAAGCCACAGATGT ATTCATCTTCCTCTTCCACCTTTTGCCTACT GCCTCGGA
ILF2.1851	TGATATTCTAGTTTACTCTG GT	TGCTGTTGACAGTGAGCGCCCAGAGTAAA CTAGAATATCATAGTGAAGCCACAGATGTA TGATATTCTAGTTTACTCTGGTTGCCTACT GCCTCGGA
KLF10.1084	TATGTCTTGCCACATCCTGG GT	TGCTGTTGACAGTGAGCGCCCCAGGATGT GGCAAGACATATAGTGAAGCCACAGATGT ATATGTCTTGCCACATCCTGGGTTGCCTAC TGCCTCGGA
KLF10.1822v	TACATCTCCATGTCTGTACC GT	TGCTGTTGACAGTGAGCGCCGGTACAGAC ATGGAGATGTATAGTGAAGCCACAGATGTA TACATCTCCATGTCTGTACCGTTGCCTACT GCCTCGGA
MED8.561	TTAAAGGTCTGCTTGTTCGG CC	TGCTGTTGACAGTGAGCGAGCCGAACAAG CAGACCTTTAATAGTGAAGCCACAGATGTA TTAAAGGTCTGCTTGTTCGGCCTGCCTACT GCCTCGGA
PPP1R15A.1494	TTCTCTTTCATCCTCGGCTG AT	TGCTGTTGACAGTGAGCGCTCAGCCGAGG ATGAAAGAGAATAGTGAAGCCACAGATGT ATTCTCTTTCATCCTCGGCTGATTGCCTAC TGCCTCGGA
PPP1R15A.49v	TTGCATAAGATCAACAACTG GG	TGCTGTTGACAGTGAGCGACCAGTTGTTGA TCTTATGCAATAGTGAAGCCACAGATGTAT TGCATAAGATCAACAACTGGGTGCCTACTG CCTCGGA
PPP2R5A.183	TACTATATCAGAATACGCTG AT	TGCTGTTGACAGTGAGCGCTCAGCGTATTC TGATATAGTATAGTGAAGCCACAGATGTAT ACTATATCAGAATACGCTGATTGCCTACTG CCTCGGA
PPP2R5B.1879	TTGAGCACATTGTAGATCAG TG	TGCTGTTGACAGTGAGCGAACTGATCTACA ATGTGCTCAATAGTGAAGCCACAGATGTAT TGAGCACATTGTAGATCAGTGTGCCTACTG CCTCGGA
PPP2R5E.2031	TTCTACTACATAAACGTGTG AC	TGCTGTTGACAGTGAGCGATCACACGTTTA TGTAGTAGAATAGTGAAGCCACAGATGTAT TCTACTACATAAACGTGTGACTGCCTACTG CCTCGGA
SPRY1.137	TCATAGTCTAATCTCTGACG GC	TGCTGTTGACAGTGAGCGACCGTCAGAGAT TAGACTATGATAGTGAAGCCACAGATGTAT CATAGTCTAATCTCTGACGGCTGCCTACTG CCTCGGA
RASA4.3049	TTTGAGGAGAGAACAGCTGG TT	TGCTGTTGACAGTGAGCGCACCAGCTGTTC TCTCCTCAAATAGTGAAGCCACAGATGTAT TTGAGGAGAGAACAGCTGGTTTGCCTACTG CCTCGGA
WBP11.1135	TTGAAGAGGAGTCAGTTCCT TC	TGCTGTTGACAGTGAGCGAAAGGAACTGA CTCCTCTTCAATAGTGAAGCCACAGATGTA TTGAAGAGGAGTCAGTTCCTTCTGCCTACT GCCTCGGA

4.1.9. Primer

Table 17: Primer

Name	Sequence (5' - 3')
p5 SOLEXA adapter	AATGATACGGCGACCACCGATGGATGTGGAATGTGTGCGAGG
p7loop_AAGC	CAAGCAGAAGACGGCATACGAAAGCTAGTGAAGCCACAGATGT
p7loop_AGAC	CAAGCAGAAGACGGCATACGAAGACTAGTGAAGCCACAGATGT
p7loop_CAAC	CAAGCAGAAGACGGCATACGACAACTAGTGAAGCCACAGATGT
p7loop_CGAA	CAAGCAGAAGACGGCATACGACGAATAGTGAAGCCACAGATGT
p7loop_GAGT	CAAGCAGAAGACGGCATACGAGAGTTAGTGAAGCCACAGATGT
p7loop_GGAT	CAAGCAGAAGACGGCATACGAGGATTAGTGAAGCCACAGATGT
MCM7 qPCR fwd	GTTTGACCTCCTCTGGCTGA
MCM7 qPCR rev	AGAGGTTCAAACTGGGAGGG
UBE2D2 fwd	ATGGCGCTGAAGAGGATTC
UBE2D2 rev	CTTGCCAGTGGAACAAGTCA
ZUB-SEQ-SH	TGTTTGAATGAGGCTTCAGTAC
mirE-XhoI	TACAATACTCGAGAAGGTATATTGCTGTTGACAGTGAGCG
mirE-EcoRI	TTAGATGAATTCTAGCCCCTTGAAGTCCGAGGCAGTAGGCA

4.1.10. Software

Table 18: Software and databases

Name	Version	Company/Institute	License	Website
ApE	2.0.47	M. Wayne Davis	Freeware	
BD CSampler C6 software	1.0.264 .21	BD Bioscience	Charité	
cBio Portal	1.11.3	Center for Molecular Oncology, Memorial Sloan Kettering Cancer Center	---	http://www.cbioportal.org/
CellProfiler	2.2.0	Broad Institute	Freeware	
ClinicalTrials.gov	January 2018	National Institutes of Health (NIH)	---	http://www.clinicaltrials.gov/
COSMIC	v83	Wellcome Sanger Institute	---	https://cancer.sanger.ac.uk/cosmic
FlowJo	v10.2	FlowJo	Freeware	
Gen5	2.04	BioTek	Charité	
GraphPad Prism	6.07	GraphPad Software	Charité	
Illustrator	CS6	Adobe	Charité	
Image Studio	3.1	LI-COR Bioscience	Charité	
ImageJ	1.48v	NIH	Freeware	
IncuCyte Zoom	2016B	Essen BioScience	Charité	
LAS AF	1.0	Leica Microsystems	Charité	
Mendeley Desktop	1.17.11	Mendeley	Freeware	
Microsoft Excel	2016	Microsoft	Charité	

Microsoft Word	2016	Microsoft	Charité
Photoshop	CS6	Adobe	Charité
R	3.2.1	The R Foundation for Statistical Computing	Freeware
R Studio	1.0.44	Rstudio	Freeware
SnapGene viewer	4.0.2	GSL Biotech	Freeware
StepOne Software	2.3	Applied Biosystems	Charité

4.2. Methods

4.2.1. Cell culture

Cell lines were cultured in their respective medium with antibiotic selection as indicated in Table 13: Human cell lines and culture conditions with 10% fetal calf serum and 1% Penicillin/Streptomycin at 37°C and 5% CO_2. Transgene expression was induced with 2 µg/ml of doxycycline immediately after seeding the cells (if indicated). For drug treatment experiments, transgene expression was induced immediately after seeding and drugs were added one night after seeding the cells. Long-term storage of all cells was achieved by resuspending the cells in their respective medium and 10% DMSO without selection antibiotics and freezing them in liquid nitrogen.

4.2.2. Retrovirus production and transduction

Twenty µg of the target plasmid and 7.5 µg of gag plasmid (encoding gag and pol) were diluted in a total of 440 µl H_2O and incubated at 37 °C for 5 h while shaking. Plat-E cells were seeded at a confluency of $4x10^6$ cells in a 10 cm dish in 9 ml medium and cultured for at least 4 h. When cells were approx. 75% confluent, 10 µl PO_4 solution was added to 0.5 ml 2x HBS. Then, 60 µl 2 M $CaCl_2$ was mixed with the DNA solution and added dropwise to the 2x HBS-PO_4 solution while gently shaking. The mixture was incubated for 1 min at room temperature and then distributed dropwise onto the cells. 20 h after the transfection the medium was exchanged and reduced to 5 ml per plate. The virus-containing supernatant was harvested 34 h after transfection. At this point, the supernatant could be stored for up to two weeks at 4 °C. The virus-containing supernatant was then diluted 1:1 with medium and polybrene was added in a dilution of 1:1,200 to the final volume before the mixture was added to cell lines (previously transduced with a lentivirus containing an ecotropic receptor) for 24 h.

4.2.3. RNAi screen

4.2.3.1. Library transduction and proliferation screen.

CaCo2 cells with doxycycline-inducible $KRAS^{G12V}$ were transfected by retroviral transduction with a custom-designed shRNA library containing 625 shRNAs against 121 different targets (Table A 1; purchased from CustomArray Inc. and prepared by Kathleen Klotz-Noack, Institute of Pathology, Charité) with less than 20% transduction efficiency to predominantly integrate a single shRNA construct per cell. This was achieved by diluting the retrovirus library 1:7. Three days after transfection and G418 selection, a fraction of cells was sorted for $mCherry^+$ cells ($shRNA^+$) using a FACSAria II and frozen down as the baseline control. The remaining cells were split in half and cultured in the presence or absence of doxycycline for 14 and 21 more days, respectively, before the two fractions were sorted for $mCherry^+$ cells and frozen down. Before cell sorting, the cell populations were filtered through a 30 µm cell filter. The shRNA representation was kept over 1,000x at any given time.

4.2.3.2. Phenol extraction and precipitation of genomic DNA

To isolate the genomic DNA, the sorted cell pellets were resuspended in 400 µl DNA extraction buffer. Then, 4 µl 10% SDS and 4 µl proteinase K (20 mg/ml stock) were added to the samples. After each addition, the samples were vortexed. Next, the samples were incubated at 55 °C in a shaker (800 rpm) for 16.5 h overnight. On the next day, the samples were mixed with 400 µl phenol, transferred to PhaseLock tubes, and centrifuged at maximum speed for 8 min. The DNA containing aqueous solution was transferred to a fresh tube while leaving 30 µl of the aqueous fraction in the tube to avoid contamination with the phenol soluble fraction. The phenol extraction was repeated two more times while adjusting for the phenol volumes according to the current volume of the aqueous fraction. To precipitate the genomic DNA, 31 µl 3 M Sodium acetate pH=5.2 ($\frac{1}{10}$ the volume of the aqueous solution), 930 µl 96% ethanol (3 volumes of the aqueous solution), and 1 µl Pellet Paint Co-Precipitant were added and mixed. The DNA was then left to precipitate at -20 °C overnight. On the next day, the

DNA samples were centrifuged at maximum speed at 4 °C for 30 min. The resulting DNA pellet was then washed with 200 µl 70% ethanol and centrifuged for 5 min at 4 °C. The supernatant was discarded and the DNA pellet was air dried for 5 min at 55 °C before it was resuspended in 40 µl elution buffer (EB, provided in QIAGEN Plasmid Mini Kit). To facilitate resuspension, the DNA solution was incubated for 1.5 h at 55 °C while shaking at 800 rpm. The final DNA concentrations across all samples were then equilibrated to 0.5 µg/µl.

4.2.3.3. Barcoding and Solexa sequencing sample preparation

Samples were PCR amplified and barcoded (adapter primers: p5 SOLEXA adapter, p7loop_XYXY [XYXY = barcoding nucleotides]) according to PCR conditions shown in Table 19 and Table 20. To prevent amplification artifacts, each sample was amplified in 10 separate reactions and the resulting PCR products were mixed.

Table 19: PCR mix for shRNA cassette amplification and barcoding

Template DNA 0.5 µg/µl	1.0 µl
H_2O	36.5 µl
10x PCR buffer	5.0 µl
$MgCl_2$	3.0 µl
dNTPs (2 mM each)	1.0 µl
p7loop_XYXY (fwd) 10 µM	1.5 µl
p5 SOLEXA adapter (rev) 10 µM	1.5 µl
Amplitaq Gold	0.5 µl
total	**50.0 µl**

Table 20: PCR cycling conditions for shRNA cassette amplification and barcoding

Initial denaturation	95 °C	10 min	
Denaturation	95 °C	30 s	33x
Primer annealing	52 °C	45 s	
Extension	72 °C	60 s	
Final Extension	72 °C	7 min	

To purify the amplified DNA, one round of Phenol extraction was performed as described in 4.2.3.2 Phenol extraction and precipitation of genomic DNA. The DNA pellet was resuspended in 30 µl elution buffer (EB, provided in QIAGEN Plasmid Mini Kit) and was run through a 2% agarose gel. The correct band at 345 bp was excised and purified using a QIAGEN QIAquick gel extraction kit according to the manufacturer's instructions with following adjustments: samples were incubated for 10 min after addition of 1 volume isopropanol to increase precipitation, the optional washing step with QG buffer was skipped, samples were washed a second time with 0.5 ml PE buffer, and the DNA was eluted in 30 µl EB after 15 min of incubation at ambient temperature. The isolated DNA was then diluted to obtain a concentration of 100 nM (~22.77 ng/µl for 345 bp) per sample. The abundance of each shRNA was assessed by deep sequencing and compared to baseline control. Deep sequencing was performed on the Illumina HiSeq 2500 platform by the sequencing unit of the Campus Science Support Facilities (CSF), which was renamed to Vienna BioCenter Core Facilities GmbH (VBCF) in 2015. Mapping of the raw reads was performed by Dr. Bertram Klinger, Institute of Pathology, Charité and IRI Life Sciences, Humboldt University. Briefly, BAM files were converted into FASTQ files using BEDtools2 v2.2.3 (Quinlan and Hall, 2010). Counts were created by perfectly matching inverted reverse complement sequences for hairpin and barcode using the processAmplicon function of edgeR v3.8.6 (Robinson et al., 2010). Samples were normalized by scaling the total count of each sample to the average total count of all samples. All processing steps following FASTQ file generation were conducted in R v3.2.1.

4.2.4. Growth assays

4.2.4.1. Long-term growth assays

Approximately $5x10^3$-$1x10^4$ cells/well were seeded in 6 well plates and cultured with or without 2 µg/ml doxycycline or additional drugs as indicated in 2 ml medium. Culture medium was changed after approximately six days or every three to four days if the cells were treated with other drugs than doxycycline. After 10-13 days, cells were fixed and stained with 0.2% methylene blue in 50% methanol for 20 min before washing the

plates by submerging them in ambient temperature tap water. The final confluency was quantified using a custom pipeline in CellProfiler (Carpenter et al., 2006). Results were normalized to each respective control (no doxycycline or no drug).

4.2.4.2. Soft agar assays

10^5 CaCo2 cells or 10^3 SW480/DLD-1 cells were suspended in one part 37°C warm 2x DMEM (CaCo2, SW480) or 2x RPMI-1640 (DLD-1) with their respective selection antibiotic and mixed with one part 42°C warm 0.4% Noble Agar in T25 flasks. After thorough mixing, the flasks were set on ice for 30 min and subsequently incubated at 37 °C and 5% CO_2 for 3 weeks (SW480, DLD-1) or 5 weeks (CaCo2). All cell lines were induced with 2 µg/ml doxycycline at the time of seeding. The number of colonies was quantified using a custom pipeline in CellProfiler (Carpenter et al., 2006).

4.2.5. Protein expression analysis

4.2.5.1. Protein isolation and quantification

Cell lines were seeded at low confluency on 10 cm plates and doxycycline was added at different times according to desired end points. All cell lines in a given experiment were harvested at the same time. For whole cell extracts, cell pellets were lysed using M-PER buffer with PhosSTOP and cOmplete protease inhibitor cocktail for 10 min on ice. For chromatin fractionation, the cell pellets were first lysed in CSK buffer (+PhosSTOP and cOmplete) for 15 min on ice before centrifuging the samples at 5,000 g at 4°C for 5 min. The supernatant containing the soluble protein fraction was collected and snap frozen in liquid nitrogen. The pellets were washed twice with CSK buffer and again snap frozen in liquid nitrogen. After rethawing, the pellets were lysed in RIPA buffer (+PhosSTOP and cOmplete) for 10 min on ice. Next, the lysate was sonicated twice for 10 min with on/off intervals of 30 s using a Bioruptor before centrifuging the lysate at about 20,000 g for 10 min and collecting the supernatant

containing the chromatin-bound fraction. Protein concentrations were quantified using BCA protein quantification kit according to the manufacturer's instructions.

4.2.5.2. SDS-PAGE and western blot

Proteins were mixed with 6x SDS sample buffer and boiled for 10 min at 95 °C while shaking. After cooling the samples on ice, they were separated by SDS-PAGE using a 2% stacking gel and 8%, 10%, or 12% separation gel in a Mini-PROTEAN Tetra Handcast Systems (Bio-Rad). The gels were run at a voltage of 68 V for 20 min followed by about 2 h at 110 V. To transfer the protein samples to a nitrocellulose membrane, a semi-dry western blot was performed at a current of 0.8 to 1.2 mA/cm² of membrane area (about 100 mA per membrane) for 1-1.5 h. The membranes were then blocked with 5% milk powder in TBS + 0.1% Tween20 (TBS-T) (blocking buffer) for 1 h at ambient temperature. Next, the membranes were rinsed once with TBS-T and incubated with a primary antibody in blocking buffer at 4 °C overnight. On the next day, the membranes were washed twice with TBS-T before a secondary antibody in blocking buffer was added and incubated for 1 h at ambient temperature. The respective antibody dilutions are listed in Table 11: Primary antibodies and Table 12: Secondary antibodies. After that, the membranes were rinsed with TBS-T and then washed three times with TBS-T for 10 min each. Next, the membranes were washed once with TBS, before they were analyzed using a LI-COR Odyssey Infrared System 9120 or a Protein Simple FluorChem M System. Western blots were quantified using ImageJ 1.48v.

4.2.6. cDNA synthesis and quantitative polymerase chain reaction (qPCR)

Cells were seeded in 6 well plates and induced for two days with doxycycline before RNA was collected using a QIAGEN RNeasy Mini kit according to the manufacturer's protocol.

The collected RNA was transcribed to cDNA using the High-Capacity cDNA ReverseTranscription Kit. First, 1 µl of anchored-oligo$(dT)_{18}$ primer and random

hexamer primer each was added to 1 µg RNA in 9.4 µl RNase free H_2O and incubated at 65 °C for 10 min. Next, 8.6 µl master mix (4 µl buffer, 0.5 µl RNase inhibitor, 2 µl dNTPs, 1 µl DTT, and 1.1 µl reverse transcriptase) were added to the RNA/primer mix. The cDNA synthesis was carried out using the following conditions: 10 min at 29 °C, 60 min at 48 °C, and 5 min at 85 °C.

Quantitative PCR (qPCR) was performed using the Promega GoTaq qPCR Master Mix. First, the transcribed cDNA was diluted 1:100 in nuclease-free H_2O. Then 1 µl of diluted cDNA was added to 7.5 µl SybrGreen Master Mix and 5.5 µl nuclease-free H_2O. The total 14 µl were pipetted on a 96-well PCR plate, before adding 1 µl of the primer mix to reach a final primer concentration of 333 nM per primer. All samples were run as technical triplicates. The qPCR was run on an Applied Biosystems StepOnePlus Real-Time PCR System using the cycle conditions in Table 21.

Table 21: qPCR cycling conditions

Initial denaturation	95 °C	2 min	
Denaturation	95 °C	15 s	40x
Primer annealing	60 °C	30 s	

The Ct values (threshold cycle value) were normalized to the values of the endogenous control UBE2D2 (ΔCt values). Next, the ΔCt values were normalized to the control sample (ΔΔCt values).

4.2.7. Cell cycle analysis

Cells were seeded at low confluency and induced with 2 µg/ml doxycycline for 7 days. Prior to harvesting, the cells were treated with 20 µM BrdU for 30 min. Afterwards, cells were trypsinized, washed twice with PBS and fixed with ice-cold 70% ethanol. Next, cells were washed with 1 ml washing buffer (1 % BSA, 0.2 % Triton X-100 in PBS) twice and denatured in 2 M HCl + 0.2% Triton-X for 30 min at ambient temperature under gentle agitation. Thereafter, cells were washed twice with washing buffer and blocked with blocking buffer (5% BSA, 0.2% Triton X-100 in PBS) for 1 h at ambient temperature

under gentle agitation. The blocking buffer was replaced with anti-BrdU antibody in blocking buffer and incubated for 1 h at ambient temperature under gentle agitation. Cells were then washed twice with washing buffer and incubated with anti-mouse Alexa Fluor 488 in blocking buffer under gentle agitation. Lastly, cells were washed with washing buffer and stained with PI staining solution (50 µg/ml Propidium iodide, 50 µg/ml RNase, 0.1% Triton X-100 in PBS) for 10-20 min at ambient temperature. Samples were analyzed with the BD Accuri™ C6 flow cytometer. Data were analyzed with FlowJo v10.

4.2.8. Cleaved Caspase 3 flow cytometry analysis

Cells were cultured in 10 cm plates for 3 days with 2 µg/ml doxycycline. Cells were then split and cultured for 4 more days with doxycycline for a total of 7 days. Floating and adherent cells were collected and fixed in 1 ml 2% formaldehyde for 10 min at ambient temperature before chilling the fixed cells for 1 min on ice. Next, the cells were washed with 1 ml PBS and permeabilized in ice-cold 90% methanol on ice for 30 min, before storing the cells for up to several weeks at -20 °C. Subsequently, the fixed cells were washed twice with incubation buffer (0.5% BSA in PBS) and stained for 1 h with an anti-Cleaved Caspase-3 Alexa Fluor® 647 antibody at ambient temperature. Next, the cells were washed with 500 µl incubation buffer, resuspended in 200 µl PBS, and analyzed with the BD Accuri™ C6 flow cytometer. Data were analyzed with FlowJo v10.

4.2.9. pHH3 and γH2AX flow cytometry analysis

All steps until the addition of the first antibody were performed identically to 4.2.8 Cleaved Caspase 3 flow cytometry analysis. The cells were then incubated in 100 µl γH2AX antibody solution (Millipore, 05-636, 1:250 in incubation buffer [0.5% BSA in PBS]) at ambient temperature for 1 h. Then, the cells were washed with 500 µl incubation buffer by centrifugation before they were incubated with 100 µl anti-mouse antibody conjugated to Alexa Fluor 488 in incubation buffer at ambient temperature

for 1 h. This was followed by three washing steps in 500 µl incubation buffer, and one blocking step for 15-30 min in incubation buffer. After centrifugation, the cells were incubated in an 1:50 pHH3-PE in incubation buffer at ambient temperature for 1 h. Finally, the cells were washed with 500 µl incubation buffer, centrifuged, resuspended in 200 µl PBS, and analyzed with the BD Accuri™ C6 flow cytometer. Data were analyzed with FlowJo v10.

4.2.10. Immunofluorescence and confocal microscopy

Cells were seeded and induced with doxycycline 4 days prior fixation on poly-L-lysine coated coverslips. For the 7-day time point, cells were pre-induced 3 days before seeding. On the day of the staining, cells were washed once with PBS and fixed with 3% PFA in PBS + 0.1% Triton-X100 for 10 min. (In case of the *in situ* chromatin fractionation of adherent cells for the MCM2 staining, cells were, prior to fixation, incubated in ice-cold CSK buffer for 15 min and then washed 2x with CSK buffer and 1x with PBS.) The fixation buffer was washed off 3x briefly and 2x for 5 min with PBS. Next, the cells were permeabilized with 0.3% Triton-X100 in PBS for 2 min before washing the cells again 3x briefly and 2x for 5 min with PBS. The cells were subsequently incubated in blocking buffer (3% BSA in PBS + 0.1% Tween-20) for 1 h before washing them briefly 2x with PBS-T (PBS + 0.1% Tween-20). Next, the cells were incubated with the primary antibody in blocking buffer for 1 h, washed 3x for 5 min with PBS-T, incubated in the secondary antibody in blocking buffer for 1 h, and washed again 3x for 5 min with PBS-T. To visualize DNA, the cells were incubated in 2 µg/ml DAPI (in PBS) for 15 min and washed 2x with dH_2O. The coverslips were air dried and mounted on microscope slides in VECTASHIELD HardSet Mounting Medium and stored at 4 °C. All steps were carried out at ambient temperature. Images were taken with a Leica TCS SPE confocal system. Image analysis was performed using ImageJ (https://imagej.nih.gov/ij/) after projecting the maximum intensity of each z-stack into a single image. The “Find Maxima…” tool was used to quantify the number of RPA2 and γH2AX foci per cell.

4.2.11. Nocodazole cell cycle synchronization and release

Cells were seeded on 10 cm dishes and induced with doxycycline for 3 days before they were treated with 1 µM nocodazole for 21 h. The cells were then washed three times with PBS and 10 ml fresh medium was added. The cells were then harvested by trypsinization after 0-8 h in 1 h intervals and washed two times with PBS before fixing the cells with ice-cold 70% ethanol. For FACS analysis, the cells were washed twice with 1 ml washing buffer (1% BSA, 0.2% Triton X-100 in PBS) and stained for their DNA content in 350 µl PI staining solution (50 µg/ml propidium iodide, 50 µg/ml RNase, 0.1% Triton X-100 in PBS) for 30 min before they were analyzed with the BD Accuri™ C6 flow cytometer. Data were analyzed with FlowJo v10.

4.2.12. Knockdown construct cloning and bacterial transformation

97mere DNA oligos containing the shRNA sequence were purchased from Integrated DNA Technologies. Johannes Zuber, IMP (Vienna), kindly provided the shRNA sequences, which were generated using a proprietary algorithm (Fellmann et al., 2011). First, the oligos were PCR amplified with mirE-XhoI and mirE-EcoRI primers to extend the sequence for XhoI and EcoRI restriction recognition sites. PCR conditions are listed in Table 22 and Table 23. The PCR product was then purified using a QIAquick PCR Purification kit according to the manufacturer's instructions.

Table 22: PCR mix for primer extension of 97mere oligos

Template DNA (0.1 ng/µl)	1.0 µl
H_2O	29.5 µl
5X Phusion HF reaction buffer	10.0 µl
$MgCl_2$	3.0 µl
dNTPs (10 mM)	1.0 µl
mirE-XhoI (fwd) 10 mM	2.5 µl
mirE-EcoRI (rev) 10 mM	2.5 µl
Phusion DNA Polymerase	0.5 µl
total	**50.0 µl**

Table 23: PCR cycling conditions for primer extension of 97mere oligos

Initial denaturation	98 °C	2 min	
Denaturation	98 °C	15 s	33x
Primer annealing	54 °C	30 s	
Extension	72 °C	25 s	
Final Extension	72 °C	5 min	

One µg of the purified PCR product, as well as 2.3 µg of the backbone plasmid p425, were then digested with EcoRI and XhoI in NEBuffer 3.1 digestion buffer for 4 h at 37 °C. The resulting 5’ and 3’ ends of the backbone vector were additionally dephosphorylated by adding 1 µl of calf intestinal alkaline phosphatase (CIP) to the reaction for 1 h at 37 °C. The digestion of the backbone and insert DNA was next separated on a 2% agarose gel and the 131 bp band of the insert as well as the 7,721 bp band of the backbone were excised and purified using a QIAquick gel extraction kit according to the manufacturer’s instructions. Next, the ligation was set up at an insert to backbone ratio of 3:1. The ligation reaction was performed using the T4 DNA ligase at 15 °C for 16 h before the ligase was inactivated at 65 °C for 10 min.

To amplify the ligated plasmid, OneShot Stbl3 *Escherichia coli* were transformed via heat shock transformation. First, 50 µl of *E. coli* suspension was incubated in a 1.5 ml reaction tube on ice for 15 min. Next, 5 µl ligation product (~26 ng DNA) were mixed with the bacteria suspension by gently flicking the tube. The DNA/bacteria mix was then incubated for additional 5 min on ice before applying a heat shocking at 42 °C in a water bath for 60 s. The reaction tube was then incubated on ice for 2 min before plating the bacteria suspension on a pre-warmed LB agar plate. The LB agar plate contained 100 µg/ml ampicillin for the selection of successfully transformed bacteria. The plates were incubated at 37 °C overnight. Successfully transformed bacteria formed colonies, which were further expanded in LB medium in a shaking incubator at 37 °C overnight. Plasmid DNA was then isolated using a QIAGEN Plasmid Midi kit. The plasmid was then Sanger sequenced by Eurofins Genomics using the ZUB-SEQ-SH sequencing primer to assure the sequence was correctly amplified and ligated.

4.2.13. Statistical analysis

Unpaired, two-sided Student's t-tests, Fisher's exact test, and nonlinear regressions were performed using GraphPad Prism 6. To assess statistically significant differences in drug sensitivity, the drug concentrations were first transformed on a $\log_{10}$ scale. All data points were then normalized in a way that the smallest and highest value in each data set represents 0% and 100%, respectively. On these data, a nonlinear regression was performed using the corresponding "log(inhibitor) vs. normalized response -- Variable slope" setting. The curves were compared using the extra sum-of-squares F test. Alternatively, the IC_{50} values of every single replicate were calculated individually and subsequently compared via an unpaired, two-sided Student's t-test.

Bibliography

Aarts, M., Sharpe, R., Garcia-Murillas, I., Gevensleben, H., Hurd, M.S., Shumway, S.D., Toniatti, C., Ashworth, A., and Turner, N.C. (2012). Forced mitotic entry of S-phase cells as a therapeutic strategy induced by inhibition of WEE1. Cancer Discov. *2*, 524–539.

Ahearn, I.M., Haigis, K., Bar-Sagi, D., and Philips, M.R. (2011). Regulating the regulator: post-translational modification of RAS. Nat. Rev. Mol. Cell Biol. *13*, 39–51.

Ahmed, D., Eide, P.W., Eilertsen, I.A., Danielsen, S.A., Eknæs, M., Hektoen, M., Lind, G.E., and Lothe, R.A. (2013). Epigenetic and genetic features of 24 colon cancer cell lines. Oncogenesis *2*, e71.

Aird, K.M., Zhang, G., Li, H., Tu, Z., Bitler, B.G., Garipov, A., Wu, H., Wei, Z., Wagner, S.N., Herlyn, M., et al. (2013). Suppression of Nucleotide Metabolism Underlies the Establishment and Maintenance of Oncogene-Induced Senescence. Cell Rep. *3*, 1252–1265.

Alcindor, T., and Beauger, N. (2011). Oxaliplatin: a review in the era of molecularly targeted therapy. Curr. Oncol. *18*, 18–25.

Amado, R.G., Wolf, M., Peeters, M., Van Cutsem, E., Siena, S., Freeman, D.J., Juan, T., Sikorski, R., Suggs, S., Radinsky, R., et al. (2008). Wild-Type *KRAS* Is Required for Panitumumab Efficacy in Patients With Metastatic Colorectal Cancer. J. Clin. Oncol. *26*, 1626–1634.

Athuluri-Divakar, S.K., Vasquez-Del Carpio, R., Dutta, K., Baker, S.J., Cosenza, S.C., Basu, I., Gupta, Y.K., Reddy, M.V.R., Ueno, L., Hart, J.R., et al. (2016). A Small Molecule RAS-Mimetic Disrupts RAS Association with Effector Proteins to Block Signaling. Cell *165*, 643–655.

Bailey, P., Chang, D.K., Nones, K., Johns, A.L., Patch, A.-M., Gingras, M.-C., Miller, D.K., Christ, A.N., Bruxner, T.J.C., Quinn, M.C., et al. (2016). Genomic analyses identify molecular subtypes of pancreatic cancer. Nature *531*, 47–52.

Barbie, D.A., Tamayo, P., Boehm, J.S., Kim, S.Y., Moody, S.E., Dunn, I.F., Schinzel, A.C., Sandy, P., Meylan, E., Scholl, C., et al. (2009). Systematic RNA interference reveals that oncogenic KRAS-driven cancers require TBK1. Nature *462*, 108–112.

Barretina, J., Caponigro, G., Stransky, N., Venkatesan, K., Margolin, A.A., Kim, S., Wilson, C.J., Lehár, J., Kryukov, G. V., Sonkin, D., et al. (2012). The Cancer Cell Line Encyclopedia enables predictive modelling of anticancer drug sensitivity. Nature *483*, 603–607.

Barrière, C., Santamaría, D., Cerqueira, A., Galán, J., Martín, A., Ortega, S., Malumbres, M., Dubus, P., and Barbacid, M. (2007). Mice thrive without Cdk4 and Cdk2. Mol. Oncol. *1*, 72–83.

Bartek, J., and Lukas, J. (2003). Chk1 and Chk2 kinases in checkpoint control and cancer. 421–429.

Beronja, S., Janki, P., Heller, E., Lien, W.-H., Keyes, B.E., Oshimori, N., and Fuchs, E. (2013). RNAi

screens in mice identify physiological regulators of oncogenic growth. Nature *501*, 185–190.

Berthet, C., Aleem, E., Coppola, V., Tessarollo, L., and Kaldis, P. (2003). Cdk2 knockout mice are viable. Curr. Biol. *13*, 1775–1785.

Bester, A.C., Roniger, M., Oren, Y.S., Im, M.M., Sarni, D., Chaoat, M., Bensimon, A., Zamir, G., Shewach, D.S., and Kerem, B. (2011). Nucleotide Deficiency Promotes Genomic Instability in Early Stages of Cancer Development. Cell *145*, 435–446.

Bicknell, L.S., Bongers, E.M.H.F., Leitch, A., Brown, S., Schoots, J., Harley, M.E., Aftimos, S., Al-Aama, J.Y., Bober, M., Brown, P.A.J., et al. (2011). Mutations in the pre-replication complex cause Meier-Gorlin syndrome. Nat. Genet. *43*, 356–359.

Blow, J.J., Ge, X.Q., and Jackson, D.A. (2011). How dormant origins promote complete genome replication. Trends Biochem. Sci. *36*, 405–414.

Blum, R., Jacob-Hirsch, J., Amariglio, N., Rechavi, G., and Kloog, Y. (2005). Ras inhibition in glioblastoma down-regulates hypoxia-inducible factor-1alpha, causing glycolysis shutdown and cell death. Cancer Res. *65*, 999–1006.

Bochman, M.L., and Schwacha, A. (2008). The Mcm2-7 Complex Has In Vitro Helicase Activity.

Bochman, M.L., and Schwacha, A. (2009). The Mcm complex: unwinding the mechanism of a replicative helicase. Microbiol. Mol. Biol. Rev. *73*, 652–683.

Bongers, E.M.H.F., Opitz, J.M., Fryer, A., Sarda, P., Hennekam, R.C.M., Hall, B.D., Superneau, D.W., Harbison, M., Poss, A., Bokhoven, H. van, et al. (2001). Meier-Gorlin syndrome: Report of eight additional cases and review. Am. J. Med. Genet. *102*, 115–124.

Booher, R.N., Holman, P.S., and Fattaey, A. (1997). Human Myt1 is a cell cycle-regulated kinase that inhibits Cdc2 but not Cdk2 activity. J. Biol. Chem. *272*, 22300–22306.

Breasted, J.H. (1930). The Edwin Smith Surgical Papyrus, Volume 1: Hieroglyphic Transliteration, Translation, and Commentary (Chicago: The University of Chicago Press).

Bryant, H.E., Schultz, N., Thomas, H.D., Parker, K.M., Flower, D., Lopez, E., Kyle, S., Meuth, M., Curtin, N.J., and Helleday, T. (2005). Specific killing of BRCA2-deficient tumours with inhibitors of poly(ADP-ribose) polymerase. Nature *434*, 913–917.

Bryant, K.L., Mancias, J.D., Kimmelman, A.C., and Der, C.J. (2014). KRAS: feeding pancreatic cancer proliferation.

Burkhart, R., Schulte, D., Hu, B., Musahl, C., Gohring, F., and Knippers, R. (1995). Interactions of Human Nuclear Proteins P1Mcm3 and P1Cdc46. Eur. J. Biochem. *228*, 431–438.

Cancer Genome Atlas Network, R., Akdemir, K.C., Aksoy, B.A., Albert, M., Ally, A., Amin, S.B., Arachchi, H., Arora, A., Auman, J.T., Ayala, B., et al. (2015). Genomic Classification of Cutaneous Melanoma. Cell *161*, 1681–1696.

Carpenter, A.E., Jones, T.R., Lamprecht, M.R., Clarke, C., Kang, I.H., Friman, O., Guertin, D.A.,

Chang, J.H., Lindquist, R.A., Moffat, J., et al. (2006). CellProfiler: image analysis software for identifying and quantifying cell phenotypes. Genome Biol. *7*, R100.

Castedo, M., Perfettini, J.-L., Roumier, T., Andreau, K., Medema, R., and Kroemer, G. (2004). Cell death by mitotic catastrophe: a molecular definition. Oncogene *23*, 2825–2837.

Cerami, E., Gao, J., Dogrusoz, U., Gross, B.E., Sumer, S.O., Aksoy, B.A., Jacobsen, A., Byrne, C.J., Heuer, M.L., Larsson, E., et al. (2012). The cBio cancer genomics portal: an open platform for exploring multidimensional cancer genomics data. Cancer Discov. *2*, 401–404.

Chen, C., Pore, N., Behrooz, A., Ismail-Beigi, F., and Maity, A. (2001). Regulation of glut1 mRNA by hypoxia-inducible factor-1. Interaction between H-ras and hypoxia. J. Biol. Chem. *276*, 9519–9525.

Chen, W., Dong, J., Haiech, J., Kilhoffer, M.-C., and Zeniou, M. (2016). Cancer Stem Cell Quiescence and Plasticity as Major Challenges in Cancer Therapy. Stem Cells Int. *2016*, 1740936.

Chiaradonna, F., Sacco, E., Manzoni, R., Giorgio, M., Vanoni, M., and Alberghina, L. (2006). Ras-dependent carbon metabolism and transformation in mouse fibroblasts. Oncogene *25*, 5391–5404.

Chow, J.P.H., and Poon, R.Y.C. (2013). The CDK1 inhibitory kinase MYT1 in DNA damage checkpoint recovery. Oncogene *32*, 4778–4788.

Ciombor, K.K., and Berlin, J. (2014). Targeting metastatic colorectal cancer - present and emerging treatment options. Pharmgenomics. Pers. Med. *7*, 137–144.

Ciriello, G., Gatza, M.L., Beck, A.H., Wilkerson, M.D., Rhie, S.K., Pastore, A., Zhang, H., McLellan, M., Yau, C., Kandoth, C., et al. (2015). Comprehensive Molecular Portraits of Invasive Lobular Breast Cancer. Cell *163*, 506–519.

Collisson, E.A., Trejo, C., Silva, J., Gu, S., Korkola, J.E., Heiser, L., Charles, R.-P., Rabinovich, B.A., Hann, B., Dankort, D., et al. (2012). A Central Role for RAF→MEK→ERK Signaling in the Genesis of Pancreatic Ductal Adenocarcinoma. Cancer Discov. *2*, 685.

Collisson, E.A., Campbell, J.D., Brooks, A.N., Berger, A.H., Lee, W., Chmielecki, J., Beer, D.G., Cope, L., Creighton, C.J., Danilova, L., et al. (2014). Comprehensive molecular profiling of lung adenocarcinoma. Nature *511*, 543–550.

Commisso, C., Davidson, S.M., Soydaner-Azeloglu, R.G., Parker, S.J., Kamphorst, J.J., Hackett, S., Grabocka, E., Nofal, M., Drebin, J.A., Thompson, C.B., et al. (2013). Macropinocytosis of protein is an amino acid supply route in Ras-transformed cells. Nature *497*, 633–637.

Corcoran, R.B., Cheng, K.A., Hata, A.N., Faber, A.C., Ebi, H., Coffee, E.M., Greninger, P., Brown, R.D., Godfrey, J.T., Cohoon, T.J., et al. (2013). Synthetic Lethal Interaction of Combined BCL-XL and MEK Inhibition Promotes Tumor Regressions in KRAS Mutant Cancer Models. Cancer Cell *23*, 121–128.

Costa-Cabral, S., Brough, R., Konde, A., Aarts, M., Campbell, J., Marinari, E., Riffell, J., Bardelli, A., Torrance, C., Lord, C.J., et al. (2016). CDK1 Is a Synthetic Lethal Target for KRAS Mutant Tumours. PLoS One *11*, e0149099.

Cox, A.D., Fesik, S.W., Kimmelman, A.C., Luo, J., and Der, C.J. (2014). Drugging the undruggable RAS: Mission Possible? Nat. Rev. Drug Discov. *13*, 828–851.

Cullis, J., Meiri, D., Sandi, M.J., Radulovich, N., Kent, O.A., Medrano, M., Mokady, D., Normand, J., Larose, J., Marcotte, R., et al. (2014). The RhoGEF GEF-H1 Is Required for Oncogenic RAS Signaling via KSR-1. Cancer Cell *25*, 181–195.

Van Cutsem, E., Cervantes, A., Nordlinger, B., and Arnold, D. (2014). Metastatic colorectal cancer: ESMO Clinical Practice Guidelines for diagnosis, treatment and follow-up. Ann. Oncol. *25*, iii1-iii9.

Davies, H., Bignell, G.R., Cox, C., Stephens, P., Edkins, S., Clegg, S., Teague, J., Woffendin, H., Garnett, M.J., Bottomley, W., et al. (2002). Mutations of the BRAF gene in human cancer. Nature *417*, 949–954.

Deegan, T.D., and Diffley, J.F.X. (2016). MCM: One ring to rule them all. Curr. Opin. Struct. Biol. *37*, 145–151.

Dewar, J.M., Budzowska, M., and Walter, J.C. (2015). The mechanism of DNA replication termination in vertebrates. Nature *525*, 345–350.

Dietlein, F., Kalb, B., Jokic, M., Noll, E.M., Strong, A., Tharun, L., Ozretić, L., Künstlinger, H., Kambartel, K., Randerath, W.J., et al. (2015). A Synergistic Interaction between Chk1- and MK2 Inhibitors in KRAS-Mutant Cancer. Cell *162*, 146–159.

Dimauro, T., and David, G. (2010). Ras-induced senescence and its physiological relevance in cancer. Curr. Cancer Drug Targets *10*, 869–876.

Diril, M.K., Ratnacaram, C.K., Padmakumar, V.C., Du, T., Wasser, M., Coppola, V., Tessarollo, L., and Kaldis, P. (2012). Cyclin-dependent kinase 1 (Cdk1) is essential for cell division and suppression of DNA re-replication but not for liver regeneration. Proc. Natl. Acad. Sci. *109*, 3826–3831.

Dobzhansky, T. (1946). Genetics of natural populations; recombination and variability in populations of Drosophila pseudoobscura. Genetics *31*, 269–290.

Donegang, W. (2006). Breast Cancer. In Breast Cancer, D. Winchester, D. Winchester, C. Hudis, and L. Norton, eds. (Ontario: BC Dekker), pp. 1–14.

Donzelli, M., and Draetta, G.F. (2003). Regulating mammalian checkpoints through Cdc25 inactivation. EMBO Rep. *4*, 671–677.

Douillard, J.-Y., Oliner, K.S., Siena, S., Tabernero, J., Burkes, R., Barugel, M., Humblet, Y., Bodoky, G., Cunningham, D., Jassem, J., et al. (2013). Panitumumab–FOLFOX4 Treatment and *RAS*

Mutations in Colorectal Cancer. N. Engl. J. Med. *369*, 1023–1034.

Downward, J. (2003). Targeting RAS signalling pathways in cancer therapy. Nat Rev Cancer *3*, 11–22.

Downward, J. (2015). RAS Synthetic Lethal Screens Revisited: Still Seeking the Elusive Prize? Clin. Cancer Res. *21*, 1802–1809.

Duncan, J.S., Whittle, M.C., Nakamura, K., Abell, A.N., Midland, A.A., Zawistowski, J.S., Johnson, N.L., Granger, D.A., Jordan, N.V., Darr, D.B., et al. (2012). Dynamic Reprogramming of the Kinome in Response to Targeted MEK Inhibition in Triple-Negative Breast Cancer. Cell *149*, 307–321.

Dziadkowiec, K.N., Gąsiorowska, E., Nowak-Markwitz, E., and Jankowska, A. (2016). PARP inhibitors: review of mechanisms of action and BRCA1/2 mutation targeting. Prz. Menopauzalny = Menopause Rev. *15*, 215–219.

Esteban, L.M., Vicario-Abejón, C., Fernández-Salguero, P., Fernández-Medarde, A., Swaminathan, N., Yienger, K., Lopez, E., Malumbres, M., McKay, R., Ward, J.M., et al. (2001). Targeted genomic disruption of H-ras and N-ras, individually or in combination, reveals the dispensability of both loci for mouse growth and development. Mol. Cell. Biol. *21*, 1444–1452.

Evers, B., Jastrzebski, K., Heijmans, J.P.M., Grernrum, W., Beijersbergen, R.L., and Bernards, R. (2016). CRISPR knockout screening outperforms shRNA and CRISPRi in identifying essential genes. Nat. Biotechnol. *34*, 631–633.

Evrin, C., Clarke, P., Zech, J., Lurz, R., Sun, J., Uhle, S., Li, H., Stillman, B., and Speck, C. (2009). A double-hexameric MCM2-7 complex is loaded onto origin DNA during licensing of eukaryotic DNA replication. Proc. Natl. Acad. Sci. U. S. A. *106*, 20240–20245.

Faltas, B. (2011). Cancer is an ancient disease: the case for better palaeoepidemiological and molecular studies. Nat. Rev. Cancer *11*, 76–76.

Farmer, H., McCabe, N., Lord, C.J., Tutt, A.N.J., Johnson, D.A., Richardson, T.B., Santarosa, M., Dillon, K.J., Hickson, I., Knights, C., et al. (2005). Targeting the DNA repair defect in BRCA mutant cells as a therapeutic strategy. Nature *434*, 917–921.

Fellmann, C., Zuber, J., McJunkin, K., Chang, K., Malone, C.D., Dickins, R. a., Xu, Q., Hengartner, M.O., Elledge, S.J., Hannon, G.J., et al. (2011). Functional Identification of Optimized RNAi Triggers Using a Massively Parallel Sensor Assay. Mol. Cell *41*, 733–746.

Feng, D., Tu, Z., Wu, W., and Liang, C. (2003). Inhibiting the expression of DNA replication-initiation proteins induces apoptosis in human cancer cells. Cancer Res. *63*, 7356–7364.

Ferlay, J., Soerjomataram, I., Dikshit, R., Eser, S., Mathers, C., Rebelo, M., Parkin, D.M., Forman, D., and Bray, F. (2015). Cancer incidence and mortality worldwide: Sources, methods and major patterns in GLOBOCAN 2012. Int. J. Cancer *136*, E359–E386.

Filmus, J., Robles, A.I., Shi, W., Wong, M.J., Colombo, L.L., and Conti, C.J. (1994). Induction of cyclin D1 overexpression by activated ras. Oncogene *9*, 3627–3633.

Flier, J.S., Mueckler, M.M., Usher, P., and Lodish, H.F. (1987). Elevated levels of glucose transport and transporter messenger RNA are induced by ras or src oncogenes. Science *235*, 1492–1495.

Forbes, S.A., Beare, D., Boutselakis, H., Bamford, S., Bindal, N., Tate, J., Cole, C.G., Ward, S., Dawson, E., Ponting, L., et al. (2017). COSMIC: somatic cancer genetics at high-resolution. Nucleic Acids Res. *45*, D777–D783.

Gaglio, D., Metallo, C.M., Gameiro, P.A., Hiller, K., Danna, L.S., Balestrieri, C., Alberghina, L., Stephanopoulos, G., and Chiaradonna, F. (2011). Oncogenic K-Ras decouples glucose and glutamine metabolism to support cancer cell growth. Mol. Syst. Biol. *7*, 523.

Gambus, A., Jones, R.C., Sanchez-Diaz, A., Kanemaki, M., van Deursen, F., Edmondson, R.D., and Labib, K. (2006). GINS maintains association of Cdc45 with MCM in replisome progression complexes at eukaryotic DNA replication forks. Nat. Cell Biol. *8*, 358–366.

Gambus, A., Khoudoli, G.A., Jones, R.C., and Blow, J.J. (2011). MCM2-7 form double hexamers at licensed origins in Xenopus egg extract. J. Biol. Chem. *286*, 11855–11864.

Garnett, M.J., Edelman, E.J., Heidorn, S.J., Greenman, C.D., Dastur, A., Lau, K.W., Greninger, P., Thompson, I.R., Luo, X., Soares, J., et al. (2012). Systematic identification of genomic markers of drug sensitivity in cancer cells. Nature *483*, 570–575.

Ge, X.Q., and Blow, J.J. (2010). Chk1 inhibits replication factory activation but allows dormant origin firing in existing factories. J. Cell Biol. *191*, 1285–1297.

Ge, X.Q., Jackson, D.A., and Blow, J.J. (2007). Dormant origins licensed by excess Mcm2-7 are required for human cells to survive replicative stress. Genes Dev. *21*, 3331–3341.

Getz, G., Gabriel, S.B., Cibulskis, K., Lander, E., Sivachenko, A., Sougnez, C., Lawrence, M., Kandoth, C., Dooling, D., Fulton, R., et al. (2013). Integrated genomic characterization of endometrial carcinoma. Nature *497*, 67–73.

Grabocka, E., Pylayeva-Gupta, Y., Jones, M.K., Lubkov, V., Yemanaberhan, E., Taylor, L., Jeng, H., and Bar-Sagi, D. (2014). Wild-Type H- and N-Ras Promote Mutant K-Ras-Driven Tumorigenesis by Modulating the DNA Damage Response. Cancer Cell *25*, 243–256.

Grabocka, E., Commisso, C., and Bar-Sagi, D. (2015). Molecular pathways: Targeting the dependence of mutant RAS cancers on the DNA damage response. Clin. Cancer Res. *21*, 1243–1247.

Guinney, J., Dienstmann, R., Wang, X., de Reyniès, A., Schlicker, A., Soneson, C., Marisa, L., Roepman, P., Nyamundanda, G., Angelino, P., et al. (2015). The consensus molecular subtypes of colorectal cancer. Nat. Med. *21*, 1350–1356.

Guo, J.Y., Chen, H.-Y., Mathew, R., Fan, J., Strohecker, A.M., Karsli-Uzunbas, G., Kamphorst, J.J.,

Chen, G., Lemons, J.M.S., Karantza, V., et al. (2011). Activated Ras requires autophagy to maintain oxidative metabolism and tumorigenesis. Genes Dev. *25*, 460–470.

Hajdu, S.I. (2011). A note from history: Landmarks in history of cancer, part 1. Cancer *117*, 1097–1102.

Hanahan, D., and Weinberg, R.A. (2000). The Hallmarks of Cancer. Cell *100*, 57–70.

Hanahan, D., and Weinberg, R.A. (2011). Hallmarks of cancer: the next generation. Cell *144*, 646–674.

Hans, F., and Dimitrov, S. (2001). Histone H3 phosphorylation and cell division. Oncogene *20*, 3021–3027.

Heller, R.C., Kang, S., Lam, W.M., Chen, S., Chan, C.S., and Bell, S.P. (2011). Eukaryotic origin-dependent DNA replication in vitro reveals sequential action of DDK and S-CDK kinases. Cell *146*, 80–91.

Hills, S.A., and Diffley, J.F.X. (2014). DNA replication and oncogene-induced replicative stress. Curr. Biol. *24*, R435–R444.

Hitomi, M., and Stacey, D.W. (1999). Cyclin D1 production in cycling cells depends on Ras in a cell-cycle-specific manner. Curr. Biol. *9*, 1075-S2.

Hobbs, G.A., Der, C.J., and Rossman, K.L. (2016). RAS isoforms and mutations in cancer at a glance. J. Cell Sci. *129*, 1287–1292.

Holderfield, M., Nagel, T.E., and Stuart, D.D. (2014). Mechanism and consequences of RAF kinase activation by small-molecule inhibitors. Br. J. Cancer *111*, 640–645.

Housman, G., Byler, S., Heerboth, S., Lapinska, K., Longacre, M., Snyder, N., and Sarkar, S. (2014). Drug resistance in cancer: an overview. Cancers (Basel). *6*, 1769–1792.

Ibarra, A., Schwob, E., and Méndez, J. (2008). Excess MCM proteins protect human cells from replicative stress by licensing backup origins of replication. Proc. Natl. Acad. Sci. U. S. A. *105*, 8956–8961.

Ilves, I., Petojevic, T., Pesavento, J.J., and Botchan, M.R. (2010). Activation of the MCM2-7 Helicase by Association with Cdc45 and GINS Proteins. Mol. Cell *37*, 247–258.

Irani, K., Xia, Y., Zweier, J.L., Sollott, S.J., Der, C.J., Fearon, E.R., Sundaresan, M., Finkel, T., and Goldschmidt-Clermont, P.J. (1997). Mitogenic signaling mediated by oxidants in Ras-transformed fibroblasts. Science *275*, 1649–1652.

Janes, M.R., Zhang, J., Li, L.-S., Hansen, R., Peters, U., Guo, X., Chen, Y., Babbar, A., Firdaus, S.J., Darjania, L., et al. (2018). Targeting KRAS Mutant Cancers with a Covalent G12C-Specific Inhibitor. Cell *172*, 578–589.e17.

Jass, J.R. (2007). Classification of colorectal cancer based on correlation of clinical, morphological and molecular features. Histopathology *50*, 113–130.

Johnson, L., Greenbaum, D., Cichowski, K., Mercer, K., Murphy, E., Schmitt, E., Bronson, R.T., Umanoff, H., Edelmann, W., Kucherlapati, R., et al. (1997). K-ras is an essential gene in the mouse with partial functional overlap with N-ras. Genes Dev. *11*, 2468–2481.

Jost, M., Chen, Y., Gilbert, L.A., Horlbeck, M.A., Krenning, L., Menchon, G., Rai, A., Cho, M.Y., Stern, J.J., Prota, A.E., et al. (2017). Combined CRISPRi/a-Based Chemical Genetic Screens Reveal that Rigosertib Is a Microtubule-Destabilizing Agent. Mol. Cell *68*, 210–223.e6.

Jürchott, K., Kuban, R.-J., Krech, T., Blüthgen, N., Stein, U., Walther, W., Friese, C., Kiełbasa, S.M., Ungethüm, U., Lund, P., et al. (2010). Identification of Y-Box Binding Protein 1 As a Core Regulator of MEK/ERK Pathway-Dependent Gene Signatures in Colorectal Cancer Cells. PLoS Genet. *6*, e1001231.

Kang, J.S., and Krauss, R.S. (1996). Ras induces anchorage-independent growth by subverting multiple adhesion-regulated cell cycle events. Mol. Cell. Biol. *16*, 3370–3380.

Kastan, M.B., and Bartek, J. (2004). Cell-cycle checkpoints and cancer. Nature *432*, 316–323.

Kilbey, A., Terry, A., Cameron, E.R., and Neil, J.C. (2008). Oncogene-induced senescence: an essential role for Runx. Cell Cycle *7*, 2333–2340.

Kim, H.S., Mendiratta, S., Kim, J., Pecot, C.V., Larsen, J.E., Zubovych, I., Seo, B.Y., Kim, J., Eskiocak, B., Chung, H., et al. (2013). Systematic Identification of Molecular Subtype-Selective Vulnerabilities in Non-Small-Cell Lung Cancer. Cell *155*, 552–566.

Kim, J., McMillan, E., Kim, H.S., Venkateswaran, N., Makkar, G., Rodriguez-Canales, J., Villalobos, P., Neggers, J.E., Mendiratta, S., Wei, S., et al. (2016). XPO1-dependent nuclear export is a druggable vulnerability in KRAS-mutant lung cancer. Nature *538*, 114–117.

Klinger, B., Sieber, A., Fritsche-Guenther, R., Witzel, F., Berry, L., Schumacher, D., Yan, Y., Durek, P., Merchant, M., Schäfer, R., et al. (2013). Network quantification of EGFR signaling unveils potential for targeted combination therapy. Mol. Syst. Biol. *9*, 673.

Klingseisen, A., and Jackson, A.P. (2011). Mechanisms and pathways of growth failure in primordial dwarfism. Genes Dev. *25*, 2011–2024.

Klotz-Noack, K., McIntosh, D., Schurch, N., Pratt, N., and Blow, J.J. (2012). Re-replication induced by geminin depletion occurs from G2 and is enhanced by checkpoint activation. J. Cell Sci. *125*, 2436–2445.

Knauf, J.A., Ouyang, B., Knudsen, E.S., Fukasawa, K., Babcock, G., and Fagin, J.A. (2006). Oncogenic RAS induces accelerated transition through G2/M and promotes defects in the G2 DNA damage and mitotic spindle checkpoints. J. Biol. Chem. *281*, 3800–3809.

Kole, H.K., Resnick, R.J., Van Doren, M., and Racker, E. (1991). Regulation of 6-phosphofructo-1-kinase activity in ras-transformed rat-1 fibroblasts. Arch. Biochem. Biophys. *286*, 586–590.

Kotsantis, P., Silva, L.M., Irmscher, S., Jones, R.M., Folkes, L., Gromak, N., and Petermann, E. (2016). Increased global transcription activity as a mechanism of replication stress in cancer.

Nat. Commun. *7*, 13087.

Kumar, M.S., Hancock, D.C., Molina-Arcas, M., Steckel, M., East, P., Diefenbacher, M., Armenteros-Monterroso, E., Lassailly, F., Matthews, N., Nye, E., et al. (2012). The GATA2 Transcriptional Network Is Requisite for RAS Oncogene-Driven Non-Small Cell Lung Cancer. Cell *149*, 642–655.

Labib, K., Tercero, J.A., Diffley, J.F., and Labib, K. (2000). Uninterrupted MCM2-7 function required for DNA replication fork progression. Science *288*, 1643–1647.

Lane, K.T., and Beese, L.S. (2006). Thematic review series: lipid posttranslational modifications. Structural biology of protein farnesyltransferase and geranylgeranyltransferase type I. J. Lipid Res. *47*, 681–699.

Lawrence, M.S., Sougnez, C., Lichtenstein, L., Cibulskis, K., Lander, E., Gabriel, S.B., Getz, G., Ally, A., Balasundaram, M., Birol, I., et al. (2015). Comprehensive genomic characterization of head and neck squamous cell carcinomas. Nature *517*, 576–582.

Lee, A.C., Fenster, B.E., Ito, H., Takeda, K., Bae, N.S., Hirai, T., Yu, Z.X., Ferrans, V.J., Howard, B.H., and Finkel, T. (1999). Ras proteins induce senescence by altering the intracellular levels of reactive oxygen species. J. Biol. Chem. *274*, 7936–7940.

Lim, S.M., Westover, K.D., Ficarro, S.B., Harrison, R.A., Choi, H.G., Pacold, M.E., Carrasco, M., Hunter, J., Kim, N.D., Xie, T., et al. (2014). Therapeutic targeting of oncogenic K-Ras by a covalent catalytic site inhibitor. Angew. Chem. Int. Ed. Engl. *53*, 199–204.

Lin, Y.-L., Liang, Y.-H., Tsai, J.-H., Liau, J.-Y., Liang, J.-T., Lin, B.-R., Hung, J.-S., Lin, L.-I., Tseng, L.-H., Chang, Y.-L., et al. (2014). Oxaliplatin-Based Chemotherapy Is More Beneficial in KRAS Mutant than in KRAS Wild-Type Metastatic Colorectal Cancer Patients. PLoS One *9*, e86789.

Liu, J.J., Chao, J.R., Jiang, M.C., Ng, S.Y., Yen, J.J., and Yang-Yen, H.F. (1995). Ras transformation results in an elevated level of cyclin D1 and acceleration of G1 progression in NIH 3T3 cells. Mol. Cell. Biol. *15*, 3654–3663.

Lock, R., Roy, S., Kenific, C.M., Su, J.S., Salas, E., Ronen, S.M., and Debnath, J. (2011). Autophagy facilitates glycolysis during Ras-mediated oncogenic transformation. Mol. Biol. Cell *22*, 165–178.

Lohr, J.G., Stojanov, P., Carter, S.L., Cruz-Gordillo, P., Lawrence, M.S., Auclair, D., Sougnez, C., Knoechel, B., Gould, J., Saksena, G., et al. (2014). Widespread genetic heterogeneity in multiple myeloma: implications for targeted therapy. Cancer Cell *25*, 91–101.

Lukas, C., Savic, V., Bekker-Jensen, S., Doil, C., Neumann, B., Sølvhøj Pedersen, R., Grøfte, M., Chan, K.L., Hickson, I.D., Bartek, J., et al. (2011). 53BP1 nuclear bodies form around DNA lesions generated by mitotic transmission of chromosomes under replication stress. Nat. Cell Biol. *13*, 243–253.

Luo, J., Emanuele, M.J., Li, D., Creighton, C.J., Schlabach, M.R., Westbrook, T.F., Wong, K.K., and Elledge, S.J. (2009). A Genome-wide RNAi Screen Identifies Multiple Synthetic Lethal

Interactions with the Ras Oncogene. Cell *137*, 835–848.

Machida, Y.J., Teer, J.K., and Dutta, A. (2005). Acute reduction of an origin recognition complex (ORC) subunit in human cells reveals a requirement of ORC for Cdk2 activation. J. Biol. Chem. *280*, 27624–27630.

Maculins, T., Nkosi, P.J., Nishikawa, H., and Labib, K. (2015). Tethering of SCF(Dia2) to the Replisome Promotes Efficient Ubiquitylation and Disassembly of the CMG Helicase. Curr. Biol. *25*, 2254–2259.

Maertens, O., and Cichowski, K. (2014). An expanding role for RAS GTPase activating proteins (RAS GAPs) in cancer. Adv. Biol. Regul. *55*, 1–14.

Mahbubani, H.M., Chong, J.P., Chevalier, S., Thömmes, P., and Blow, J.J. (1997). Cell cycle regulation of the replication licensing system: involvement of a Cdk-dependent inhibitor. J. Cell Biol. *136*, 125–135.

Malumbres, M., and Barbacid, M. (2003). RAS oncogenes: the first 30 years. Nat. Rev. Cancer *3*, 459–465.

Malumbres, M., and Barbacid, M. (2009). Cell cycle, CDKs and cancer: a changing paradigm. Nat. Rev. Cancer *9*, 153–166.

Malumbres, M., Sotillo, R., Santamaría, D., Galán, J., Cerezo, A., Ortega, S., Dubus, P., and Barbacid, M. (2004). Mammalian Cells Cycle without the D-Type Cyclin-Dependent Kinases Cdk4 and Cdk6. Cell *118*, 493–504.

Mannava, S., Moparthy, K.C., Wheeler, L.J., Natarajan, V., Zucker, S.N., Fink, E.E., Im, M., Flanagan, S., Burhans, W.C., Zeitouni, N.C., et al. (2013). Depletion of deoxyribonucleotide pools is an endogenous source of DNA damage in cells undergoing oncogene-induced senescence. Am. J. Pathol. *182*, 142–151.

Martin, T.D., Cook, D.R., Choi, M.Y., Li, M.Z., Haigis, K.M., and Elledge, S.J. (2017). A Role for Mitochondrial Translation in Promotion of Viability in K-Ras Mutant Cells. Cell Rep. *20*, 427–438.

Martini, G., Troiani, T., Cardone, C., Vitiello, P., Sforza, V., Ciardiello, D., Napolitano, S., Della Corte, C.M., Morgillo, F., Raucci, A., et al. (2017). Present and future of metastatic colorectal cancer treatment: A review of new candidate targets. World J. Gastroenterol. *23*, 4675–4688.

Matsuo, Y., Campbell, P.M., Brekken, R.A., Sung, B., Ouellette, M.M., Fleming, J.B., Aggarwal, B.B., Der, C.J., and Guha, S. (2009). K-Ras promotes angiogenesis mediated by immortalized human pancreatic epithelial cells through mitogen-activated protein kinase signaling pathways. Mol. Cancer Res. *7*, 799–808.

Maya-Mendoza, A., Ostrakova, J., Kosar, M., Hall, A., Duskova, P., Mistrik, M., Merchut-Maya,

J.M., Hodny, Z., Bartkova, J., Christensen, C., et al. (2015). Myc and Ras oncogenes engage different energy metabolism programs and evoke distinct patterns of oxidative and DNA replication stress. Mol. Oncol. *9*, 601–616.

McGranahan, N., Burrell, R.A., Endesfelder, D., Novelli, M.R., and Swanton, C. (2012). Cancer chromosomal instability: therapeutic and diagnostic challenges. EMBO Rep. *13*, 528–538.

McIntosh, D., and Blow, J.J. (2012). Dormant origins, the licensing checkpoint, and the response to replicative stresses. Cold Spring Harb. Perspect. Biol. *4*.

Di Micco, R., Fumagalli, M., Cicalese, A., Piccinin, S., Gasparini, P., Luise, C., Schurra, C., Garre, M., Nuciforo, P.G., Bensimon, A., et al. (2006). Oncogene-induced senescence is a DNA damage response triggered by DNA hyper-replication. Nature *444*, 638–642.

Michel, B., Flores, M.J., Viguera, E., Grompone, G., Seigneur, M., and Bidnenko, V. (2001). Rescue of arrested replication forks by homologous recombination. Proc. Natl. Acad. Sci. U. S. A. *98*, 8181–8188.

Mitsushita, J., Lambeth, J.D., and Kamata, T. (2004). The Superoxide-Generating Oxidase Nox1 Is Functionally Required for Ras Oncogene Transformation. CANCER Res. *64*, 3580–3585.

Montagnoli, A., Valsasina, B., Brotherton, D., Troiani, S., Rainoldi, S., Tenca, P., Molinari, A., and Santocanale, C. (2006). Identification of Mcm2 phosphorylation sites by S-phase-regulating kinases. J. Biol. Chem. *281*, 10281–10290.

Montagnoli, A., Valsasina, B., Croci, V., Menichincheri, M., Rainoldi, S., Marchesi, V., Tibolla, M., Tenca, P., Brotherton, D., Albanese, C., et al. (2008). A Cdc7 kinase inhibitor restricts initiation of DNA replication and has antitumor activity. Nat. Chem. Biol. *4*, 357–365.

Moreno, A., Carrington, J.T., Albergante, L., Al Mamun, M., Haagensen, E.J., Komseli, E.-S., Gorgoulis, V.G., Newman, T.J., and Blow, J.J. (2016). Unreplicated DNA remaining from unperturbed S phases passes through mitosis for resolution in daughter cells. Proc. Natl. Acad. Sci. U. S. A. *113*, E5757-64.

Morgan-Lappe, S.E., Tucker, L.A., Huang, X., Zhang, Q., Sarthy, A. V., Zakula, D., Vernetti, L., Schurdak, M., Wang, J., and Fesik, S.W. (2007). Identification of Ras-Related Nuclear Protein, Targeting Protein for Xenopus Kinesin-like Protein 2, and Stearoyl-CoA Desaturase 1 as Promising Cancer Targets from an RNAi-Based Screen. Cancer Res. *67*, 4390–4398.

Moyer, S.E., Lewis, P.W., and Botchan, M.R. (2006). Isolation of the Cdc45/Mcm2-7/GINS (CMG) complex, a candidate for the eukaryotic DNA replication fork helicase. Proc. Natl. Acad. Sci. U. S. A. *103*, 10236–10241.

Mueller, P.R., Coleman, T.R., Kumagai, A., and Dunphy, W.G. (1995). Myti: A Membrane-Associated Inhibitory Kinas That Phosphorylates Cdc2. *270*.

Muzny, D.M., Bainbridge, M.N., Chang, K., Dinh, H.H., Drummond, J.A., Fowler, G., Kovar, C.L., Lewis, L.R., Morgan, M.B., Newsham, I.F., et al. (2012). Comprehensive molecular characterization of human colon and rectal cancer. Nature *487*, 330–337.

National Institutes of Health (NIH) clinicaltrials.gov https://clinicaltrials.gov/. accessed January 17, 2018.

Neel, N.F., Martin, T.D., Stratford, J.K., Zand, T.P., Reiner, D.J., and Der, C.J. (2011). The RalGEF-Ral Effector Signaling Network: The Road Less Traveled for Anti-Ras Drug Discovery. Genes Cancer *2*, 275–287.

Nevis, K.R., Cordeiro-Stone, M., and Cook, J.G. (2009). Origin licensing and p53 status regulate Cdk2 activity during G(1). Cell Cycle *8*, 1952–1963.

Nigg, E.A. (2001). Mitotic kinases as regulators of cell division and its checkpoints. Nat. Rev. Mol. Cell Biol. *2*, 21–32.

Nijman, S.M.B. (2011). Synthetic lethality: general principles, utility and detection using genetic screens in human cells. FEBS Lett. *585*, 1–6.

Nishitani, H., and Lygerou, Z. (2002). Control of DNA replication licensing in a cell cycle. Genes Cells *7*, 523–534.

O'Connor, M.J. (2015). Targeting the DNA Damage Response in Cancer. Mol. Cell *60*, 547–560.

Ogrunc, M., Di Micco, R., Liontos, M., Bombardelli, L., Mione, M., Fumagalli, M., Gorgoulis, V.G., and d'Adda di Fagagna, F. (2014). Oncogene-induced reactive oxygen species fuel hyperproliferation and DNA damage response activation. Cell Death Differ. *21*, 998–1012.

Ortega, S., Prieto, I., Odajima, J., Martín, A., Dubus, P., Sotillo, R., Barbero, J.L., Malumbres, M., and Barbacid, M. (2003). Cyclin-dependent kinase 2 is essential for meiosis but not for mitotic cell division in mice. Nat. Genet. *35*, 25–31.

Ostrem, J.M., Peters, U., Sos, M.L., Wells, J.A., and Shokat, K.M. (2013). K-Ras(G12C) inhibitors allosterically control GTP affinity and effector interactions. Nature *503*, 548–551.

Padmanabhan, V., Callas, P., Philips, G., Trainer, T.D., and Beatty, B.G. (2004). DNA replication regulation protein Mcm7 as a marker of proliferation in prostate cancer. J. Clin. Pathol. *57*, 1057–1062.

Palmer, A., Gavin, A.C., and Nebreda, A.R. (1998). A link between MAP kinase and p34(cdc2)/cyclin B during oocyte maturation: p90(rsk) phosphorylates and inactivates the p34(cdc2) inhibitory kinase Myt1. EMBO J. *17*, 5037–5047.

Papke, B., and Der, C.J. (2017). Drugging RAS: Know the enemy. Science (80-.). *355*, 1158–1163.

Papke, B., Murarka, S., Vogel, H.A., Martín-Gago, P., Kovacevic, M., Truxius, D.C., Fansa, E.K., Ismail, S., Zimmermann, G., Heinelt, K., et al. (2016). Identification of pyrazolopyridazinones as PDEδ inhibitors. Nat. Commun. *7*, 11360.

Peng, S.-B., Henry, J.R., Kaufman, M.D., Lu, W.-P., Smith, B.D., Vogeti, S., Rutkoski, T.J., Wise, S.,

Chun, L., Zhang, Y., et al. (2015). Inhibition of RAF Isoforms and Active Dimers by LY3009120 Leads to Anti-tumor Activities in RAS or BRAF Mutant Cancers. Cancer Cell *28*, 384–398.

Phipps, A.I., Limburg, P.J., Baron, J.A., Burnett-Hartman, A.N., Weisenberger, D.J., Laird, P.W., Sinicrope, F.A., Rosty, C., Buchanan, D.D., Potter, J.D., et al. (2015). Association between molecular subtypes of colorectal cancer and patient survival. Gastroenterology *148*, 77–87.e2.

Prahallad, A., Sun, C., Huang, S., Di Nicolantonio, F., Salazar, R., Zecchin, D., Beijersbergen, R.L., Bardelli, A., and Bernards, R. (2012). Unresponsiveness of colon cancer to BRAF(V600E) inhibition through feedback activation of EGFR. Nature *483*, 100–103.

Pruitt, S.C., Bailey, K.J., and Freeland, A. (2007). Reduced Mcm2 Expression Results in Severe Stem/Progenitor Cell Deficiency and Cancer. Stem Cells *25*, 3121–3132.

Pylayeva-Gupta, Y., Grabocka, E., and Bar-Sagi, D. (2011). RAS oncogenes: weaving a tumorigenic web. Nat. Rev. Cancer *11*, 761–774.

Qu, K., Wang, Z., Fan, H., Li, J., Liu, J., Li, P., Liang, Z., An, H., Jiang, Y., Lin, Q., et al. (2017). MCM7 promotes cancer progression through cyclin D1-dependent signaling and serves as a prognostic marker for patients with hepatocellular carcinoma. Cell Death Dis. *8*, e2603–e2603.

Quinlan, A.R., and Hall, I.M. (2010). BEDTools: a flexible suite of utilities for comparing genomic features. Bioinformatics *26*, 841–842.

Rai, P., Onder, T.T., Young, J.J., McFaline, J.L., Pang, B., Dedon, P.C., and Weinberg, R.A. (2009). Continuous elimination of oxidized nucleotides is necessary to prevent rapid onset of cellular senescence. Proc. Natl. Acad. Sci. U. S. A. *106*, 169–174.

Ray-David, H., Romeo, Y., Lavoie, G., Déléris, P., Tcherkezian, J., Galan, J. a, and Roux, P.P. (2013). RSK promotes G2 DNA damage checkpoint silencing and participates in melanoma chemoresistance. Oncogene *32*, 4480–4489.

Remus, D., Beuron, F., Tolun, G., Griffith, J.D., Morris, E.P., and Diffley, J.F.X. (2009). Concerted Loading of Mcm2–7 Double Hexamers around DNA during DNA Replication Origin Licensing. Cell *139*, 719–730.

Ren, B., Yu, G., Tseng, G.C., Cieply, K., Gavel, T., Nelson, J., Michalopoulos, G., Yu, Y.P., and Luo, J.-H. (2006). MCM7 amplification and overexpression are associated with prostate cancer progression. Oncogene *25*, 1090–1098.

Ritt, D.A., Abreu-Blanco, M.T., Bindu, L., Durrant, D.E., Zhou, M., Specht, S.I., Stephen, A.G., Holderfield, M., and Morrison, D.K. (2016). Inhibition of Ras/Raf/MEK/ERK Pathway Signaling by a Stress-Induced Phospho-Regulatory Circuit. Mol. Cell *64*, 875–887.

Robinson, M.D., McCarthy, D.J., and Smyth, G.K. (2010). edgeR: a Bioconductor package for differential expression analysis of digital gene expression data. Bioinformatics *26*, 139–140.

Ryan, M.B., Der, C.J., Wang-Gillam, A., and Cox, A.D. (2015). Targeting RAS-mutant cancers: is ERK the key? Trends in Cancer *1*, 183–198.

Santamaría, D., Barrière, C., Cerqueira, A., Hunt, S., Tardy, C., Newton, K., Cáceres, J.F., Dubus, P., Malumbres, M., and Barbacid, M. (2007). Cdk1 is sufficient to drive the mammalian cell cycle. Nature *448*, 811–815.

Sarthy, A. V., Morgan-Lappe, S.E., Zakula, D., Vernetti, L., Schurdak, M., Packer, J.C.L., Anderson, M.G., Shirasawa, S., Sasazuki, T., and Fesik, S.W. (2007). Survivin depletion preferentially reduces the survival of activated K-Ras-transformed cells. Mol. Cancer Ther. *6*, 269–276.

Schafer, K.A. (1998). The Cell Cycle: A Review. Vet. Pathol. *35*, 461–478.

Scholl, C., Fröhling, S., Dunn, I.F., Schinzel, A.C., Barbie, D.A., Kim, S.Y., Silver, S.J., Tamayo, P., Wadlow, R.C., Ramaswamy, S., et al. (2009). Synthetic Lethal Interaction between Oncogenic KRAS Dependency and STK33 Suppression in Human Cancer Cells. Cell *137*, 821–834.

Shirasawa, S., Furuse, M., Yokoyama, N., and Sasazuki, T. (1993). Altered growth of human colon cancer cell lines disrupted at activated Ki-ras. Science (80-.). *260*.

Shreeram, S., Sparks, A., Lane, D.P., and Blow, J.J. (2002). Cell type-specific responses of human cells to inhibition of replication licensing. Oncogene *21*, 6624–6632.

Singh, A., and Xu, Y.-J. (2016). The Cell Killing Mechanisms of Hydroxyurea. Genes (Basel). *7*.

Singh, A., Sweeney, M.F., Yu, M., Burger, A., Greninger, P., Benes, C., Haber, D.A., and Settleman, J. (2012). TAK1 Inhibition Promotes Apoptosis in KRAS-Dependent Colon Cancers. Cell *148*, 639–650.

Son, J., Lyssiotis, C.A., Ying, H., Wang, X., Hua, S., Ligorio, M., Perera, R.M., Ferrone, C.R., Mullarky, E., Shyh-Chang, N., et al. (2013). Glutamine supports pancreatic cancer growth through a KRAS-regulated metabolic pathway. Nature *496*, 101–105.

Song, J., Wang, Z., and Ewing, R.M. (2013). Integrated analysis of the Wnt responsive proteome in human cells reveals diverse and cell-type specific networks. Mol. Biosyst. *10*, 45–53.

Steckel, M., Molina-Arcas, M., Weigelt, B., Marani, M., Warne, P.H., Kuznetsov, H., Kelly, G., Saunders, B., Howell, M., Downward, J., et al. (2012). Determination of synthetic lethal interactions in KRAS oncogene-dependent cancer cells reveals novel therapeutic targeting strategies. Cell Res. *22*, 1227–1245.

Sudhakar, A. (2009). History of Cancer, Ancient and Modern Treatment Methods. J. Cancer Sci. Ther. *1*, 1–4.

TCGA provisional The Cancer Genome Atlas - Data Portal https://tcga-data.nci.nih.gov/docs/publications/tcga/? accessed April 18, 2018.

The Cancer Genome Atlas (2012). Comprehensive molecular characterization of human colon and rectal cancer. Nature *487*, 330–337.

Tsutsui, T., Hesabi, B., Moons, D.S., Pandolfi, P.P., Hansel, K.S., Koff, A., and Kiyokawa, H. (1999). Targeted disruption of CDK4 delays cell cycle entry with enhanced p27(Kip1) activity. Mol. Cell. Biol. *19*, 7011–7019.

U.S. Food & Drug Administration (2018). Approved Drugs - FDA approves olaparib for germline BRCA-mutated metastatic breast cancer https://www.fda.gov/drugs/informationondrugs/approveddrugs/ucm592357.htm. accessed January 18, 2018.

Vakifahmetoglu, H., Olsson, M., and Zhivotovsky, B. (2008). Death through a tragedy: mitotic catastrophe. Cell Death Differ. *15*, 1153–1162.

Vicent, S., Chen, R., Sayles, L.C., Lin, C., Walker, R.G., Gillespie, A.K., Subramanian, A., Hinkle, G., Yang, X., Saif, S., et al. (2010). Wilms tumor 1 (WT1) regulates KRAS-driven oncogenesis and senescence in mouse and human models. J. Clin. Invest. *120*, 3940–3952.

Vitale, I., Galluzzi, L., Castedo, M., and Kroemer, G. (2011). Mitotic catastrophe: a mechanism for avoiding genomic instability. Nat. Rev. Mol. Cell Biol. *12*, 385–392.

Wang, J., Hu, K., Guo, J., Cheng, F., Lv, J., Jiang, W., Lu, W., Liu, J., Pang, X., and Liu, M. (2016). Suppression of KRas-mutant cancer through the combined inhibition of KRAS with PLK1 and ROCK. Nat. Commun. *7*, 11363.

Wang, T., Birsoy, K., Hughes, N.W., Krupczak, K.M., Post, Y., Wei, J.J., Lander, E.S., and Sabatini, D.M. (2015). Identification and characterization of essential genes in the human genome. Science *350*, 1096–1101.

Wang, T., Yu, H., Hughes, N.W., Liu, B., Kendirli, A., Klein, K., Chen, W.W., Lander, E.S., and Sabatini, D.M. (2017). Gene Essentiality Profiling Reveals Gene Networks and Synthetic Lethal Interactions with Oncogenic Ras. Cell *168*, 890–903.e15.

Wang, Y., Ngo, V.N., Marani, M., Yang, Y., Wright, G., Staudt, L.M., and Downward, J. (2010). Critical role for transcriptional repressor Snail2 in transformation by oncogenic RAS in colorectal carcinoma cells. Oncogene *29*, 4658–4670.

Weinstein, J.N., Akbani, R., Broom, B.M., Wang, W., Verhaak, R.G.W., McConkey, D., Lerner, S., Morgan, M., Creighton, C.J., Smith, C., et al. (2014). Comprehensive molecular characterization of urothelial bladder carcinoma. Nature *507*, 315–322.

Wellcome Sanger Institute (2018). COSMIC v83 https://cancer.sanger.ac.uk/cosmic. accessed January 9, 2018.

Weyemi, U., Lagente-Chevallier, O., Boufraqech, M., Prenois, F., Courtin, F., Caillou, B., Talbot, M., Dardalhon, M., Al Ghuzlan, A., Bidart, J.-M., et al. (2012). ROS-generating NADPH oxidase NOX4 is a critical mediator in oncogenic H-Ras-induced DNA damage and subsequent senescence. Oncogene *31*, 1117–1129.

White, E. (2013). Exploiting the bad eating habits of Ras-driven cancers. Genes Dev. *27*, 2065–2071.

Whyte, D.B., Kirschmeier, P., Hockenberry, T.N., Nunez-Oliva, I., James, L., Catino, J.J., Bishop, W.R., and Pai, J.K. (1997). K- and N-Ras are geranylgeranylated in cells treated with farnesyl protein transferase inhibitors. J. Biol. Chem. *272*, 14459–14464.

Witkiewicz, A.K., McMillan, E.A., Balaji, U., Baek, G., Lin, W.-C., Mansour, J., Mollaee, M., Wagner, K.-U., Koduru, P., Yopp, A., et al. (2015). Whole-exome sequencing of pancreatic cancer defines genetic diversity and therapeutic targets. Nat. Commun. *6*, 6744.

Wong, P.G., Winter, S.L., Zaika, E., Cao, T. V., Oguz, U., Koomen, J.M., Hamlin, J.L., and Alexandrow, M.G. (2011). Cdc45 Limits Replicon Usage from a Low Density of preRCs in Mammalian Cells. PLoS One *6*, e17533.

World Health Organization (2015). Summary tables of mortality estimates by cause, age and sex, by country http://www.who.int/healthinfo/global_burden_disease/estimates/en/index1.html. accessed January 5, 2018.

Yang, G., Mercado-Uribe, I., Multani, A.S., Sen, S., Shih, I.-M., Wong, K.-K., Gershenson, D.M., and Liu, J. (2013). RAS promotes tumorigenesis through genomic instability induced by imbalanced expression of Aurora-A and BRCA2 in midbody during cytokinesis. Int. J. Cancer *133*, 275–285.

Yang, S., Wang, X., Contino, G., Liesa, M., Sahin, E., Ying, H., Bause, A., Li, Y., Stommel, J.M., Dell'antonio, G., et al. (2011). Pancreatic cancers require autophagy for tumor growth. Genes Dev. *25*, 717–729.

Yarbro, J.W. (1992). Mechanism of action of hydroxyurea. Semin. Oncol. *19*, 1–10.

Yeeles, J.T.P., Deegan, T.D., Janska, A., Early, A., and Diffley, J.F.X. (2015). Regulated eukaryotic DNA replication origin firing with purified proteins. Nature *519*, 431–435.

Zeman, M.K., and Cimprich, K.A. (2014). Causes and consequences of replication stress. Nat. Cell Biol. *16*, 2–9.

Zeng, M., Lu, J., Li, L., Feru, F., Quan, C., Gero, T.W., Ficarro, S.B., Xiong, Y., Ambrogio, C., Paranal, R.M., et al. (2017). Potent and Selective Covalent Quinazoline Inhibitors of KRAS G12C. Cell Chem. Biol. *24*, 1005–1016.e3.

Zhang, C., Spevak, W., Zhang, Y., Burton, E.A., Ma, Y., Habets, G., Zhang, J., Lin, J., Ewing, T., Matusow, B., et al. (2015). RAF inhibitors that evade paradoxical MAPK pathway activation. Nature *526*, 583–586.

Zheng, J. (2015). Diagnostic value of MCM2 immunocytochemical staining in cervical lesions and its relationship with HPV infection. Int. J. Clin. Exp. Pathol. *8*, 875–880.

Zimmermann, G., Papke, B., Ismail, S., Vartak, N., Chandra, A., Hoffmann, M., Hahn, S.A., Triola, G., Wittinghofer, A., Bastiaens, P.I.H., et al. (2013). Small molecule inhibition of the KRAS–PDEδ interaction impairs oncogenic KRAS signalling. Nature *497*, 638–642.

Zou, L., and Elledge, S.J. (2003). Sensing DNA Damage Through ATRIP Recognition of RPA-ssDNA Complexes. Science (80-.). *300*.

Zou, L., Stillman, B., Ishimi, Y., Cvetic, C., Walter, J., Dutta, A., Leone, G., and Knudsen, E. (2000). Assembly of a complex containing Cdc45p, replication protein A, and Mcm2p at replication origins controlled by S-phase cyclin-dependent kinases and Cdc7p-Dbf4p kinase. Mol. Cell. Biol. *20*, 3086–3096.

Abbreviations

2D	two-dimensional
3D	three-dimensional
53BP1	p53-Binding Protein 1
5-FU	5-fluorouracil
AF	Alexa Fluor™
AKT	AKT Serine/Threonine Kinase
APC	Adenomatosis Polyposis Coli Tumor Suppressor
ATM	Ataxia Telangiectasia Mutated
ATP	Adenosine triphosphate
ATR	Ataxia Telangiectasia And Rad3-Related Protein
BAD	BCL2 Associated Agonist Of Cell Death
BC	before Christ
bp	base pair
BRCA	Breast Cancer
BrdU	Bromodeoxyuridine
CDC25	Cell Division Cycle 25
CDC45	Cell Division Cycle 45
CDC6	Cell Division Cycle 6
CDC7	Cell division cycle 7-related protein kinase
CDK	Cyclin-dependent kinase
CDK1	Cyclin-dependent kinase 1
CDK2	Cyclin-dependent kinase 2
CDK4	Cyclin-dependent kinase 4
CDK6	Cyclin-dependent kinase 6
cDNA	complementary DNA
CDT1	Chromatin Licensing And DNA Replication Factor 1
CHK1	Checkpoint Kinase 1
CHK2	Checkpoint Kinase 2
CI	confidence interval
CIMP	CpG island methylator phenotype
CIN	chromosome instability
c-JUN	Jun proto-oncogene
clCaspase 3	cleaved Caspase 3
clPARP	cleaved poly(ADP ribose) polymerase
CMG	CDC45-MCM-GINS
COSMIC	Catalogue of Somatic Mutations in Cancer
CRC	colorectal cancer
CRISPR	Clustered Regularly Interspaced Short Palindromic Repeats
CSK	Cytoskeletal (buffer)
DAB2IP	DAB2 Interacting Protein
DAPI	4',6-diamidino-2-phenylindole
DDK	Dbf4-dependent kinase
DNA	deoxyribonucleic acid
DNA Pol.	DNA polymerase
DNAJC2	DnaJ Heat Shock Protein Family (Hsp40) Member C2
DNMT1	DNA (cytosine-5)-methyltransferase 1

dNTP	deoxyribose nucleoside triphosphate
DOX	Doxycycline
DSB	DNA double-strand break
dsDNA	double-stranded DNA
E2F	E2F Transcription Factor
EGF	epidermal growth factor
EGFR	epidermal growth factor receptor
ELK1	ETS Transcription Factor
ENO1	Enolase 1
ERK	extracellular signal-regulated kinase
FACS	Fluorescence-activated cell sorting
FDA	United States Food and Drug Administration
FITC	Fluorescein isothiocyanate
FOXM1	Forkhead box protein M1
FTase	farnesyltransferase
GAP	GTPase activating protein
GDP	Guanosine diphosphate
GEF	guanine nucleotide exchange factor
GGTase	geranylgeranyltransferase
GINS	DNA Replication Complex GINS
GLUT1	glucose transporter 1
GPCR	G-protein-coupled-receptors
GRB2	growth-factor-receptor-bound protein 2
GSK3	Glycogen Synthase Kinase 3
GTP	Guanosine triphosphate
HIF1α	hypoxia-inducible factor 1α
HMGB3	High mobility group protein B3
HR	homologous recombination
HRAS	Harvey rat sarcoma viral oncogene homolog
IC_{50}	half maximal inhibitory concentration
ILF2	Interleukin enhancer binding factor 2
JNK	c-Jun N-terminal kinase
KLF10	Krueppel-like factor 10
KRAS	Kirsten rat sarcoma viral oncogene homolog
MAPK	Mitogen-activated protein kinase
MCM	Minichromosome Maintenance protein complex
MCM2	Minichromosome Maintenance Complex Component 2
MCM7	Minichromosome Maintenance Complex Component 7
MED8	Mediator of RNA polymerase II transcription subunit 8
MEK	mitogen-activated protein kinase kinase
MSI	microsatellite instability
mut	mutant
NADP+/NADPH	Nicotinamide adenine dinucleotide phosphate
NHEJ	non-homologous end joining
NOX1	NADPH Oxidase 1
NOX4	NADPH Oxidase 4
NRAS	neuroblastoma RAS viral oncogene homolog
NS	not significant

ORC	origin recognition complex
p90RSK	p90 ribosomal s6 kinase
PARP	poly (ADP-ribose) polymerase
PCNA	Proliferating Cell Nuclear Antigen
PCR	Polymerase chain reaction
PDAC	Pancreatic ductal adenocarcinoma
PDEδ	phosphodiesterase δ
Pen/Strep	Penicillin/Streptomycin
PI3K	Phosphatidylinositol 3-kinase
PKC	Protein Kinase C
PLCε	1-phosphatidylinositol-4,5-bisphosphate phosphodiesterase ε
PLD	Phospholipase D
PPP1R15A	Protein phosphatase 1 regulatory subunit 15A
PPP2R5A	Protein Phosphatase 2 Regulatory Subunit B'Alpha
PPP2R5B	Protein Phosphatase 2 Regulatory Subunit B'Beta
PPP2R5E	Protein Phosphatase 2 Regulatory Subunit B'Epsilon
pre-RC	pre-replication complex
PTEN	Phosphatase And Tensin Homolog
qPCR	quantitative polymerase chain reaction
RAF	rat fibrosarcoma
RAL	RAS Like Proto-Oncogene
RALGDS	Ral guanine nucleotide dissociation stimulator
RAS	rat sarcoma
RASA4	RAS P21 Protein Activator 4
Rb	Retinoblastoma
RIPA	Radioimmunoprecipitation assay (buffer)
RNA	ribonucleic acid
RNAi	RNA interference
ROS	reactive oxygen species
RPA	replication protein A
RTK	receptor tyrosine kinase
scrbl	scrambled shRNA
SD	Standard deviation
SDS	Sodium dodecyl sulfate
SEM	Standard error of the mean
shRNA	short hairpin RNA
SOS	son of sevenless
SPRY1	Sprouty RTK Signaling Antagonist 1
SSB	single-strand break
ssDNA	single-stranded DNA
TCA cycle	tricarboxylic acid cycle
TP53	Tumor Protein P53
VEGFR	vascular endothelial growth factor receptor
WBP11	WW Domain Binding Protein 11
wt	wild-type
XRCC6	X-ray repair cross-complementing protein 6

Appendix

Table A 1: shRNAs contained in shRNA library

Gene	shRNA name	Guide	97mer
DUSP4	DUSP4.1283	TTAAGCATAATTATTCATCTGT	TGCTGTTGACAGTGAGCGCCAGATGAATAAT TATGCTTAATAGTGAAGCCACAGATGTATTA AGCATAATTATTCATCTGTTGCCTACTGCCT CGGA
DUSP4	DUSP4.31	TTTTAGAACAGAATTCTGGGTA	TGCTGTTGACAGTGAGCGCACCCAGAATTCT GTTCTAAAATAGTGAAGCCACAGATGTATTT TAGAACAGAATTCTGGGTATGCCTACTGCCT CGGA
DUSP4	DUSP4.1193	TACAACAACGACAACAAAGGGA	TGCTGTTGACAGTGAGCGCCCCTTTGTTGTC GTTGTTGTATAGTGAAGCCACAGATGTATAC AACAACGACAACAAAGGGATGCCTACTGCC TCGGA
DUSP4	DUSP4.1545	TTAAAAAGCAATTCAAACCTAA	TGCTGTTGACAGTGAGCGCTAGGTTTGAATT GCTTTTTAATAGTGAAGCCACAGATGTATTA AAAAGCAATTCAAACCTAATGCCTACTGCCT CGGA
DUSP4	DUSP4.2934	TATTTCTAGAGGAAGCAGGGAG	TGCTGTTGACAGTGAGCGATCCCTGCTTCCT CTAGAAATATAGTGAAGCCACAGATGTATAT TTCTAGAGGAAGCAGGGAGTGCCTACTGCC TCGGA
DUSP6	DUSP6.1299	TTGTCTAGTACAGACAGCTGGT	TGCTGTTGACAGTGAGCGCCCAGCTGTCTGT ACTAGACAATAGTGAAGCCACAGATGTATTG TCTAGTACAGACAGCTGGTTGCCTACTGCCT CGGA
DUSP6	DUSP6.1902	TTAGTGATAATAGTGTCCGTAA	TGCTGTTGACAGTGAGCGCTACGGACACTAT TATCACTAATAGTGAAGCCACAGATGTATTA GTGATAATAGTGTCCGTAATGCCTACTGCCT CGGA
DUSP6	DUSP6.1330	TTAGTATTAACCAATTCCGCAC	TGCTGTTGACAGTGAGCGATGCGGAATTGG TTAATACTAATAGTGAAGCCACAGATGTATT AGTATTAACCAATTCCGCACTGCCTACTGCC TCGGA
DUSP6	DUSP6.1382	TATCTATACAGCATGTCCTGTT	TGCTGTTGACAGTGAGCGCACAGGACATGC TGTATAGATATAGTGAAGCCACAGATGTATA TCTATACAGCATGTCCTGTTTGCCTACTGCC TCGGA
DUSP6	DUSP6.2099	TATACTGTTTAGCACAGCTGAA	TGCTGTTGACAGTGAGCGCTCAGCTGTGCTA AACAGTATATAGTGAAGCCACAGATGTATAT ACTGTTTAGCACAGCTGAATGCCTACTGCCT CGGA
ELK1	ELK1.447	TTGTAGACGAACTTCTGGCCGC	TGCTGTTGACAGTGAGCGACGGCCAGAAGT TCGTCTACAATAGTGAAGCCACAGATGTATT GTAGACGAACTTCTGGCCGCTGCCTACTGCC TCGGA
ELK1	ELK1.1078	TAACTCTTCTACTCACATCCAA	TGCTGTTGACAGTGAGCGCTGGATGTGAGT AGAAGAGTTATAGTGAAGCCACAGATGTATA ACTCTTCTACTCACATCCAATGCCTACTGCC TCGGA
ELK1	ELK1.408	TTCTTGTCATAGTAGTACCGCA	TGCTGTTGACAGTGAGCGCGCGGTACTACTA TGACAAGAATAGTGAAGCCACAGATGTATTC TTGTCATAGTAGTACCGCATGCCTACTGCCT CGGA
ELK1	ELK1.1708	TTGCCTAGAATAGAGACAGGAC	TGCTGTTGACAGTGAGCGATCCTGTCTCTAT TCTAGGCAATAGTGAAGCCACAGATGTATTG CCTAGAATAGAGACAGGACTGCCTACTGCC TCGGA
ELK1	ELK1.1488	TATAGGAAGAGATGACTCCCTC	TGCTGTTGACAGTGAGCGAAGGGAGTCATC TCTTCCTATATAGTGAAGCCACAGATGTATA

			TAGGAAGAGATGACTCCCTCTGCCTACTGCC TCGGA
MAPK1	MAPK1.1316	TTTAAGATCTGTATCCTGGCTG	TGCTGTTGACAGTGAGCGAAGCCAGGATAC AGATCTTAAATAGTGAAGCCACAGATGTATT TAAGATCTGTATCCTGGCTGTGCCTACTGCC TCGGA
MAPK1	MAPK1.1233	TCCATGTCGAACTTGAATGGTG	TGCTGTTGACAGTGAGCGAACCATTCAAGTT CGACATGGATAGTGAAGCCACAGATGTATC CATGTCGAACTTGAATGGTGTGCCTACTGCC TCGGA
MAPK1	MAPK1.1121	TGAATGTCAACATTTTGTCCAA	TGCTGTTGACAGTGAGCGCTGGACAAAATGT TGACATTCATAGTGAAGCCACAGATGTATGA ATGTCAACATTTTGTCCAATGCCTACTGCCT CGGA
MAPK1	MAPK1.528	TTCATTTGCTCGATGGTTGGTG	TGCTGTTGACAGTGAGCGAACCAACCATCG AGCAAATGAATAGTGAAGCCACAGATGTATT CATTTGCTCGATGGTTGGTGTGCCTACTGCC TCGGA
MAPK1	MAPK1.537	TATACATCTTTCATTTGCTCGA	TGCTGTTGACAGTGAGCGCCGAGCAAATGA AAGATGTATATAGTGAAGCCACAGATGTATA TACATCTTTCATTTGCTCGATGCCTACTGCC TCGGA
MAPK3	MAPK3.1741	TATATTTATATATTAGACGGGT	TGCTGTTGACAGTGAGCGCCCCGTCTAATAT ATAAATATATAGTGAAGCCACAGATGTATAT ATTTATATATTAGACGGGTTGCCTACTGCCT CGGA
MAPK3	MAPK3.1200	TTTTCTAACAGTCTGGCGGGAG	TGCTGTTGACAGTGAGCGATCCCGCCAGAC TGTTAGAAAATAGTGAAGCCACAGATGTATT TTCTAACAGTCTGGCGGGAGTGCCTACTGCC TCGGA
MAPK3	MAPK3.912	TAAAGGTTAACATCCGGTCCAG	TGCTGTTGACAGTGAGCGATGGACCGGATG TTAACCTTTATAGTGAAGCCACAGATGTATA AAGGTTAACATCCGGTCCAGTGCCTACTGCC TCGGA
MAPK3	MAPK3.751	TTGGAGTTCAGCATGATCTCTG	TGCTGTTGACAGTGAGCGAAGAGATCATGCT GAACTCCAATAGTGAAGCCACAGATGTATTG GAGTTCAGCATGATCTCTGTGCCTACTGCCT CGGA
MAPK3	MAPK3.616	TTGATGAGCAGGTTGGAGGGCT	TGCTGTTGACAGTGAGCGCGCCCTCCAACCT GCTCATCAATAGTGAAGCCACAGATGTATTG ATGAGCAGGTTGGAGGGCTTGCCTACTGCC TCGGA
SRF	SRF.2720	TTTGTTTTCACTTCGTCTCCTC	TGCTGTTGACAGTGAGCGAAGGAGACGAAG TGAAAACAAATAGTGAAGCCACAGATGTATT TGTTTTCACTTCGTCTCCTCTGCCTACTGCC TCGGA
SRF	SRF.901	TCCATCTTGATCTTCACGCGGC	TGCTGTTGACAGTGAGCGACCGCGTGAAGA TCAAGATGGATAGTGAAGCCACAGATGTATC CATCTTGATCTTCACGCGGCTGCCTACTGCC TCGGA
SRF	SRF.85	TAAAGAGATACAATGTTTCCTT	TGCTGTTGACAGTGAGCGCAGGAAACATTGT ATCTCTTTATAGTGAAGCCACAGATGTATAA AGAGATACAATGTTTCCTTTGCCTACTGCCT CGGA
SRF	SRF.3603	TTCACCTAATCACAGAAGCCAG	TGCTGTTGACAGTGAGCGATGGCTTCTGTGA TTAGGTGAATAGTGAAGCCACAGATGTATTC ACCTAATCACAGAAGCCAGTGCCTACTGCCT CGGA
SRF	SRF.1868	TGAAACAGGGATCTGCACTGTC	TGCTGTTGACAGTGAGCGAACAGTGCAGAT CCCTGTTTCATAGTGAAGCCACAGATGTATG AAACAGGGATCTGCACTGTCTGCCTACTGCC TCGGA
AATF	AATF.1732	TTTTGCTTCGTAACTTCTGGAT	TGCTGTTGACAGTGAGCGCTCCAGAAGTTAC GAAGCAAAATAGTGAAGCCACAGATGTATTT

			TGCTTCGTAACTTCTGGATTGCCTACTGCCTCGGA
AATF	AATF.1150	TAGATATCTAGTGTCTGGGTAC	TGCTGTTGACAGTGAGCGATACCCAGACACTAGATATCTATAGTGAAGCCACAGATGTATAGATATCTAGTGTCTGGGTACTGCCTACTGCCTCGGA
AATF	AATF.968	TTTTGTAGTTTGATCCTTCCTT	TGCTGTTGACAGTGAGCGCAGGAAGGATCAAACTACAAAATAGTGAAGCCACAGATGTATTTTGTAGTTTGATCCTTCCTTTGCCTACTGCCTCGGA
AATF	AATF.1152	TACTAGATATCTAGTGTCTGGG	TGCTGTTGACAGTGAGCGACCAGACACTAGATATCTAGTATAGTGAAGCCACAGATGTATACTAGATATCTAGTGTCTGGGTGCCTACTGCCTCGGA
AATF	AATF.1223	TTCTTCTCTTCTACCAGCTCAT	TGCTGTTGACAGTGAGCGCTGAGCTGGTAGAAGAGAAGAATAGTGAAGCCACAGATGTATTCTTCTCTTCTACCAGCTCATTGCCTACTGCCTCGGA
ANKRD57	ANKRD57.2246	TTGCATTTCAACTTTGATCTGA	TGCTGTTGACAGTGAGCGCCAGATCAAAGTTGAAATGCAATAGTGAAGCCACAGATGTATTGCATTTCAACTTTGATCTGATGCCTACTGCCTCGGA
ANKRD57	ANKRD57.2974	TTAAATATAGAAATAGTCCCAT	TGCTGTTGACAGTGAGCGCTGGGACTATTTCTATATTTAATAGTGAAGCCACAGATGTATTAAATATAGAAATAGTCCCATTGCCTACTGCCTCGGA
ANKRD57	ANKRD57.3667	TTTTGAGACAGAGTCTCCGTTG	TGCTGTTGACAGTGAGCGAAACGGAGACTCTGTCTCAAAATAGTGAAGCCACAGATGTATTTTGAGACAGAGTCTCCGTTGTGCCTACTGCCTCGGA
AREG	AREG.517	TTAACTACCTGTTCAACTCTGA	TGCTGTTGACAGTGAGCGCCAGAGTTGAACAGGTAGTTAATAGTGAAGCCACAGATGTATTAACTACCTGTTCAACTCTGATGCCTACTGCCTCGGA
AREG	AREG.677	TATATATTTGCATTCTCCGTGA	TGCTGTTGACAGTGAGCGCCACGGAGAATGCAAATATATATAGTGAAGCCACAGATGTATATATATTTGCATTCTCCGTGATGCCTACTGCCTCGGA
AREG	AREG.868	TTGTCTTCTAAGCTGGACTGTA	TGCTGTTGACAGTGAGCGCACAGTCCAGCTTAGAAGACAATAGTGAAGCCACAGATGTATTGTCTTCTAAGCTGGACTGTATGCCTACTGCCTCGGA
AREG	AREG.850	TGTAATAACAGCAACAGCTGTG	TGCTGTTGACAGTGAGCGAACAGCTGTTGCTGTTATTACATAGTGAAGCCACAGATGTATGTAATAACAGCAACAGCTGTGTGCCTACTGCCTCGGA
AREG	AREG.460	TTCGTTATCATACTCTTCTGAG	TGCTGTTGACAGTGAGCGATCAGAAGAGTATGATAACGAATAGTGAAGCCACAGATGTATTCGTTATCATACTCTTCTGAGTGCCTACTGCCTCGGA
ARNTL2	ARNTL2.1018	TTGTCTTTCTTACTGTTCCTTT	TGCTGTTGACAGTGAGCGCAAGGAACAGTAAGAAAGACAATAGTGAAGCCACAGATGTATTGTCTTTCTTACTGTTCCTTTTGCCTACTGCCTCGGA
ARNTL2	ARNTL2.674	TTGTCCAGTCAAACTAGCCTGA	TGCTGTTGACAGTGAGCGCCAGGCTAGTTTGACTGGACAATAGTGAAGCCACAGATGTATTGTCCAGTCAAACTAGCCTGATGCCTACTGCCTCGGA
ARNTL2	ARNTL2.111	TAGCTGTTGGTCTTGTCCCTGG	TGCTGTTGACAGTGAGCGACAGGGACAAGACCAACAGCTATAGTGAAGCCACAGATGTATAGCTGTTGGTCTTGTCCCTGGTGCCTACTGCCTCGGA
ARNTL2	ARNTL2.2192	TATGTAAGTAGTATTCTTGGTT	TGCTGTTGACAGTGAGCGCACCAAGAATACTACTTACATATAGTGAAGCCACAGATGTATAT

			GTAAGTAGTATTCTTGGTTTGCCTACTGCCT CGGA
ARNTL2	ARNTL2.3342	TTTTGTTTTATTACCTTTGGTT	TGCTGTTGACAGTGAGCGCACCAAAGGTAA TAAAACAAAATAGTGAAGCCACAGATGTATT TTGTTTTATTACCTTTGGTTTGCCTACTGCC TCGGA
ATAD2	ATAD2.1342	TTGCATTGGATCAACATCGGCA	TGCTGTTGACAGTGAGCGCGCCGATGTTGAT CCAATGCAATAGTGAAGCCACAGATGTATTG CATTGGATCAACATCGGCATGCCTACTGCCT CGGA
ATAD2	ATAD2.569	TAATCCTACAACTTCGACGCAC	TGCTGTTGACAGTGAGCGATGCGTCGAAGTT GTAGGATTATAGTGAAGCCACAGATGTATAA TCCTACAACTTCGACGCACTGCCTACTGCCT CGGA
ATAD2	ATAD2.1599	TACTTAGACAATCAGCACCTTT	TGCTGTTGACAGTGAGCGCAAGGTGCTGATT GTCTAAGTATAGTGAAGCCACAGATGTATAC TTAGACAATCAGCACCTTTTGCCTACTGCCT CGGA
ATAD2	ATAD2.4380	TACTATTTTAATCTTTTCCTTA	TGCTGTTGACAGTGAGCGCAAGGAAAAGAT TAAAATAGTATAGTGAAGCCACAGATGTATA CTATTTTAATCTTTTCCTTATGCCTACTGCCT CGGA
ATAD2	ATAD2.3499	TTTATCACCAACAAGAGTGGAA	TGCTGTTGACAGTGAGCGCTCCACTCTTGTT GGTGATAAATAGTGAAGCCACAGATGTATTT ATCACCAACAAGAGTGGAATGCCTACTGCCT CGGA
BARD1	BARD1.548	TTTAATTGAATTCTTCTTGTTT	TGCTGTTGACAGTGAGCGCAACAAGAAGAA TTCAATTAAATAGTGAAGCCACAGATGTATT TAATTGAATTCTTCTTGTTTTGCCTACTGCC TCGGA
BARD1	BARD1.1690	TATATTAACAGCATTTCTGGAG	TGCTGTTGACAGTGAGCGATCCAGAAATGCT GTTAATATATAGTGAAGCCACAGATGTATAT ATTAACAGCATTTCTGGAGTGCCTACTGCCT CGGA
BARD1	BARD1.543	TTGAATTCTTCTTGTTTCCTGC	TGCTGTTGACAGTGAGCGACAGGAAACAAG AAGAATTCAATAGTGAAGCCACAGATGTATT GAATTCTTCTTGTTTCCTGCTGCCTACTGCC TCGGA
BARD1	BARD1.582	TATCTGACTTTCTTACTTCGAG	TGCTGTTGACAGTGAGCGATCGAAGTAAGA AAGTCAGATATAGTGAAGCCACAGATGTATA TCTGACTTTCTTACTTCGAGTGCCTACTGCC TCGGA
BARD1	BARD1.1647	TTGACTATATCCACATGCCCAT	TGCTGTTGACAGTGAGCGCTGGGCATGTGG ATATAGTCAATAGTGAAGCCACAGATGTATT GACTATATCCACATGCCCATTGCCTACTGCC TCGGA
BAZ1A	BAZ1A.1434	TTTATTAGCAACATTGTCCTCT	TGCTGTTGACAGTGAGCGCGAGGACAATGT TGCTAATAAATAGTGAAGCCACAGATGTATT TATTAGCAACATTGTCCTCTTGCCTACTGCC TCGGA
BAZ1A	BAZ1A.5651	TAAACTTGGACTTAATACCTGC	TGCTGTTGACAGTGAGCGACAGGTATTAAGT CCAAGTTTATAGTGAAGCCACAGATGTATAA ACTTGGACTTAATACCTGCTGCCTACTGCCT CGGA
BAZ1A	BAZ1A.4264	TAACTTGTGGTCTTCCTCGTTT	TGCTGTTGACAGTGAGCGCAACGAGGAAGA CCACAAGTTATAGTGAAGCCACAGATGTATA ACTTGTGGTCTTCCTCGTTTTGCCTACTGCC TCGGA
BAZ1A	BAZ1A.5297	TATCTTTCCTACATTCTCCTGA	TGCTGTTGACAGTGAGCGCCAGGAGAATGT AGGAAAGATATAGTGAAGCCACAGATGTAT ATCTTTCCTACATTCTCCTGATGCCTACTGC CTCGGA
BAZ1A	BAZ1A.4218	TTGAGAGTCATCTTCATCTTGT	TGCTGTTGACAGTGAGCGCCAAGATGAAGA TGACTCTCAATAGTGAAGCCACAGATGTATT

			GAGAGTCATCTTCATCTTGTTGCCTACTGCC TCGGA
BAZ1B	BAZ1B.5150	TAAACATTTAAATTCTTCCTGC	TGCTGTTGACAGTGAGCGACAGGAAGAATTT AAATGTTTATAGTGAAGCCACAGATGTATAA ACATTTAAATTCTTCCTGCTGCCTACTGCCT CGGA
BAZ1B	BAZ1B.3381	TTGACTTTCTCTTATTCCCTGA	TGCTGTTGACAGTGAGCGCCAGGGAATAAG AGAAAGTCAATAGTGAAGCCACAGATGTATT GACTTTCTCTTATTCCCTGATGCCTACTGCC TCGGA
BAZ1B	BAZ1B.2041	TTTCTTTCTCTCTTCGTTCTTT	TGCTGTTGACAGTGAGCGCAAGAACGAAGA GAGAAAGAAATAGTGAAGCCACAGATGTAT TTCTTTCTCTCTTCGTTCTTTTGCCTACTGCC TCGGA
BAZ1B	BAZ1B.2230	TAATAGGATACTGAGCATCTGG	TGCTGTTGACAGTGAGCGACAGATGCTCAGT ATCCTATTATAGTGAAGCCACAGATGTATAA TAGGATACTGAGCATCTGGTGCCTACTGCCT CGGA
BAZ1B	BAZ1B.3695	TTTTCTTCTCTTTTGCTTGGGA	TGCTGTTGACAGTGAGCGCCCCAAGCAAAA GAGAAGAAAATAGTGAAGCCACAGATGTAT TTTCTTCTCTTTTGCTTGGGATGCCTACTGC CTCGGA
BRCA1	BRCA1.656	TTCAGTATTTGTTACATCCGTC	TGCTGTTGACAGTGAGCGAACGGATGTAAC AAATACTGAATAGTGAAGCCACAGATGTATT CAGTATTTGTTACATCCGTCTGCCTACTGCC TCGGA
BRCA1	BRCA1.2561	TAAACTTAGGGAAACCAGCTAT	TGCTGTTGACAGTGAGCGCTAGCTGGTTTCC CTAAGTTTATAGTGAAGCCACAGATGTATAA ACTTAGGGAAACCAGCTATTGCCTACTGCCT CGGA
BRCA1	BRCA1.1108	TTTTACTGGTAGAACTATCTGC	TGCTGTTGACAGTGAGCGACAGATAGTTCTA CCAGTAAAATAGTGAAGCCACAGATGTATTT TACTGGTAGAACTATCTGCTGCCTACTGCCT CGGA
BRCA1	BRCA1.37	TTTTGTACTTCTTCAACGCGAA	TGCTGTTGACAGTGAGCGCTCGCGTTGAAG AAGTACAAAATAGTGAAGCCACAGATGTATT TTGTACTTCTTCAACGCGAATGCCTACTGCC TCGGA
BRCA1	BRCA1.190	TAAATCTCGTACTTTCTTGTAG	TGCTGTTGACAGTGAGCGATACAAGAAAGT ACGAGATTTATAGTGAAGCCACAGATGTATA AATCTCGTACTTTCTTGTAGTGCCTACTGCC TCGGA
CBFB	CBFB.3057	TAAACAAACAAACACACAGTAT	TGCTGTTGACAGTGAGCGCTACTGTGTGTTT GTTTGTTTATAGTGAAGCCACAGATGTATAA ACAAACAAACACACAGTATTGCCTACTGCCT CGGA
CBFB	CBFB.2451	TAACAATTTAAACACACTCCTT	TGCTGTTGACAGTGAGCGCAGGAGTGTGTTT AAATTGTTATAGTGAAGCCACAGATGTATAA CAATTTAAACACACTCCTTTGCCTACTGCCT CGGA
CBFB	CBFB.507	TCTAAGTCGACATACTCTCGGC	TGCTGTTGACAGTGAGCGACCGAGAGTATG TCGACTTAGATAGTGAAGCCACAGATGTATC TAAGTCGACATACTCTCGGCTGCCTACTGCC TCGGA
CBFB	CBFB.665	TTGTGCTAATGCATCCTCCTGC	TGCTGTTGACAGTGAGCGACAGGAGGATGC ATTAGCACAATAGTGAAGCCACAGATGTATT GTGCTAATGCATCCTCCTGCTGCCTACTGCC TCGGA
CBFB	CBFB.2457	AACAATTTAAACACACTCCTTT	TGCTGTTGACAGTGAGCGCAAGGAGTGTGT TTAAATTGTTTAGTGAAGCCACAGATGTAAA CAATTTAAACACACTCCTTTTGCCTACTGCC TCGGA
CBX3	CBX3.1941	TTTAATGAGACAATTGACCCTA	TGCTGTTGACAGTGAGCGCAGGGTCAATTGT CTCATTAAATAGTGAAGCCACAGATGTATTT

			AATGAGACAATTGACCCTATGCCTACTGCCTCGGA
CBX3	CBX3.560	TTATTGAGCTTCATCTTCTGGA	TGCTGTTGACAGTGAGCGCCCAGAAGATGAAGCTCAATAATAGTGAAGCCACAGATGTATTATTGAGCTTCATCTTCTGGATGCCTACTGCCTCGGA
CBX3	CBX3.1278	TTGTCTAGTTTCCTCATCTGGA	TGCTGTTGACAGTGAGCGCCCAGATGAGGAAACTAGACAATAGTGAAGCCACAGATGTATTGTCTAGTTTCCTCATCTGGATGCCTACTGCCTCGGA
CBX3	CBX3.1081	TTATCTCTTATTTTGCTTGGAA	TGCTGTTGACAGTGAGCGCTCCAAGCAAAATAAGAGATAATAGTGAAGCCACAGATGTATTATCTCTTATTTTGCTTGGAATGCCTACTGCCTCGGA
CBX3	CBX3.628	TAAATCAAAATCTAAGACCCAA	TGCTGTTGACAGTGAGCGCTGGGTCTTAGATTTTGATTTATAGTGAAGCCACAGATGTATAAATCAAAATCTAAGACCCAATGCCTACTGCCTCGGA
CHAF1A	CHAF1A.1387	TTCTCTTCTTCTCTTAACCGTT	TGCTGTTGACAGTGAGCGCACGGTTAAGAGAAGAAGAGAATAGTGAAGCCACAGATGTATTCTCTTCTTCTCTTAACCGTTTGCCTACTGCCTCGGA
CHAF1A	CHAF1A.3082	TAGAACTCTGCACACTTTGGGG	TGCTGTTGACAGTGAGCGACCCAAAGTGTGCAGAGTTCTATAGTGAAGCCACAGATGTATAGAACTCTGCACACTTTGGGGTGCCTACTGCCTCGGA
CHAF1A	CHAF1A.182	TTGTATTAACTTCTTAACTGGA	TGCTGTTGACAGTGAGCGCCCAGTTAAGAAGTTAATACAATAGTGAAGCCACAGATGTATTGTATTAACTTCTTAACTGGATGCCTACTGCCTCGGA
CHAF1A	CHAF1A.1374	TAACCGTTTCTCTTCTTCCTTT	TGCTGTTGACAGTGAGCGCAAGGAAGAAGAGAAACGGTTATAGTGAAGCCACAGATGTATAACCGTTTCTCTTCTTCCTTTTGCCTACTGCCTCGGA
CHAF1A	CHAF1A.3031	TTACACAGGAATTGAGTCGGTT	TGCTGTTGACAGTGAGCGCACCGACTCAATTCCTGTGTAATAGTGAAGCCACAGATGTATTACACAGGAATTGAGTCGGTTTGCCTACTGCCTCGGA
CTNNBL1	CTNNBL1.388	TTGTCTGGAAACTTAATCCGCA	TGCTGTTGACAGTGAGCGCGCGGATTAAGTTTCCAGACAATAGTGAAGCCACAGATGTATTGTCTGGAAACTTAATCCGCATGCCTACTGCCTCGGA
CTNNBL1	CTNNBL1.961	TTAAACACGGATAACTGCTGAA	TGCTGTTGACAGTGAGCGCTCAGCAGTTATCCGTGTTTAATAGTGAAGCCACAGATGTATTAAACACGGATAACTGCTGAATGCCTACTGCCTCGGA
CTNNBL1	CTNNBL1.1828	TTGTGTAGAAACTGATCCTGGG	TGCTGTTGACAGTGAGCGACCAGGATCAGTTTCTACACAATAGTGAAGCCACAGATGTATTGTGTAGAAACTGATCCTGGGTGCCTACTGCCTCGGA
CTNNBL1	CTNNBL1.1653	TTTTGATGGAGCTTCCTCGCAT	TGCTGTTGACAGTGAGCGCTGCGAGGAAGCTCCATCAAAATAGTGAAGCCACAGATGTATTTTGATGGAGCTTCCTCGCATTGCCTACTGCCTCGGA
CTNNBL1	CTNNBL1.1495	TTGTCGATGATCTCTCCTCGCC	TGCTGTTGACAGTGAGCGAGCGAGGAGAGATCATCGACAATAGTGAAGCCACAGATGTATTGTCGATGATCTCTCCTCGCCTGCCTACTGCCTCGGA
DAB2IP	DAB2IP.2670	TCGTCTTCTAACAACTGCGCGT	TGCTGTTGACAGTGAGCGCCGCGCAGTTGTTAGAAGACGATAGTGAAGCCACAGATGTATCGTCTTCTAACAACTGCGCGTTGCCTACTGCCTCGGA
DAB2IP	DAB2IP.468	TTCTTCTTGTCGGTCTCCCGGT	TGCTGTTGACAGTGAGCGCCCGGGAGACCGACAAGAAGAATAGTGAAGCCACAGATGTAT

			TCTTCTTGTCGGTCTCCCGGTTGCCTACTGC CTCGGA
DAB2IP	DAB2IP.2316	TTTTCAGTCAGTGACATCTGTC	TGCTGTTGACAGTGAGCGAACAGATGTCACT GACTGAAAATAGTGAAGCCACAGATGTATTT TCAGTCAGTGACATCTGTCTGCCTACTGCCT CGGA
DAB2IP	DAB2IP.411	TTGTGGAACTCGAAGTGCTCGC	TGCTGTTGACAGTGAGCGACGAGCACTTCG AGTTCCACAATAGTGAAGCCACAGATGTATT GTGGAACTCGAAGTGCTCGCTGCCTACTGC CTCGGA
DAB2IP	DAB2IP.957	TACAGCGCTTTGATGAACTCAC	TGCTGTTGACAGTGAGCGATGAGTTCATCAA AGCGCTGTATAGTGAAGCCACAGATGTATAC AGCGCTTTGATGAACTCACTGCCTACTGCCT CGGA
DDX54	DDX54.301	TTCTTCTTCTTCTTGTTCTGGG	TGCTGTTGACAGTGAGCGACCAGAACAAGA AGAAGAAGAATAGTGAAGCCACAGATGTAT TCTTCTTCTTCTTGTTCTGGGTGCCTACTGC CTCGGA
DDX54	DDX54.421	TTGCCATCCAAGATCACCGGGA	TGCTGTTGACAGTGAGCGCCCCGGTGATCTT GGATGGCAATAGTGAAGCCACAGATGTATT GCCATCCAAGATCACCGGGATGCCTACTGC CTCGGA
DDX54	DDX54.2274	TAATCTTCTTCTTGTCTTCCTG	TGCTGTTGACAGTGAGCGAAGGAAGACAAG AAGAAGATTATAGTGAAGCCACAGATGTATA ATCTTCTTCTTGTCTTCCTGTGCCTACTGCC TCGGA
DDX54	DDX54.1756	TTGATCTCAAAGATAGTCGCCC	TGCTGTTGACAGTGAGCGAGGCGACTATCTT TGAGATCAATAGTGAAGCCACAGATGTATTG ATCTCAAAGATAGTCGCCCTGCCTACTGCCT CGGA
DDX54	DDX54.2269	TTCTTCTTGTCTTCCTGTCCTG	TGCTGTTGACAGTGAGCGAAGGACAGGAAG ACAAGAAGAATAGTGAAGCCACAGATGTAT TCTTCTTGTCTTCCTGTCCTGTGCCTACTGC CTCGGA
DEK	DEK.2225	TTAGTCATAATCGTGAAGCTGG	TGCTGTTGACAGTGAGCGACAGCTTCACGAT TATGACTAATAGTGAAGCCACAGATGTATTA GTCATAATCGTGAAGCTGGTGCCTACTGCCT CGGA
DEK	DEK.398	TAGATTTCTAAGTTCATCGGTT	TGCTGTTGACAGTGAGCGCACCGATGAACTT AGAAATCTATAGTGAAGCCACAGATGTATAG ATTTCTAAGTTCATCGGTTTGCCTACTGCCT CGGA
DEK	DEK.448	TTAATGAGGACACAGTGCCTGG	TGCTGTTGACAGTGAGCGACAGGCACTGTG TCCTCATTAATAGTGAAGCCACAGATGTATT AATGAGGACACAGTGCCTGGTGCCTACTGC CTCGGA
DEK	DEK.508	TTTTATATTGGACACTTCCTTT	TGCTGTTGACAGTGAGCGCAAGGAAGTGTC CAATATAAAATAGTGAAGCCACAGATGTATT TTATATTGGACACTTCCTTTTGCCTACTGCC TCGGA
DEK	DEK.829	TTTCTTTATCTTCATCATCTGA	TGCTGTTGACAGTGAGCGCCAGATGATGAA GATAAAGAAATAGTGAAGCCACAGATGTATT TCTTTATCTTCATCATCTGATGCCTACTGCC TCGGA
DNAJC2	DNAJC2.1165	TTCTTTAGCTTCTTGCTCCTTC	TGCTGTTGACAGTGAGCGAAAGGAGCAAGA AGCTAAAGAATAGTGAAGCCACAGATGTATT CTTTAGCTTCTTGCTCCTTCTGCCTACTGCC TCGGA
DNAJC2	DNAJC2.1455	TAATTGTAGATCATCTTCTGAC	TGCTGTTGACAGTGAGCGATCAGAAGATGAT CTACAATTATAGTGAAGCCACAGATGTATAA TTGTAGATCATCTTCTGACTGCCTACTGCCT CGGA
DNAJC2	DNAJC2.1157	TTAGCTTCTTGCTCCTTCCGTT	TGCTGTTGACAGTGAGCGCACGGAAGGAGC AAGAAGCTAATAGTGAAGCCACAGATGTATT

			AGCTTCTTGCTCCTTCCGTTTGCCTACTGCC TCGGA
DNAJC2	DNAJC2.429	TTCATCTTCTGATTCCTCGGAT	TGCTGTTGACAGTGAGCGCTCCGAGGAATC AGAAGATGAATAGTGAAGCCACAGATGTATT CATCTTCTGATTCCTCGGATTGCCTACTGCC TCGGA
DNAJC2	DNAJC2.1466	TTAGTAATTGTAGATCATCTTC	TGCTGTTGACAGTGAGCGAAAGATGATCTAC AATTACTAATAGTGAAGCCACAGATGTATTA GTAATTGTAGATCATCTTCTGCCTACTGCCT CGGA
DNMT1	DNMT1.884	TTCATCTCTTTCTTCTTCCTTT	TGCTGTTGACAGTGAGCGCAAGGAAGAAGA AAGAGATGAATAGTGAAGCCACAGATGTATT CATCTCTTTCTTCTTCCTTTTGCCTACTGCCT CGGA
DNMT1	DNMT1.3991	TTGAAGGAGACAAAGTTCCTGA	TGCTGTTGACAGTGAGCGCCAGGAACTTTGT CTCCTTCAATAGTGAAGCCACAGATGTATTG AAGGAGACAAAGTTCCTGATGCCTACTGCCT CGGA
DNMT1	DNMT1.3205	TTTGATGTCAGTCTCATTGGGC	TGCTGTTGACAGTGAGCGACCCAATGAGAC TGACATCAAATAGTGAAGCCACAGATGTATT TGATGTCAGTCTCATTGGGCTGCCTACTGCC TCGGA
DNMT1	DNMT1.2410	TTATAGTAACTCTTCTTCCCAT	TGCTGTTGACAGTGAGCGCTGGGAAGAAGA GTTACTATAATAGTGAAGCCACAGATGTATT ATAGTAACTCTTCTTCCCATTGCCTACTGCC TCGGA
DNMT1	DNMT1.2839	TTGAACTTGTTGTCCTCTGTTG	TGCTGTTGACAGTGAGCGAAACAGAGGACA ACAAGTTCAATAGTGAAGCCACAGATGTATT GAACTTGTTGTCCTCTGTTGTGCCTACTGCC TCGGA
DR1	DR1.1454	ATTGATATTATACTGAACCTTA	TGCTGTTGACAGTGAGCGCAAGGTTCAGTAT AATATCAATTAGTGAAGCCACAGATGTAATT GATATTATACTGAACCTTATGCCTACTGCCT CGGA
DR1	DR1.1779	TAAACAAGTATATTGATCTGAG	TGCTGTTGACAGTGAGCGATCAGATCAATAT ACTTGTTTATAGTGAAGCCACAGATGTATAA ACAAGTATATTGATCTGAGTGCCTACTGCCT CGGA
DR1	DR1.2938	TTAACTTATCGTTCTAGACTAG	TGCTGTTGACAGTGAGCGATAGTCTAGAACG ATAAGTTAATAGTGAAGCCACAGATGTATTA ACTTATCGTTCTAGACTAGTGCCTACTGCCT CGGA
DR1	DR1.2574	TATCTTAAGTGACTTTTCCTTT	TGCTGTTGACAGTGAGCGCAAGGAAAAGTC ACTTAAGATATAGTGAAGCCACAGATGTATA TCTTAAGTGACTTTTCCTTTTGCCTACTGCC TCGGA
DR1	DR1.766	TTTATTGATAGCAGCTCTGGGG	TGCTGTTGACAGTGAGCGACCCAGAGCTGC TATCAATAAATAGTGAAGCCACAGATGTATT TATTGATAGCAGCTCTGGGGTGCCTACTGCC TCGGA
EGR1	EGR1.2823	TTTTGTTTTCTTACATTCTGGA	TGCTGTTGACAGTGAGCGCCCAGAATGTAA GAAAACAAAATAGTGAAGCCACAGATGTATT TTGTTTTCTTACATTCTGGATGCCTACTGCC TCGGA
EGR1	EGR1.2815	TCTTACATTCTGGAGAACCGAA	TGCTGTTGACAGTGAGCGCTCGGTTCTCCAG AATGTAAGATAGTGAAGCCACAGATGTATCT TACATTCTGGAGAACCGAATGCCTACTGCCT CGGA
EGR1	EGR1.2822	TTTGTTTTCTTACATTCTGGAG	TGCTGTTGACAGTGAGCGATCCAGAATGTAA GAAAACAAATAGTGAAGCCACAGATGTATTT GTTTTCTTACATTCTGGAGTGCCTACTGCCT CGGA
EGR1	EGR1.2946	TAACATACAAAAATCGCCGCCT	TGCTGTTGACAGTGAGCGCGGCGGCGATTTT TGTATGTTATAGTGAAGCCACAGATGTATAA

			CATACAAAAATCGCCGCCTTGCCTACTGCCT CGGA
EGR1	EGR1.2525	TAACGGAACAACACTCTGACAC	TGCTGTTGACAGTGAGCGATGTCAGAGTGTT GTTCCGTTATAGTGAAGCCACAGATGTATAA CGGAACAACACTCTGACACTGCCTACTGCCT CGGA
ENO1	ENO1.261	TTGATGACATTGAACGCCGGGA	TGCTGTTGACAGTGAGCGCCCCGGCGTTCA ATGTCATCAATAGTGAAGCCACAGATGTATT GATGACATTGAACGCCGGGATGCCTACTGC CTCGGA
ENO1	ENO1.1440	TTTGAGCACAAAACCACCGGGG	TGCTGTTGACAGTGAGCGACCCGGTGGTTTT GTGCTCAAATAGTGAAGCCACAGATGTATTT GAGCACAAAACCACCGGGGTGCCTACTGCC TCGGA
ENO1	ENO1.1437	TTTTGAGCACAAAACCACCGGG	TGCTGTTGACAGTGAGCGACCGGTGGTTTTG TGCTCAAAATAGTGAAGCCACAGATGTATTT TGAGCACAAAACCACCGGGTGCCTACTGCC TCGGA
ENO1	ENO1.1441	TTTATTTTGAGCACAAAACCAC	TGCTGTTGACAGTGAGCGATGGTTTTGTGCT CAAAATAAATAGTGAAGCCACAGATGTATTT ATTTTGAGCACAAAACCACTGCCTACTGCCT CGGA
ENO1	ENO1.681	TCTTCGATAGACACCACTGGGT	TGCTGTTGACAGTGAGCGCCCCAGTGGTGT CTATCGAAGATAGTGAAGCCACAGATGTATC TTCGATAGACACCACTGGGTTGCCTACTGCC TCGGA
EREG	EREG.1324	TAGATGAGTGACTAGTACCTGT	TGCTGTTGACAGTGAGCGCCAGGTACTAGTC ACTCATCTATAGTGAAGCCACAGATGTATAG ATGAGTGACTAGTACCTGTTGCCTACTGCCT CGGA
EREG	EREG.1188	TAGTGTTTAACACAGGACCTAT	TGCTGTTGACAGTGAGCGCTAGGTCCTGTGT TAAACACTATAGTGAAGCCACAGATGTATAG TGTTTAACACAGGACCTATTGCCTACTGCCT CGGA
EREG	EREG.3002	TAACCTATTCACATCCTCCTGT	TGCTGTTGACAGTGAGCGCCAGGAGGATGT GAATAGGTTATAGTGAAGCCACAGATGTATA ACCTATTCACATCCTCCTGTTGCCTACTGCC TCGGA
EREG	EREG.3718	TTATAGAACTTAATATTCCTGG	TGCTGTTGACAGTGAGCGACAGGAATATTAA GTTCTATAATAGTGAAGCCACAGATGTATTA TAGAACTTAATATTCCTGGTGCCTACTGCCT CGGA
EREG	EREG.993	TTGCTAACAATTCTTGAGCTAT	TGCTGTTGACAGTGAGCGCTAGCTCAAGAAT TGTTAGCAATAGTGAAGCCACAGATGTATTG CTAACAATTCTTGAGCTATTGCCTACTGCCT CGGA
ESPL1	ESPL1.267	TAGCTTAGCAGTCAGCTGCTGG	TGCTGTTGACAGTGAGCGACAGCAGCTGAC TGCTAAGCTATAGTGAAGCCACAGATGTATA GCTTAGCAGTCAGCTGCTGGTGCCTACTGCC TCGGA
ESPL1	ESPL1.1362	TACAACTGTCCACTAGTTGGGT	TGCTGTTGACAGTGAGCGCCCCAACTAGTG GACAGTTGTATAGTGAAGCCACAGATGTATA CAACTGTCCACTAGTTGGGTTGCCTACTGCC TCGGA
ESPL1	ESPL1.1897	TCACAGATGATGTTGAAGCGTT	TGCTGTTGACAGTGAGCGCACGCTTCAACAT CATCTGTGATAGTGAAGCCACAGATGTATCA CAGATGATGTTGAAGCGTTTGCCTACTGCCT CGGA
ESPL1	ESPL1.1771	TTTAGCTGTAGCTCCTTGTCTC	TGCTGTTGACAGTGAGCGAAGACAAGGAGC TACAGCTAAATAGTGAAGCCACAGATGTATT TAGCTGTAGCTCCTTGTCTCTGCCTACTGCC TCGGA
ESPL1	ESPL1.2669	TTGACTTCGAAGCAGATCACAG	TGCTGTTGACAGTGAGCGATGTGATCTGCTT CGAAGTCAATAGTGAAGCCACAGATGTATTG

			ACTTCGAAGCAGATCACAGTGCCTACTGCCT CGGA
ETV4	ETV4.686	TTCATTTATATGTACACAGGGC	TGCTGTTGACAGTGAGCGACCCTGTGTACAT ATAAATGAATAGTGAAGCCACAGATGTATTC ATTTATATGTACACAGGGCTGCCTACTGCCT CGGA
ETV4	ETV4.380	TAATAGTATCGGAGCGAGCGGC	TGCTGTTGACAGTGAGCGACCGCTCGCTCC GATACTATTATAGTGAAGCCACAGATGTATA ATAGTATCGGAGCGAGCGGCTGCCTACTGC CTCGGA
ETV4	ETV4.806	TTTCCTTCCCAATGACTCCGGT	TGCTGTTGACAGTGAGCGCCCGGAGTCATT GGGAAGGAAATAGTGAAGCCACAGATGTAT TTCCTTCCCAATGACTCCGGTTGCCTACTGC CTCGGA
ETV4	ETV4.385	TCTCATAATAGTATCGGAGCGA	TGCTGTTGACAGTGAGCGCCGCTCCGATACT ATTATGAGATAGTGAAGCCACAGATGTATCT CATAATAGTATCGGAGCGATGCCTACTGCCT CGGA
ETV4	ETV4.816	TTTCTCCACTTTTCCTTCCCAA	TGCTGTTGACAGTGAGCGCTGGGAAGGAAA AGTGGAGAAATAGTGAAGCCACAGATGTAT TTCTCCACTTTTCCTTCCCAATGCCTACTGC CTCGGA
ETV5	ETV5.390	TTGAAGTTGACTGAGATCCTGA	TGCTGTTGACAGTGAGCGCCAGGATCTCAGT CAACTTCAATAGTGAAGCCACAGATGTATTG AAGTTGACTGAGATCCTGATGCCTACTGCCT CGGA
ETV5	ETV5.3563	TTTGATTAGAGTACAATGCTAA	TGCTGTTGACAGTGAGCGCTAGCATTGTACT CTAATCAAATAGTGAAGCCACAGATGTATTT GATTAGAGTACAATGCTAATGCCTACTGCCT CGGA
ETV5	ETV5.2355	TATGATTTTGAGAACCACGGAG	TGCTGTTGACAGTGAGCGATCCGTGGTTCTC AAAATCATATAGTGAAGCCACAGATGTATAT GATTTTGAGAACCACGGAGTGCCTACTGCCT CGGA
ETV5	ETV5.3085	TTACCTGTCAGTATCACACGTA	TGCTGTTGACAGTGAGCGCACGTGTGATACT GACAGGTAATAGTGAAGCCACAGATGTATTA CCTGTCAGTATCACACGTATGCCTACTGCCT CGGA
ETV5	ETV5.2130	TAGTAGTCCATGATCGATGCAG	TGCTGTTGACAGTGAGCGATGCATCGATCAT GGACTACTATAGTGAAGCCACAGATGTATAG TAGTCCATGATCGATGCAGTGCCTACTGCCT CGGA
EZH2	EZH2.292	TTCAATGAAAGTACCATCCTGA	TGCTGTTGACAGTGAGCGCCAGGATGGTAC TTTCATTGAATAGTGAAGCCACAGATGTATT CAATGAAAGTACCATCCTGATGCCTACTGCC TCGGA
EZH2	EZH2.578	TTTCCTTTAGTTCTTCTGCTGT	TGCTGTTGACAGTGAGCGCCAGCAGAAGAA CTAAAGGAAATAGTGAAGCCACAGATGTATT TCCTTTAGTTCTTCTGCTGTTGCCTACTGCC TCGGA
EZH2	EZH2.1100	TTTATTGGTGTTTGACACCGAG	TGCTGTTGACAGTGAGCGATCGGTGTCAAAC ACCAATAAATAGTGAAGCCACAGATGTATTT ATTGGTGTTTGACACCGAGTGCCTACTGCCT CGGA
EZH2	EZH2.1112	TTTGGCTTCATCTTTATTGGTG	TGCTGTTGACAGTGAGCGAACCAATAAAGAT GAAGCCAAATAGTGAAGCCACAGATGTATTT GGCTTCATCTTTATTGGTGTGCCTACTGCCT CGGA
EZH2	EZH2.1700	TATTTATCATACACTTTCCCTC	TGCTGTTGACAGTGAGCGAAGGGAAAGTGT ATGATAAATATAGTGAAGCCACAGATGTATA TTTATCATACACTTTCCCTCTGCCTACTGCC TCGGA
FOS	FOS.1690	TTAATTCCAATAATGAACCCAA	TGCTGTTGACAGTGAGCGCTGGGTTCATTAT TGGAATTAATAGTGAAGCCACAGATGTATTA

			ATTCCAATAATGAACCCAATGCCTACTGCCT CGGA
FOS	FOS.1804	TTTTCTTAGTATAATATTGGTC	TGCTGTTGACAGTGAGCGAACCAATATTATA CTAAGAAAATAGTGAAGCCACAGATGTATTT TCTTAGTATAATATTGGTCTGCCTACTGCCT CGGA
FOS	FOS.1894	TAACATTACAATGAACATTGAT	TGCTGTTGACAGTGAGCGCTCAATGTTCATT GTAATGTTATAGTGAAGCCACAGATGTATAA CATTACAATGAACATTGATTGCCTACTGCCT CGGA
FOS	FOS.2115	TTTTATTGACAATGTCTTGGAA	TGCTGTTGACAGTGAGCGCTCCAAGACATTG TCAATAAAATAGTGAAGCCACAGATGTATTT TATTGACAATGTCTTGGAATGCCTACTGCCT CGGA
FOS	FOS.703	TCTAGTTGGTCTGTCTCCGCTT	TGCTGTTGACAGTGAGCGCAGCGGAGACAG ACCAACTAGATAGTGAAGCCACAGATGTATC TAGTTGGTCTGTCTCCGCTTTGCCTACTGCC TCGGA
FOSL1	FOSL1.1280	TAAGGATCTACAAAGTCTCTGG	TGCTGTTGACAGTGAGCGACAGAGACTTTGT AGATCCTTATAGTGAAGCCACAGATGTATAA GGATCTACAAAGTCTCTGGTGCCTACTGCCT CGGA
FOSL1	FOSL1.90	TATGAATGAAAAGTTCTCGGGC	TGCTGTTGACAGTGAGCGACCCGAGAACTTT TCATTCATATAGTGAAGCCACAGATGTATAT GAATGAAAAGTTCTCGGGCTGCCTACTGCCT CGGA
FOSL1	FOSL1.1634	TTTTATTCCATTTTGGTAGGTT	TGCTGTTGACAGTGAGCGCACCTACCAAAAT GGAATAAAATAGTGAAGCCACAGATGTATTT TATTCCATTTTGGTAGGTTTGCCTACTGCCT CGGA
FOSL1	FOSL1.91	TTATGAATGAAAAGTTCTCGGG	TGCTGTTGACAGTGAGCGACCGAGAACTTTT CATTCATAATAGTGAAGCCACAGATGTATTA TGAATGAAAAGTTCTCGGGTGCCTACTGCCT CGGA
FOSL1	FOSL1.1405	TGAGTTAGTGTTCTAGGTGGGT	TGCTGTTGACAGTGAGCGCCCCACCTAGAA CACTAACTCATAGTGAAGCCACAGATGTATG AGTTAGTGTTCTAGGTGGGTTGCCTACTGCC TCGGA
FOXM1	FOXM1.1812	TTGAATCACAAGCATTTCCGAG	TGCTGTTGACAGTGAGCGATCGGAAATGCTT GTGATTCAATAGTGAAGCCACAGATGTATTG AATCACAAGCATTTCCGAGTGCCTACTGCCT CGGA
FOXM1	FOXM1.725	TCTAGGAAGATTCACATCCCTA	TGCTGTTGACAGTGAGCGCAGGGATGTGAA TCTTCCTAGATAGTGAAGCCACAGATGTATC TAGGAAGATTCACATCCCTATGCCTACTGCC TCGGA
FOXM1	FOXM1.1277	TTGATGGTCATGTTCCGGCGGA	TGCTGTTGACAGTGAGCGCCCGCCGGAACA TGACCATCAATAGTGAAGCCACAGATGTATT GATGGTCATGTTCCGGCGGATGCCTACTGCC TCGGA
FOXM1	FOXM1.2496	TAGCTCAGGAATAAACTGGGAC	TGCTGTTGACAGTGAGCGATCCCAGTTTATT CCTGAGCTATAGTGAAGCCACAGATGTATAG CTCAGGAATAAACTGGGACTGCCTACTGCCT CGGA
FOXM1	FOXM1.463	TGGTTAATAATCTTGATCCCAG	TGCTGTTGACAGTGAGCGATGGGATCAAGA TTATTAACCATAGTGAAGCCACAGATGTATG GTTAATAATCTTGATCCCAGTGCCTACTGCC TCGGA
FUBP1	FUBP1.2714	TATAGCAGCAGTACAGGTCTGA	TGCTGTTGACAGTGAGCGCCAGACCTGTACT GCTGCTATATAGTGAAGCCACAGATGTATAT AGCAGCAGTACAGGTCTGATGCCTACTGCCT CGGA
FUBP1	FUBP1.1846	TTTCTTGTAGTACTCTTCCCAA	TGCTGTTGACAGTGAGCGCTGGGAAGAGTA CTACAAGAAATAGTGAAGCCACAGATGTATT

			TCTTGTAGTACTCTTCCCAATGCCTACTGCC TCGGA
FUBP1	FUBP1.521	TTAACATACAGGACCTTTCTGG	TGCTGTTGACAGTGAGCGACAGAAAGGTCC TGTATGTTAATAGTGAAGCCACAGATGTATT AACATACAGGACCTTTCTGGTGCCTACTGCC TCGGA
FUBP1	FUBP1.236	TTGAATTCAGTGATGTCCCTGC	TGCTGTTGACAGTGAGCGACAGGGACATCA CTGAATTCAATAGTGAAGCCACAGATGTATT GAATTCAGTGATGTCCCTGCTGCCTACTGCC TCGGA
FUBP1	FUBP1.1932	TTGTCTATAATACTCAGCCCAG	TGCTGTTGACAGTGAGCGATGGGCTGAGTA TTATAGACAATAGTGAAGCCACAGATGTATT GTCTATAATACTCAGCCCAGTGCCTACTGCC TCGGA
FUS	FUS.212	ATAACCACTGTAACTCTGCTGT	TGCTGTTGACAGTGAGCGCCAGCAGAGTTA CAGTGGTTATTAGTGAAGCCACAGATGTAAT AACCACTGTAACTCTGCTGTTGCCTACTGCC TCGGA
FUS	FUS.2807	TTGAGAGGAAAGCACTTCCCAA	TGCTGTTGACAGTGAGCGCTGGGAAGTGCTT TCCTCTCAATAGTGAAGCCACAGATGTATTG AGAGGAAAGCACTTCCCAATGCCTACTGCCT CGGA
FUS	FUS.960	TTGTTGTCTGAATTATCCTGTT	TGCTGTTGACAGTGAGCGCACAGGATAATTC AGACAACAATAGTGAAGCCACAGATGTATT GTTGTCTGAATTATCCTGTTTGCCTACTGCC TCGGA
FUS	FUS.1050	TTGTTTGTCTTAATAATACCAA	TGCTGTTGACAGTGAGCGCTGGTATTATTAA GACAAACAATAGTGAAGCCACAGATGTATT GTTTGTCTTAATAATACCAATGCCTACTGCC TCGGA
FUS	FUS.1028	TCTGCTTGAAGTAATCAGCCAC	TGCTGTTGACAGTGAGCGATGGCTGATTACT TCAAGCAGATAGTGAAGCCACAGATGTATCT GCTTGAAGTAATCAGCCACTGCCTACTGCCT CGGA
HMGA1	HMGA1.211	TTTTGCTTCCCTTTGGTCGGCC	TGCTGTTGACAGTGAGCGAGCCGACCAAAG GGAAGCAAAATAGTGAAGCCACAGATGTAT TTTGCTTCCCTTTGGTCGGCCTGCCTACTGC CTCGGA
HMGA1	HMGA1.155	TCCTTGAATTCCTCGAGCGGAG	TGCTGTTGACAGTGAGCGATCCGCTCGAGG AATTCAAGGATAGTGAAGCCACAGATGTATC CTTGAATTCCTCGAGCGGAGTGCCTACTGCC TCGGA
HMGA1	HMGA1.40	TCATCTTCCCTTCTCTAAGGAG	TGCTGTTGACAGTGAGCGATCCTTAGAGAAG GGAAGATGATAGTGAAGCCACAGATGTATC ATCTTCCCTTCTCTAAGGAGTGCCTACTGCC TCGGA
HMGA1	HMGA1.1061	TATGTACTCAGATCCCAGGCGG	TGCTGTTGACAGTGAGCGACGCCTGGGATC TGAGTACATATAGTGAAGCCACAGATGTATA TGTACTCAGATCCCAGGCGGTGCCTACTGCC TCGGA
HMGA1	HMGA1.1391	TGAGGATGAACATTTGGCGCTG	TGCTGTTGACAGTGAGCGAAGCGCCAAATG TTCATCCTCATAGTGAAGCCACAGATGTATG AGGATGAACATTTGGCGCTGTGCCTACTGCC TCGGA
HMGB1	HMGB1.2309	TTAACTAGTATTTAAAACCTCT	TGCTGTTGACAGTGAGCGCGAGGTTTTAAAT ACTAGTTAATAGTGAAGCCACAGATGTATTA ACTAGTATTTAAAACCTCTTGCCTACTGCCT CGGA
HMGB1	HMGB1.2683	TACAGTAGAAACTTCCATCTAA	TGCTGTTGACAGTGAGCGCTAGATGGAAGTT TCTACTGTATAGTGAAGCCACAGATGTATAC AGTAGAAACTTCCATCTAATGCCTACTGCCT CGGA
HMGB1	HMGB1.1726	TTGTATTTTAAGCTCACGCTTT	TGCTGTTGACAGTGAGCGCAAGCGTGAGCT TAAAATACAATAGTGAAGCCACAGATGTATT

			GTATTTTAAGCTCACGCTTTTGCCTACTGCC TCGGA
HMGB1	HMGB1.1534	TTGAGTAGATTGATTACTCTTC	TGCTGTTGACAGTGAGCGAAAGAGTAATCA ATCTACTCAATAGTGAAGCCACAGATGTATT GAGTAGATTGATTACTCTTCTGCCTACTGCC TCGGA
HMGB1	HMGB1.2936	TTAGACATCCAACTTCTAGGGG	TGCTGTTGACAGTGAGCGACCCTAGAAGTTG GATGTCTAATAGTGAAGCCACAGATGTATTA GACATCCAACTTCTAGGGGTGCCTACTGCCT CGGA
HMGB2	HMGB2.635	TTATTCTTCATCTTCATCCTCT	TGCTGTTGACAGTGAGCGCGAGGATGAAGA TGAAGAATAATAGTGAAGCCACAGATGTATT ATTCTTCATCTTCATCCTCTTGCCTACTGCC TCGGA
HMGB2	HMGB2.1295	TTAGCTAATAAACAGAAACGTC	TGCTGTTGACAGTGAGCGAACGTTTCTGTTT ATTAGCTAATAGTGAAGCCACAGATGTATTA GCTAATAAACAGAAACGTCTGCCTACTGCCT CGGA
HMGB2	HMGB2.102	TTCTTCTTGTGCTCTTCCCGGC	TGCTGTTGACAGTGAGCGACCGGGAAGAGC ACAAGAAGAATAGTGAAGCCACAGATGTAT TCTTCTTGTGCTCTTCCCGGCTGCCTACTGC CTCGGA
HMGB2	HMGB2.952	TTACTATTGATACTAATTCCTA	TGCTGTTGACAGTGAGCGCAGGAATTAGTAT CAATAGTAATAGTGAAGCCACAGATGTATTA CTATTGATACTAATTCCTATGCCTACTGCCT CGGA
HMGB2	HMGB2.849	TCTAACTGTATGAGTAGCCCAT	TGCTGTTGACAGTGAGCGCTGGGCTACTCAT ACAGTTAGATAGTGAAGCCACAGATGTATCT AACTGTATGAGTAGCCCATTGCCTACTGCCT CGGA
HMGB3	HMGB3.2264	TTAACATTGAACATCAATCTAC	TGCTGTTGACAGTGAGCGATAGATTGATGTT CAATGTTAATAGTGAAGCCACAGATGTATTA ACATTGAACATCAATCTACTGCCTACTGCCT CGGA
HMGB3	HMGB3.1909	TTTGACACACCATACACTCTGA	TGCTGTTGACAGTGAGCGCCAGAGTGTATG GTGTGTCAAATAGTGAAGCCACAGATGTATT TGACACACCATACACTCTGATGCCTACTGCC TCGGA
HMGB3	HMGB3.628	TTCATCTTCCTCTTCCACCTTT	TGCTGTTGACAGTGAGCGCAAGGTGGAAGA GGAAGATGAATAGTGAAGCCACAGATGTAT TCATCTTCCTCTTCCACCTTTTGCCTACTGC CTCGGA
HMGB3	HMGB3.1249	TACAGAAACAAGACAACCTGAA	TGCTGTTGACAGTGAGCGCTCAGGTTGTCTT GTTTCTGTATAGTGAAGCCACAGATGTATAC AGAAACAAGACAACCTGAATGCCTACTGCC TCGGA
HMGB3	HMGB3.2531	TAATAGCACAAAAACACTCCTG	TGCTGTTGACAGTGAGCGAAGGAGTGTTTTT GTGCTATTATAGTGAAGCCACAGATGTATAA TAGCACAAAAACACTCCTGTGCCTACTGCCT CGGA
HNRNPAB	HNRNPAB.1243	TTAAATAAGATGCACATGGGAC	TGCTGTTGACAGTGAGCGATCCCATGTGCAT CTTATTTAATAGTGAAGCCACAGATGTATTA AATAAGATGCACATGGGACTGCCTACTGCCT CGGA
HNRNPAB	HNRNPAB.608	TCTTTGAACAGGATAAACCCAA	TGCTGTTGACAGTGAGCGCTGGGTTTATCCT GTTCAAAGATAGTGAAGCCACAGATGTATCT TTGAACAGGATAAACCCAATGCCTACTGCCT CGGA
HNRNPAB	HNRNPAB.829	TTTTGTTCAACTTTGGATCCAT	TGCTGTTGACAGTGAGCGCTGGATCCAAAGT TGAACAAAATAGTGAAGCCACAGATGTATTT TGTTCAACTTTGGATCCATTGCCTACTGCCT CGGA
HNRNPAB	HNRNPAB.1575	TTACAATACATTAGATTCCCAA	TGCTGTTGACAGTGAGCGCTGGGAATCTAAT GTATTGTAATAGTGAAGCCACAGATGTATTA

			CAATACATTAGATTCCCAATGCCTACTGCCTCGGA
HNRNPAB	HNRNPAB.1063	TTGTACTACCGAATTCCTCGAG	TGCTGTTGACAGTGAGCGATCGAGGAATTCGGTAGTACAATAGTGAAGCCACAGATGTATTGTACTACCGAATTCCTCGAGTGCCTACTGCCTCGGA
HNRNPD	HNRNPD.1275	TTGAACTGCTATTAGCAGGTGG	TGCTGTTGACAGTGAGCGACACCTGCTAATAGCAGTTCAATAGTGAAGCCACAGATGTATTGAACTGCTATTAGCAGGTGGTGCCTACTGCCTCGGA
HNRNPD	HNRNPD.2045	TATATTTCTTTAATCCTCCCTC	TGCTGTTGACAGTGAGCGAAGGGAGGATTAAAGAAATATATAGTGAAGCCACAGATGTATATATTTCTTTAATCCTCCCTCTGCCTACTGCCTCGGA
HNRNPD	HNRNPD.774	TTAGGATCAATCACCTTCCCAT	TGCTGTTGACAGTGAGCGCTGGGAAGGTGATTGATCCTAATAGTGAAGCCACAGATGTATTAGGATCAATCACCTTCCCATTGCCTACTGCCTCGGA
HNRNPD	HNRNPD.988	TTCCATTATCTTCTTCACTGGT	TGCTGTTGACAGTGAGCGCCCAGTGAAGAAGATAATGGAATAGTGAAGCCACAGATGTATTCCATTATCTTCTTCACTGGTTGCCTACTGCCTCGGA
HNRNPD	HNRNPD.1060	TTGCTGATATTGTTCCTTCGAC	TGCTGTTGACAGTGAGCGATCGAAGGAACAATATCAGCAATAGTGAAGCCACAGATGTATTGCTGATATTGTTCCTTCGACTGCCTACTGCCTCGGA
HNRNPR	HNRNPR.2400	TTTAAAAACACAGTTAACCTAC	TGCTGTTGACAGTGAGCGATAGGTTAACTGTGTTTTTAAATAGTGAAGCCACAGATGTATTTAAAAACACAGTTAACCTACTGCCTACTGCCTCGGA
HNRNPR	HNRNPR.777	TTCTTTAGTCTTATTCTTCGGA	TGCTGTTGACAGTGAGCGCCCGAAGAATAAGACTAAAGAATAGTGAAGCCACAGATGTATTCTTTAGTCTTATTCTTCGGATGCCTACTGCCTCGGA
HNRNPR	HNRNPR.1892	TACTTGTCTACTTCCACTGTTG	TGCTGTTGACAGTGAGCGAAACAGTGGAAGTAGACAAGTATAGTGAAGCCACAGATGTATACTTGTCTACTTCCACTGTTGTGCCTACTGCCTCGGA
HNRNPR	HNRNPR.1919	TTACTTGTCTACTTCCACTGTT	TGCTGTTGACAGTGAGCGCACAGTGGAAGTAGACAAGTAATAGTGAAGCCACAGATGTATTACTTGTCTACTTCCACTGTTTGCCTACTGCCTCGGA
HNRNPR	HNRNPR.510	TTTGCCTACAAATACCTCCGTT	TGCTGTTGACAGTGAGCGCACGGAGGTATTTGTAGGCAAATAGTGAAGCCACAGATGTATTTGCCTACAAATACCTCCGTTTGCCTACTGCCTCGGA
IL17RD	IL17RD.5166	TTTTGAAGGACAGTCTTCCTGC	TGCTGTTGACAGTGAGCGACAGGAAGACTGTCCTTCAAAATAGTGAAGCCACAGATGTATTTTGAAGGACAGTCTTCCTGCTGCCTACTGCCTCGGA
IL17RD	IL17RD.4714	TAACCTATCTACACAAGCCTTT	TGCTGTTGACAGTGAGCGCAAGGCTTGTGTAGATAGGTTATAGTGAAGCCACAGATGTATAACCTATCTACACAAGCCTTTTGCCTACTGCCTCGGA
IL17RD	IL17RD.660	TTTACAAGCTAGATTGTCCGGC	TGCTGTTGACAGTGAGCGACCGGACAATCTAGCTTGTAAATAGTGAAGCCACAGATGTATTTACAAGCTAGATTGTCCGGCTGCCTACTGCCTCGGA
IL17RD	IL17RD.1052	TTTTCTTGTTGCTTCTTGCGGC	TGCTGTTGACAGTGAGCGACCGCAAGAAGCAACAAGAAAATAGTGAAGCCACAGATGTATTTTCTTGTTGCTTCTTGCGGCTGCCTACTGCCTCGGA
IL17RD	IL17RD.493	TTTGAAGCTACTGTTGAGCTGC	TGCTGTTGACAGTGAGCGACAGCTCAACAGTAGCTTCAAATAGTGAAGCCACAGATGTATT

			TGAAGCTACTGTTGAGCTGCTGCCTACTGCC TCGGA
ILF2	ILF2.527	TAAAACTTCAGAAGGATCCTGT	TGCTGTTGACAGTGAGCGCCAGGATCCTTCT GAAGTTTTATAGTGAAGCCACAGATGTATAA AACTTCAGAAGGATCCTGTTGCCTACTGCCT CGGA
ILF2	ILF2.45	TAGCAGACAACTGAAGAGGCGT	TGCTGTTGACAGTGAGCGCCGCCTCTTCAGT TGTCTGCTATAGTGAAGCCACAGATGTATAG CAGACAACTGAAGAGGCGTTGCCTACTGCC TCGGA
ILF2	ILF2.1584	TTTCACAACATTTCAACAGCAA	TGCTGTTGACAGTGAGCGCTGCTGTTGAAAT GTTGTGAAATAGTGAAGCCACAGATGTATTT CACAACATTTCAACAGCAATGCCTACTGCCT CGGA
ILF2	ILF2.1851	TGATATTCTAGTTTACTCTGGT	TGCTGTTGACAGTGAGCGCCCAGAGTAAAC TAGAATATCATAGTGAAGCCACAGATGTATG ATATTCTAGTTTACTCTGGTTGCCTACTGCC TCGGA
ILF2	ILF2.785	TCTGATGAGAACTTTAACTGTG	TGCTGTTGACAGTGAGCGAACAGTTAAAGTT CTCATCAGATAGTGAAGCCACAGATGTATCT GATGAGAACTTTAACTGTGTGCCTACTGCCT CGGA
ILF3	ILF3.2024	TTTTGTTGGAACCAGCACCTTG	TGCTGTTGACAGTGAGCGAAAGGTGCTGGT TCCAACAAAATAGTGAAGCCACAGATGTATT TTGTTGGAACCAGCACCTTGTGCCTACTGCC TCGGA
ILF3	ILF3.1480	TTTCTTCTGAATCTTCTTCTTC	TGCTGTTGACAGTGAGCGAAAGAAGAAGAT TCAGAAGAAATAGTGAAGCCACAGATGTATT TCTTCTGAATCTTCTTCTTCTGCCTACTGCC TCGGA
ILF3	ILF3.724	TTCTGTTACAGCAGCAAGCTGG	TGCTGTTGACAGTGAGCGACAGCTTGCTGCT GTAACAGAATAGTGAAGCCACAGATGTATTC TGTTACAGCAGCAAGCTGGTGCCTACTGCCT CGGA
ILF3	ILF3.299	TTACTTCTTCTGTAGTGTCTGG	TGCTGTTGACAGTGAGCGACAGACACTACA GAAGAAGTAATAGTGAAGCCACAGATGTATT ACTTCTTCTGTAGTGTCTGGTGCCTACTGCC TCGGA
ILF3	ILF3.534	TTCTTTACTGTCGTCCTCTGGG	TGCTGTTGACAGTGAGCGACCAGAGGACGA CAGTAAAGAATAGTGAAGCCACAGATGTATT CTTTACTGTCGTCCTCTGGGTGCCTACTGCC TCGGA
IQGAP1	IQGAP1.7193	TTAACATGAACAAATGACCTTT	TGCTGTTGACAGTGAGCGCAAGGTCATTTGT TCATGTTAATAGTGAAGCCACAGATGTATTA ACATGAACAAATGACCTTTTGCCTACTGCCT CGGA
IQGAP1	IQGAP1.622	TTCTTCTGTGAAGTCAACCTTT	TGCTGTTGACAGTGAGCGCAAGGTTGACTTC ACAGAAGAATAGTGAAGCCACAGATGTATT CTTCTGTGAAGTCAACCTTTTGCCTACTGCC TCGGA
IQGAP1	IQGAP1.5499	TAACATGACATTTTAGTTGTGT	TGCTGTTGACAGTGAGCGCCACAACTAAAAT GTCATGTTATAGTGAAGCCACAGATGTATAA CATGACATTTTAGTTGTGTTGCCTACTGCCT CGGA
IQGAP1	IQGAP1.4793	TTTCATGTAGTCTTGCTGCTGT	TGCTGTTGACAGTGAGCGCCAGCAGCAAGA CTACATGAAATAGTGAAGCCACAGATGTATT TCATGTAGTCTTGCTGCTGTTGCCTACTGCC TCGGA
IQGAP1	IQGAP1.3207	TTGAATCTGATCTACCTTCGAC	TGCTGTTGACAGTGAGCGATCGAAGGTAGA TCAGATTCAATAGTGAAGCCACAGATGTATT GAATCTGATCTACCTTCGACTGCCTACTGCC TCGGA
JUNB	JUNB.308	TAGCTGTGTATGAGTCGTCGTG	TGCTGTTGACAGTGAGCGAACGACGACTCA TACACAGCTATAGTGAAGCCACAGATGTATA

			GCTGTGTATGAGTCGTCGTGTGCCTACTGCC TCGGA
JUNB	JUNB.273	TCCATTTTAGTGCACATCCGGG	TGCTGTTGACAGTGAGCGACCGGATGTGCA CTAAAATGGATAGTGAAGCCACAGATGTATC CATTTTAGTGCACATCCGGGTGCCTACTGCC TCGGA
JUNB	JUNB.1535	TATGAATCGAGTCTGTTTCCAG	TGCTGTTGACAGTGAGCGATGGAAACAGAC TCGATTCATATAGTGAAGCCACAGATGTATA TGAATCGAGTCTGTTTCCAGTGCCTACTGCC TCGGA
JUNB	JUNB.363	TTCAGGAGTTTGTAGTCGTGTA	TGCTGTTGACAGTGAGCGCACACGACTACA AACTCCTGAATAGTGAAGCCACAGATGTATT CAGGAGTTTGTAGTCGTGTATGCCTACTGCC TCGGA
JUNB	JUNB.1241	TGACCTTCTGTTTGAGCTGGGC	TGCTGTTGACAGTGAGCGACCCAGCTCAAA CAGAAGGTCATAGTGAAGCCACAGATGTAT GACCTTCTGTTTGAGCTGGGCTGCCTACTGC CTCGGA
KLF10	KLF10.622	TTGCTTTCTCATCAACATCTGC	TGCTGTTGACAGTGAGCGACAGATGTTGATG AGAAAGCAATAGTGAAGCCACAGATGTATT GCTTTCTCATCAACATCTGCTGCCTACTGCC TCGGA
KLF10	KLF10.1350	TAGCTTGCTCACTTCCATCTGC	TGCTGTTGACAGTGAGCGACAGATGGAAGT GAGCAAGCTATAGTGAAGCCACAGATGTAT AGCTTGCTCACTTCCATCTGCTGCCTACTGC CTCGGA
KLF10	KLF10.1822	TACATCTCCATGTCTGTACCGT	TGCTGTTGACAGTGAGCGCCGGTACAGACA TGGAGATGTATAGTGAAGCCACAGATGTATA CATCTCCATGTCTGTACCGTTGCCTACTGCC TCGGA
KLF10	KLF10.1084	TATGTCTTGCCACATCCTGGGT	TGCTGTTGACAGTGAGCGCCCCAGGATGTG GCAAGACATATAGTGAAGCCACAGATGTAT ATGTCTTGCCACATCCTGGGTTGCCTACTGC CTCGGA
KLF10	KLF10.1413	TTCTGACTCTTCACTTTCCGGT	TGCTGTTGACAGTGAGCGCCCGGAAAGTGA AGAGTCAGAATAGTGAAGCCACAGATGTATT CTGACTCTTCACTTTCCGGTTGCCTACTGCC TCGGA
LRRFIP1	LRRFIP1.595	TCTTTTGTCATCTTGGTAGGAC	TGCTGTTGACAGTGAGCGATCCTACCAAGAT GACAAAAGATAGTGAAGCCACAGATGTATC TTTTGTCATCTTGGTAGGACTGCCTACTGCC TCGGA
LRRFIP1	LRRFIP1.259	TATTTCTCTTCAACTTCTGCTA	TGCTGTTGACAGTGAGCGCAGCAGAAGTTG AAGAGAAATATAGTGAAGCCACAGATGTAT ATTTCTCTTCAACTTCTGCTATGCCTACTGC CTCGGA
LRRFIP1	LRRFIP1.445	TGAAATTGCAGTATACTGTGGG	TGCTGTTGACAGTGAGCGACCACAGTATACT GCAATTTCATAGTGAAGCCACAGATGTATGA AATTGCAGTATACTGTGGGTGCCTACTGCCT CGGA
LRRFIP1	LRRFIP1.592	TTTGTCATCTTGGTAGGACCTT	TGCTGTTGACAGTGAGCGCAGGTCCTACCA AGATGACAAATAGTGAAGCCACAGATGTATT TGTCATCTTGGTAGGACCTTTGCCTACTGCC TCGGA
LRRFIP1	LRRFIP1.262	TTATATTTCTCTTCAACTTCTG	TGCTGTTGACAGTGAGCGAAGAAGTTGAAG AGAAATATAATAGTGAAGCCACAGATGTATT ATATTTCTCTTCAACTTCTGTGCCTACTGCC TCGGA
MAFF	MAFF.970	TTTCACTAGTCTTCCCACCCAC	TGCTGTTGACAGTGAGCGATGGGTGGGAAG ACTAGTGAAATAGTGAAGCCACAGATGTATT TCACTAGTCTTCCCACCCACTGCCTACTGCC TCGGA
MAFF	MAFF.1993	TAAATAAATTCTAGGAGCCGGG	TGCTGTTGACAGTGAGCGACCGGCTCCTAG AATTTATTTATAGTGAAGCCACAGATGTATA

			AATAAATTCTAGGAGCCGGGTGCCTACTGCC TCGGA
MAFF	MAFF.708	TAAACTTTCAGCCAAGGGCGAT	TGCTGTTGACAGTGAGCGCTCGCCCTTGGCT GAAAGTTTATAGTGAAGCCACAGATGTATAA ACTTTCAGCCAAGGGCGATTGCCTACTGCCT CGGA
MAFF	MAFF.2	TCGCTTGATCGAATTCCTCGAG	TGCTGTTGACAGTGAGCGATCGAGGAATTC GATCAAGCGATAGTGAAGCCACAGATGTAT CGCTTGATCGAATTCCTCGAGTGCCTACTGC CTCGGA
MAFF	MAFF.839	TAGCTTTGAATCCTGGGAGGGT	TGCTGTTGACAGTGAGCGCCCCTCCCAGGA TTCAAAGCTATAGTGAAGCCACAGATGTATA GCTTTGAATCCTGGGAGGGTTGCCTACTGCC TCGGA
MCM2	MCM2.715	TTCTCTTTGCACATGTCGCTGA	TGCTGTTGACAGTGAGCGCCAGCGACATGT GCAAAGAGAATAGTGAAGCCACAGATGTAT TCTCTTTGCACATGTCGCTGATGCCTACTGC CTCGGA
MCM2	MCM2.1397	TACAGCAACCTTGTTGTCCTTC	TGCTGTTGACAGTGAGCGAAAGGACAACAA GGTTGCTGTATAGTGAAGCCACAGATGTATA CAGCAACCTTGTTGTCCTTCTGCCTACTGCC TCGGA
MCM2	MCM2.1017	TACTTGACCATGCTGAGCTGGG	TGCTGTTGACAGTGAGCGACCAGCTCAGCA TGGTCAAGTATAGTGAAGCCACAGATGTATA CTTGACCATGCTGAGCTGGGTGCCTACTGCC TCGGA
MCM2	MCM2.1427	TCATCTTCACATCTTCATCGGT	TGCTGTTGACAGTGAGCGCCCGATGAAGAT GTGAAGATGATAGTGAAGCCACAGATGTAT CATCTTCACATCTTCATCGGTTGCCTACTGC CTCGGA
MCM2	MCM2.1302	TAGTTGTTGTGATAGATGCCAG	TGCTGTTGACAGTGAGCGATGGCATCTATCA CAACAACTATAGTGAAGCCACAGATGTATAG TTGTTGTGATAGATGCCAGTGCCTACTGCCT CGGA
MCM3	MCM3.246	TTCACATTGACAATCAGCCGGT	TGCTGTTGACAGTGAGCGCCCGGCTGATTGT CAATGTGAATAGTGAAGCCACAGATGTATTC ACATTGACAATCAGCCGGTTGCCTACTGCCT CGGA
MCM3	MCM3.957	TTACTGAACTTCTTGATCTTGG	TGCTGTTGACAGTGAGCGACAAGATCAAGA AGTTCAGTAATAGTGAAGCCACAGATGTATT ACTGAACTTCTTGATCTTGGTGCCTACTGCC TCGGA
MCM3	MCM3.958	TTTACTGAACTTCTTGATCTTG	TGCTGTTGACAGTGAGCGAAAGATCAAGAA GTTCAGTAAATAGTGAAGCCACAGATGTATT TACTGAACTTCTTGATCTTGTGCCTACTGCC TCGGA
MCM3	MCM3.2977	TTTCTTGACCTGCATGACGTGC	TGCTGTTGACAGTGAGCGACACGTCATGCA GGTCAAGAAATAGTGAAGCCACAGATGTATT TCTTGACCTGCATGACGTGCTGCCTACTGCC TCGGA
MCM3	MCM3.3080	TAAGTTTATTCAACATCTCGGA	TGCTGTTGACAGTGAGCGCCCGAGATGTTG AATAAACTTATAGTGAAGCCACAGATGTATA AGTTTATTCAACATCTCGGATGCCTACTGCC TCGGA
MCM4	MCM4.216	TTATCGAGGAACAAACTTGGAA	TGCTGTTGACAGTGAGCGCTCCAAGTTTGTT CCTCGATAATAGTGAAGCCACAGATGTATTA TCGAGGAACAAACTTGGAATGCCTACTGCCT CGGA
MCM4	MCM4.3163	TTTTGAGACAGTCTCACTCTAT	TGCTGTTGACAGTGAGCGCTAGAGTGAGAC TGTCTCAAAATAGTGAAGCCACAGATGTATT TTGAGACAGTCTCACTCTATTGCCTACTGCC TCGGA
MCM4	MCM4.86	TAGGTTTCCATGTTGATTCGGG	TGCTGTTGACAGTGAGCGACCGAATCAACAT GGAAACCTATAGTGAAGCCACAGATGTATA

			GGTTTCCATGTTGATTCGGGTGCCTACTGCC TCGGA
MCM4	MCM4.1641	TATTCTTAGTCTTCAATGCGTT	TGCTGTTGACAGTGAGCGCACGCATTGAAG ACTAAGAATATAGTGAAGCCACAGATGTATA TTCTTAGTCTTCAATGCGTTTGCCTACTGCC TCGGA
MCM4	MCM4.217	TTTATCGAGGAACAAACTTGGA	TGCTGTTGACAGTGAGCGCCCAAGTTTGTTC CTCGATAAATAGTGAAGCCACAGATGTATTT ATCGAGGAACAAACTTGGATGCCTACTGCCT CGGA
MCM5	MCM5.2528	TTTACCTGAACACACCGTGGCT	TGCTGTTGACAGTGAGCGCGCCACGGTGTG TTCAGGTAAATAGTGAAGCCACAGATGTATT TACCTGAACACACCGTGGCTTGCCTACTGCC TCGGA
MCM5	MCM5.2529	TTTTACCTGAACACACCGTGGC	TGCTGTTGACAGTGAGCGACCACGGTGTGTT CAGGTAAAATAGTGAAGCCACAGATGTATTT TACCTGAACACACCGTGGCTGCCTACTGCCT CGGA
MCM5	MCM5.1636	TTGACGATGAAGATCATGTCGA	TGCTGTTGACAGTGAGCGCCGACATGATCTT CATCGTCAATAGTGAAGCCACAGATGTATTG ACGATGAAGATCATGTCGATGCCTACTGCCT CGGA
MCM5	MCM5.240	TGTATTTGAAGGTGAAGCCCGT	TGCTGTTGACAGTGAGCGCCGGGCTTCACCT TCAAATACATAGTGAAGCCACAGATGTATGT ATTTGAAGGTGAAGCCCGTTGCCTACTGCCT CGGA
MCM5	MCM5.343	TTGTACAAGTAGTCGGCCAGGT	TGCTGTTGACAGTGAGCGCCCTGGCCGACT ACTTGTACAATAGTGAAGCCACAGATGTATT GTACAAGTAGTCGGCCAGGTTGCCTACTGC CTCGGA
MCM6	MCM6.1479	ATGAATAGCAACTTGATCCCGC	TGCTGTTGACAGTGAGCGACGGGATCAAGT TGCTATTCATTAGTGAAGCCACAGATGTAAT GAATAGCAACTTGATCCCGCTGCCTACTGCC TCGGA
MCM6	MCM6.2172	TTGATTTATGTCTTCATTGTAG	TGCTGTTGACAGTGAGCGATACAATGAAGA CATAAATCAATAGTGAAGCCACAGATGTATT GATTTATGTCTTCATTGTAGTGCCTACTGCC TCGGA
MCM6	MCM6.2798	TTTGGTTCCAACTTCACTGGGA	TGCTGTTGACAGTGAGCGCCCCAGTGAAGTT GGAACCAAATAGTGAAGCCACAGATGTATTT GGTTCCAACTTCACTGGGATGCCTACTGCCT CGGA
MCM6	MCM6.2096	TTGATCTAGATTGACATCAGGT	TGCTGTTGACAGTGAGCGCCCTGATGTCAAT CTAGATCAATAGTGAAGCCACAGATGTATTG ATCTAGATTGACATCAGGTTGCCTACTGCCT CGGA
MCM6	MCM6.2807	TTACACATGAAAACAAAGGTAT	TGCTGTTGACAGTGAGCGCTACCTTTGTTTT CATGTGTAATAGTGAAGCCACAGATGTATTA CACATGAAAACAAAGGTATTGCCTACTGCCT CGGA
MCM7	MCM7.1879	TTTGACATCTCCATTAGCCTGA	TGCTGTTGACAGTGAGCGCCAGGCTAATGG AGATGTCAAATAGTGAAGCCACAGATGTATT TGACATCTCCATTAGCCTGATGCCTACTGCC TCGGA
MCM7	MCM7.897	TTGTTCATCTTCACAATCCGAT	TGCTGTTGACAGTGAGCGCTCGGATTGTGAA GATGAACAATAGTGAAGCCACAGATGTATTG TTCATCTTCACAATCCGATTGCCTACTGCCT CGGA
MCM7	MCM7.8	TTGTAAGAACTTCTTAACCTTT	TGCTGTTGACAGTGAGCGCAAGGTTAAGAA GTTCTTACAATAGTGAAGCCACAGATGTATT GTAAGAACTTCTTAACCTTTTGCCTACTGCC TCGGA
MCM7	MCM7.60	TACTTGAACTGCTTCTTCCCGA	TGCTGTTGACAGTGAGCGCCGGGAAGAAGC AGTTCAAGTATAGTGAAGCCACAGATGTATA

			CTTGAACTGCTTCTTCCCGATGCCTACTGCC TCGGA
MCM7	MCM7.674	TTCTTGCATCTTCATCTCCTGG	TGCTGTTGACAGTGAGCGACAGGAGATGAA GATGCAAGAATAGTGAAGCCACAGATGTATT CTTGCATCTTCATCTCCTGGTGCCTACTGCC TCGGA
MED8	MED8.2	TTTTCCAGTCGAATTCCTCGAG	TGCTGTTGACAGTGAGCGATCGAGGAATTC GACTGGAAAATAGTGAAGCCACAGATGTATT TTCCAGTCGAATTCCTCGAGTGCCTACTGCC TCGGA
MED8	MED8.561	TTAAAGGTCTGCTTGTTCGGCC	TGCTGTTGACAGTGAGCGAGCCGAACAAGC AGACCTTTAATAGTGAAGCCACAGATGTATT AAAGGTCTGCTTGTTCGGCCTGCCTACTGCC TCGGA
MED8	MED8.222	TTGTTCAGAGTGTTCAGCTGTC	TGCTGTTGACAGTGAGCGAACAGCTGAACA CTCTGAACAATAGTGAAGCCACAGATGTATT GTTCAGAGTGTTCAGCTGTCTGCCTACTGCC TCGGA
MED8	MED8.405	TTCTCCTGTTCTTCCACTTCAG	TGCTGTTGACAGTGAGCGATGAAGTGGAAG AACAGGAGAATAGTGAAGCCACAGATGTAT TCTCCTGTTCTTCCACTTCAGTGCCTACTGC CTCGGA
MED8	MED8.474	TTATTCAAGCTCTGGATCTGCT	TGCTGTTGACAGTGAGCGCGCAGATCCAGA GCTTGAATAATAGTGAAGCCACAGATGTATT ATTCAAGCTCTGGATCTGCTTGCCTACTGCC TCGGA
MYBL2	MYBL2.2073	TTCTTTGATACCTGACAGGGTG	TGCTGTTGACAGTGAGCGAACCCTGTCAGGT ATCAAAGAATAGTGAAGCCACAGATGTATTC TTTGATACCTGACAGGGTGTGCCTACTGCCT CGGA
MYBL2	MYBL2.2234	TTCTCCTGCATGAAAAGCTGGT	TGCTGTTGACAGTGAGCGCCCAGCTTTTCAT GCAGGAGAATAGTGAAGCCACAGATGTATT CTCCTGCATGAAAAGCTGGTTGCCTACTGCC TCGGA
MYBL2	MYBL2.1874	TCGATGATGAGTTCGATGCCAG	TGCTGTTGACAGTGAGCGATGGCATCGAACT CATCATCGATAGTGAAGCCACAGATGTATCG ATGATGAGTTCGATGCCAGTGCCTACTGCCT CGGA
MYBL2	MYBL2.875	TTGGTCAGAAGACTTCCCTGGC	TGCTGTTGACAGTGAGCGACCAGGGAAGTC TTCTGACCAATAGTGAAGCCACAGATGTATT GGTCAGAAGACTTCCCTGGCTGCCTACTGCC TCGGA
MYBL2	MYBL2.1535	TTAACAGGTGTGCTCTTGGGCG	TGCTGTTGACAGTGAGCGAGCCCAAGAGCA CACCTGTTAATAGTGAAGCCACAGATGTATT AACAGGTGTGCTCTTGGGCGTGCCTACTGCC TCGGA
NAP1L4	NAP1L4.362	TATGTGAGCACATCTCACCTGA	TGCTGTTGACAGTGAGCGCCAGGTGAGATG TGCTCACATATAGTGAAGCCACAGATGTATA TGTGAGCACATCTCACCTGATGCCTACTGCC TCGGA
NAP1L4	NAP1L4.2472	TAGAATATTCTAACTATTCTGT	TGCTGTTGACAGTGAGCGCCAGAATAGTTAG AATATTCTATAGTGAAGCCACAGATGTATAG AATATTCTAACTATTCTGTTGCCTACTGCCT CGGA
NAP1L4	NAP1L4.740	TAACACAAAAGACATAGGCTGT	TGCTGTTGACAGTGAGCGCCAGCCTATGTCT TTTGTGTTATAGTGAAGCCACAGATGTATAA CACAAAAGACATAGGCTGTTGCCTACTGCCT CGGA
NAP1L4	NAP1L4.909	TTGACAGTAACATTCTTTCCTT	TGCTGTTGACAGTGAGCGCAGGAAAGAATG TTACTGTCAATAGTGAAGCCACAGATGTATT GACAGTAACATTCTTTCCTTTGCCTACTGCC TCGGA
NAP1L4	NAP1L4.885	TTCCAGTCAATAGTACACCCGT	TGCTGTTGACAGTGAGCGCCGGGTGTACTAT TGACTGGAATAGTGAAGCCACAGATGTATTC

			CAGTCAATAGTACACCCGTTGCCTACTGCCT CGGA
NF1	NF1.898	TATATCATGAACATCAACATTG	TGCTGTTGACAGTGAGCGAAATGTTGATGTT CATGATATATAGTGAAGCCACAGATGTATAT ATCATGAACATCAACATTGTGCCTACTGCCT CGGA
NF1	NF1.898	TATATCATGAACATCAACATTG	TGCTGTTGACAGTGAGCGAAATGTTGATGTT CATGATATATAGTGAAGCCACAGATGTATAT ATCATGAACATCAACATTGTGCCTACTGCCT CGGA
NF1	NF1.1588	TAGAAGGTGAATTCTGAGCCAG	TGCTGTTGACAGTGAGCGATGGCTCAGAATT CACCTTCTATAGTGAAGCCACAGATGTATAG AAGGTGAATTCTGAGCCAGTGCCTACTGCCT CGGA
NF1	NF1.1588	TAGAAGGTGAATTCTGAGCCAG	TGCTGTTGACAGTGAGCGATGGCTCAGAATT CACCTTCTATAGTGAAGCCACAGATGTATAG AAGGTGAATTCTGAGCCAGTGCCTACTGCCT CGGA
NF1	NF1.561	TAAAATAGTAGTGAGGCCGCTT	TGCTGTTGACAGTGAGCGCAGCGGCCTCAC TACTATTTTATAGTGAAGCCACAGATGTATA AAATAGTAGTGAGGCCGCTTTGCCTACTGCC TCGGA
NF1	NF1.561	TAAAATAGTAGTGAGGCCGCTT	TGCTGTTGACAGTGAGCGCAGCGGCCTCAC TACTATTTTATAGTGAAGCCACAGATGTATA AAATAGTAGTGAGGCCGCTTTGCCTACTGCC TCGGA
NF1	NF1.1785	TTCTTTAAATGTAAGACTCGGT	TGCTGTTGACAGTGAGCGCCCGAGTCTTACA TTTAAAGAATAGTGAAGCCACAGATGTATTC TTTAAATGTAAGACTCGGTTGCCTACTGCCT CGGA
NF1	NF1.1785	TTCTTTAAATGTAAGACTCGGT	TGCTGTTGACAGTGAGCGCCCGAGTCTTACA TTTAAAGAATAGTGAAGCCACAGATGTATTC TTTAAATGTAAGACTCGGTTGCCTACTGCCT CGGA
NF1	NF1.1361	TTACACAGTTTGACACAGGCAA	TGCTGTTGACAGTGAGCGCTGCCTGTGTCAA ACTGTGTAATAGTGAAGCCACAGATGTATTA CACAGTTTGACACAGGCAATGCCTACTGCCT CGGA
NF1	NF1.1361	TTACACAGTTTGACACAGGCAA	TGCTGTTGACAGTGAGCGCTGCCTGTGTCAA ACTGTGTAATAGTGAAGCCACAGATGTATTA CACAGTTTGACACAGGCAATGCCTACTGCCT CGGA
NFE2L3	NFE2L3.943	TTCATCATCATCATTCTGCTGA	TGCTGTTGACAGTGAGCGCCAGCAGAATGA TGATGATGAATAGTGAAGCCACAGATGTATT CATCATCATCATTCTGCTGATGCCTACTGCC TCGGA
NFE2L3	NFE2L3.1541	TATTATTGTGACTTGAATCTAA	TGCTGTTGACAGTGAGCGCTAGATTCAAGTC ACAATAATATAGTGAAGCCACAGATGTATAT TATTGTGACTTGAATCTAATGCCTACTGCCT CGGA
NFE2L3	NFE2L3.3599	TACTCTACACTGTAGCTCCTAT	TGCTGTTGACAGTGAGCGCTAGGAGCTACA GTGTAGAGTATAGTGAAGCCACAGATGTATA CTCTACACTGTAGCTCCTATTGCCTACTGCC TCGGA
NFE2L3	NFE2L3.350	TAAAGATCTAGGTCTACGCGGA	TGCTGTTGACAGTGAGCGCCCGCGTAGACC TAGATCTTTATAGTGAAGCCACAGATGTATA AAGATCTAGGTCTACGCGGATGCCTACTGCC TCGGA
NFE2L3	NFE2L3.1962	TAATATCTACTTAACATGCTAT	TGCTGTTGACAGTGAGCGCTAGCATGTTAAG TAGATATTATAGTGAAGCCACAGATGTATAA TATCTACTTAACATGCTATTGCCTACTGCCT CGGA
NFKB1	NFKB1.1378	TTGTCTATGAACATCTGTGGGG	TGCTGTTGACAGTGAGCGACCCACAGATGTT CATAGACAATAGTGAAGCCACAGATGTATTG

			TCTATGAACATCTGTGGGGTGCCTACTGCCT CGGA
NFKB1	NFKB1.2926	TTCTAGTAACTTATACAGCTGC	TGCTGTTGACAGTGAGCGACAGCTGTATAAG TTACTAGAATAGTGAAGCCACAGATGTATTC TAGTAACTTATACAGCTGCTGCCTACTGCCT CGGA
NFKB1	NFKB1.3703	TTTAATGACAATAGGAACGTAG	TGCTGTTGACAGTGAGCGATACGTTCCTATT GTCATTAAATAGTGAAGCCACAGATGTATTT AATGACAATAGGAACGTAGTGCCTACTGCCT CGGA
NFKB1	NFKB1.2920	TAACTTATACAGCTGCAGCTTC	TGCTGTTGACAGTGAGCGAAAGCTGCAGCT GTATAAGTTATAGTGAAGCCACAGATGTATA ACTTATACAGCTGCAGCTTCTGCCTACTGCC TCGGA
NFKB1	NFKB1.2367	TTGTGCTTGAGTAAGATACTGA	TGCTGTTGACAGTGAGCGCCAGTATCTTACT CAAGCACAATAGTGAAGCCACAGATGTATT GTGCTTGAGTAAGATACTGATGCCTACTGCC TCGGA
PA2G4	PA2G4.706	TTCCTTGAGAATATAATCCTGG	TGCTGTTGACAGTGAGCGACAGGATTATATT CTCAAGGAATAGTGAAGCCACAGATGTATTC CTTGAGAATATAATCCTGGTGCCTACTGCCT CGGA
PA2G4	PA2G4.994	TTCTCCATCGATGACATGCTGC	TGCTGTTGACAGTGAGCGACAGCATGTCATC GATGGAGAATAGTGAAGCCACAGATGTATT CTCCATCGATGACATGCTGCTGCCTACTGCC TCGGA
PA2G4	PA2G4.1492	TTCGACTTGCAGAACTCTGGAG	TGCTGTTGACAGTGAGCGATCCAGAGTTCTG CAAGTCGAATAGTGAAGCCACAGATGTATTC GACTTGCAGAACTCTGGAGTGCCTACTGCCT CGGA
PA2G4	PA2G4.1812	TCATTTAAAGTAGTCTTCCGTG	TGCTGTTGACAGTGAGCGAACGGAAGACTA CTTTAAATGATAGTGAAGCCACAGATGTATC ATTTAAAGTAGTCTTCCGTGTGCCTACTGCC TCGGA
PA2G4	PA2G4.1809	TTTAAAGTAGTCTTCCGTGGTT	TGCTGTTGACAGTGAGCGCACCACGGAAGA CTACTTTAAATAGTGAAGCCACAGATGTATT TAAAGTAGTCTTCCGTGGTTTGCCTACTGCC TCGGA
PHTF2	PHTF2.323	TTACTTGTAACCACCACCGGAA	TGCTGTTGACAGTGAGCGCTCCGGTGGTGG TTACAAGTAATAGTGAAGCCACAGATGTATT ACTTGTAACCACCACCGGAATGCCTACTGCC TCGGA
PHTF2	PHTF2.269	TACAACTCGAACAATTCCCTTT	TGCTGTTGACAGTGAGCGCAAGGGAATTGTT CGAGTTGTATAGTGAAGCCACAGATGTATAC AACTCGAACAATTCCCTTTTGCCTACTGCCT CGGA
PHTF2	PHTF2.808	TTGTATTCCATCTTCACCGCTT	TGCTGTTGACAGTGAGCGCAGCGGTGAAGA TGGAATACAATAGTGAAGCCACAGATGTATT GTATTCCATCTTCACCGCTTTGCCTACTGCC TCGGA
PHTF2	PHTF2.993	TTCTATTCCGAAGAACACCTTC	TGCTGTTGACAGTGAGCGAAAGGTGTTCTTC GGAATAGAATAGTGAAGCCACAGATGTATTC TATTCCGAAGAACACCTTCTGCCTACTGCCT CGGA
PHTF2	PHTF2.714	TATCAATTGAATTCTTTGCTTT	TGCTGTTGACAGTGAGCGCAAGCAAAGAAT TCAATTGATATAGTGAAGCCACAGATGTATA TCAATTGAATTCTTTGCTTTTGCCTACTGCC TCGGA
PMEPA1	PMEPA1.4210	TTAACTTGAACAGAGCTTGGGA	TGCTGTTGACAGTGAGCGCCCCAAGCTCTGT TCAAGTTAATAGTGAAGCCACAGATGTATTA ACTTGAACAGAGCTTGGGATGCCTACTGCCT CGGA
PMEPA1	PMEPA1.3541	TAACGTGACAACTACCATCTAG	TGCTGTTGACAGTGAGCGATAGATGGTAGTT GTCACGTTATAGTGAAGCCACAGATGTATAA

			CGTGACAACTACCATCTAGTGCCTACTGCCT CGGA
PMEPA1	PMEPA1.4018	TTTTCTTTCCTTATCGACGGGA	TGCTGTTGACAGTGAGCGCCCCGTCGATAA GGAAAGAAAATAGTGAAGCCACAGATGTAT TTTCTTTCCTTATCGACGGGATGCCTACTGC CTCGGA
PMEPA1	PMEPA1.2011	TTAAGTGAGAATTGATCCGTGA	TGCTGTTGACAGTGAGCGCCACGGATCAATT CTCACTTAATAGTGAAGCCACAGATGTATTA AGTGAGAATTGATCCGTGATGCCTACTGCCT CGGA
PMEPA1	PMEPA1.2873	TTAATCATCTTTACAAGTGCGT	TGCTGTTGACAGTGAGCGCCGCACTTGTAAA GATGATTAATAGTGAAGCCACAGATGTATTA ATCATCTTTACAAGTGCGTTGCCTACTGCCT CGGA
PML	PML.1271	TTGAACTCGTCGAAGCCATCGG	TGCTGTTGACAGTGAGCGACGATGGCTTCG ACGAGTTCAATAGTGAAGCCACAGATGTATT GAACTCGTCGAAGCCATCGGTGCCTACTGC CTCGGA
PML	PML.105	TTTAGATCTTGGAGTGCGTGAA	TGCTGTTGACAGTGAGCGCTCACGCACTCCA AGATCTAAATAGTGAAGCCACAGATGTATTT AGATCTTGGAGTGCGTGAATGCCTACTGCCT CGGA
PML	PML.109	TCGGTTTAGATCTTGGAGTGCG	TGCTGTTGACAGTGAGCGAGCACTCCAAGA TCTAAACCGATAGTGAAGCCACAGATGTATC GGTTTAGATCTTGGAGTGCGTGCCTACTGCC TCGGA
PML	PML.1148	TAGCACTTCATCCTCTGCACCA	TGCTGTTGACAGTGAGCGCGGTGCAGAGGA TGAAGTGCTATAGTGAAGCCACAGATGTATA GCACTTCATCCTCTGCACCATGCCTACTGCC TCGGA
PML	PML.111	TCTCGGTTTAGATCTTGGAGTG	TGCTGTTGACAGTGAGCGAACTCCAAGATCT AAACCGAGATAGTGAAGCCACAGATGTATC TCGGTTTAGATCTTGGAGTGTGCCTACTGCC TCGGA
PNN	PNN.401	TTTAACATCATCATCCTCCGGG	TGCTGTTGACAGTGAGCGACCGGAGGATGA TGATGTTAAATAGTGAAGCCACAGATGTATT TAACATCATCATCCTCCGGGTGCCTACTGCC TCGGA
PNN	PNN.1071	TATTTCTACATCATTGTGCTGA	TGCTGTTGACAGTGAGCGCCAGCACAATGA TGTAGAAATATAGTGAAGCCACAGATGTATA TTTCTACATCATTGTGCTGATGCCTACTGCC TCGGA
PNN	PNN.2904	TACTGTTTAGTTATCTACCGAA	TGCTGTTGACAGTGAGCGCTCGGTAGATAAC TAAACAGTATAGTGAAGCCACAGATGTATAC TGTTTAGTTATCTACCGAATGCCTACTGCCT CGGA
PNN	PNN.2847	TTAGATTAAAATAACAAGGGAG	TGCTGTTGACAGTGAGCGATCCCTTGTTATT TTAATCTAATAGTGAAGCCACAGATGTATTA GATTAAAATAACAAGGGAGTGCCTACTGCCT CGGA
PNN	PNN.400	TTAACATCATCATCCTCCGGGT	TGCTGTTGACAGTGAGCGCCCCGGAGGATG ATGATGTTAATAGTGAAGCCACAGATGTATT AACATCATCATCCTCCGGGTTGCCTACTGCC TCGGA
POLR1E	POLR1E.1199	TTGGCTATCTCCATCATCCTTT	TGCTGTTGACAGTGAGCGCAAGGATGATGG AGATAGCCAATAGTGAAGCCACAGATGTATT GGCTATCTCCATCATCCTTTTGCCTACTGCC TCGGA
POLR1E	POLR1E.501	TTCAATACAAGAATCCATCTTT	TGCTGTTGACAGTGAGCGCAAGATGGATTCT TGTATTGAATAGTGAAGCCACAGATGTATTC AATACAAGAATCCATCTTTTGCCTACTGCCT CGGA
POLR1E	POLR1E.815	TTCAGTATTTCTTCTGACGTGA	TGCTGTTGACAGTGAGCGCCACGTCAGAAG AAATACTGAATAGTGAAGCCACAGATGTATT

			CAGTATTTCTTCTGACGTGATGCCTACTGCC TCGGA
POLR1E	POLR1E.1264	TTGTGATCTTCTTCACTGCCGG	TGCTGTTGACAGTGAGCGACGGCAGTGAAG AAGATCACAATAGTGAAGCCACAGATGTATT GTGATCTTCTTCACTGCCGGTGCCTACTGCC TCGGA
POLR1E	POLR1E.467	TTTGGTCTGACTCTCTAGCGCC	TGCTGTTGACAGTGAGCGAGCGCTAGAGAG TCAGACCAAATAGTGAAGCCACAGATGTATT TGGTCTGACTCTCTAGCGCCTGCCTACTGCC TCGGA
POLR2F	POLR2F.1308	TCTGACTTAATGTAACACCTGG	TGCTGTTGACAGTGAGCGACAGGTGTTACAT TAAGTCAGATAGTGAAGCCACAGATGTATCT GACTTAATGTAACACCTGGTGCCTACTGCCT CGGA
POLR2F	POLR2F.1300	TAATGTAACACCTGGAACCCAG	TGCTGTTGACAGTGAGCGATGGGTTCCAGGT GTTACATTATAGTGAAGCCACAGATGTATAA TGTAACACCTGGAACCCAGTGCCTACTGCCT CGGA
POLR2F	POLR2F.112	TTGTCTGACATGACACCCTCGC	TGCTGTTGACAGTGAGCGACGAGGGTGTCA TGTCAGACAATAGTGAAGCCACAGATGTATT GTCTGACATGACACCCTCGCTGCCTACTGCC TCGGA
POLR2F	POLR2F.181	TTCTCCAAGTCATCTAGCCCTT	TGCTGTTGACAGTGAGCGCAGGGCTAGATG ACTTGGAGAATAGTGAAGCCACAGATGTATT CTCCAAGTCATCTAGCCCTTTGCCTACTGCC TCGGA
POLR2F	POLR2F.1305	TGACTTAATGTAACACCTGGAA	TGCTGTTGACAGTGAGCGCTCCAGGTGTTAC ATTAAGTCATAGTGAAGCCACAGATGTATGA CTTAATGTAACACCTGGAATGCCTACTGCCT CGGA
POLR3K	POLR3K.166	TTCAGTTTTGGGTACTTCCGAT	TGCTGTTGACAGTGAGCGCTCGGAAGTACC CAAAACTGAATAGTGAAGCCACAGATGTATT CAGTTTTGGGTACTTCCGATTGCCTACTGCC TCGGA
POLR3K	POLR3K.726	TAACAGTTAAATATTTAGGGAC	TGCTGTTGACAGTGAGCGATCCCTAAATATT TAACTGTTATAGTGAAGCCACAGATGTATAA CAGTTAAATATTTAGGGACTGCCTACTGCCT CGGA
POLR3K	POLR3K.313	TTGTAGAAGGTGGTCATCGGCT	TGCTGTTGACAGTGAGCGCGCCGATGACCA CCTTCTACAATAGTGAAGCCACAGATGTATT GTAGAAGGTGGTCATCGGCTTGCCTACTGCC TCGGA
POLR3K	POLR3K.676	TATTTAAGAGTGTTGATTGGGA	TGCTGTTGACAGTGAGCGCCCCAATCAACA CTCTTAAATATAGTGAAGCCACAGATGTATA TTTAAGAGTGTTGATTGGGATGCCTACTGCC TCGGA
POLR3K	POLR3K.151	TTCCGATTTGTTACCTTGCGGG	TGCTGTTGACAGTGAGCGACCGCAAGGTAA CAAATCGGAATAGTGAAGCCACAGATGTATT CCGATTTGTTACCTTGCGGGTGCCTACTGCC TCGGA
PPP1R15A	PPP1R15A.49	TTGCATAAGATCAACAACTGGG	TGCTGTTGACAGTGAGCGACCAGTTGTTGAT CTTATGCAATAGTGAAGCCACAGATGTATTG CATAAGATCAACAACTGGGTGCCTACTGCCT CGGA
PPP1R15A	PPP1R15A.963	TTCTGTTCTTTTATCCTCCGTG	TGCTGTTGACAGTGAGCGAACGGAGGATAA AAGAACAGAATAGTGAAGCCACAGATGTAT TCTGTTCTTTTATCCTCCGTGTGCCTACTGC CTCGGA
PPP1R15A	PPP1R15A.1494	TTCTCTTTCATCCTCGGCTGAT	TGCTGTTGACAGTGAGCGCTCAGCCGAGGA TGAAAGAGAATAGTGAAGCCACAGATGTATT CTCTTTCATCCTCGGCTGATTGCCTACTGCC TCGGA
PPP1R15A	PPP1R15A.2344	TTTATTCCTTATATAAACCCAC	TGCTGTTGACAGTGAGCGATGGGTTTATATA AGGAATAAATAGTGAAGCCACAGATGTATTT

			ATTCCTTATATAAACCCACTGCCTACTGCCTCGGA
PPP1R15A	PPP1R15A.964	TTTCTGTTCTTTTATCCTCCGT	TGCTGTTGACAGTGAGCGCCGGAGGATAAAAGAACAGAAATAGTGAAGCCACAGATGTATTTCTGTTCTTTTATCCTCCGTTGCCTACTGCCTCGGA
PPP2R5A	PPP2R5A.694	TACAACACAATATGCTAGCTGA	TGCTGTTGACAGTGAGCGCCAGCTAGCATATTGTGTTGTATAGTGAAGCCACAGATGTATACAACACAATATGCTAGCTGATGCCTACTGCCTCGGA
PPP2R5A	PPP2R5A.49	AAACAGTATACAACACTGCTGC	TGCTGTTGACAGTGAGCGACAGCAGTGTTGTATACTGTTTTAGTGAAGCCACAGATGTAAAACAGTATACAACACTGCTGCTGCCTACTGCCTCGGA
PPP2R5A	PPP2R5A.730	TTAGTGTTGTATCTTTCTCCAG	TGCTGTTGACAGTGAGCGATGGAGAAAGATACAACACTAATAGTGAAGCCACAGATGTATTAGTGTTGTATCTTTCTCCAGTGCCTACTGCCTCGGA
PPP2R5A	PPP2R5A.96	TTCTTTGCTCTTCAAGTCTGAA	TGCTGTTGACAGTGAGCGCTCAGACTTGAAGAGCAAAGAATAGTGAAGCCACAGATGTATTCTTTGCTCTTCAAGTCTGAATGCCTACTGCCTCGGA
PPP2R5A	PPP2R5A.183	TACTATATCAGAATACGCTGAT	TGCTGTTGACAGTGAGCGCTCAGCGTATTCTGATATAGTATAGTGAAGCCACAGATGTATACTATATCAGAATACGCTGATTGCCTACTGCCTCGGA
PPP2R5B	PPP2R5B.1181	TTTTGATCCACATATCTCTTGG	TGCTGTTGACAGTGAGCGACAAGAGATATGTGGATCAAAATAGTGAAGCCACAGATGTATTTTGATCCACATATCTCTTGGTGCCTACTGCCTCGGA
PPP2R5B	PPP2R5B.2733	TTTTCTTGAATTTCTCTCTTTA	TGCTGTTGACAGTGAGCGCAAAGAGAGAAATTCAAGAAAATAGTGAAGCCACAGATGTATTTTCTTGAATTTCTCTCTTTATGCCTACTGCCTCGGA
PPP2R5B	PPP2R5B.1342	TCGAATTCATAGATGAACCGGA	TGCTGTTGACAGTGAGCGCCCGGTTCATCTATGAATTCGATAGTGAAGCCACAGATGTATCGAATTCATAGATGAACCGGATGCCTACTGCCTCGGA
PPP2R5B	PPP2R5B.1178	TTGATCCACATATCTCTTGGCC	TGCTGTTGACAGTGAGCGAGCCAAGAGATATGTGGATCAATAGTGAAGCCACAGATGTATTGATCCACATATCTCTTGGCCTGCCTACTGCCTCGGA
PPP2R5B	PPP2R5B.1879	TTGAGCACATTGTAGATCAGTG	TGCTGTTGACAGTGAGCGAACTGATCTACAATGTGCTCAATAGTGAAGCCACAGATGTATTGAGCACATTGTAGATCAGTGTGCCTACTGCCTCGGA
PPP2R5C	PPP2R5C.1208	TAGATTTTCTATTTTAACCCAT	TGCTGTTGACAGTGAGCGCTGGGTTAAAATAGAAAATCTATAGTGAAGCCACAGATGTATAGATTTTCTATTTTAACCCATTGCCTACTGCCTCGGA
PPP2R5C	PPP2R5C.118	TTTCACTTAAAGCAGCTCGTTT	TGCTGTTGACAGTGAGCGCAACGAGCTGCTTTAAGTGAAATAGTGAAGCCACAGATGTATTTCACTTAAAGCAGCTCGTTTTGCCTACTGCCTCGGA
PPP2R5C	PPP2R5C.1159	TTCTCTTTTAGTTTCTCTGCTT	TGCTGTTGACAGTGAGCGCAGCAGAGAAACTAAAAGAGAATAGTGAAGCCACAGATGTATTCTCTTTTAGTTTCTCTGCTTTGCCTACTGCCTCGGA
PPP2R5C	PPP2R5C.631	TTGTGCTCTTCTTTTAGTGGTA	TGCTGTTGACAGTGAGCGCACCACTAAAAGAAGAGCACAATAGTGAAGCCACAGATGTATTGTGCTCTTCTTTTAGTGGTATGCCTACTGCCTCGGA
PPP2R5C	PPP2R5C.362	TATATTAGGTTGGAAATCTGGA	TGCTGTTGACAGTGAGCGCCCAGATTTCCAACCTAATATATAGTGAAGCCACAGATGTATAT

			ATTAGGTTGGAAATCTGGATGCCTACTGCCTCGGA
PPP2R5E	PPP2R5E.679	TAAACTGTGAGGAACTTTGCGA	TGCTGTTGACAGTGAGCGCCGCAAAGTTCCTCACAGTTTATAGTGAAGCCACAGATGTATAAACTGTGAGGAACTTTGCGATGCCTACTGCCTCGGA
PPP2R5E	PPP2R5E.2683	TAAACTGATGCATGAATCCGAT	TGCTGTTGACAGTGAGCGCTCGGATTCATGCATCAGTTTATAGTGAAGCCACAGATGTATAAACTGATGCATGAATCCGATTGCCTACTGCCTCGGA
PPP2R5E	PPP2R5E.1240	TATTGTTAATCTGTTTTCGGAT	TGCTGTTGACAGTGAGCGCTCCGAAAACAGATTAACAATATAGTGAAGCCACAGATGTATATTGTTAATCTGTTTTCGGATTGCCTACTGCCTCGGA
PPP2R5E	PPP2R5E.1269	TTCTGTTTCATAAACAAACCTT	TGCTGTTGACAGTGAGCGCAGGTTTGTTTATGAAACAGAATAGTGAAGCCACAGATGTATTCTGTTTCATAAACAAACCTTTGCCTACTGCCTCGGA
PPP2R5E	PPP2R5E.2031	TTCTACTACATAAACGTGTGAC	TGCTGTTGACAGTGAGCGATCACACGTTTATGTAGTAGAATAGTGAAGCCACAGATGTATTCTACTACATAAACGTGTGACTGCCTACTGCCTCGGA
PTTG1	PTTG1.670	TACAAATACACACAAACTCTGA	TGCTGTTGACAGTGAGCGCCAGAGTTTGTGTGTATTTGTATAGTGAAGCCACAGATGTATACAAATACACACAAACTCTGATGCCTACTGCCTCGGA
PTTG1	PTTG1.327	TTTGCTTTAACAGTCTTCTCAG	TGCTGTTGACAGTGAGCGATGAGAAGACTGTTAAAGCAAATAGTGAAGCCACAGATGTATTTGCTTTAACAGTCTTCTCAGTGCCTACTGCCTCGGA
PTTG1	PTTG1.18	TATTGCAGGTCTTAACAGCCGC	TGCTGTTGACAGTGAGCGACGGCTGTTAAGACCTGCAATATAGTGAAGCCACAGATGTATATTGCAGGTCTTAACAGCCGCTGCCTACTGCCTCGGA
PTTG1	PTTG1.236	TAGCTCTGTTGACAGTTCCCAA	TGCTGTTGACAGTGAGCGCTGGGAACTGTCAACAGAGCTATAGTGAAGCCACAGATGTATAGCTCTGTTGACAGTTCCCAATGCCTACTGCCTCGGA
PTTG1	PTTG1.7	TTAACAGCCGCATTCATCTGAG	TGCTGTTGACAGTGAGCGATCAGATGAATGCGGCTGTTAATAGTGAAGCCACAGATGTATTAACAGCCGCATTCATCTGAGTGCCTACTGCCTCGGA
RASA1	RASA1.1954	TTATCTTTAAAATAGAGTCTTT	TGCTGTTGACAGTGAGCGCAAGACTCTATTTTAAAGATAATAGTGAAGCCACAGATGTATTATCTTTAAAATAGAGTCTTTTGCCTACTGCCTCGGA
RASA1	RASA1.1954	TTATCTTTAAAATAGAGTCTTT	TGCTGTTGACAGTGAGCGCAAGACTCTATTTTAAAGATAATAGTGAAGCCACAGATGTATTATCTTTAAAATAGAGTCTTTTGCCTACTGCCTCGGA
RASA1	RASA1.396	TAGAATAGCTCGTACACGCCTT	TGCTGTTGACAGTGAGCGCAGGCGTGTACGAGCTATTCTATAGTGAAGCCACAGATGTATAGAATAGCTCGTACACGCCTTTGCCTACTGCCTCGGA
RASA1	RASA1.396	TAGAATAGCTCGTACACGCCTT	TGCTGTTGACAGTGAGCGCAGGCGTGTACGAGCTATTCTATAGTGAAGCCACAGATGTATAGAATAGCTCGTACACGCCTTTGCCTACTGCCTCGGA
RASA1	RASA1.573	TTCATGTGGATCTTCTTCCCGG	TGCTGTTGACAGTGAGCGACGGGAAGAAGATCCACATGAATAGTGAAGCCACAGATGTATTCATGTGGATCTTCTTCCCGGTGCCTACTGCCTCGGA
RASA1	RASA1.573	TTCATGTGGATCTTCTTCCCGG	TGCTGTTGACAGTGAGCGACGGGAAGAAGATCCACATGAATAGTGAAGCCACAGATGTATT

			CATGTGGATCTTCTTCCCGGTGCCTACTGCC TCGGA
RASA1	RASA1.2153	TAAATATATCTCAATGTCGGTG	TGCTGTTGACAGTGAGCGAACCGACATTGA GATATATTTATAGTGAAGCCACAGATGTATA AATATATCTCAATGTCGGTGTGCCTACTGCC TCGGA
RASA1	RASA1.2153	TAAATATATCTCAATGTCGGTG	TGCTGTTGACAGTGAGCGAACCGACATTGA GATATATTTATAGTGAAGCCACAGATGTATA AATATATCTCAATGTCGGTGTGCCTACTGCC TCGGA
RASA1	RASA1.3593	TAAAACTATACAGTTGAACTAA	TGCTGTTGACAGTGAGCGCTAGTTCAACTGT ATAGTTTTATAGTGAAGCCACAGATGTATAA AACTATACAGTTGAACTAATGCCTACTGCCT CGGA
RASA1	RASA1.3593	TAAAACTATACAGTTGAACTAA	TGCTGTTGACAGTGAGCGCTAGTTCAACTGT ATAGTTTTATAGTGAAGCCACAGATGTATAA AACTATACAGTTGAACTAATGCCTACTGCCT CGGA
RASA2	RASA2.1380	TTGTATTGAATAACTTGTCTAC	TGCTGTTGACAGTGAGCGATAGACAAGTTAT TCAATACAATAGTGAAGCCACAGATGTATTG TATTGAATAACTTGTCTACTGCCTACTGCCT CGGA
RASA2	RASA2.1380	TTGTATTGAATAACTTGTCTAC	TGCTGTTGACAGTGAGCGATAGACAAGTTAT TCAATACAATAGTGAAGCCACAGATGTATTG TATTGAATAACTTGTCTACTGCCTACTGCCT CGGA
RASA2	RASA2.1884	TTGTTAAGCAGAACCATCGTTT	TGCTGTTGACAGTGAGCGCAACGATGGTTCT GCTTAACAATAGTGAAGCCACAGATGTATTG TTAAGCAGAACCATCGTTTTGCCTACTGCCT CGGA
RASA2	RASA2.1884	TTGTTAAGCAGAACCATCGTTT	TGCTGTTGACAGTGAGCGCAACGATGGTTCT GCTTAACAATAGTGAAGCCACAGATGTATTG TTAAGCAGAACCATCGTTTTGCCTACTGCCT CGGA
RASA2	RASA2.760	TTGTTCCACAAGTCGATCCTGA	TGCTGTTGACAGTGAGCGCCAGGATCGACTT GTGGAACAATAGTGAAGCCACAGATGTATT GTTCCACAAGTCGATCCTGATGCCTACTGCC TCGGA
RASA2	RASA2.760	TTGTTCCACAAGTCGATCCTGA	TGCTGTTGACAGTGAGCGCCAGGATCGACTT GTGGAACAATAGTGAAGCCACAGATGTATT GTTCCACAAGTCGATCCTGATGCCTACTGCC TCGGA
RASA2	RASA2.449	TTCAAGGTGAACTTTACCCTGA	TGCTGTTGACAGTGAGCGCCAGGGTAAAGT TCACCTTGAATAGTGAAGCCACAGATGTATT CAAGGTGAACTTTACCCTGATGCCTACTGCC TCGGA
RASA2	RASA2.449	TTCAAGGTGAACTTTACCCTGA	TGCTGTTGACAGTGAGCGCCAGGGTAAAGT TCACCTTGAATAGTGAAGCCACAGATGTATT CAAGGTGAACTTTACCCTGATGCCTACTGCC TCGGA
RASA2	RASA2.2057	TTCTACACAGTTATTTGCCTGG	TGCTGTTGACAGTGAGCGACAGGCAAATAA CTGTGTAGAATAGTGAAGCCACAGATGTATT CTACACAGTTATTTGCCTGGTGCCTACTGCC TCGGA
RASA2	RASA2.2057	TTCTACACAGTTATTTGCCTGG	TGCTGTTGACAGTGAGCGACAGGCAAATAA CTGTGTAGAATAGTGAAGCCACAGATGTATT CTACACAGTTATTTGCCTGGTGCCTACTGCC TCGGA
RASA3	RASA3.2532	TATTTCGTCTTCTTGAACTTGT	TGCTGTTGACAGTGAGCGCCAAGTTCAAGA AGACGAAATATAGTGAAGCCACAGATGTAT ATTTCGTCTTCTTGAACTTGTTGCCTACTGC CTCGGA
RASA3	RASA3.3525	TTACTTTGTATCAAAGAGCTAA	TGCTGTTGACAGTGAGCGCTAGCTCTTTGAT ACAAAGTAATAGTGAAGCCACAGATGTATTA

			CTTTGTATCAAAGAGCTAATGCCTACTGCCTCGGA
RASA3	RASA3.276	TTTTCCACAATTTTGGTCCTGA	TGCTGTTGACAGTGAGCGCCAGGACCAAAATTGTGGAAAATAGTGAAGCCACAGATGTATTTTCCACAATTTTGGTCCTGATGCCTACTGCCTCGGA
RASA3	RASA3.4009	TTTGTGACAAGAAAGTTCCTAT	TGCTGTTGACAGTGAGCGCTAGGAACTTTCTTGTCACAAATAGTGAAGCCACAGATGTATTTGTGACAAGAAAGTTCCTATTGCCTACTGCCTCGGA
RASA3	RASA3.707	TAAAACACTTCATCGAACTGGG	TGCTGTTGACAGTGAGCGACCAGTTCGATGAAGTGTTTTATAGTGAAGCCACAGATGTATAAAACACTTCATCGAACTGGGTGCCTACTGCCTCGGA
RASA4	RASA4.4988	TTAATAATTCCAATCATCCTAT	TGCTGTTGACAGTGAGCGCTAGGATGATTGGAATTATTAATAGTGAAGCCACAGATGTATTAATAATTCCAATCATCCTATTGCCTACTGCCTCGGA
RASA4	RASA4.4126	TTTCGTGATCTCTTCTTCCCTT	TGCTGTTGACAGTGAGCGCAGGGAAGAAGAGATCACGAAATAGTGAAGCCACAGATGTATTTCGTGATCTCTTCTTCCCTTTGCCTACTGCCTCGGA
RASA4	RASA4.4422	TAAAAATACAAGAATTAGCTGG	TGCTGTTGACAGTGAGCGACAGCTAATTCTTGTATTTTTATAGTGAAGCCACAGATGTATAAAAATACAAGAATTAGCTGGTGCCTACTGCCTCGGA
RASA4	RASA4.3049	TTTGAGGAGAGAACAGCTGGTT	TGCTGTTGACAGTGAGCGCACCAGCTGTTCTCTCCTCAAATAGTGAAGCCACAGATGTATTTGAGGAGAGAACAGCTGGTTTGCCTACTGCCTCGGA
RASA4	RASA4.3459	TCAAGTTTTGCCAACCATCGGA	TGCTGTTGACAGTGAGCGCCCGATGGTTGGCAAAACTTGATAGTGAAGCCACAGATGTATCAAGTTTTGCCAACCATCGGATGCCTACTGCCTCGGA
RASAL1	RASAL1.3203	TTCTAGCAGACATTCTAGCGGG	TGCTGTTGACAGTGAGCGACCGCTAGAATGTCTGCTAGAATAGTGAAGCCACAGATGTATTCTAGCAGACATTCTAGCGGGTGCCTACTGCCTCGGA
RASAL1	RASAL1.3203	TTCTAGCAGACATTCTAGCGGG	TGCTGTTGACAGTGAGCGACCGCTAGAATGTCTGCTAGAATAGTGAAGCCACAGATGTATTCTAGCAGACATTCTAGCGGGTGCCTACTGCCTCGGA
RASAL1	RASAL1.3202	TCTAGCAGACATTCTAGCGGGT	TGCTGTTGACAGTGAGCGCCCCGCTAGAATGTCTGCTAGATAGTGAAGCCACAGATGTATCTAGCAGACATTCTAGCGGGTTGCCTACTGCCTCGGA
RASAL1	RASAL1.3202	TCTAGCAGACATTCTAGCGGGT	TGCTGTTGACAGTGAGCGCCCCGCTAGAATGTCTGCTAGATAGTGAAGCCACAGATGTATCTAGCAGACATTCTAGCGGGTTGCCTACTGCCTCGGA
RASAL1	RASAL1.3144	TTCTTGAACTACCTCATTGGAA	TGCTGTTGACAGTGAGCGCTCCAATGAGGTAGTTCAAGAATAGTGAAGCCACAGATGTATTCTTGAACTACCTCATTGGAATGCCTACTGCCTCGGA
RASAL1	RASAL1.3144	TTCTTGAACTACCTCATTGGAA	TGCTGTTGACAGTGAGCGCTCCAATGAGGTAGTTCAAGAATAGTGAAGCCACAGATGTATTCTTGAACTACCTCATTGGAATGCCTACTGCCTCGGA
RASAL1	RASAL1.2886	TTAGCAGACATGAAAACAGGAA	TGCTGTTGACAGTGAGCGCTCCTGTTTTCATGTCTGCTAATAGTGAAGCCACAGATGTATTAGCAGACATGAAAACAGGAATGCCTACTGCCTCGGA
RASAL1	RASAL1.2886	TTAGCAGACATGAAAACAGGAA	TGCTGTTGACAGTGAGCGCTCCTGTTTTCATGTCTGCTAATAGTGAAGCCACAGATGTATTA

			GCAGACATGAAAACAGGAATGCCTACTGCC TCGGA
RASAL1	RASAL1.1181	TAAACTGTTCCATCGACTTGGA	TGCTGTTGACAGTGAGCGCCCAAGTCGATG GAACAGTTTATAGTGAAGCCACAGATGTATA AACTGTTCCATCGACTTGGATGCCTACTGCC TCGGA
RASAL1	RASAL1.1181	TAAACTGTTCCATCGACTTGGA	TGCTGTTGACAGTGAGCGCCCAAGTCGATG GAACAGTTTATAGTGAAGCCACAGATGTATA AACTGTTCCATCGACTTGGATGCCTACTGCC TCGGA
RASAL2	RASAL2.9009	TATAGTAGCAACTTTAGTCTGA	TGCTGTTGACAGTGAGCGCCAGACTAAAGTT GCTACTATATAGTGAAGCCACAGATGTATAT AGTAGCAACTTTAGTCTGATGCCTACTGCCT CGGA
RASAL2	RASAL2.9009	TATAGTAGCAACTTTAGTCTGA	TGCTGTTGACAGTGAGCGCCAGACTAAAGTT GCTACTATATAGTGAAGCCACAGATGTATAT AGTAGCAACTTTAGTCTGATGCCTACTGCCT CGGA
RASAL2	RASAL2.6025	TAACTTAACATTTAACATCTAT	TGCTGTTGACAGTGAGCGCTAGATGTTAAAT GTTAAGTTATAGTGAAGCCACAGATGTATAA CTTAACATTTAACATCTATTGCCTACTGCCT CGGA
RASAL2	RASAL2.6025	TAACTTAACATTTAACATCTAT	TGCTGTTGACAGTGAGCGCTAGATGTTAAAT GTTAAGTTATAGTGAAGCCACAGATGTATAA CTTAACATTTAACATCTATTGCCTACTGCCT CGGA
RASAL2	RASAL2.3477	TTGTGAAGTAGCAACATTCTGT	TGCTGTTGACAGTGAGCGCCAGAATGTTGCT ACTTCACAATAGTGAAGCCACAGATGTATTG TGAAGTAGCAACATTCTGTTGCCTACTGCCT CGGA
RASAL2	RASAL2.3477	TTGTGAAGTAGCAACATTCTGT	TGCTGTTGACAGTGAGCGCCAGAATGTTGCT ACTTCACAATAGTGAAGCCACAGATGTATTG TGAAGTAGCAACATTCTGTTGCCTACTGCCT CGGA
RASAL2	RASAL2.8696	TATCATTGTAAAATAGTCGTGT	TGCTGTTGACAGTGAGCGCCACGACTATTTT ACAATGATATAGTGAAGCCACAGATGTATAT CATTGTAAAATAGTCGTGTTGCCTACTGCCT CGGA
RASAL2	RASAL2.8696	TATCATTGTAAAATAGTCGTGT	TGCTGTTGACAGTGAGCGCCACGACTATTTT ACAATGATATAGTGAAGCCACAGATGTATAT CATTGTAAAATAGTCGTGTTGCCTACTGCCT CGGA
RASAL2	RASAL2.459	TTAGGTTGAACTGTCCTGCGAA	TGCTGTTGACAGTGAGCGCTCGCAGGACAG TTCAACCTAATAGTGAAGCCACAGATGTATT AGGTTGAACTGTCCTGCGAATGCCTACTGCC TCGGA
RASAL2	RASAL2.459	TTAGGTTGAACTGTCCTGCGAA	TGCTGTTGACAGTGAGCGCTCGCAGGACAG TTCAACCTAATAGTGAAGCCACAGATGTATT AGGTTGAACTGTCCTGCGAATGCCTACTGCC TCGGA
RASGRF1	RASGRF1.2658	TACATTACTATATTCCTGCTAG	TGCTGTTGACAGTGAGCGATAGCAGGAATAT AGTAATGTATAGTGAAGCCACAGATGTATAC ATTACTATATTCCTGCTAGTGCCTACTGCCT CGGA
RASGRF1	RASGRF1.3029	TATGGTGTCCTTGACACTCTGG	TGCTGTTGACAGTGAGCGACAGAGTGTCAA GGACACCATATAGTGAAGCCACAGATGTAT ATGGTGTCCTTGACACTCTGGTGCCTACTGC CTCGGA
RASGRF1	RASGRF1.1738	TACAGTATCATCTAGCACATGT	TGCTGTTGACAGTGAGCGCCATGTGCTAGAT GATACTGTATAGTGAAGCCACAGATGTATAC AGTATCATCTAGCACATGTTGCCTACTGCCT CGGA
RASGRF1	RASGRF1.2342	TAATCCTAGAGCAAGGAGCGAC	TGCTGTTGACAGTGAGCGATCGCTCCTTGCT CTAGGATTATAGTGAAGCCACAGATGTATAA

			TCCTAGAGCAAGGAGCGACTGCCTACTGCC TCGGA
RASGRF 1	RASGRF1.277 1	TTGTCTGTCTGTTGTAGTGGAG	TGCTGTTGACAGTGAGCGATCCACTACAACA GACAGACAATAGTGAAGCCACAGATGTATT GTCTGTCTGTTGTAGTGGAGTGCCTACTGCC TCGGA
RBM14	RBM14.1421	TTTAGCTATCATGTCTTCCTGG	TGCTGTTGACAGTGAGCGACAGGAAGACAT GATAGCTAAATAGTGAAGCCACAGATGTATT TAGCTATCATGTCTTCCTGGTGCCTACTGCC TCGGA
RBM14	RBM14.3781	TAAATCTAGACATAAAACCCAG	TGCTGTTGACAGTGAGCGATGGGTTTTATGT CTAGATTTATAGTGAAGCCACAGATGTATAA ATCTAGACATAAAACCCAGTGCCTACTGCCT CGGA
RBM14	RBM14.1281	TTTTCTAACACCACCTACTTGG	TGCTGTTGACAGTGAGCGACAAGTAGGTGG TGTTAGAAAATAGTGAAGCCACAGATGTATT TTCTAACACCACCTACTTGGTGCCTACTGCC TCGGA
RBM14	RBM14.1437	TTAGCTATCATGTCTTCCTGGA	TGCTGTTGACAGTGAGCGCCCAGGAAGACA TGATAGCTAATAGTGAAGCCACAGATGTATT AGCTATCATGTCTTCCTGGATGCCTACTGCC TCGGA
RBM14	RBM14.1332	TTGTAGTCCATACAAAAGGGAA	TGCTGTTGACAGTGAGCGCTCCCTTTTGTAT GGACTACAATAGTGAAGCCACAGATGTATTG TAGTCCATACAAAAGGGAATGCCTACTGCCT CGGA
RNF138	RNF138.759	TTACATTAGTGAAACATCTTTT	TGCTGTTGACAGTGAGCGCAAAGATGTTTCA CTAATGTAATAGTGAAGCCACAGATGTATTA CATTAGTGAAACATCTTTTTGCCTACTGCCT CGGA
RNF138	RNF138.2339	TAACTTGACATATTGGATGTAT	TGCTGTTGACAGTGAGCGCTACATCCAATAT GTCAAGTTATAGTGAAGCCACAGATGTATAA CTTGACATATTGGATGTATTGCCTACTGCCT CGGA
RNF138	RNF138.2861	TACATCTCAAATAAGACTCTGT	TGCTGTTGACAGTGAGCGCCAGAGTCTTATT TGAGATGTATAGTGAAGCCACAGATGTATAC ATCTCAAATAAGACTCTGTTGCCTACTGCCT CGGA
RNF138	RNF138.481	TTGGGTTTCTTCATCTAGCTGA	TGCTGTTGACAGTGAGCGCCAGCTAGATGA AGAAACCCAATAGTGAAGCCACAGATGTATT GGGTTTCTTCATCTAGCTGATGCCTACTGCC TCGGA
RNF138	RNF138.2166	TAAAATGACAGAACAAAGGCGT	TGCTGTTGACAGTGAGCGCCGCCTTTGTTCT GTCATTTTATAGTGAAGCCACAGATGTATAA AATGACAGAACAAAGGCGTTGCCTACTGCC TCGGA
RUVBL1	RUVBL1.487	TTCACCTTCATAAACTTCCTTG	TGCTGTTGACAGTGAGCGAAAGGAAGTTTAT GAAGGTGAATAGTGAAGCCACAGATGTATT CACCTTCATAAACTTCCTTGTGCCTACTGCC TCGGA
RUVBL1	RUVBL1.907	TTTGTCTGTGATTTCTGTCTTC	TGCTGTTGACAGTGAGCGAAAGACAGAAAT CACAGACAAATAGTGAAGCCACAGATGTATT TGTCTGTGATTTCTGTCTTCTGCCTACTGCC TCGGA
RUVBL1	RUVBL1.1673	TTATAGAAAACACACCAGGTAA	TGCTGTTGACAGTGAGCGCTACCTGGTGTGT TTTCTATAATAGTGAAGCCACAGATGTATTA TAGAAAACACACCAGGTAATGCCTACTGCCT CGGA
RUVBL1	RUVBL1.989	TCAACAAACAGCACACCCGGGA	TGCTGTTGACAGTGAGCGCCCCGGGTGTGC TGTTTGTTGATAGTGAAGCCACAGATGTATC AACAAACAGCACACCCGGGATGCCTACTGC CTCGGA
RUVBL1	RUVBL1.1338	TTTAGCAAGCAAGTTGGCCGGG	TGCTGTTGACAGTGAGCGACCGGCCAACTT GCTTGCTAAATAGTGAAGCCACAGATGTATT

			TAGCAAGCAAGTTGGCCGGGTGCCTACTGC CTCGGA
SFPQ	SFPQ.2323	TATTAGGTCAATAAACTGCTAA	TGCTGTTGACAGTGAGCGCTAGCAGTTTATT GACCTAATATAGTGAAGCCACAGATGTATAT TAGGTCAATAAACTGCTAATGCCTACTGCCT CGGA
SFPQ	SFPQ.1022	TAGTCTTTTGAATTCATCCTCC	TGCTGTTGACAGTGAGCGAGAGGATGAATT CAAAAGACTATAGTGAAGCCACAGATGTATA GTCTTTTGAATTCATCCTCCTGCCTACTGCC TCGGA
SFPQ	SFPQ.1062	TTGTTGATAAAAACTTCTCCTG	TGCTGTTGACAGTGAGCGAAGGAGAAGTTTT TATCAACAATAGTGAAGCCACAGATGTATTG TTGATAAAAACTTCTCCTGTGCCTACTGCCT CGGA
SFPQ	SFPQ.1734	TTGTGAAGTTCTTCCATGCGTC	TGCTGTTGACAGTGAGCGAACGCATGGAAG AACTTCACAATAGTGAAGCCACAGATGTATT GTGAAGTTCTTCCATGCGTCTGCCTACTGCC TCGGA
SFPQ	SFPQ.1059	TTGATAAAAACTTCTCCTGGTT	TGCTGTTGACAGTGAGCGCACCAGGAGAAG TTTTTATCAATAGTGAAGCCACAGATGTATT GATAAAAACTTCTCCTGGTTTGCCTACTGCC TCGGA
SKI	SKI.3286	TTGACTGCTCTATAAATCGGTA	TGCTGTTGACAGTGAGCGCACCGATTTATAG AGCAGTCAATAGTGAAGCCACAGATGTATTG ACTGCTCTATAAATCGGTATGCCTACTGCCT CGGA
SKI	SKI.4039	TTGCATAACAAAACCGACCCTT	TGCTGTTGACAGTGAGCGCAGGGTCGGTTTT GTTATGCAATAGTGAAGCCACAGATGTATTG CATAACAAAACCGACCCTTTGCCTACTGCCT CGGA
SKI	SKI.5673	TTATTGTACAATGTCATCTGTT	TGCTGTTGACAGTGAGCGCACAGATGACATT GTACAATAATAGTGAAGCCACAGATGTATTA TTGTACAATGTCATCTGTTTGCCTACTGCCT CGGA
SKI	SKI.4968	TACATGTATAATACAACGGTGA	TGCTGTTGACAGTGAGCGCCACCGTTGTATT ATACATGTATAGTGAAGCCACAGATGTATAC ATGTATAATACAACGGTGATGCCTACTGCCT CGGA
SKI	SKI.5667	TACAATGTCATCTGTTTCGGGG	TGCTGTTGACAGTGAGCGACCCGAAACAGA TGACATTGTATAGTGAAGCCACAGATGTATA CAATGTCATCTGTTTCGGGGTGCCTACTGCC TCGGA
SMAD6	SMAD6.865	TACATTGTAAAAATGACTCCAT	TGCTGTTGACAGTGAGCGCTGGAGTCATTTT TACAATGTATAGTGAAGCCACAGATGTATAC ATTGTAAAAATGACTCCATTGCCTACTGCCT CGGA
SMAD6	SMAD6.941	TATTGAAAGAATTATAAGCCAA	TGCTGTTGACAGTGAGCGCTGGCTTATAATT CTTTCAATATAGTGAAGCCACAGATGTATAT TGAAAGAATTATAAGCCAATGCCTACTGCCT CGGA
SMAD6	SMAD6.82	TTTCAGTGTAAGACAATGTGGA	TGCTGTTGACAGTGAGCGCCCACATTGTCTT ACACTGAAATAGTGAAGCCACAGATGTATTT CAGTGTAAGACAATGTGGATGCCTACTGCCT CGGA
SMAD6	SMAD6.81	TTCAGTGTAAGACAATGTGGAA	TGCTGTTGACAGTGAGCGCTCCACATTGTCT TACACTGAATAGTGAAGCCACAGATGTATTC AGTGTAAGACAATGTGGAATGCCTACTGCCT CGGA
SMAD6	SMAD6.1061	TATCTCAAAAACCATACACCAA	TGCTGTTGACAGTGAGCGCTGGTGTATGGTT TTTGAGATATAGTGAAGCCACAGATGTATAT CTCAAAAACCATACACCAATGCCTACTGCCT CGGA
SMAD7	SMAD7.390	TTGTGTACCAACAGCGTCCTGG	TGCTGTTGACAGTGAGCGACAGGACGCTGT TGGTACACAATAGTGAAGCCACAGATGTATT

			GTGTACCAACAGCGTCCTGGTGCCTACTGCC TCGGA
SMAD7	SMAD7.1703	TTGAGCTAAGAACAGTGTCGAA	TGCTGTTGACAGTGAGCGCTCGACACTGTTC TTAGCTCAATAGTGAAGCCACAGATGTATTG AGCTAAGAACAGTGTCGAATGCCTACTGCCT CGGA
SMAD7	SMAD7.1953	TTCTTGTTTATACACATTGCAC	TGCTGTTGACAGTGAGCGATGCAATGTGTAT AAACAAGAATAGTGAAGCCACAGATGTATTC TTGTTTATACACATTGCACTGCCTACTGCCT CGGA
SMAD7	SMAD7.2099	TTTAATGGAACATAAACTCCTT	TGCTGTTGACAGTGAGCGCAGGAGTTTATGT TCCATTAAATAGTGAAGCCACAGATGTATTT AATGGAACATAAACTCCTTTGCCTACTGCCT CGGA
SMAD7	SMAD7.239	TTGTTGTCCGAATTGAGCTGTC	TGCTGTTGACAGTGAGCGAACAGCTCAATTC GGACAACAATAGTGAAGCCACAGATGTATT GTTGTCCGAATTGAGCTGTCTGCCTACTGCC TCGGA
SMC3	SMC3.1337	TTTCTTGTCATTAATAGCCTGA	TGCTGTTGACAGTGAGCGCCAGGCTATTAAT GACAAGAAATAGTGAAGCCACAGATGTATTT CTTGTCATTAATAGCCTGATGCCTACTGCCT CGGA
SMC3	SMC3.1442	TTTGACTTCATTAAGATCCTGG	TGCTGTTGACAGTGAGCGACAGGATCTTAAT GAAGTCAAATAGTGAAGCCACAGATGTATTT GACTTCATTAAGATCCTGGTGCCTACTGCCT CGGA
SMC3	SMC3.860	TTCTCCACTAGTCTCTCGCTTA	TGCTGTTGACAGTGAGCGCAAGCGAGAGAC TAGTGGAGAATAGTGAAGCCACAGATGTATT CTCCACTAGTCTCTCGCTTATGCCTACTGCC TCGGA
SMC3	SMC3.905	TTTATCTCTTGCATCCTGCTGA	TGCTGTTGACAGTGAGCGCCAGCAGGATGC AAGAGATAAATAGTGAAGCCACAGATGTATT TATCTCTTGCATCCTGCTGATGCCTACTGCC TCGGA
SMC3	SMC3.3106	TAACTTTTCTTTCTGCTCGGAG	TGCTGTTGACAGTGAGCGATCCGAGCAGAA AGAAAAGTTATAGTGAAGCCACAGATGTATA ACTTTTCTTTCTGCTCGGAGTGCCTACTGCC TCGGA
SMURF2	SMURF2.1967	TAAACTGTTGTGAAGATCCGGA	TGCTGTTGACAGTGAGCGCCCGGATCTTCAC AACAGTTTATAGTGAAGCCACAGATGTATAA ACTGTTGTGAAGATCCGGATGCCTACTGCCT CGGA
SMURF2	SMURF2.1494	TTTCTGAACCAGGTCTCGCTTG	TGCTGTTGACAGTGAGCGAAAGCGAGACCT GGTTCAGAAATAGTGAAGCCACAGATGTATT TCTGAACCAGGTCTCGCTTGTGCCTACTGCC TCGGA
SMURF2	SMURF2.3699	TTTAGAGCAAAATTCTTCCTTT	TGCTGTTGACAGTGAGCGCAAGGAAGAATTT TGCTCTAAATAGTGAAGCCACAGATGTATTT AGAGCAAAATTCTTCCTTTTGCCTACTGCCT CGGA
SMURF2	SMURF2.3622	TTAATGGAAACTTACACTGTAG	TGCTGTTGACAGTGAGCGATACAGTGTAAGT TTCCATTAATAGTGAAGCCACAGATGTATTA ATGGAAACTTACACTGTAGTGCCTACTGCCT CGGA
SMURF2	SMURF2.633	TTTCTTATGGATCTTCTTGTGA	TGCTGTTGACAGTGAGCGCCACAAGAAGAT CCATAAGAAATAGTGAAGCCACAGATGTATT TCTTATGGATCTTCTTGTGATGCCTACTGCC TCGGA
SNRPB	SNRPB.928	TAAAAGGACTATGTACAGCCTT	TGCTGTTGACAGTGAGCGCAGGCTGTACATA GTCCTTTTATAGTGAAGCCACAGATGTATAA AAGGACTATGTACAGCCTTTGCCTACTGCCT CGGA
SNRPB	SNRPB.20	TAGAAACCTACTTCCGGTCCAG	TGCTGTTGACAGTGAGCGATGGACCGGAAG TAGGTTTCTATAGTGAAGCCACAGATGTATA

			GAAACCTACTTCCGGTCCAGTGCCTACTGCC TCGGA
SNRPB	SNRPB.391	TCTACTGTCATTGAGACCAGAT	TGCTGTTGACAGTGAGCGCTCTGGTCTCAAT GACAGTAGATAGTGAAGCCACAGATGTATCT ACTGTCATTGAGACCAGATTGCCTACTGCCT CGGA
SNRPB	SNRPB.292	TTTCTGAACTCATCACAGTCAC	TGCTGTTGACAGTGAGCGATGACTGTGATGA GTTCAGAAATAGTGAAGCCACAGATGTATTT CTGAACTCATCACAGTCACTGCCTACTGCCT CGGA
SNRPB	SNRPB.329	TTCCCTTTCTGCTTGTTTGGAG	TGCTGTTGACAGTGAGCGATCCAAACAAGC AGAAAGGGAATAGTGAAGCCACAGATGTAT TCCCTTTCTGCTTGTTTGGAGTGCCTACTGC CTCGGA
SNRPD1	SNRPD1.1118	TATATTGTTAAGTTTAGCCTAA	TGCTGTTGACAGTGAGCGCTAGGCTAAACTT AACAATATATAGTGAAGCCACAGATGTATAT ATTGTTAAGTTTAGCCTAATGCCTACTGCCT CGGA
SNRPD1	SNRPD1.1049	TAGAACTGTAGCCTAACTGGAC	TGCTGTTGACAGTGAGCGATCCAGTTAGGCT ACAGTTCTATAGTGAAGCCACAGATGTATAG AACTGTAGCCTAACTGGACTGCCTACTGCCT CGGA
SNRPD1	SNRPD1.582	TAAATAGACAGCTCTGTCCCAC	TGCTGTTGACAGTGAGCGATGGGACAGAGC TGTCTATTTATAGTGAAGCCACAGATGTATA AATAGACAGCTCTGTCCCACTGCCTACTGCC TCGGA
SNRPD1	SNRPD1.1061	TTTCTCAGTACATAGAACTGTA	TGCTGTTGACAGTGAGCGCACAGTTCTATGT ACTGAGAAATAGTGAAGCCACAGATGTATTT CTCAGTACATAGAACTGTATGCCTACTGCCT CGGA
SNRPD1	SNRPD1.1469	TAACTGATAATCTAGTGACCAT	TGCTGTTGACAGTGAGCGCTGGTCACTAGAT TATCAGTTATAGTGAAGCCACAGATGTATAA CTGATAATCTAGTGACCATTGCCTACTGCCT CGGA
SOWAHC	SOWAHC.2451	TTAATGTACCTTAACACTGGTG	TGCTGTTGACAGTGAGCGAACCAGTGTTAAG GTACATTAATAGTGAAGCCACAGATGTATTA ATGTACCTTAACACTGGTGTGCCTACTGCCT CGGA
SOWAHC	SOWAHC.3222	TTAGGTTTCAGCAACTACGCGA	TGCTGTTGACAGTGAGCGCCGCGTAGTTGCT GAAACCTAATAGTGAAGCCACAGATGTATTA GGTTTCAGCAACTACGCGATGCCTACTGCCT CGGA
SPRED1	SPRED1.5564	TTCAACACAAGAAATATCCTTA	TGCTGTTGACAGTGAGCGCAAGGATATTTCT TGTGTTGAATAGTGAAGCCACAGATGTATTC AACACAAGAAATATCCTTATGCCTACTGCCT CGGA
SPRED1	SPRED1.5123	TAAAATACCAAAACTTAGCTGG	TGCTGTTGACAGTGAGCGACAGCTAAGTTTT GGTATTTTATAGTGAAGCCACAGATGTATAA AATACCAAAACTTAGCTGGTGCCTACTGCCT CGGA
SPRED1	SPRED1.1060	TATTCTGACAATCTCATCCTCA	TGCTGTTGACAGTGAGCGCGAGGATGAGAT TGTCAGAATATAGTGAAGCCACAGATGTATA TTCTGACAATCTCATCCTCATGCCTACTGCC TCGGA
SPRED1	SPRED1.6831	TATTACTGTCCTAATAACCTTT	TGCTGTTGACAGTGAGCGCAAGGTTATTAGG ACAGTAATATAGTGAAGCCACAGATGTATAT TACTGTCCTAATAACCTTTTGCCTACTGCCT CGGA
SPRED1	SPRED1.5651	TACACTTGCTTAATGCACCTTT	TGCTGTTGACAGTGAGCGCAAGGTGCATTAA GCAAGTGTATAGTGAAGCCACAGATGTATAC ACTTGCTTAATGCACCTTTTGCCTACTGCCT CGGA
SPRED2	SPRED2.418	TAGAAGAACTGTCTGTAGCTGT	TGCTGTTGACAGTGAGCGCCAGCTACAGAC AGTTCTTCTATAGTGAAGCCACAGATGTATA

			GAAGAACTGTCTGTAGCTGTTGCCTACTGCC TCGGA
SPRED2	SPRED2.1853	TAAAGATAGAAACTGCAGCTTA	TGCTGTTGACAGTGAGCGCAAGCTGCAGTTT CTATCTTTATAGTGAAGCCACAGATGTATAA AGATAGAAACTGCAGCTTATGCCTACTGCCT CGGA
SPRED2	SPRED2.2948	TAATCTACTAAAGAAAATCGAT	TGCTGTTGACAGTGAGCGCTCGATTTTCTTT AGTAGATTATAGTGAAGCCACAGATGTATAA TCTACTAAAGAAAATCGATTGCCTACTGCCT CGGA
SPRED2	SPRED2.1588	TTGCAGACTCCTTTGAACTGGA	TGCTGTTGACAGTGAGCGCCCAGTTCAAAG GAGTCTGCAATAGTGAAGCCACAGATGTATT GCAGACTCCTTTGAACTGGATGCCTACTGCC TCGGA
SPRED2	SPRED2.1496	TAGTACAGGAGTCTGTGGCGAA	TGCTGTTGACAGTGAGCGCTCGCCACAGAC TCCTGTACTATAGTGAAGCCACAGATGTATA GTACAGGAGTCTGTGGCGAATGCCTACTGC CTCGGA
SPRY1	SPRY1.2179	TAACATATGTACTTTCTTCGTG	TGCTGTTGACAGTGAGCGAACGAAGAAAGT ACATATGTTATAGTGAAGCCACAGATGTATA ACATATGTACTTTCTTCGTGTGCCTACTGCC TCGGA
SPRY1	SPRY1.587	TTCACAAATGAACTTGTGCTGT	TGCTGTTGACAGTGAGCGCCAGCACAAGTT CATTTGTGAATAGTGAAGCCACAGATGTATT CACAAATGAACTTGTGCTGTTGCCTACTGCC TCGGA
SPRY1	SPRY1.718	TTGACTAAGCACATGCAGGTTC	TGCTGTTGACAGTGAGCGAAACCTGCATGTG CTTAGTCAATAGTGAAGCCACAGATGTATTG ACTAAGCACATGCAGGTTCTGCCTACTGCCT CGGA
SPRY1	SPRY1.311	TTATTATTCACATTAATTGGTA	TGCTGTTGACAGTGAGCGCACCAATTAATGT GAATAATAATAGTGAAGCCACAGATGTATTA TTATTCACATTAATTGGTATGCCTACTGCCT CGGA
SPRY1	SPRY1.137	TCATAGTCTAATCTCTGACGGC	TGCTGTTGACAGTGAGCGACCGTCAGAGATT AGACTATGATAGTGAAGCCACAGATGTATCA TAGTCTAATCTCTGACGGCTGCCTACTGCCT CGGA
SPRY2	SPRY2.328	TAGAACACATCTGAACTCCGTG	TGCTGTTGACAGTGAGCGAACGGAGTTCAG ATGTGTTCTATAGTGAAGCCACAGATGTATA GAACACATCTGAACTCCGTGTGCCTACTGCC TCGGA
SPRY2	SPRY2.1747	TAGTATAATATTTTGTGTCTGT	TGCTGTTGACAGTGAGCGCCAGACACAAAA TATTATACTATAGTGAAGCCACAGATGTATA GTATAATATTTTGTGTCTGTTGCCTACTGCC TCGGA
SPRY2	SPRY2.2060	TATATTGGACATATGCATCTGT	TGCTGTTGACAGTGAGCGCCAGATGCATATG TCCAATATATAGTGAAGCCACAGATGTATAT ATTGGACATATGCATCTGTTGCCTACTGCCT CGGA
SPRY2	SPRY2.1553	TTAGCTTATGCAATACATGGGT	TGCTGTTGACAGTGAGCGCCCCATGTATTGC ATAAGCTAATAGTGAAGCCACAGATGTATTA GCTTATGCAATACATGGGTTGCCTACTGCCT CGGA
SPRY2	SPRY2.329	TTAGAACACATCTGAACTCCGT	TGCTGTTGACAGTGAGCGCCGGAGTTCAGA TGTGTTCTAATAGTGAAGCCACAGATGTATT AGAACACATCTGAACTCCGTTGCCTACTGCC TCGGA
SPRY3	SPRY3.6580	TTTAACAGCAGCAACACTGGTA	TGCTGTTGACAGTGAGCGCACCAGTGTTGCT GCTGTTAAATAGTGAAGCCACAGATGTATTT AACAGCAGCAACACTGGTATGCCTACTGCCT CGGA
SPRY3	SPRY3.6604	TTCCTTATCTTGTCCATCCTGG	TGCTGTTGACAGTGAGCGACAGGATGGACA AGATAAGGAATAGTGAAGCCACAGATGTATT

			CCTTATCTTGTCCATCCTGGTGCCTACTGCC TCGGA
SPRY3	SPRY3.7990	TTGCATATTATAATCATCTGGG	TGCTGTTGACAGTGAGCGACCAGATGATTAT AATATGCAATAGTGAAGCCACAGATGTATTG CATATTATAATCATCTGGGTGCCTACTGCCT CGGA
SPRY3	SPRY3.2842	TTCTTTTCCACACTTGAGCTTC	TGCTGTTGACAGTGAGCGAAAGCTCAAGTGT GGAAAAGAATAGTGAAGCCACAGATGTATT CTTTTCCACACTTGAGCTTCTGCCTACTGCC TCGGA
SPRY3	SPRY3.7497	TTAGGTGAGAGAAACACACTGA	TGCTGTTGACAGTGAGCGCCAGTGTGTTTCT CTCACCTAATAGTGAAGCCACAGATGTATTA GGTGAGAGAAACACACTGATGCCTACTGCC TCGGA
SPRY4	SPRY4.4393	TTCAAGGTGACAGTCATCCGGG	TGCTGTTGACAGTGAGCGACCGGATGACTG TCACCTTGAATAGTGAAGCCACAGATGTATT CAAGGTGACAGTCATCCGGGTGCCTACTGC CTCGGA
SPRY4	SPRY4.2099	TAAAACACCGTTAGCATCCGGT	TGCTGTTGACAGTGAGCGCCCGGATGCTAA CGGTGTTTTATAGTGAAGCCACAGATGTATA AAACACCGTTAGCATCCGGTTGCCTACTGCC TCGGA
SPRY4	SPRY4.2909	TAAGATGTTACTACTAGTCTTC	TGCTGTTGACAGTGAGCGAAAGACTAGTAGT AACATCTTATAGTGAAGCCACAGATGTATAA GATGTTACTACTAGTCTTCTGCCTACTGCCT CGGA
SPRY4	SPRY4.4659	TTGTAACATGAAACCAAGCTGT	TGCTGTTGACAGTGAGCGCCAGCTTGGTTTC ATGTTACAATAGTGAAGCCACAGATGTATTG TAACATGAAACCAAGCTGTTGCCTACTGCCT CGGA
SPRY4	SPRY4.2067	TATAAAAACATAATGACTGGAT	TGCTGTTGACAGTGAGCGCTCCAGTCATTAT GTTTTTATATAGTGAAGCCACAGATGTATAT AAAAACATAATGACTGGATTGCCTACTGCCT CGGA
SRSF1	SRSF1.3300	TTAACATTTAATACTTACCTTT	TGCTGTTGACAGTGAGCGCAAGGTAAGTATT AAATGTTAATAGTGAAGCCACAGATGTATTA ACATTTAATACTTACCTTTTGCCTACTGCCT CGGA
SRSF1	SRSF1.4112	TAAACTTACACTAAGTACTTAG	TGCTGTTGACAGTGAGCGATAAGTACTTAGT GTAAGTTTATAGTGAAGCCACAGATGTATAA ACTTACACTAAGTACTTAGTGCCTACTGCCT CGGA
SRSF1	SRSF1.3678	TAATCTTGTGCACTCTTCCCTT	TGCTGTTGACAGTGAGCGCAGGGAAGAGTG CACAAGATTATAGTGAAGCCACAGATGTATA ATCTTGTGCACTCTTCCCTTTGCCTACTGCC TCGGA
SRSF1	SRSF1.1216	TTACACAATATCACAGTCTGAA	TGCTGTTGACAGTGAGCGCTCAGACTGTGAT ATTGTGTAATAGTGAAGCCACAGATGTATTA CACAATATCACAGTCTGAATGCCTACTGCCT CGGA
SRSF1	SRSF1.2656	TTTATCTCCAGGTCCTCGCTTT	TGCTGTTGACAGTGAGCGCAAGCGAGGACC TGGAGATAAATAGTGAAGCCACAGATGTATT TATCTCCAGGTCCTCGCTTTTGCCTACTGCC TCGGA
SRSF10	SRSF10.613	TAGTTGTAATCAAAAGACCGAC	TGCTGTTGACAGTGAGCGATCGGTCTTTTGA TTACAACTATAGTGAAGCCACAGATGTATAG TTGTAATCAAAAGACCGACTGCCTACTGCCT CGGA
SRSF10	SRSF10.371	TTGAACATAAGCAAATCCTCTT	TGCTGTTGACAGTGAGCGCAGAGGATTTGCT TATGTTCAATAGTGAAGCCACAGATGTATTG AACATAAGCAAATCCTCTTTGCCTACTGCCT CGGA
SRSF10	SRSF10.567	TTCGGCTTCTAGAACGTCTGTA	TGCTGTTGACAGTGAGCGCACAGACGTTCTA GAAGCCGAATAGTGAAGCCACAGATGTATT

			CGGCTTCTAGAACGTCTGTATGCCTACTGCC TCGGA
SRSF10	SRSF10.319	TACACATCAACTATAGGACCAT	TGCTGTTGACAGTGAGCGCTGGTCCTATAGT TGATGTGTATAGTGAAGCCACAGATGTATAC ACATCAACTATAGGACCATTGCCTACTGCCT CGGA
SRSF10	SRSF10.571	TAACTTCGGCTTCTAGAACGTC	TGCTGTTGACAGTGAGCGAACGTTCTAGAAG CCGAAGTTATAGTGAAGCCACAGATGTATAA CTTCGGCTTCTAGAACGTCTGCCTACTGCCT CGGA
SRSF2	SRSF2.1937	TTAAACTACAGAAACAATGGTT	TGCTGTTGACAGTGAGCGCACCATTGTTTCT GTAGTTTAATAGTGAAGCCACAGATGTATTA AACTACAGAAACAATGGTTTGCCTACTGCCT CGGA
SRSF2	SRSF2.1488	TTGTGTTTGATAAACAATCCTT	TGCTGTTGACAGTGAGCGCAGGATTGTTTAT CAAACACAATAGTGAAGCCACAGATGTATTG TGTTTGATAAACAATCCTTTGCCTACTGCCT CGGA
SRSF2	SRSF2.1919	TAAACTACAGAAACAATGGTTA	TGCTGTTGACAGTGAGCGCAACCATTGTTTC TGTAGTTTATAGTGAAGCCACAGATGTATAA ACTACAGAAACAATGGTTATGCCTACTGCCT CGGA
SRSF2	SRSF2.1545	TCAACTGCTACACAACTGCGCC	TGCTGTTGACAGTGAGCGAGCGCAGTTGTGT AGCAGTTGATAGTGAAGCCACAGATGTATCA ACTGCTACACAACTGCGCCTGCCTACTGCCT CGGA
SRSF2	SRSF2.1723	TTATTTATATGCAAGGCCCGGG	TGCTGTTGACAGTGAGCGACCGGGCCTTGC ATATAAATAATAGTGAAGCCACAGATGTATT ATTTATATGCAAGGCCCGGGTGCCTACTGCC TCGGA
SRSF3	SRSF3.2297	TTAACTTTAAGGCTGAACCTTC	TGCTGTTGACAGTGAGCGAAAGGTTCAGCCT TAAAGTTAATAGTGAAGCCACAGATGTATTA ACTTTAAGGCTGAACCTTCTGCCTACTGCCT CGGA
SRSF3	SRSF3.1983	TTACATTTGAACCATATTGTGA	TGCTGTTGACAGTGAGCGCCACAATATGGTT CAAATGTAATAGTGAAGCCACAGATGTATTA CATTTGAACCATATTGTGATGCCTACTGCCT CGGA
SRSF3	SRSF3.774	TTGAACAGCTAAAACATCTTAA	TGCTGTTGACAGTGAGCGCTAAGATGTTTTA GCTGTTCAATAGTGAAGCCACAGATGTATTG AACAGCTAAAACATCTTAATGCCTACTGCCT CGGA
SRSF3	SRSF3.1204	TTCTTGAAACTTAACATTCTAT	TGCTGTTGACAGTGAGCGCTAGAATGTTAAG TTTCAAGAATAGTGAAGCCACAGATGTATTC TTGAAACTTAACATTCTATTGCCTACTGCCT CGGA
SRSF3	SRSF3.941	TAGAGGTTTATTATCAGTCTGT	TGCTGTTGACAGTGAGCGCCAGACTGATAAT AAACCTCTATAGTGAAGCCACAGATGTATAG AGGTTTATTATCAGTCTGTTGCCTACTGCCT CGGA
SSRP1	SSRP1.2236	TTGCTCTTGAAGCTCTCGCTTA	TGCTGTTGACAGTGAGCGCAAGCGAGAGCT TCAAGAGCAATAGTGAAGCCACAGATGTATT GCTCTTGAAGCTCTCGCTTATGCCTACTGCC TCGGA
SSRP1	SSRP1.1950	TCTGACTTGATCTTCTCTCGGC	TGCTGTTGACAGTGAGCGACCGAGAGAAGA TCAAGTCAGATAGTGAAGCCACAGATGTATC TGACTTGATCTTCTCTCGGCTGCCTACTGCC TCGGA
SSRP1	SSRP1.2168	TTTCTTTTCCATCTTTACCTTT	TGCTGTTGACAGTGAGCGCAAGGTAAAGAT GGAAAAGAAATAGTGAAGCCACAGATGTAT TTCTTTTCCATCTTTACCTTTTGCCTACTGCC TCGGA
SSRP1	SSRP1.2149	TTTACTTTCTTCTTCTTCTTTG	TGCTGTTGACAGTGAGCGAAAAGAAGAAGA AGAAAGTAAATAGTGAAGCCACAGATGTATT

			TACTTTCTTCTTCTTCTTTGTGCCTACTGCCTCGGA
SSRP1	SSRP1.2143	TTCTTCTTCTTCTTTGACTTGT	TGCTGTTGACAGTGAGCGCCAAGTCAAAGAAGAAGAAGAATAGTGAAGCCACAGATGTATTCTTCTTCTTCTTTGACTTGTTGCCTACTGCCTCGGA
STRAP	STRAP.683	TAACAAATAATTACTATCCTGC	TGCTGTTGACAGTGAGCGACAGGATAGTAATTATTTGTTATAGTGAAGCCACAGATGTATAACAAATAATTACTATCCTGCTGCCTACTGCCTCGGA
STRAP	STRAP.1693	TAAACAGCTACAAGAACCCTAA	TGCTGTTGACAGTGAGCGCTAGGGTTCTTGTAGCTGTTTATAGTGAAGCCACAGATGTATAAACAGCTACAAGAACCCTAATGCCTACTGCCTCGGA
STRAP	STRAP.683	TTAACAAATAATTACTATCCTG	TGCTGTTGACAGTGAGCGAAGGATAGTAATTATTTGTTAATAGTGAAGCCACAGATGTATTAACAAATAATTACTATCCTGTGCCTACTGCCTCGGA
STRAP	STRAP.859	TGTCATAGTAGCATGATCCCAA	TGCTGTTGACAGTGAGCGCTGGGATCATGCTACTATGACATAGTGAAGCCACAGATGTATGTCATAGTAGCATGATCCCAATGCCTACTGCCTCGGA
STRAP	STRAP.1476	TAAGCAGACAGTAACTCTGGAA	TGCTGTTGACAGTGAGCGCTCCAGAGTTACTGTCTGCTTATAGTGAAGCCACAGATGTATAAGCAGACAGTAACTCTGGAATGCCTACTGCCTCGGA
TCERG1	TCERG1.2467	TTGATGAACTATCTACTGCTTT	TGCTGTTGACAGTGAGCGCAAGCAGTAGATAGTTCATCAATAGTGAAGCCACAGATGTATTGATGAACTATCTACTGCTTTTGCCTACTGCCTCGGA
TCERG1	TCERG1.1866	TTTATTATCGTCTCTCTTCCGT	TGCTGTTGACAGTGAGCGCCGGAAGAGAGACGATAATAAATAGTGAAGCCACAGATGTATTTATTATCGTCTCTCTTCCGTTGCCTACTGCCTCGGA
TCERG1	TCERG1.3848	TAAACAACAAGACTCGGTCTAT	TGCTGTTGACAGTGAGCGCTAGACCGAGTCTTGTTGTTTATAGTGAAGCCACAGATGTATAAACAACAAGACTCGGTCTATTGCCTACTGCCTCGGA
TCERG1	TCERG1.1882	TTATTATCGTCTCTCTTCCGTT	TGCTGTTGACAGTGAGCGCACGGAAGAGAGACGATAATAATAGTGAAGCCACAGATGTATTATTATCGTCTCTCTTCCGTTTGCCTACTGCCTCGGA
TCERG1	TCERG1.2725	TATCAGACCATGACACATCTGA	TGCTGTTGACAGTGAGCGCCAGATGTGTCATGGTCTGATATAGTGAAGCCACAGATGTATATCAGACCATGACACATCTGATGCCTACTGCCTCGGA
TCOF1	TCOF1.313	TTTCTTAGCTTGCAGTGCCGCA	TGCTGTTGACAGTGAGCGCGCGGCACTGCAAGCTAAGAAATAGTGAAGCCACAGATGTATTTCTTAGCTTGCAGTGCCGCATGCCTACTGCCTCGGA
TCOF1	TCOF1.2214	TTTACTGAGGTTTTCACCTGTG	TGCTGTTGACAGTGAGCGAACAGGTGAAAACCTCAGTAAATAGTGAAGCCACAGATGTATTTACTGAGGTTTTCACCTGTGTGCCTACTGCCTCGGA
TCOF1	TCOF1.459	TTTTCTTTCATGCTTGATGGCA	TGCTGTTGACAGTGAGCGCGCCATCAAGCATGAAAGAAAATAGTGAAGCCACAGATGTATTTTCTTTCATGCTTGATGGCATGCCTACTGCCTCGGA
TCOF1	TCOF1.458	TTTCTTTCATGCTTGATGGCAA	TGCTGTTGACAGTGAGCGCTGCCATCAAGCATGAAAGAAATAGTGAAGCCACAGATGTATTTCTTTCATGCTTGATGGCAATGCCTACTGCCTCGGA
TCOF1	TCOF1.312	TTCTTAGCTTGCAGTGCCGCAT	TGCTGTTGACAGTGAGCGCTGCGGCACTGCAAGCTAAGAATAGTGAAGCCACAGATGTATT

			CTTAGCTTGCAGTGCCGCATTGCCTACTGCC TCGGA
TFAM	TFAM.455	TATCTCTTCTTTATATACCTGC	TGCTGTTGACAGTGAGCGACAGGTATATAAA GAAGAGATATAGTGAAGCCACAGATGTATAT CTCTTCTTTATATACCTGCTGCCTACTGCCT CGGA
TFAM	TFAM.2312	TTCTAAAACAAGAACATCTGAA	TGCTGTTGACAGTGAGCGCTCAGATGTTCTT GTTTTAGAATAGTGAAGCCACAGATGTATTC TAAAACAAGAACATCTGAATGCCTACTGCCT CGGA
TFAM	TFAM.465	TAAATCTGCTTATCTCTTCTTT	TGCTGTTGACAGTGAGCGCAAGAAGAGATA AGCAGATTTATAGTGAAGCCACAGATGTATA AATCTGCTTATCTCTTCTTTTGCCTACTGCC TCGGA
TFAM	TFAM.674	TTCCTTTACAGTCTTCAGCTTT	TGCTGTTGACAGTGAGCGCAAGCTGAAGAC TGTAAAGGAATAGTGAAGCCACAGATGTATT CCTTTACAGTCTTCAGCTTTTGCCTACTGCC TCGGA
TFAM	TFAM.3304	TTAAGTATAAAATAATACGGGT	TGCTGTTGACAGTGAGCGCCCCGTATTATTT TATACTTAATAGTGAAGCCACAGATGTATTA AGTATAAAATAATACGGGTTGCCTACTGCCT CGGA
TFDP1	TFDP1.1542	TAGCTTACCAATATCTTCTTGG	TGCTGTTGACAGTGAGCGACAAGAAGATATT GGTAAGCTATAGTGAAGCCACAGATGTATA GCTTACCAATATCTTCTTGGTGCCTACTGCC TCGGA
TFDP1	TFDP1.865	TTGAAGTTGAGACTGTTTCTGT	TGCTGTTGACAGTGAGCGCCAGAAACAGTC TCAACTTCAATAGTGAAGCCACAGATGTATT GAAGTTGAGACTGTTTCTGTTGCCTACTGCC TCGGA
TFDP1	TFDP1.2514	TTCAATAAAAAGACTATCGTTT	TGCTGTTGACAGTGAGCGCAACGATAGTCTT TTTATTGAATAGTGAAGCCACAGATGTATTC AATAAAAAGACTATCGTTTTGCCTACTGCCT CGGA
TFDP1	TFDP1.841	TATTCTTTCAAGTCTCCTCTGT	TGCTGTTGACAGTGAGCGCCAGAGGAGACT TGAAAGAATATAGTGAAGCCACAGATGTATA TTCTTTCAAGTCTCCTCTGTTGCCTACTGCC TCGGA
TFDP1	TFDP1.2064	TTTGTTGCTGCAAAACAGGGAG	TGCTGTTGACAGTGAGCGATCCCTGTTTTGC AGCAACAAATAGTGAAGCCACAGATGTATTT GTTGCTGCAAAACAGGGAGTGCCTACTGCC TCGGA
TGIF1	TGIF1.787	TTAAGCTGTAAGTTTTGCCTGA	TGCTGTTGACAGTGAGCGCCAGGCAAAACT TACAGCTTAATAGTGAAGCCACAGATGTATT AAGCTGTAAGTTTTGCCTGATGCCTACTGCC TCGGA
TGIF1	TGIF1.962	TTTAAGTTTATAGTTCTTGGAA	TGCTGTTGACAGTGAGCGCTCCAAGAACTAT AAACTTAAATAGTGAAGCCACAGATGTATTT AAGTTTATAGTTCTTGGAATGCCTACTGCCT CGGA
TGIF1	TGIF1.954	TATAGTTCTTGGAATGACTGTA	TGCTGTTGACAGTGAGCGCACAGTCATTCCA AGAACTATATAGTGAAGCCACAGATGTATAT AGTTCTTGGAATGACTGTATGCCTACTGCCT CGGA
TGIF1	TGIF1.199	TAGACAGGTGTGTTTGCTGGGA	TGCTGTTGACAGTGAGCGCCCCAGCAAACA CACCTGTCTATAGTGAAGCCACAGATGTATA GACAGGTGTGTTTGCTGGGATGCCTACTGCC TCGGA
TGIF1	TGIF1.510	TTTCAATGCAGTCACAGTGGTA	TGCTGTTGACAGTGAGCGCACCACTGTGACT GCATTGAAATAGTGAAGCCACAGATGTATTT CAATGCAGTCACAGTGGTATGCCTACTGCCT CGGA
TIMELESS	TIMELESS.4012	TAAATCTCCAGAGAGCTGCTGG	TGCTGTTGACAGTGAGCGACAGCAGCTCTCT GGAGATTTATAGTGAAGCCACAGATGTATAA

			ATCTCCAGAGAGCTGCTGGTGCCTACTGCCT CGGA
TIMELESS	TIMELESS.4984	TTGCAGTATTTATCCATCCTTT	TGCTGTTGACAGTGAGCGCAAGGATGGATA AATACTGCAATAGTGAAGCCACAGATGTATT GCAGTATTTATCCATCCTTTTGCCTACTGCC TCGGA
TIMELESS	TIMELESS.939	TTTTCTGCCATCTCTCGCTGGC	TGCTGTTGACAGTGAGCGACCAGCGAGAGA TGGCAGAAAATAGTGAAGCCACAGATGTATT TTCTGCCATCTCTCGCTGGCTGCCTACTGCC TCGGA
TIMELESS	TIMELESS.1233	TTTACTGATCCCATGAGCCGGT	TGCTGTTGACAGTGAGCGCCCGGCTCATGG GATCAGTAAATAGTGAAGCCACAGATGTATT TACTGATCCCATGAGCCGGTTGCCTACTGCC TCGGA
TIMELESS	TIMELESS.2900	TATTCTTCATGATATGACCCAG	TGCTGTTGACAGTGAGCGATGGGTCATATCA TGAAGAATATAGTGAAGCCACAGATGTATAT TCTTCATGATATGACCCAGTGCCTACTGCCT CGGA
TOP2B	TOP2B.232	TACATCTTCATCATACACCCAC	TGCTGTTGACAGTGAGCGATGGGTGTATGAT GAAGATGTATAGTGAAGCCACAGATGTATAC ATCTTCATCATACACCCACTGCCTACTGCCT CGGA
TOP2B	TOP2B.849	TAAAGATCTACATAACTGCGAA	TGCTGTTGACAGTGAGCGCTCGCAGTTATGT AGATCTTTATAGTGAAGCCACAGATGTATAA AGATCTACATAACTGCGAATGCCTACTGCCT CGGA
TOP2B	TOP2B.1679	TTTTATGTGAGAACCATCTTGA	TGCTGTTGACAGTGAGCGCCAAGATGGTTCT CACATAAAATAGTGAAGCCACAGATGTATTT TATGTGAGAACCATCTTGATGCCTACTGCCT CGGA
TOP2B	TOP2B.4436	TTTACTTGGAACTTTATCTGTC	TGCTGTTGACAGTGAGCGAACAGATAAAGTT CCAAGTAAATAGTGAAGCCACAGATGTATTT ACTTGGAACTTTATCTGTCTGCCTACTGCCT CGGA
TOP2B	TOP2B.2861	TAGCATAGGTTCTAAAACCTGT	TGCTGTTGACAGTGAGCGCCAGGTTTTAGAA CCTATGCTATAGTGAAGCCACAGATGTATAG CATAGGTTCTAAAACCTGTTGCCTACTGCCT CGGA
TRIP13	TRIP13.858	TTTATCATCAATCAAATCCTGA	TGCTGTTGACAGTGAGCGCCAGGATTTGATT GATGATAAATAGTGAAGCCACAGATGTATTT ATCATCAATCAAATCCTGATGCCTACTGCCT CGGA
TRIP13	TRIP13.264	TAGCTTTCTAACACTCAGGTTT	TGCTGTTGACAGTGAGCGCAACCTGAGTGTT AGAAAGCTATAGTGAAGCCACAGATGTATA GCTTTCTAACACTCAGGTTTTGCCTACTGCC TCGGA
TRIP13	TRIP13.839	TGAATCTTCTGAAACATCTTGG	TGCTGTTGACAGTGAGCGACAAGATGTTTCA GAAGATTCATAGTGAAGCCACAGATGTATGA ATCTTCTGAAACATCTTGGTGCCTACTGCCT CGGA
TRIP13	TRIP13.989	TTTAATCTGATCAATTTGGGTC	TGCTGTTGACAGTGAGCGAACCCAAATTGAT CAGATTAAATAGTGAAGCCACAGATGTATTT AATCTGATCAATTTGGGTCTGCCTACTGCCT CGGA
TRIP13	TRIP13.241	TTTATGTCTTCTTTCTTTGCAG	TGCTGTTGACAGTGAGCGATGCAAAGAAAG AAGACATAAATAGTGAAGCCACAGATGTATT TATGTCTTCTTTCTTTGCAGTGCCTACTGCC TCGGA
WBP11	WBP11.2579	TAATTGTACATATTCTTCCCAC	TGCTGTTGACAGTGAGCGATGGGAAGAATA TGTACAATTATAGTGAAGCCACAGATGTATA ATTGTACATATTCTTCCCACTGCCTACTGCC TCGGA
WBP11	WBP11.846	TAACATGTCTTCATCTCGCCTA	TGCTGTTGACAGTGAGCGCAGGCGAGATGA AGACATGTTATAGTGAAGCCACAGATGTATA

			ACATGTCTTCATCTCGCCTATGCCTACTGCC TCGGA
WBP11	WBP11.236	TTCTTTAATTCTCTCTTCCGGG	TGCTGTTGACAGTGAGCGACCGGAAGAGAG AATTAAAGAATAGTGAAGCCACAGATGTATT CTTTAATTCTCTCTTCCGGGTGCCTACTGCC TCGGA
WBP11	WBP11.2271	TTCAATAACTGATCTATTCTGG	TGCTGTTGACAGTGAGCGACAGAATAGATC AGTTATTGAATAGTGAAGCCACAGATGTATT CAATAACTGATCTATTCTGGTGCCTACTGCC TCGGA
WBP11	WBP11.1135	TTGAAGAGGAGTCAGTTCCTTC	TGCTGTTGACAGTGAGCGAAAGGAACTGAC TCCTCTTCAATAGTGAAGCCACAGATGTATT GAAGAGGAGTCAGTTCCTTCTGCCTACTGCC TCGGA
WHSC1	WHSC1.1087	TTGAGGGTTGAGATGAAGCTGG	TGCTGTTGACAGTGAGCGACAGCTTCATCTC AACCCTCAATAGTGAAGCCACAGATGTATTG AGGGTTGAGATGAAGCTGGTGCCTACTGCC TCGGA
WHSC1	WHSC1.767	TTAAGTTTGGTATAGCTGTGAA	TGCTGTTGACAGTGAGCGCTCACAGCTATAC CAAACTTAATAGTGAAGCCACAGATGTATTA AGTTTGGTATAGCTGTGAATGCCTACTGCCT CGGA
WHSC1	WHSC1.67	TTATGCACTTTACAACACTCTG	TGCTGTTGACAGTGAGCGAAGAGTGTTGTAA AGTGCATAATAGTGAAGCCACAGATGTATTA TGCACTTTACAACACTCTGTGCCTACTGCCT CGGA
WHSC1	WHSC1.777	TTTCTGACCTTTAAGTTTGGTA	TGCTGTTGACAGTGAGCGCACCAAACTTAAA GGTCAGAAATAGTGAAGCCACAGATGTATTT CTGACCTTTAAGTTTGGTATGCCTACTGCCT CGGA
WHSC1	WHSC1.279	TTCTCCATTAAACACCCGGGAA	TGCTGTTGACAGTGAGCGCTCCCGGGTGTTT AATGGAGAATAGTGAAGCCACAGATGTATTC TCCATTAAACACCCGGGAATGCCTACTGCCT CGGA
XRCC6	XRCC6.842	TTGAGCTTCAGCTTTAACCTGC	TGCTGTTGACAGTGAGCGACAGGTTAAAGCT GAAGCTCAATAGTGAAGCCACAGATGTATTG AGCTTCAGCTTTAACCTGCTGCCTACTGCCT CGGA
XRCC6	XRCC6.1682	TTTCTCTTGGTAACTTTCCCTT	TGCTGTTGACAGTGAGCGCAGGGAAAGTTA CCAAGAGAAATAGTGAAGCCACAGATGTAT TTCTCTTGGTAACTTTCCCTTTGCCTACTGC CTCGGA
XRCC6	XRCC6.480	TGAGTGAGTAGTCAGATCCGTG	TGCTGTTGACAGTGAGCGAACGGATCTGACT ACTCACTCATAGTGAAGCCACAGATGTATGA GTGAGTAGTCAGATCCGTGTGCCTACTGCCT CGGA
XRCC6	XRCC6.828	TTAACCTGCTGAGTGCTCGCTT	TGCTGTTGACAGTGAGCGCAGCGAGCACTC AGCAGGTTAATAGTGAAGCCACAGATGTATT AACCTGCTGAGTGCTCGCTTTGCCTACTGCC TCGGA
XRCC6	XRCC6.270	TACTGATGTACACACTTTGGAT	TGCTGTTGACAGTGAGCGCTCCAAAGTGTGT ACATCAGTATAGTGAAGCCACAGATGTATAC TGATGTACACACTTTGGATTGCCTACTGCCT CGGA
ZNF207	ZNF207.1823	TAAGCTTACAGAACTTGCCTTT	TGCTGTTGACAGTGAGCGCAAGGCAAGTTCT GTAAGCTTATAGTGAAGCCACAGATGTATAA GCTTACAGAACTTGCCTTTTGCCTACTGCCT CGGA
ZNF207	ZNF207.1051	TTGTACTAGTTGTTGAAGCTGT	TGCTGTTGACAGTGAGCGCCAGCTTCAACAA CTAGTACAATAGTGAAGCCACAGATGTATTG TACTAGTTGTTGAAGCTGTTGCCTACTGCCT CGGA
ZNF207	ZNF207.318	TATTGTTTCTTTATGTACCTGC	TGCTGTTGACAGTGAGCGACAGGTACATAA AGAAACAATATAGTGAAGCCACAGATGTATA

			TTGTTTCTTTATGTACCTGCTGCCTACTGCCTCGGA
ZNF207	ZNF207.1042	TTGTTGAAGCTGTAGACTGTGT	TGCTGTTGACAGTGAGCGCCACAGTCTACAGCTTCAACAATAGTGAAGCCACAGATGTATTGTTGAAGCTGTAGACTGTGTTGCCTACTGCCTCGGA
ZNF207	ZNF207.257	TTTCTTGTGACATATATGGCAT	TGCTGTTGACAGTGAGCGCTGCCATATATGTCACAAGAAATAGTGAAGCCACAGATGTATTTCTTGTGACATATATGGCATTGCCTACTGCCTCGGA

Table A 2: Table of all screened shRNAs and their respective abundance after 14 and 21 days with or without KRAS^{G12V}. Values indicate the log_2 fold change of shRNA abundance after massive parallel sequencing compared to the control sample. (blue = depletion; red = enrichment; n.a. = not available)

	14 days		21 days		
shRNA	**+KRAS^{G12V}**	**-KRAS^{G12V}**	**+KRAS^{G12V}**	**-KRAS^{G12V}**	**shRNA library pre-transduction**
AATF.1150	0.226	0.475	0.224	0.067	0.15
AATF.1152	0.388	0.0319	0.621	0.0264	0.0852
AATF.1223	-0.701	-0.171	-1.28	-0.785	-0.0732
AATF.1732	-0.994	-0.114	-0.791	0.583	0.000896
AATF.968	0.232	0.389	0.0751	0.123	0.0206
ANKRD57.2246	-0.619	-0.203	-0.714	-0.229	-0.0732
ANKRD57.2974	-0.183	-0.312	-0.0894	-0.522	0.436
ANKRD57.3667	0.0606	0.463	-0.564	-0.128	-0.394
AREG.460	0.375	0.686	-0.66	0.135	0.455
AREG.517	-0.0539	-0.0704	-0.241	-0.335	-0.0823
AREG.677	0.131	-0.0251	0.0594	-0.408	0.427
AREG.850	0.424	-0.144	0.753	-0.188	-0.207
AREG.868	-0.178	-1.77	-0.805	-1.48	-0.336
ARNTL2.1018	0.066	0.0505	0.216	-0.168	0.00292
ARNTL2.111	0.276	-0.344	0.383	0.317	-0.593
ARNTL2.2192	-0.447	0.174	-0.536	0.142	-0.527
ARNTL2.3342	0.219	-0.0256	-0.001	-0.0198	-0.268
ARNTL2.674	-0.185	0.212	-0.48	-0.183	-0.466
ATAD2.1342	0.458	-0.406	0.19	-0.225	-0.00205
ATAD2.1599	0.232	0.322	0.531	0.651	-0.182
ATAD2.3499	-0.432	-1.02	-0.929	-1.36	-0.0609
ATAD2.4380	0.249	0.356	0.18	0.17	0.335
ATAD2.569	-0.598	-0.466	-0.571	-0.402	-0.00413
BARD1.1647	-0.346	-0.166	-1.46	0.722	0.356
BARD1.1690	0.222	-0.327	-0.0201	0.193	0.251
BARD1.543	n.a.	n.a.	-0.917	0.754	0.144
BARD1.548	1.26	n.a.	0.868	n.a.	1.64
BARD1.582	0.363	0.0779	-0.257	0.131	0.303
BAZ1A.1434	-0.0826	0.000422	0.214	-0.531	-0.467
BAZ1A.4218	0.604	0.031	0.227	0.136	-0.0858
BAZ1A.4264	0.0116	-0.436	0.00433	0.593	-0.405
BAZ1A.5297	0.102	-0.115	-0.0887	-0.818	0.267
BAZ1A.5651	0.359	-0.0661	0.0158	0.0747	0.163
BAZ1B.2041	-0.15	0.206	0.016	0.492	0.0413
BAZ1B.2230	0.227	-0.314	-0.00934	-0.175	-0.235

BAZ1B.3381	-0.456	0.0329	-0.451	-0.0821	0.272
BAZ1B.3695	-0.228	0.118	-0.373	-0.659	-0.193
BAZ1B.5150	-0.323	0.108	-0.42	-0.109	0.123
BRCA1.1108	0.0988	0.233	-0.174	0.702	0.0873
BRCA1.190	0.502	-0.146	0.412	0.187	0.353
BRCA1.2561	0.234	0.0768	0.266	-0.494	-0.037
BRCA1.37	-0.872	-0.241	0.0793	-0.00707	-0.0614
BRCA1.656	-0.258	-0.153	-0.396	-0.31	-0.172
CBFB.2451	0.0201	-0.792	0.768	-0.746	0.00253
CBFB.2457	0.69	-0.143	0.894	-0.341	-0.0581
CBFB.3057	-0.403	-0.313	0.0876	0.186	-0.343
CBFB.507	0.0893	-0.0212	0.859	-0.111	-0.143
CBFB.665	0.367	0.0303	0.0406	0.556	-0.333
CBX3.1081	-0.859	-0.205	-0.273	0.15	0.202
CBX3.1278	-0.198	-0.162	-0.42	-0.134	-0.213
CBX3.1941	-0.0129	-0.247	0.217	-0.0306	-0.158
CBX3.560	-0.405	0.212	-0.845	0.124	0.0591
CBX3.628	-0.324	-0.271	-0.815	-0.333	-0.149
CHAF1A.1374	0.56	0.13	0.0381	0.547	0.0547
CHAF1A.1387	0.248	0.484	0.32	-0.0841	-0.0612
CHAF1A.182	-0.828	-0.00399	-0.491	0.273	0.123
CHAF1A.3031	-0.873	-0.884	-0.198	-3.1	-0.446
CHAF1A.3082	-0.524	-0.0135	-0.0331	-0.52	-0.461
CTNNBL1.1495	-0.31	0.89	-1.63	1.38	0.0403
CTNNBL1.1653	-0.4	-0.991	0.499	-1.46	-0.714
CTNNBL1.1828	0.371	0.329	-0.122	0.0964	-0.276
CTNNBL1.388	-0.0258	-0.0514	0.0519	-0.159	-0.572
CTNNBL1.961	1.35	0.488	2.08	0.21	0.00168
DAB2IP.2316	0.125	-0.0503	0.519	-0.909	-0.348
DAB2IP.2670	-0.61	0.283	-0.272	0.818	-0.307
DAB2IP.411	-0.0802	-0.266	-0.969	0.678	-0.823
DAB2IP.468	-0.565	-0.555	-0.334	-0.488	-0.911
DAB2IP.957	-0.112	1.23	-0.65	1.06	-0.159
DDX54.1756	-0.3	-0.0433	0.38	0.564	0.152
DDX54.2269	-0.639	-0.229	-0.543	-0.169	0.0177
DDX54.2274	0.0659	-0.645	-0.0163	-0.727	0.377
DDX54.301	0.0779	-0.147	0.184	-0.571	0.315
DDX54.421	-0.539	-0.457	0.0965	-0.587	-0.541
DEK.2225	-0.236	0.344	0.0927	-0.366	-0.0629
DEK.398	-0.626	-0.118	-0.545	0.172	-0.16
DEK.448	-0.0645	0.0921	-0.168	-0.701	-0.441
DEK.508	0.348	0.347	0.22	0.0499	-0.0209
DEK.829	-0.117	0.388	-0.00686	0.687	0.383
DNAJC2.1157	-0.23	-0.592	0.284	-0.66	-0.375
DNAJC2.1165	0.492	0.178	0.382	-0.359	0.00444
DNAJC2.1455	0.067	-0.269	-0.147	0.0637	0.32
DNAJC2.1466	0.0944	-0.094	-0.154	0.0276	0.165
DNAJC2.429	-0.893	-0.449	-1.13	-0.468	-0.0269
DNMT1.2410	0.231	0.182	0.135	0.529	0.294
DNMT1.2839	-0.683	-0.218	-0.753	-0.243	-0.278
DNMT1.3205	-0.279	0.0502	-0.704	0.214	-0.145
DNMT1.3991	-1.1	-0.657	-0.52	-0.107	-0.31
DNMT1.884	0.141	-0.116	0.00221	-0.353	0.149
DR1.1454	0.69	1.19	1.25	1.6	0.615
DR1.1779	0.44	0.32	0.184	0.224	0.312
DR1.2574	-0.409	-0.291	-0.258	0.00295	0.0151
DR1.2938	0.168	0.14	-0.0389	0.201	0.113
DR1.766	-0.025	-0.000725	0.405	0.325	-0.074
DUSP4.1193	-0.862	-1.07	-1.64	-1.26	-0.599
DUSP4.1283	-0.81	0.19	-0.353	-0.145	-0.113
DUSP4.1545	-0.129	0.218	0.615	0.0574	0.0684
DUSP4.2934	-0.314	-0.411	0.358	-0.256	-0.0383
DUSP6.1299	-0.0155	-0.189	-0.736	0.404	-0.837
DUSP6.1330	-0.0233	0.344	-0.441	0.366	-0.128
DUSP6.1382	0.0948	-0.254	-0.111	-0.105	-0.0269

DUSP6.1902	0.102	-0.198	-0.513	-0.14	-0.0435
DUSP6.2099	0.777	0.282	1.05	0.449	0.341
EGR1.2525	0.253	0.0255	-0.102	-0.053	-0.128
EGR1.2815	0.224	0.0141	0.515	-0.797	-0.191
EGR1.2822	0.306	0.401	-0.0206	0.473	0.19
EGR1.2823	-0.0544	-0.0544	-0.114	-0.255	0.0558
EGR1.2946	-0.613	-1.36	-0.199	-0.253	-0.649
ELK1.1078	-0.0178	0.0451	0.132	0.448	0.00481
ELK1.1488	-0.559	0.0786	-0.62	0.0387	-0.548
ELK1.1708	-0.763	-0.143	-1.51	-0.13	-0.164
ELK1.408	-0.781	0.476	-0.382	0.331	-0.315
ELK1.447	-0.305	0.233	-8.09	-0.185	0.0912
ENO1.1437	0.225	0.193	0.106	-0.159	-0.568
ENO1.1440	-1.5	0.037	-1.18	0.118	-0.946
ENO1.1441	-0.0211	-0.128	-0.215	-0.79	-0.437
ENO1.261	-1.09	-2.05	-0.381	-1.21	-0.43
ENO1.681	-1.72	-0.0155	-2.15	-1.49	-0.538
EREG.1188	0.158	-0.224	-0.564	-0.583	-0.0708
EREG.1324	0.75	0.128	0.638	0.224	0.249
EREG.3002	-0.364	-0.464	0.268	-0.347	-0.255
EREG.3718	0.296	0.348	0.162	0.213	0.425
EREG.993	-0.29	0.399	-0.0705	0.614	-0.033
ESPL1.1362	-0.449	-0.179	-0.552	-0.236	-0.451
ESPL1.1771	0.345	0.425	-0.149	0.144	-0.323
ESPL1.1897	0.25	-0.0337	-0.889	-0.0308	-0.281
ESPL1.2669	-0.138	-0.336	-1.23	0.0821	-0.423
ESPL1.267	-0.315	-0.594	0.136	-0.661	-0.549
ETV4.380	-1.61	-0.562	-0.807	-1.96	-0.62
ETV4.385	-1.02	-0.707	-0.411	-0.372	0.236
ETV4.686	-0.0526	0.0198	-0.544	0.391	-0.0841
ETV4.806	-0.0838	0.97	1.35	0.862	-0.446
ETV4.816	0.558	0.518	0.344	0.18	0.169
ETV5.2130	0.5	-0.0407	0.42	-0.633	-0.212
ETV5.2355	-0.333	-0.604	0.123	-0.747	-0.0562
ETV5.3085	-0.714	-0.507	-1.04	0.153	-0.47
ETV5.3563	0.124	-0.291	0.32	0.0614	0.0228
ETV5.390	-1.27	-1.55	-1.45	-1.28	-0.452
EZH2.1100	0.704	-0.0898	0.0284	-0.492	-0.0177
EZH2.1112	-0.261	0.282	0.153	0.00835	0.146
EZH2.1700	-0.4	-0.295	-0.405	-0.432	-0.0952
EZH2.292	0.321	0.0269	0.297	-0.372	0.105
EZH2.578	-0.216	0.315	-0.0669	0.372	0.0628
FOS.1690	0.34	0.0147	0.184	-0.245	0.352
FOS.1804	0.655	-0.0715	0.498	0.00816	0.16
FOS.1894	-0.407	0.0884	-0.647	0.269	0.197
FOS.2115	0.128	0.153	0.222	-0.504	0.349
FOS.703	0.765	0.415	1.31	-0.0119	-0.549
FOSL1.1280	0.00899	-0.187	-0.334	0.231	-0.042
FOSL1.1405	-0.415	0.0132	-0.949	0.355	-0.189
FOSL1.1634	0.188	0.264	0.796	1.02	0.183
FOSL1.90	-0.138	0.535	0.0878	-0.53	0.108
FOSL1.91	-0.297	0.274	-0.39	0.587	0.106
FOXM1.1277	-0.425	-0.933	-0.737	-1.71	-0.403
FOXM1.1812	0.0653	0.476	0.385	0.22	-0.0828
FOXM1.2496	-0.849	-0.186	-0.665	-0.389	-0.468
FOXM1.463	-0.472	-0.615	0.04	-0.441	0.0231
FOXM1.725	-0.8	-0.392	-0.474	-1.06	-0.298
FUBP1.1846	0.0676	0.209	-0.194	-0.109	0.142
FUBP1.1932	0.273	0.429	-0.125	0.148	-0.439
FUBP1.236	n.a.	n.a.	n.a.	n.a.	n.a.
FUBP1.2714	-0.164	0.297	-0.902	0.0172	-0.423
FUBP1.521	-0.0598	-0.0598	0.243	0.069	-0.148
FUS.1028	0.131	0.135	-0.42	0.597	0.139
FUS.1050	0.142	-0.326	-0.167	-0.916	0.288
FUS.212	0.156	-0.521	0.312	0.436	-0.222

FUS.2807	-0.438	-0.971	-0.547	-1.14	-0.524
FUS.960	-0.606	0.0117	-0.403	0.0855	-0.205
HMGA1.1061	0.00397	-0.212	0.668	-0.201	0.0622
HMGA1.1391	-2.22	-0.985	-0.57	-0.835	-1.29
HMGA1.155	n.a.	n.a.	n.a.	n.a.	n.a.
HMGA1.211	0.0693	0.117	0.032	0.196	-0.562
HMGA1.40	0.0619	-0.0113	0.716	-0.0214	0.188
HMGB1.1534	-0.0584	-0.268	0.198	0.0379	0.287
HMGB1.1726	0.472	0.844	-0.0148	0.751	-0.167
HMGB1.2309	0.116	0.484	-0.496	0.396	0.113
HMGB1.2683	-0.753	-0.189	-0.72	-0.475	0.257
HMGB1.2936	-0.731	0.107	-0.427	-0.288	-0.22
HMGB2.102	-0.897	-0.0749	-1.55	-1.3	-0.714
HMGB2.1295	0.687	0.383	0.7	0.53	0.222
HMGB2.635	0.264	-0.0549	0.15	0.235	0.165
HMGB2.849	0.112	0.501	1.29	0.749	-0.105
HMGB2.952	0.322	-0.197	0.6	0.345	0.269
HMGB3.1249	0.347	-0.295	0.613	-1.06	-0.0948
HMGB3.1909	-0.00944	0.707	-0.47	0.529	-0.421
HMGB3.2264	0.1	0.113	0.704	0.0173	0.176
HMGB3.2531	0.233	1.37	0.698	0.819	0.33
HMGB3.628	-0.616	-0.13	-0.892	0.0718	-0.241
HNRNPAB.1243	0.468	0.297	0.874	0.196	0.254
HNRNPAB.1575	-0.0302	-0.0597	-0.0245	-0.0542	0.0366
HNRNPAB.608	-0.89	-0.092	-0.271	-0.391	-0.243
HNRNPAB.829	-0.411	-0.494	-0.048	-0.531	0.176
HNRNPD.1060	0.471	0.0227	-0.274	0.46	0.0601
HNRNPD.1275	-0.161	-0.421	0.19	0.144	0.0468
HNRNPD.2045	0.507	0.184	-0.338	0.405	0.21
HNRNPD.774	-0.235	0.356	0.0472	-0.0322	-0.0599
HNRNPD.988	0.267	0.564	0.194	0.507	0.316
HNRNPR.1892	-0.0762	0.243	0.283	-0.0343	0.000676
HNRNPR.1919	-0.216	0.391	-0.247	0.348	-0.172
HNRNPR.2400	0.095	0.32	0.339	0.639	0.152
HNRNPR.510	-1.17	-0.251	-0.527	-1.33	-0.527
HNRNPR.777	0.171	0.21	0.329	0.0708	0.554
IL17RD.1052	0.179	0.215	0.145	0.0349	-0.0103
IL17RD.4714	-0.316	-0.825	0.632	-0.129	-0.361
IL17RD.493	-0.000402	-0.384	-0.0237	0.453	-0.223
IL17RD.5166	-0.517	-0.0783	-1.59	-0.207	-0.299
IL17RD.660	0.485	0.0212	0.0321	0.000448	-0.438
ILF2.1584	0.0956	-0.336	0.348	-0.153	-0.301
ILF2.1851	0.492	-2.15	-0.489	-2.29	-0.0742
ILF2.45	-1.06	-0.67	-1.6	-0.205	-0.64
ILF2.527	0.756	-0.161	0.612	-0.32	-0.252
ILF2.785	-0.568	-0.354	-0.231	-0.0845	-0.167
ILF3.1480	0.0201	0.292	-0.24	0.0445	0.316
ILF3.2024	0.51	0.219	1.15	0.225	-0.156
ILF3.299	-0.0203	0.422	-0.0316	0.481	0.27
ILF3.534	0.0336	0.271	-0.0244	0.199	-0.295
ILF3.724	0.056	0.00336	-0.107	-0.409	-0.483
IQGAP1.3207	0.322	-0.0673	-0.277	-0.307	0.303
IQGAP1.4793	-0.238	0.2	0.173	-0.26	0.136
IQGAP1.5499	-0.333	0.459	0.25	0.895	0.226
IQGAP1.622	-0.3	0.0521	-0.0295	0.511	-0.256
IQGAP1.7193	-0.443	-1.14	-0.404	-0.942	-0.434
JUNB.1241	0.226	-0.462	0.0315	-0.775	-0.172
JUNB.1535	-0.181	-0.18	0.199	-0.107	-0.0863
JUNB.273	-0.0734	0.0629	-0.0228	-0.00325	-0.631
JUNB.308	-0.591	-0.565	-1.08	-0.93	-0.462
JUNB.363	-0.262	0.138	-0.318	0.358	-0.51
KLF10.1084	-3.08	-1.61	-2.71	-2.04	-1.15
KLF10.1350	-0.28	-0.29	0.307	-0.219	0.0541
KLF10.1413	-0.98	-0.704	-0.761	-1.16	-0.582
KLF10.1822	-0.00357	-0.741	0.249	-0.694	-0.395

KLF10.622	-0.47	-0.0528	-0.282	0.0768	0.186
LRRFIP1.259	0.213	0.155	-0.107	0.0903	0.339
LRRFIP1.262	-0.0116	0.0419	-0.0613	0.336	0.343
LRRFIP1.445	-0.569	-0.482	-0.627	-0.536	-0.273
LRRFIP1.592	-0.692	-0.216	-0.476	-0.477	-0.33
LRRFIP1.595	-0.104	-0.873	0.128	-0.454	0.176
MAFF.1993	0.0277	-0.0627	-0.263	0.164	0.017
MAFF.2	0.396	1.01	1.81	n.a.	0.376
MAFF.708	-0.585	0.0734	-0.998	-1.04	-0.462
MAFF.839	-0.0663	-0.535	-0.799	0.0485	-0.193
MAFF.970	1.1	1.37	1.24	0.712	0.861
MAPK1.1121	0.312	-0.541	-0.337	-0.548	-0.0632
MAPK1.1233	-0.0432	-0.552	-0.249	-0.344	-0.356
MAPK1.1316	0.114	0.138	0.112	0.0349	0.1
MAPK1.528	-0.283	-0.338	0.338	0.0855	-0.56
MAPK1.537	-0.00725	0.308	-0.347	0.595	0.268
MAPK3.1200	0.537	-0.13	-0.0771	-0.554	-0.489
MAPK3.1741	-0.0882	-0.77	0.289	-0.263	0.47
MAPK3.616	0.583	0.294	0.222	0.136	-0.525
MAPK3.751	0.18	-0.743	-0.693	-0.12	-0.215
MAPK3.912	-0.81	-0.399	-0.643	-0.471	-0.292
MCM2.1017	-0.189	0.15	0.444	0.178	-0.203
MCM2.1302	0.244	-0.362	-0.943	0.258	-0.0612
MCM2.1397	-0.168	-0.979	-0.415	0.081	-0.205
MCM2.1427	-1.14	-0.134	0.153	0.0458	-0.143
MCM2.715	-0.377	-0.185	0.161	-1.05	-0.116
MCM3.246	-1.33	-0.625	0.192	-0.944	-0.804
MCM3.2977	0.344	0.26	0.281	-0.0215	-0.204
MCM3.3080	-1.14	-0.328	-0.437	-0.24	-0.0924
MCM3.957	-0.177	-0.36	-0.438	-0.224	0.255
MCM3.958	0.112	0.406	0.34	0.286	0.329
MCM4.1641	0.0144	-0.46	-1.48	-0.647	-0.0547
MCM4.216	-0.566	-0.586	-0.158	-0.427	-0.302
MCM4.217	0.0334	-0.673	-0.236	-1.27	-0.0176
MCM4.3163	-0.138	-0.307	-0.505	-0.157	-0.586
MCM4.86	0.459	-0.271	0.28	-0.52	-0.194
MCM5.1636	0.26	-0.0601	-0.143	-0.677	0.0603
MCM5.240	0.194	-0.0636	1	-0.341	-0.165
MCM5.2528	-0.0343	0.79	0.176	0.952	-0.22
MCM5.2529	0.624	0.503	1.23	1.51	-0.318
MCM5.343	-0.659	-3.57	0.648	-3.45	-1.91
MCM6.1479	-0.201	-0.145	-0.999	0.215	-0.206
MCM6.2096	-0.0123	-0.489	0.31	-0.939	-0.368
MCM6.2172	-0.332	-0.296	-0.352	-0.253	0.135
MCM6.2798	-0.294	-0.331	0.542	-0.15	-0.382
MCM6.2807	-0.303	0.37	-0.483	-0.172	-0.036
MCM7.1879	-1.07	0.219	-1.41	0.0575	0.0033
MCM7.60	0.32	0.606	0.0715	-0.312	0.22
MCM7.674	-0.0164	-0.3	-0.308	-0.248	0.0635
MCM7.8	0.42	0.143	0.313	-0.523	-0.078
MCM7.897	-0.469	-0.0828	-0.0407	-0.198	-0.163
MED8.2	n.a.	n.a.	n.a.	n.a.	n.a.
MED8.222	0.852	0.194	1.33	0.0639	-0.221
MED8.405	-0.296	0.272	-0.11	-0.0826	0.00297
MED8.474	-0.0875	-0.381	-1.75	-1.77	-0.219
MED8.561	-1.07	0.168	-1.13	0.655	-0.286
MYBL2.1535	0.586	-1.4	0.00922	-0.891	-0.456
MYBL2.1874	-0.392	-0.491	-0.234	-0.296	-0.232
MYBL2.2073	-0.485	-0.0732	-0.289	0.0479	-0.337
MYBL2.2234	0.331	-0.515	-0.675	-1.04	-0.417
MYBL2.875	-1.27	-1.12	-0.367	-1.27	-0.814
NAP1L4.2472	0.575	-0.399	0.317	-0.177	0.253
NAP1L4.362	-1	-0.665	-1.5	-0.245	-0.0507
NAP1L4.740	0.33	-0.389	0.403	0.139	-0.392
NAP1L4.885	0.148	0.395	0.135	0.15	-0.589

NAP1L4.909	0.00591	0.4	-0.104	0.25	-0.154
NF1.1361	-0.153	-0.589	-1.46	0.624	0.0412
NF1.1588	2.98	0.757	2.5	0.784	1.14
NF1.1785	-0.238	0.226	-0.484	-0.829	-0.0802
NF1.561	0.108	-0.119	0.812	-0.0635	-0.48
NF1.898	0.0669	0.138	0.251	0.00658	0.294
NFE2L3.1541	0.307	-0.214	0.625	-0.716	0.361
NFE2L3.1962	0.453	0.389	0.308	0.839	0.162
NFE2L3.350	-0.206	0.0351	-0.188	0.32	-0.0801
NFE2L3.3599	-0.241	0.5	0.0387	0.174	-0.00575
NFE2L3.943	-0.425	-0.753	-1.04	-0.25	0.0327
NFKB1.1378	-0.0514	-0.146	-0.335	-0.288	0.149
NFKB1.2367	0.146	0.67	1.61	-0.0531	0.247
NFKB1.2920	0.21	-0.287	-0.71	0.124	-0.0427
NFKB1.2926	0.228	0.782	0.389	0.202	0.00236
NFKB1.3703	-0.00817	-0.0647	-0.142	-0.074	0.0921
PA2G4.1492	-0.641	-0.00866	-0.726	-0.655	-0.288
PA2G4.1809	0.0831	-0.67	0.661	0.117	0.102
PA2G4.1812	0.438	-0.0881	0.273	-0.0877	0.184
PA2G4.706	0.0289	0.384	0.378	0.253	0.112
PA2G4.994	-0.0193	-0.625	0.166	-1.73	-0.128
PHTF2.269	-0.583	0.354	-0.123	-0.0404	-0.304
PHTF2.323	-0.472	-0.188	-1.04	-1.28	-0.375
PHTF2.714	1.22	n.a.	3.51	n.a.	0.236
PHTF2.808	0.448	0.896	0.526	0.459	0.123
PHTF2.993	-0.435	0.372	-0.0717	0.0598	-0.142
PMEPA1.2011	-0.146	0.00471	-0.0797	-0.106	0.129
PMEPA1.2873	-0.235	-0.554	-0.678	-1.19	0.139
PMEPA1.3541	0.165	0.206	0.271	0.203	-0.165
PMEPA1.4018	0.189	-0.301	0.162	0.155	0.172
PMEPA1.4210	-0.286	-0.0959	-0.307	0.0393	-0.326
PML.105	0.283	0.217	0.211	-0.139	0.0419
PML.109	0.125	0.124	0.698	-1.39	-0.395
PML.111	-0.118	-0.167	0.167	-0.503	-0.0406
PML.1148	-0.193	-0.751	-0.998	-0.611	-0.537
PML.1271	-0.223	-0.558	-0.543	-0.0676	-0.466
PNN.1071	0.104	0.0103	-0.0511	0.135	0.39
PNN.2847	0.0194	-0.0442	-0.886	-0.298	0.371
PNN.2904	0.299	-0.134	0.222	-0.0703	0.219
PNN.400	-0.913	-1.13	0.851	-1.07	-0.713
PNN.401	-0.102	0.405	-0.12	0.567	-0.167
POLR1E.1199	-0.315	-0.565	-0.293	0.0709	-0.287
POLR1E.1264	-0.0238	-0.0916	-0.101	-0.403	-0.0224
POLR1E.467	0.368	0.934	-0.488	-0.14	-0.515
POLR1E.501	-0.48	-0.161	-0.228	-0.746	-0.0659
POLR1E.815	-0.581	-0.233	-0.376	-0.415	-0.0263
POLR2F.112	0.326	-0.65	0.503	-2.45	-0.336
POLR2F.1300	-0.61	-0.284	-0.759	0.453	0.044
POLR2F.1305	-0.518	-1.23	-0.951	-1.39	0.00903
POLR2F.1308	0.0413	-0.194	0.0779	-0.868	-0.211
POLR2F.181	-0.331	-0.118	-0.845	-0.539	-0.157
POLR3K.151	-0.327	-0.205	-0.267	0.058	-0.544
POLR3K.166	0.397	0.357	0.555	0.728	-0.237
POLR3K.313	0.000943	-0.0479	0.0584	-0.385	-0.594
POLR3K.676	-0.809	-0.145	-0.391	-0.403	0.34
POLR3K.726	0.0258	0.0767	-0.133	-0.155	0.398
PPP1R15A.1494	-0.801	0.169	-1.03	0.593	-0.091
PPP1R15A.2344	-0.216	0.348	0.000941	0.0223	0.258
PPP1R15A.49	-0.108	0.0641	-0.0458	-0.333	-0.29
PPP1R15A.963	0.122	-0.0326	-0.156	0.172	-0.0876
PPP1R15A.964	0.0256	0.0679	-0.0437	-0.159	-0.24
PPP2R5A.183	-3.62	1.04	-0.6	0.918	-0.414
PPP2R5A.49	-0.257	0.0102	-0.399	0.116	-0.258
PPP2R5A.694	-0.0119	-0.171	-0.387	0.336	-0.0845
PPP2R5A.730	0.096	0.195	-0.505	-0.0951	0.0212

PPP2R5A.96	-0.279	0.305	-0.678	-0.13	0.0867
PPP2R5B.1178	-0.256	0.148	0.128	0.0935	-0.221
PPP2R5B.1181	0.296	0.433	-0.0671	0.0338	0.253
PPP2R5B.1342	0.617	0.473	n.a.	n.a.	n.a.
PPP2R5B.1879	0.349	-0.381	-0.405	-1.58	-0.241
PPP2R5B.2733	0.208	-0.135	-0.0369	-0.11	0.219
PPP2R5C.1159	-0.0393	0.0271	0.216	0.223	-0.075
PPP2R5C.118	0.364	0.0847	1.05	-0.677	-0.198
PPP2R5C.1208	-0.0997	-0.574	-0.778	-0.448	0.259
PPP2R5C.362	-0.206	-0.649	-0.921	-1.01	-0.0903
PPP2R5C.631	0.537	-0.122	0.621	0.0111	0.031
PPP2R5E.1240	0.169	-0.301	-0.168	0.378	0.0815
PPP2R5E.1269	-0.112	0.27	0.44	0.397	-0.387
PPP2R5E.2031	-5.09	0.277	-1.66	0.552	0.344
PPP2R5E.2683	0.0289	-0.359	0.497	-0.107	0.151
PPP2R5E.679	-0.0973	-0.206	-0.0342	-0.243	-0.219
PTTG1.18	-0.686	-0.548	-0.106	-0.336	-0.709
PTTG1.236	0.506	-0.035	0.614	0.31	0.213
PTTG1.327	0.347	-0.112	-0.0327	-0.125	0.0831
PTTG1.670	-0.334	0.0894	0.652	-0.11	-0.166
PTTG1.7	-0.691	-0.339	-0.874	-0.254	-0.517
RASA1.1954	0.466	-0.124	0.349	0.253	0.439
RASA1.2153	0.0723	-0.116	-0.0372	-0.168	0.0643
RASA1.3593	-0.151	-0.0463	-0.1	0.193	0.298
RASA1.396	-1.23	-0.248	-0.461	-0.0798	-0.559
RASA1.573	-0.698	-0.129	-0.506	0.02	-0.1
RASA2.1380	0.351	0.466	0.206	0.886	0.607
RASA2.1884	0.0427	-0.101	0.126	-0.127	-0.322
RASA2.2057	0.241	0.143	0.88	-0.546	-0.068
RASA2.449	-0.0528	-0.267	0.26	-0.0456	-0.192
RASA2.760	-0.268	-0.432	-0.769	-0.321	-0.367
RASA3.2532	-0.00257	0.0672	0.4	0.0521	0.289
RASA3.276	0.323	0.342	-0.0539	0.307	-0.0661
RASA3.3525	0.0564	-0.305	-0.338	-0.403	-0.0793
RASA3.4009	-0.438	-0.35	-0.49	-0.32	-0.489
RASA3.707	0.182	-0.182	-0.00787	-0.374	-0.0776
RASA4.3049	-0.463	-1.55	-0.0716	-1.31	-0.641
RASA4.3459	-0.00874	-0.527	-0.0919	-0.663	-0.164
RASA4.4126	0.172	0.929	0.235	0.427	0.292
RASA4.4422	0.614	0.394	0.609	0.218	0.309
RASA4.4988	-0.0094	-0.424	0.216	-0.0172	0.17
RASAL1.1181	-0.681	-0.992	-0.0412	-0.116	-0.283
RASAL1.2886	-0.975	-0.562	-0.583	-1.4	-0.392
RASAL1.3144	-0.683	0.0195	-0.667	0.234	0.0188
RASAL1.3202	-0.0169	-0.133	0.0843	-0.145	-0.651
RASAL1.3203	-0.115	0.52	-0.0262	-0.36	-0.165
RASAL2.3477	-0.613	-0.401	-0.656	-0.175	-0.403
RASAL2.459	-0.222	-0.218	0.468	-0.0519	-0.167
RASAL2.6025	0.222	-0.134	-0.0391	0.0412	0.243
RASAL2.8696	-0.468	-0.344	-0.64	-0.199	-0.0108
RASAL2.9009	-0.131	0.228	-0.152	0.314	0.234
RASGRF1.1738	-0.348	-0.2	0.17	-0.364	0.0396
RASGRF1.2342	-0.519	-0.227	-0.444	0.104	-0.249
RASGRF1.2658	0.283	0.0622	0.275	0.117	0.248
RASGRF1.2771	-0.299	0.0994	-0.765	0.734	-0.314
RASGRF1.3029	-0.659	-0.216	-1.16	-0.159	-0.408
RBM14.1281	0.229	0.436	0.524	0.357	-0.33
RBM14.1332	-0.628	-0.774	-1.61	-0.601	-0.57
RBM14.1421	0.625	0.288	0.686	0.74	0.158
RBM14.1437	0.21	0.327	0.121	0.309	0.244
RBM14.3781	-0.018	0.203	-0.294	-0.129	0.0616
RNF138.2166	-0.345	0.326	0.0569	0.806	-0.13
RNF138.2339	-0.136	-0.827	0.519	-1.09	0.0968
RNF138.2861	0.061	-0.0722	1	-1.05	0.12
RNF138.481	-0.33	-0.282	-0.295	-0.91	-0.355

RNF138.759	-0.0656	0.323	0.321	0.677	0.138
RUVBL1.1338	0.331	-0.559	-0.142	-0.221	-0.741
RUVBL1.1673	-0.558	-0.846	-0.213	-0.498	-0.39
RUVBL1.487	0.00845	0.15	0.0843	0.0184	0.115
RUVBL1.907	0.729	0.0865	0.179	0.173	-0.143
RUVBL1.989	-1.17	-0.466	-0.944	-0.707	-0.293
SFPQ.1022	0.714	n.a.	n.a.	n.a.	0.801
SFPQ.1059	0.0733	0.144	0.328	0.0525	-0.128
SFPQ.1062	-0.183	-0.294	-0.477	-0.0841	0.0189
SFPQ.1734	-0.82	-0.464	-0.0801	-0.656	-0.413
SFPQ.2323	0.325	-0.281	-0.501	0.64	0.386
SKI.3286	-0.165	-0.186	0.691	0.151	-0.345
SKI.4039	-0.513	0.0654	-0.6	0.307	-0.782
SKI.4968	-0.389	-0.332	-0.377	-1.4	-0.116
SKI.5667	-0.251	-0.595	-0.471	-0.147	-0.289
SKI.5673	0.149	0.0627	-0.745	-0.184	-0.0513
SMAD6.1061	-0.376	-0.483	-0.0728	-0.213	-0.324
SMAD6.81	0.00159	0.301	-0.389	-0.221	0.169
SMAD6.82	-0.542	-0.0556	-0.357	-0.226	-0.251
SMAD6.865	-0.509	0.353	-1.01	0.425	0.415
SMAD6.941	-0.244	-0.15	0.0196	-0.176	0.145
SMAD7.1703	0.125	0.24	-0.385	0.547	-0.326
SMAD7.1953	0.426	0.621	0.588	0.394	-0.15
SMAD7.2099	0.68	0.186	0.146	0.237	-0.0589
SMAD7.239	0.344	-0.809	-0.547	0.0786	-0.358
SMAD7.390	-0.169	-0.0112	-0.615	0.335	-0.485
SMC3.1337	-0.187	0.13	0.206	0.0966	-0.0154
SMC3.1442	0.339	-0.211	0.894	-0.643	0.243
SMC3.3106	0.205	0.408	0.612	0.456	0.009
SMC3.860	-0.129	0.326	-0.245	0.214	-0.274
SMC3.905	-0.107	-0.843	0.342	-0.353	-0.152
SMURF2.1494	-0.372	0.0163	-0.248	0.216	-0.806
SMURF2.1967	-0.112	-0.716	-0.387	-1.96	-0.137
SMURF2.3622	0.0539	-0.0343	-0.33	-0.0196	0.0379
SMURF2.3699	0.0255	0.513	-0.244	0.373	0.0466
SMURF2.633	0.373	0.101	0.621	-0.314	0.424
SNRPB.20	-1.51	-0.487	-0.807	-0.0835	-0.428
SNRPB.292	0.00715	-0.317	0.155	0.163	-0.229
SNRPB.329	0.957	-0.0675	0.557	0.283	0.377
SNRPB.391	-0.533	-0.0236	-0.383	0.369	-0.132
SNRPB.928	0.0489	0.632	-1.22	1.16	0.176
SNRPD1.1049	0.503	-0.871	-0.123	-0.241	0.183
SNRPD1.1061	0.0188	0.652	-0.0368	0.855	0.385
SNRPD1.1118	0.657	0.0742	0.202	0.293	0.62
SNRPD1.1469	-1.09	0.053	-0.259	0.3	-0.0915
SNRPD1.582	-0.641	-0.288	-0.315	0.211	-0.217
SOWAHC.2451	0.189	0.2	0.102	0.577	0.198
SOWAHC.3222	-0.427	-0.708	-1.61	-0.474	-0.602
SPRED1.1060	-0.136	-0.226	-0.113	-0.135	-0.00872
SPRED1.5123	0.472	0.301	-0.25	0.244	0.0494
SPRED1.5564	0.188	0.0817	-0.0776	0.244	0.148
SPRED1.5651	-0.355	0.284	-0.0581	0.0581	-0.342
SPRED1.6831	0.429	-0.0657	0.0995	-0.209	-0.074
SPRED2.1496	-7.53	-1.44	-0.765	-1.85	-0.8
SPRED2.1588	-0.606	-0.604	-0.713	-2.5	-0.636
SPRED2.1853	0.151	0.263	0.294	0.384	-0.124
SPRED2.2948	0.388	0.378	0.56	0.287	0.445
SPRED2.418	-0.218	-0.648	-1.16	0.122	-0.291
SPRY1.137	-0.464	0.0883	-0.146	0.657	-0.328
SPRY1.2179	0.126	-1.08	-0.0635	-0.702	0.182
SPRY1.311	0.15	0.14	0.0251	0.433	0.523
SPRY1.587	-0.285	-0.0107	-1.18	0.0387	-0.609
SPRY1.718	0.265	-0.117	-0.709	0.602	-0.0997
SPRY2.1553	0.408	-0.243	0.0485	-0.391	0.0439
SPRY2.1747	0.569	-0.577	0.696	-0.144	0.238

SPRY2.2060	-0.386	-0.0793	-0.461	-0.251	0.154
SPRY2.328	-0.436	0.266	-0.663	0.9	-0.192
SPRY2.329	2.01	0.953	n.a.	-0.00226	0.177
SPRY3.2842	0.0677	0.638	0.428	0.792	0.0793
SPRY3.6580	-0.378	0.211	0.0651	0.267	-0.619
SPRY3.6604	0.000808	-0.235	-0.579	-0.257	-0.377
SPRY3.7497	-0.325	-0.382	-0.808	-0.109	-0.556
SPRY3.7990	-0.169	0.0222	-0.558	0.307	-0.0676
SPRY4.2067	-0.368	-1.73	-0.507	-0.189	0.184
SPRY4.2099	0.0273	-1.24	0.698	-1.99	-0.524
SPRY4.2909	-0.128	-0.444	0.13	-0.223	0.24
SPRY4.4393	0.197	0.0905	0.387	-0.152	-0.699
SPRY4.4659	-1.34	-1.88	-0.0425	-0.61	-0.301
SRF.1868	-0.101	-0.513	-0.41	-0.556	-0.499
SRF.2720	0.344	0.29	0.274	0.242	-0.111
SRF.3603	0.185	0.365	-0.179	0.389	-0.263
SRF.85	0.226	-0.17	-0.139	0.239	-0.082
SRF.901	-1.34	-2.2	-1.73	-1.25	-0.423
SRSF10.319	-0.268	-0.468	-0.836	-0.719	-0.23
SRSF10.371	-0.409	-0.179	-0.638	-0.699	-0.643
SRSF10.567	-0.632	-0.246	-0.362	0.0442	-0.323
SRSF10.571	-0.615	0.443	-0.554	-0.0715	-0.0373
SRSF10.613	0.0521	-0.229	0.544	-0.337	0.324
SRSF1.1216	-0.0153	-0.769	-0.163	-0.247	-0.0808
SRSF1.2656	-0.108	0.274	-0.347	0.134	-0.213
SRSF1.3300	0.701	0.556	0.854	0.568	-0.236
SRSF1.3678	0.0802	0.247	0.347	0.479	-0.28
SRSF1.4112	0.333	0.411	0.344	0.441	0.179
SRSF2.1488	-0.673	0.156	-0.479	0.0198	-0.327
SRSF2.1545	-0.541	-0.0658	-0.499	-0.371	-0.111
SRSF2.1723	-0.733	0.179	-0.567	0.436	-0.651
SRSF2.1919	-0.353	-0.16	-0.155	-0.489	0.103
SRSF2.1937	0.039	0.178	-0.088	-0.0715	-0.172
SRSF3.1204	0.228	0.26	0.198	0.0689	0.0761
SRSF3.1983	-0.199	0.0278	0.476	0.304	-0.0922
SRSF3.2297	-0.559	-0.334	-0.898	-0.161	-0.347
SRSF3.774	0.722	-0.707	0.517	0.122	0.192
SRSF3.941	0.488	0.00526	0.197	-0.771	0.056
SSRP1.1950	-1.34	-0.744	-0.253	-0.854	-0.381
SSRP1.2143	-0.0386	0.125	-0.347	0.118	0.11
SSRP1.2149	0.0816	0.0664	0.0287	-0.12	0.426
SSRP1.2168	0.282	0.34	0.489	0.228	-0.138
SSRP1.2236	0.377	0.417	-0.142	-0.339	-0.3
STRAP.1476	0.905	-0.475	1.11	0.0534	0.0652
STRAP.1693	0.29	-0.0996	0.112	0.0768	-0.0828
STRAP.683_1	0.153	0.0614	0.00907	0.293	0.219
STRAP.683_2	-0.0718	0.318	-0.184	0.62	0.259
STRAP.859	0.0742	0.0987	-0.879	-0.0621	0.174
TCERG1.1866	0.139	-0.142	0.425	0.067	0.0203
TCERG1.1882	-0.361	0.158	-0.4	-0.517	-0.125
TCERG1.2467	-0.441	-0.35	-0.942	-0.477	-0.161
TCERG1.2725	0.337	0.396	-0.796	-0.538	0.134
TCERG1.3848	-0.201	-0.0898	-0.299	-0.218	-0.0956
TCOF1.2214	0.16	-0.23	-0.0645	-0.117	-0.21
TCOF1.312	-0.107	0.567	-0.644	-0.159	-0.557
TCOF1.313	0.186	0.473	-0.353	-0.138	-0.485
TCOF1.458	-0.0282	-0.0851	0.319	-0.616	0.134
TCOF1.459	-0.372	-0.324	-0.701	-0.801	-0.212
TFAM.2312	-0.743	0.339	-0.0879	-0.727	0.172
TFAM.3304	-0.0157	0.722	0.000104	0.783	0.231
TFAM.455	0.28	-0.149	0.24	0.373	0.374
TFAM.465	0.148	-0.192	0.163	-0.191	0.189
TFAM.674	0.414	0.534	0.329	0.0737	-0.0479
TFDP1.1542	0.0195	-0.253	0.167	0.062	0.064
TFDP1.2064	-0.483	-0.487	-0.0806	-0.69	-0.371

TFDP1.2514	0.0915	-0.342	0.226	-0.679	0.264
TFDP1.841	-0.0299	-0.373	-0.198	-0.572	-0.0903
TFDP1.865	0.389	0.357	0.203	0.112	-0.245
TGIF1.199	-0.166	-0.00507	0.217	-0.814	-0.727
TGIF1.510	0.189	-0.278	-0.2	-0.185	-0.384
TGIF1.787	-0.129	-0.92	-0.0483	0.0636	-0.00916
TGIF1.954	-0.885	-0.667	-1.52	0.0947	0.252
TGIF1.962	0.479	0.271	0.435	0.522	0.579
TIMELESS.1233	0.888	-0.828	1.11	-0.452	-0.132
TIMELESS.2900	-0.716	-0.335	-0.72	-0.458	0.338
TIMELESS.4012	0.387	-0.046	-0.3	-0.0151	0.0697
TIMELESS.4984	-0.0706	0.3	0.495	-0.0349	-0.00965
TIMELESS.939	-0.359	0.395	-0.512	0.241	-0.524
TOP2B.1679	0.608	0.401	-0.359	0.324	0.0379
TOP2B.232	0.292	-0.259	0.458	0.138	0.00386
TOP2B.2861	0.229	-0.838	1.42	-0.411	0.0661
TOP2B.4436	0.29	-0.129	-0.0608	-0.26	-0.0407
TOP2B.849	0.0802	-0.361	-0.12	-0.0664	0.0654
TRIP13.241	0.135	0.383	0.304	-0.0511	0.43
TRIP13.264	0.00446	0.962	0.301	1.05	0.0542
TRIP13.839	-0.0535	-0.572	0.141	-0.933	0.158
TRIP13.858	-0.285	-0.197	0.189	-0.569	0.0862
TRIP13.989	0.145	0.0192	0.112	-0.513	0.0224
WBP11.1135	-0.905	-0.195	-1.22	-0.668	-0.444
WBP11.2271	-0.0697	0.173	0.128	0.404	0.246
WBP11.236	0.143	0.203	0.0647	0.0368	-0.0456
WBP11.2579	-0.138	-0.418	-0.246	-0.217	-0.00503
WBP11.846	-0.0976	-0.0914	-0.0934	-0.274	0.134
WHSC1.1087	-1.27	-0.598	-0.886	-0.847	-0.635
WHSC1.279	-0.718	0.205	0.0387	-1.87	-0.234
WHSC1.67	0.486	0.985	0.813	0.609	0.244
WHSC1.767	-0.551	0.153	-0.601	0.109	0.107
WHSC1.777	0.364	0.273	0.0673	-0.531	-0.241
XRCC6.1682	-0.189	0.606	0.474	0.591	-0.144
XRCC6.270	0.112	-0.865	0.388	-0.178	0.191
XRCC6.480	0.525	0.481	-0.0262	0.0814	-0.724
XRCC6.828	-1.64	-1.01	-2.39	-0.37	-1.28
XRCC6.842	0.2	-0.0594	0.539	0.186	-0.29
ZNF207.1042	0.201	-0.789	-0.177	-0.612	-0.456
ZNF207.1051	-3.64	-2.64	-1.77	-1.13	-0.43
ZNF207.1823	-0.306	-0.0173	0.103	0.0404	-0.171
ZNF207.257	0.994	0.195	0.321	-0.789	-0.0439
ZNF207.318	-0.174	0.231	-0.332	-0.0781	0.39

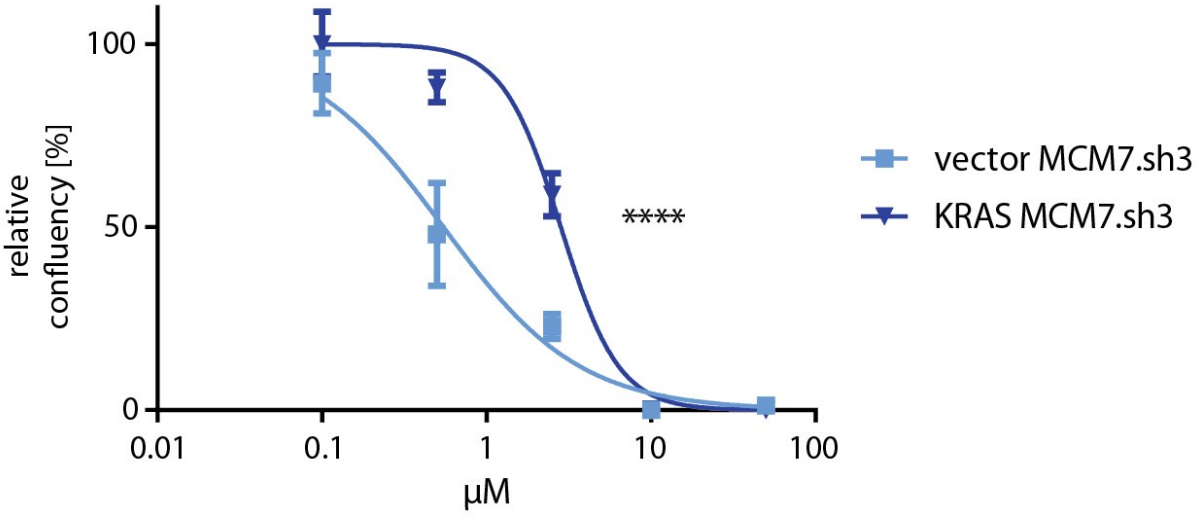

Figure A 1: CDC7 inhibition with PHA 767491in CaCo2 cells after MCM7 knockdown. $KRAS^{G12V}$ expressing CaCo2 cells exhibited a higher resistance to CDC7 inhibition ($IC_{50(vector\ MCM7.sh3)}$=0.5476 µM) after MCM7 knockdown than $KRAS^{wt}$ CaCo2 cells ($IC_{50(KRAS(G12V)\ MCM7.sh3)}$=2.833 µM). $R^2_{vector\ MCM7.sh3}$= 0.9486; $R^2_{KRAS(G12V)\ MCM7.sh3}$=0.9753. Mean relative confluency ± SEM is shown (n =4 per group). Nonlinear regression - extra sum-of-squares F test; **** = $p < 0.0001$.

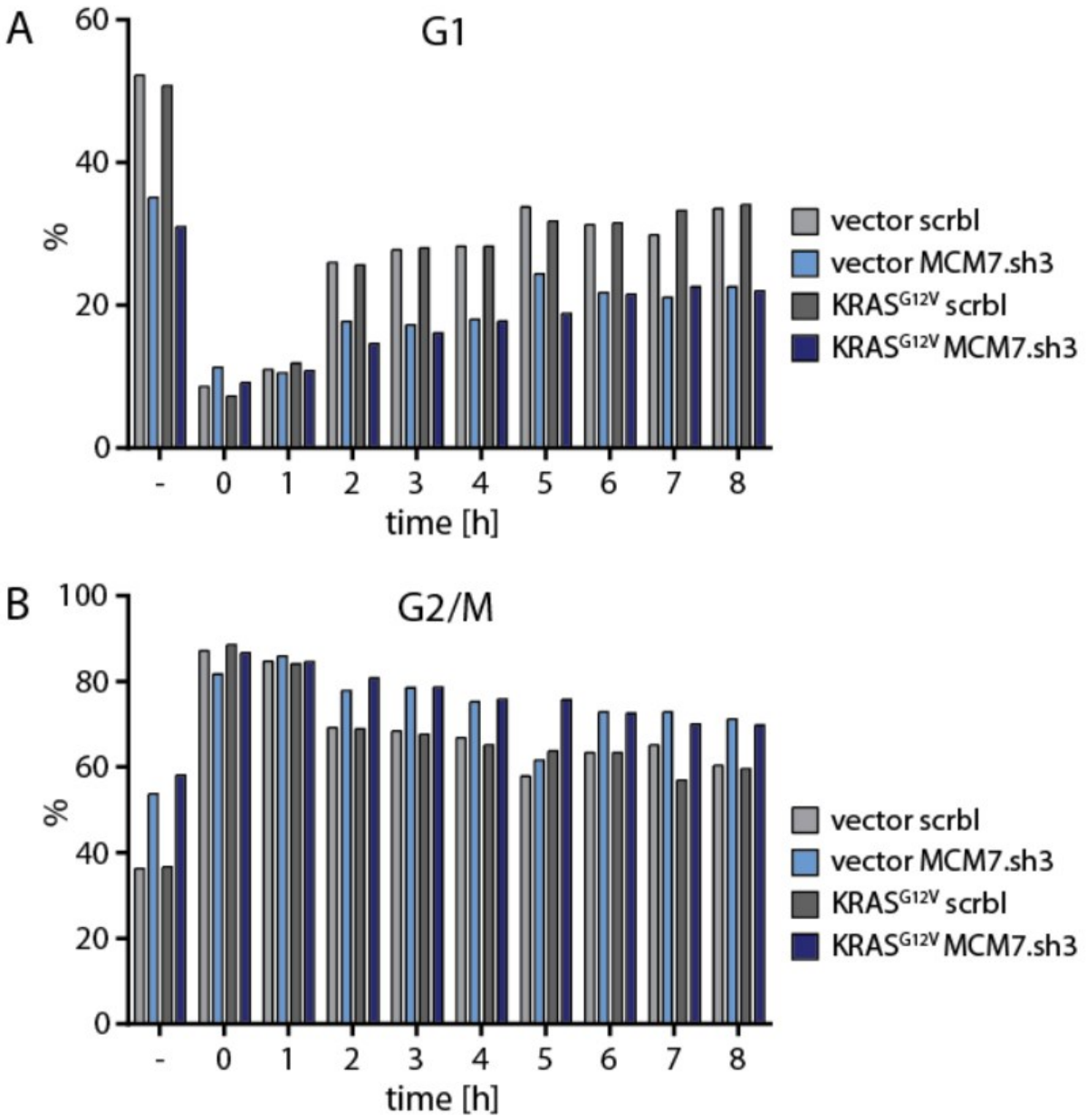

Figure A 2: Cell cycle synchronization and release with nocodazole. CaCo2 cells were induced with doxycycline for 3 days and then treated with nocodazole for 21 h before they were released for the indicated time. Nocodazole untreated sample is indicated by "-". (A) Cells of all samples entered G1 after mitotic arrest. Cells with knockdown of MCM7 showed a slower entry in G1 compared to the scrbl control. This was independent of $KRAS^{G12V}$ expression. (B) Cells in all samples were equally well synchronized in the G2/M phase after 21 h of nocodazole treatment.

Declaration of authorship

I hereby declare that I completed the doctoral thesis independently based on the stated resources and aids. I have not applied for a doctoral degree elsewhere and do not have a corresponding doctoral degree. I have not submitted the doctoral thesis or parts of it to another academic institution and the thesis has not been accepted or rejected.

I declare that I have acknowledged the Doctoral Degree Regulations, which underlie the procedure of the Faculty of Life Sciences of Humboldt-Universität zu Berlin, as amended on 5th March 2015.

Furthermore, I declare that no collaboration with commercial doctoral degree supervisors took place and that the principles of Humboldt-Universität zu Berlin for ensuring good academic practice were abided by.

Berlin, June 20th, 2018

Bastian Gastl

Publications

Articles

Gastl, B., Klotz-Noack, K., Klinger, B., Ispasanie, S., Hani Fouad Salib, K., Zuber, J., Blüthgen, N., Schäfer, R., Sers, C. (2018). **Reduced replication origin licensing selectively kills KRAS-mutant colorectal cancer cells via mitotic catastrophe**, Manuscript submitted for publication in Cell Reports on June 19th, 2018.

Mamlouk, S., Childs, L. H., Aust, D., Heim, D., Melching, F., Oliveira, C., Wolf, T., Durek, P. Schumacher, D. Bläker, H., von Winterfeld, M., Gastl, B., Möhr, K., Menne, A., Zeugner, S., Redmer, T., Lenze, D., Tierling, S., Möbs, M., Weichert, W., Folprecht, G., Blanc, E., Beule, D., Schäfer, R., Morkel, M., Klauschen, F., Leser, U., Sers, C. (2017). **DNA copy number changes define spatial patterns of heterogeneity in colorectal cancer.** ***Nature Communications***, *8*, 14093. https://doi.org/10.1038/ncomms14093

Abstracts and posters

Gastl, B., Klotz-Noack, K., Klinger, B., Zuber, J., Blüthgen, N., Schäfer, R., Sers, C. (2017). **Depletion of replication factor MCM7 is synthetically lethal to oncogenic KRAS expression**, Precision Medicine Series: Opportunities and Challenges of Exploiting Synthetic Lethality in Cancer, American Association for Cancer Research (AACR), San Diego, USA, 4th-7th Jan. 2017

Gastl, B., Klotz-Noack, K., Klinger, B., Zuber, J., Blüthgen, N., Schäfer, R., Sers, C. (2017). **Cells harboring mutant KRAS are sensitive to the depletion of replication factor MCM7**, Eukaryotic DNA Replication & Genome Maintenance, Cold Spring Harbor Laboratory, Cold Spring Harbor, USA, 1st-5th Sept. 2017

Gastl, B., Klotz-Noack, K., Klinger, B., Ispasanie, S., Zuber, J., Blüthgen, N., Schäfer, R., Sers, C. (2017). **KRAS-mutant colorectal cancer cells are sensitive to decreased DNA replication licensing through MCM7 depletion**, BIH-Symposium - Exploring Systems Medicine - The 3 Rs of Tissue Repair: Replace – Restore – Rejuvenate, Berlin Institute of Health (BIH) Berlin, Germany, 16th-17th Mar. 2018

Klotz-Noack, K., Gastl, B., Klinger, B., Rivera, M., Zuber, J., Walter. W., Blüthgen, N., Schäfer, R., Sers, C. (2016). **Functional interference screens targeting signaling components in colorectal cancer cells**, BIH-Symposium - Exploring Systems Medicine, Berlin Institute of Health (BIH), Berlin, Germany, 28th-29th Jan 2016